Defining The Role Of Oxygen Tension In Human Pluripotent Stem Cell Fate Decisions

Thesis submitted for the degree of

Doctor of Philosophy in Biochemical Engineering

By

Reema Mohammed

December 2018

Regenerative Medicine Bioprocessing Unit

Department of Biochemical Engineering

University College London

Thesis declaration

I, Reema Mohammed, confirm that the work presented in this thesis is my own. Where information has been derived from other sources, I confirm that this has been indicated in the thesis.

Abstract

Early embryo development occurs in a relatively low oxygen microenvironment in the reproductive tract (1.5- 5.3% O_2). Human Pluripotent Stem Cells (hPSCs) are routinely cultured in atmospheric condition (20% O_2). The majority of *in vitro* protocols compare 20% O_2 with one or two 'hypoxic' conditions (range from 1%-5% O_2). Therefore, there is a lack of information on how intermediate oxygen tensions might affect hPSCs behaviour. In this project, we aimed to define the role of oxygen tension in regulating self-renewal and early differentiation properties of hPSCs. Using short-term monolayer protocol, hPSCs were cultured in parallel under a full spectrum of oxygen levels (0%, 2%, 5%, 8%, 12% and 20% O_2). Cells were examined for morphological changes, growth kinetics, and expression of genes associated with pluripotency, embryonic germ layers, metabolism and hypoxia using qualitative RT-PCR, Immunostaining and Flow Cytometry. Our results revealed that culturing within a threshold of 2 to 5% O_2, was more beneficial for maintaining the self-renewal capacity of hPSCs based on morphology, cell growth and OCT4 and NANOG expression. Although cells under 2% and 5% O_2 conditions exhibited more uniform phenotypic profile which was associated with slow mitotic division, some signs of differentiation were observed under 5% O_2. Spontaneous differentiation of hPSCs under mild hypoxia (8% and 12% O_2) revealed striking morphological changes indicating the acquisition of a mesenchymal-like population that displayed positive expression of BRACHYURY, α-SMA, S100A4 and Vimentin. RT-qPCR results demonstrated cadherin switch that was coincided with SNAIL up-regulation. Which indicate the acquisition of EMT-like event during mesodermal commitment similar to that observed *in vivo* during early gastrulation. Interestingly, when mild hypoxia combined with directed mesoderm differentiation medium, a noticeable increase in mesoderm- and EMT- associated markers observed at faster kinetics. This study provides evidence for the importance of oxygen condition in regulating stem cells fate.

Impact statement

Hypoxic conditions are the physiological norms for all stem cell niches *in vivo*. Research studies looking at hypoxia have gained increasing interest over the past few decades. Nonetheless, the literature is quite controversial in which direction between self-renewal and differentiation hypoxia drives stem cells. Both an improvement and decrease of the proliferation and differentiation capacities have been reported in the literature. A key goal is to understand the fundamental properties of stem cells in order to mimic their *in vivo* microenvironment.

To date, the majority of *in vitro* maintenance and differentiation protocols compare the effect of standard culture conditions (20% O_2) with one or two hypoxic conditions on stem cell behaviour. Therefore, this thesis aims to fill a void in the literature by studying the effect of a wide range of hypoxia levels on stem cell proliferation and differentiation properties. Most of the studies have focused on the direct differentiation of hPSCs to generate mature cell types. This prompted us to mimic the early O_2 dependent events during the formation of embryonic germ layer progenitors, by allowing the cells to grow spontaneously within only 4 days without the restriction of any growth factors.

This thesis has provided evidence that stem cells are susceptible to even small changes in oxygen conditions. The results show that the decisions the cells made under a single oxygen tension (e.g. 2% O_2) were different from those made at other oxygen levels. Using a short-term culture protocol, we found that the cells deviated toward the undifferentiated state under <5% O_2, but instead shifted toward differentiation under ≥5% O_2 which mimics the situation *in vivo*.

The results from this research have shown that the manipulation of a single factor, oxygen tension, during maintenance and differentiation stages was critically important and differentially regulated hPSCs fates. Indeed, HIF-1-hypoxia main regulator- is known to regulate 5% or more of the human genome. These results have clear implications to improve the effectiveness of the *in vitro* differentiation protocols. Moving forward it is clear that the oxygen level at each stage of stem cell bioprocess development needs to be controlled individually to best recapitulate the *in*

vivo transient events during embryo development. This can be achieved by propagating the cells in a completely closed system that automatically run multiple hypoxic profiles during *in vitro* protocols.

We posit that manipulation of the oxygen level could be a possible strategy for improving the *in vitro* differentiation efficiency of hPSCs into clinically relevant populations such as Cardiomyocytes and βeta cells, holding potential for clinical applications.

“One of the most exciting things about studying HIF-1 for me is following the entire range of biological processes. You can start with the most basic, fundamental questions like ‘How does the cell sense the concentration of oxygen and respond to changes,’ all the way to the most applied, ‘How do we develop new treatments for cancer and cardiovascular disease?”

By Gregg L. Semenza

Acknowledgements

First, praises and thanks to Allah S.W.T for all the blessings he has bestowed on me. I want to thank my supervisor, Dr Farlan Veraitch, for his guidance and the valuable feedback on my thesis writing and encouragement throughout my PhD. I want to extend my gratitude to Dr Qasim Rafiq for his valuable feedback on my thesis writing. I thank Ludmila Ruban for her assistance and guidance. My sincerest thanks go to my colleagues within the Advanced Centre for Biochemical Engineering to name a few; Billy, Fair, Fatumina, Abeer, Icken, Erick and Damiano, always be happy to help. Special thanks go to Vijay Kumar, and Vaques George, your valuable assistance, critical reading and contributions are sincerely appreciated and gratefully acknowledged. I want to thank Joana Neves Dos Reis for being always there for me. Completing this work would have been more difficult without your support and friendship.

Special recognition goes out to my parents Mohammed and Hessah; I want to be more because you believe I can, and to Faisal, my partner in life, thank you for being you.

Finally, I would like to thank the Ministry of Higher Education in Saudi Arabia for providing the funding that allowed me to undertake this research project.

All the world is a laboratory to the inquiring mind. (Martin H. Fischer)

Table of Contents

List of Figures

List of Tables

List of Abbreviations

ARNT	Aryl hydrocarbon receptor nuclear translocator
ASCs	Adult Stem Cells
ATP	Adenosine-59-Triphosphate
bFGF	Basic Fibroblast Growth Factor
BM	Bone Marrow
BMP	Bone Morphogenetic Protein
BSA	Bovine Serum Albumin
C-TAD	Carboxy-terminal transactivation domain
CBP	CREB binding protein
CDH1	E-Cadherin
CDH2	N-Cadherin
cDNA	Complementary DNA
CO_2	Carbon Dioxide
DAPI	4,6-Diamidino-2-Phenylindole
DMEM	Dulbecco's Modified Eagle's Medium Dmso – Dimethyl Sulphoxide
DMOG	Dimethyloxaloylglycine
DMSO	Dimethyl Sulphoxide
DNA	Deoxyribonucleic Acid
DPBS	Dulbecco's Phosphate Buffered Saline
ECCs	Embryonic Carcinoma Cells
ECM	Extracellular Matrix
EDTA	Ethylenediaminetetraacetic Acid
ELISA	Enzyme-Linked Immunosorbent Assay
EMT	Epithelial-Mesenchymal Transition
FBS	Foetal Bovine Serum
FIH	Factor Inhibiting HIF-1
GDF3	Growth Differentiation Factor 3
gDNA	Genomic DNA
GLUT1	Glucose Transporter 1
GOI	Gene of Interest
GPR	Glucose Production Rate
GSK-3	Glycogen Synthase Kinase 3
hESCs	Human Embryonic Stem Cells
HIF	Hypoxia Inducible Factors
HKG	House Keeping Gene
hMSCs	Human Mesenchymal Stem Cells
HRE	Hypoxic-Response Element
HSC	Hematopoietic Stem Cells
iPSCs	Induced Pluripotent Stem Cells
IVF	In Vitro Fertilization
LDHA	Lactate Dehydrogenase A
LIF	Leukemia Inhibitory Factor
LPR	Lactate Production Rate
MCB	Master Cell Bank
MEFs	Mouse Embryonic Fibroblasts
MEK	Mapk/Erk Kinase
mESCs	Mouse Embryonic Stem Cells

MIM	Mesoderm Induction Medium
MMPs	Matrix Metalloproteinase
N/C	Nucleus-Cytoplasm Ratio
N2	Nitrogen
NANOG	Tír Na Nóg – Scottish Myth Mean Land of The Young
NEAA	Non-Essential Amino Acids
NRQ	Normalized Relative Quantities
NRT	No Reverse Transcription
NSCs	Neural Stem Cells
NTC	No Template Control
O_2	Oxygen
OCT4	Octamer-Binding Transcription Factor 4
ODD	Oxygen-dependent degradation
OXPHOS	Oxidative Phosphorylation
P	Passage
PAS	Per-ARNT-Sim
PAX6	Paired Box 6
PDT	Population Doubling Time
PFA	Paraformaldehyde
PHD-2	Proline-hydroxylase-2
PHDs	Prolyl Hydroxylase Proteins
PI3-K	Phosphoinositide 3-Kinase
REF	Reference Gene
RNA	Ribonucleic Acid
ROS	Reactive Oxygen Species
RT-qPCR	Real Time Quantitative Polymerase-Chain Reaction
SOX17	SRY-box 17
SOX2	SRY Sex Determining Region Y-Box 2
SP.D	Spontaneous Differentiation
SSEA	Stage-Specific Embryonic Antigen
STAT3	Signal Transducer and Activator of Transcription 3 Te-Trophectoderm
SVZ	Sub Ventricle Zone
T/E	Trypsin/EDTA
TAD	Transactivation domains
TE	Buffer – Tris-Edta Buffer
TGF-β	Transforming Growth Factor- B
TRA	Keratan Sulfate– Related Antigens
VEGF	Vascular Endothelial Growth Factor
VHL	Von Hippel Lindau
VTN	Vitronectin
WCB	Working Cell Bank

1 CHAPTER 1: LITERATURE REVIEW

1.1 HISTORY OF STEM CELLS DERIVATION

There has been a growing interest in stem cells research since the two Canadian scientists, J. Till and E. McCulloch first isolated and identified a Hematopoietic Stem Cell (HSCs). They found that HSCs from another donor effectively reconstituted the whole new haematopoietic system when introduced into an irradiated mouse (BECKER et al. 1963). This work has demonstrated the dual properties of stem cells; self-renewal and differentiation, which considered now as the hallmarks of stemness (Thomson et al. 1998).

1.1.1 Embryonic Carcinoma Cells (ECCs)

Before the discovery of stem cells, both Askanazay and Jackson & Brues had observed the presence of multipotent cells in teratocarcinoma (Askanazy 1907; Jackson & Brues 1941). Askanazay had demonstrated that the differentiated somatic cells of the teratoma were generated by embryonic differentiation from either a single or group of multi-potential cells (Askanazy 1907). Jackson & Brues had supported Askanazy's concept when they observed that in murine ovarian carcinoma, undifferentiated cells were highly mitotic than in the adult somatic cells, thought to be the stem cells of the teratocarcinoma. Another group had found when a tumour was transplanted subcutaneously; it exhibited the same pleomorphic character of the original one through serial transplants (Fekete & Ferrigno 1952). Considering that the undifferentiated cells were the essential element of a tumour, as they gave rise to the differentiated tissues, implying their pluripotency. In 1959, another study had proofed this notion when teratocarcinomas were injected into mice; free-floating aggregates that had foci of ECCs were observed. It was concluded that the ECCs were the pluripotent cells of the teratocarcinomas (Pierce et al. 1959). When these aggregates were transplanted into mice, they differentiated into teratocarcinomas (STEVENS 1960). These studies confirmed the pluripotency feature of ECCs, which further set the stage for another key study by (Kleinsmith & Pierce 1964) who demonstrated the multi-potentiality of single ECCs. Although the remarkable

similarity in morphology and differentiating potential (pluripotency) has led to the use of ECCs as the *in vitro* model to study early mouse development (Martin 1980), ECCs harbour genetic aberrations that accumulate during the development of the teratocarcinoma. These genetic abnormalities have emphasised the need to use healthy cells to study developmental biology.

1.1.2 Mouse Embryonic Stem Cells (mESCs)

ESCs were derived from Inner Cell Mass (ICM) of mouse embryos by two groups. The first group had shown that when mESCs were transplanted into the embryonic environment of the blastocyst, they underwent normal development. When mESCs were cultured on a feeder layer of Mouse Embryonic Fibroblasts (MEFs), they exhibited all the positive characteristics similar to those seen in ECCs, including the unlimited proliferative potential and the ability to differentiate into derivatives of all three germ layers, but they exhibited normal karyotype (Evans & Kaufman 1981). The other group has cultured mESCs using EC cells-conditioned medium (Martin, 1981). In 1989, mESCs were first genetically modified which has led to generating the first "knockout mice" (Mario R. Cappechi, Martin J. Evans 1989), this breakthrough has set the stage for scientists with new ways to study normal and pathological conditions.

1.1.3 Human Embryonic Stem Cells (hESCs)

Extensive work has led to the generation of first human ESCs (Thomson et al. 1998). These cells exhibited the dual properties of self-renewal and differentiation into all three embryonic germ layers *in vivo* by forming teratomas and *in vitro* by removing the co-cultured MEFs feeder layers (Thomson et al. 1998; Reubinoff et al. 2000). Additionally, hESCs exhibited surface markers previously identified in primate ESCs and human ECCs and possessed high telomerase activity rate (Huang et al. 2011). Human ESCs are derived from spare pre-implantation embryos produced by In Vitro Fertilization (IVF) that were donated to scientists at about D4 or D5 post-fertilisation. Due to their unlimited proliferative capacity and their ability to give rise any cells type; they offer a great tool to study basic developmental biology and for regenerative medicine applications. Also, derivatives of ESCs are useful as models for

understanding the biology of disease and developing new drugs, especially when there is no animal model for the disease being studied. ESCs, also, provide a potential tool for transplantation therapies in pathological conditions such as diabetes, spinal cord injury, Parkinson's disease, and myocardial infarction.

1.1.4 Induced Pluripotent Stem Cells (iPSCs)

The generation of iPSCs has revolutionised the field of regenerative medicine; such advancement makes the personalised stem cells therapies closer to be achieved; also, it eliminates the ethical controversy of using hESCs. IPSCs were first produced from mouse fibroblasts and then from human fibroblast (Takahashi & Yamanaka 2006; Takahashi et al. 2007; Ohnuki et al. 2007; Aoi et al. 2008). The generation of iPSCs was through the reprogramming of somatic cells back to an undifferentiated state by transfecting these cells with a combination of pluripotent factors. The original method, developed by (Takahashi & Yamanaka 2006), involved reprogramming of murine fibroblasts via retroviral transduction of pluripotent factors including Octamer-binding Transcription Factor 4 (OCT4), SRY sex determining region Y-Box 2 (SOX2), Kruppel-Like Factor 4 (KLF4) and C-MYC. Same factors were used to produce iPSCs from human (Takahashi et al. 2007; Yu et al. 2007; Park et al. 2008). Another group has demonstrated the reprogramming of human fibroblasts using a lentiviral-based approach to transfect with OCT4, SOX2, NANOG and LIN28 (Yu et al. 2007). This method allowed the transduction of non-dividing cells and avoided the use of C-MYC, which is known as an oncogene (Avilion et al. 2003; Takahashi & Yamanaka 2006; Fusaki et al. 2009; Ban et al. 2011). Additionally, many non-viral approaches have been identified to reprogram somatic cells such as episomal plasmid DNA (Hu & Slukvin 2013; Fontes et al. 2013; Okita et al. 2013). Safe alternatives were developed in reprogramming somatic cells by using adenoviral vectors (Stadtfeld et al. 2008), as well as transposon-based vectors, where the transgene was removed after reprogramming process (Kaji et al. 2009). Several somatic cells such as adipose cells, amniotic fluid cells, Hepatocytes, blood cells, and fibroblasts in adult tissue were used to generate iPSCs (Aoi et al. 2008; Eggenschwiler & Cantz 2009; Hanna et al. 2008; Stadtfeld et al. 2008; Kim et al. 2008). There are many similarities between ESCs and iPSCs; both cell types exhibit similar proliferation and differentiation capacities *in vitro*; Embryoid Bodies

(EBs) formation *in vitro*, teratoma and chimaera *in vivo*. ESCs and iPSCs also share relatively the same gene expression profile (Ying et al. 2003).

1.2 DEVELOPMENTAL BIOLOGY

Embryogenesis starts with the fertilisation of the egg and the formation of the zygote; this occurs in the fallopian tubes. Following fertilisation, the zygote undergoes rapid mitotic divisions with no significant growth and forms a cluster of cells called cleavage. While it travels through the fallopian tube to the uterus, cells continue to divide to form a dense ball called the morula, consisting of 16 cells (called blastomeres) within the zona pellucida (a protective membrane of glycoproteins that surrounds the zygote) (Abbott 1936; Larsen et al. 2001; Boklage 2010). After 5 to 7 days, blastomeres become bound firmly together through the formation of desmosomes and gap junctions; this process is known as compaction (Chard & Lilford 1995). Compaction continues as cellular differentiation; a cavity called blastocoel formed in the centre of the morula, which results in the formation of the blastocyst (Fong et al. 1998; Patestas & Gartner 2006). Cells differentiate into an outer layer group of cells known as the trophoblast and to the ICM. While compaction proceeds, the trophoblast become indistinguishable, they are still enclosed within the zona pellucida. Trophectoderm that is generated from the trophoblast committed to forming the placenta and extra-embryonic tissues, while ICM ultimately form the embryonic germ layers (Chazaud et al. 2006). When blastocyst moves through the fallopian tubes, the zona pellucida disappears entirely to initiate blastocyst attachment to the uterine wall at which the implantation stage starts (Forgács & Newman 2005). During implantation, ICM begins to transform into two distinct epithelial layers; epiblast and the hypoblast, which are the two layers of the bilaminar embryonic disc, occurs at the beginning of week two of gestation (Carlson 2014). The hypoblast layer will surround the epiblast, and these layers will form the embryonic disc that will eventually develop into the embryo. The trophoblast will also form two sub-layers: the cytotrophoblasts, which is in front of the syncytiotrophoblast, which in turn lies within the endometrium (Forgács & Newman 2005; Carlson 2014) (Figure 1.1). The other layer is known as the exocoelomic membrane (Heuser's membrane), which surrounds the cytotrophoblasts and the primitive yolk sac (Humana 2012). New cells that are generated from embryonic yolk sac are then established between trophoblast and exocoelomic membrane and forms the extra-embryonic mesoderm, which will form the Chorion.

Gastrulation begins after the formation of the blastocyst and its followed by organogenesis when the organs develop from the three germ layers (Hall 1998). The beginning of gastrulation marked by the appearance of the primitive streak; a central linear band of cells formed by the migrating cells from the epiblast, which takes place at week 3 after fertilisation (Figure 1.1). This creates a cavity known as the archenteron that will eventually form the primitive gut. The area at which the archenteron opens known as the blastopore. This indent causes the formation of three germ layers: ectoderm, endoderm and mesoderm (Forgács & Newman 2005) (Figure 1.1). Each germ layer generates specific tissues in the developing embryo; ectoderm gives rise to the epidermis, and the nervous system, endoderm make the epithelium of the respiratory system and digestive system, and mesoderm gives rise to bone, muscle, and connective tissue (Matsui et al. 1992).

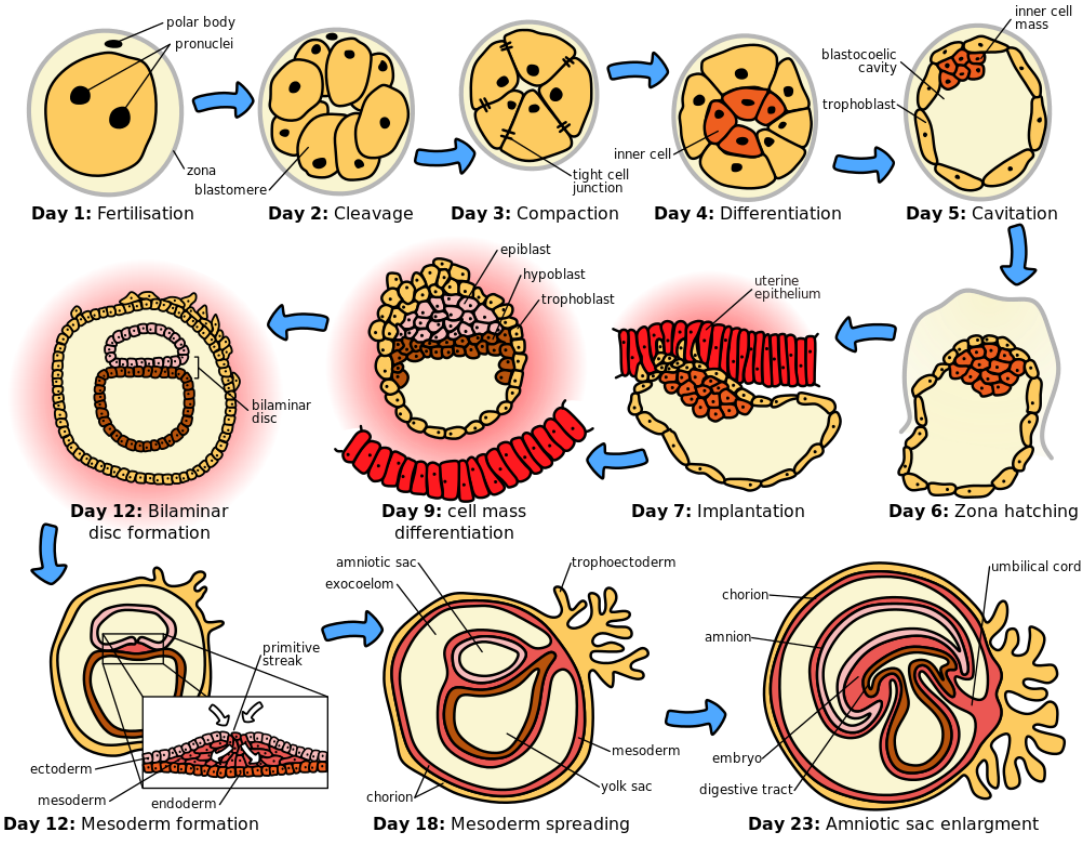

Figure 1.1 The early stages of human embryogenesis.
The first 12 days of embryogenesis in humans. Beginning at the fertilised egg and the zygote formation and ending with the establishment of three germ layers from the primitive streak. Original image created by Richard Wheeler (Zephyris)
http://en.wikipedia.org/wiki/File:HumanEmbryogenesis.svg

1.3 THE ROLE OF OXYGEN GRADIENT IN STEM CELL BIOLOGY

Stem cells reside in low oxygen microenvironments *in vivo* in the embryo as well as in the adult tissues. The following section aims to describe the role of oxygen gradient on stem cells behaviour in the context of the biology of several stem cells populations and their respective niches (embryo and adult tissue).

1.3.1 Embryonic Tissues

A connection between mammalian embryogenesis and oxygen levels was first established in the 1970s when Morriss and New showed that successful development of the cranial neurulation by ex utero rat embryos was dependent on the creation of low oxygen culture (5% O_2) (Morriss & New 1979). Early embryogenesis takes place before establishing blood circulation, indicating a low oxygen tensions microenvironment (Rodesch et al. 1992; Fischer & Bavister 1993; Burton & Jaunaiux 2001; Ottosen et al. 2006; Simon & Keith 2008; Ufer & Wang 2011; Greer et al. 2012). Direct measurement of oxygen level in the endometrial and trophoblastic tissues demonstrated that it ranges between (1.5–9% O_2) (human 3% O_2, rabbit 8.7% O_2 and monkey 1.5% O_2). (Mitchell & Yochim 1968; Rodesch et al. 1992; Maltepe & Simon 1998; James et al. 2006).

1.3.1.1 Implantation through placentation

After blastocyst implantation, cytotrophoblasts surrounds the embryo and limits the access of maternal blood by plugging the lumina of the decidual vessels, generating a low oxygen microenvironment (Jauniaux et al. 2003) (Figure 1.2). This low oxygen microenvironment plays a critical role in regulating the cytotrophoblasts invasion through the uterine epithelium. As the development proceeds, cytotrophoblasts either fuse to form multinucleated syncytiotrophoblast or columns of mononuclear cells that attach to the uterine wall (Genbacev et al. 1996; Bischof & Campana 2000). Low oxygen induces cytotrophoblasts proliferation rather than differentiation along the invasive pathway. A subset of these cells differentiates into invasive extravillous trophoblasts that migrate and reach maternal spiral arteries to enlarge and cause uteroplacental circulation blood flow to begin in the intervillous space. Accordingly, local oxygen level increases from ~2.3% to 8% O_2 by 10 to 12 weeks of

pregnancy (Jauniaux et al. 2000; Simon & Keith 2008). The differentiation of proliferating cytotrophoblasts into invasive extravillous trophoblasts is an O_2-dependent process, with O_2 levels increasing as cells migrate towards the maternal blood vessels (Staun-Ram & Shalev 2005; Rosario et al. 2008; Chang et al. 2018).

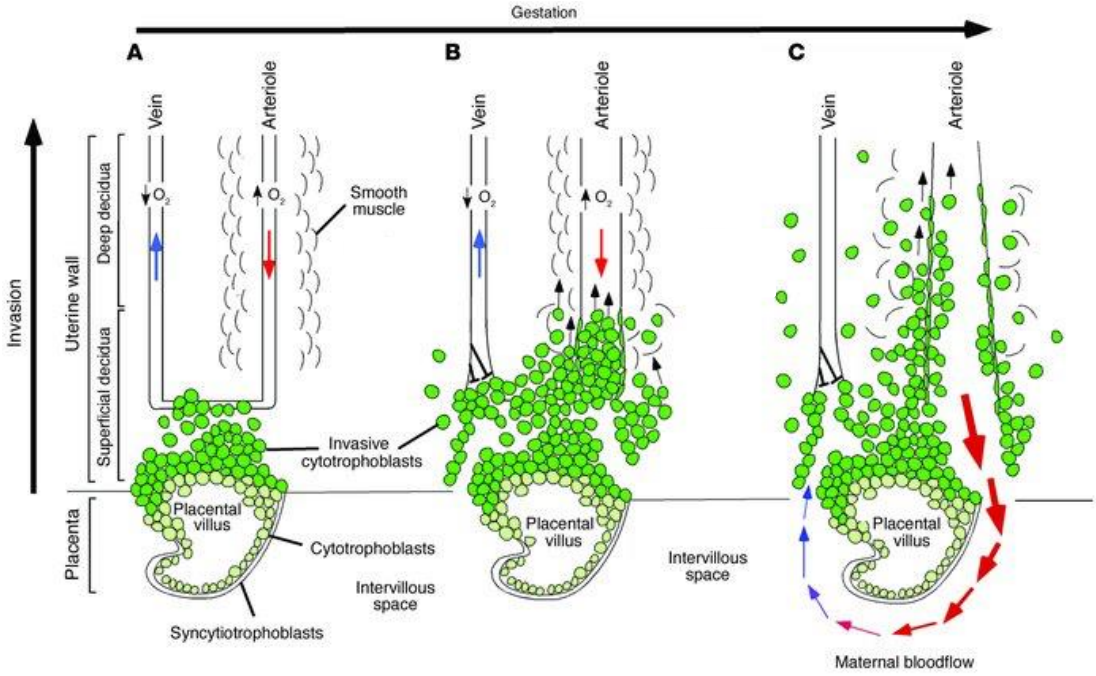

Figure 1.2 The role of oxygen tension in guiding the differentiation of Cytotrophoblasts

(A) Early stages of placental formation occur in a low O_2 microenvironment that favours Cytotrophoblasts proliferation rather than differentiation. Cytotrophoblasts (light green) rapidly divide (**B)** As development proceeds, Cytotrophoblasts (dark green) invade the uterine epithelium and block the maternal vessels, a process that maintains a state of physiological low O_2 microenvironment (**C)** Blood flow to the intervillous space begins by week 10 of human pregnancy. As the invasion progresses, the cells migrate along the lumina of spiral arterioles, replacing the maternal endothelial lining. This increases the diameter of the arterioles to accommodate the massive increase in blood flow that is required to support rapid fetal growth; consequently O_2 level rises (Red-Horse et al. 2004).

1.3.1.2 Epithelial-Mesenchymal Transition (EMT)

The concept of EMT was first proposed based on biological studies of chick embryos (Trelstad et al. 1966; Trelstad et al. 1967; Sexén 1970). Then, it has been used to describe the process of embryonic three germ layers formation in mammals (Collins & Fleming 1995; Savagner 2005; Eckert & Fleming 2008).

Following the earliest stages of embryogenesis, after implantation, two layers originate from the primitive endoderm of the blastocyst; the parietal endoderm (PE) and the visceral endoderm (VE). The trophectoderm cells (that arise from PE) undergo an EMT to facilitate the invasion of the blastocyst into the endometrium and the subsequent proper anchoring of the placenta, enabling nutrient and oxygen exchange (Vićovac & Aplin 1996; Aplin et al. 1998; Bischof et al. 2006). EMT is also associated with the embryonic gastrulation and gives rise to the mesoderm, endoderm and mobile neural crest cells. The primitive epithelium, specifically a subset of cells from the epiblast, move to the midline to form the primitive streak, a linear structure that bisects the embryo along the anteroposterior axis, these cells internalise to form the primary mesenchyme through the EMT. While the remaining cells in the epiblast from the ectoderm, therefore, the embryo is transformed from a single layer to three layers (Acloque et al. 2009) (Figure 1.3).

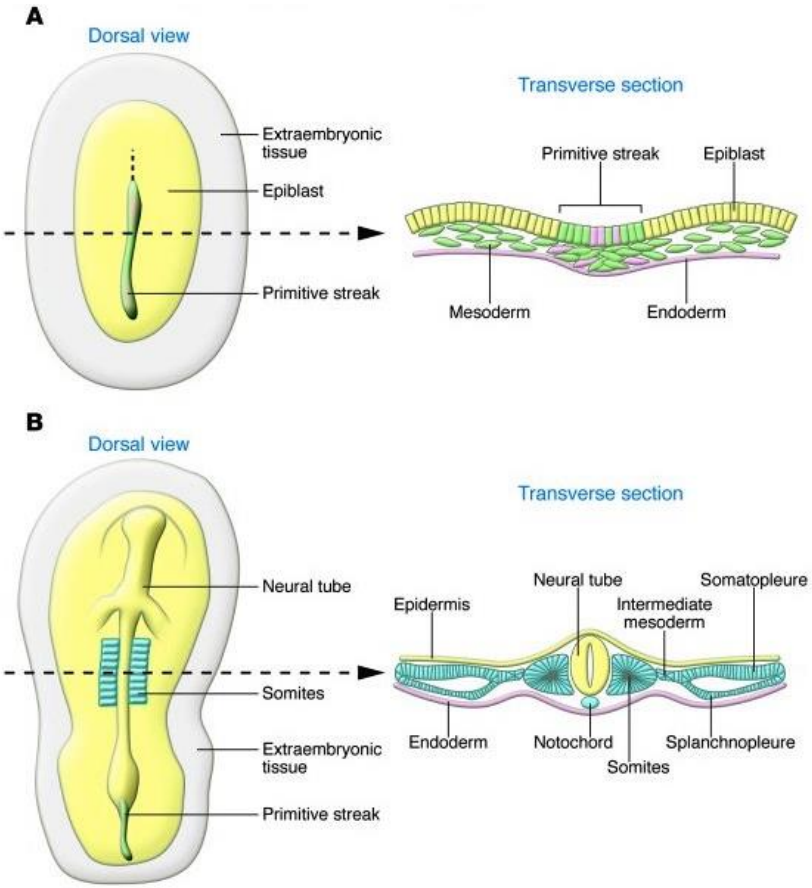

Figure 1.3 The formation of embryonic germ layers at gastrulation through EMT.
Dorsal views and transverse sections were taken at the level of the dotted lines. **(A)** The early formation of embryonic germ layers. Mesodermal (green) and endodermal progenitors (pink) are internalised at the primitive streak through the process of EMT, whereas ectodermal cells remain epithelial (yellow). **(B)** The mesodermal cells condense to form different derivatives (blue) along the mediolateral axis via the process of MET. The axial mesoderm generates the notochord, paraxial mesoderm forms the Somites (the intermediate mesoderm will later form the genitourinary system), and the lateral mesoderm condenses to form somatopleure and splanchnopleure. The ectodermal cells give rise to the neural tube and the epidermis. The endoderm is shown in pink (Acloque et al. 2009).

EMT is triggered by the naturally occurring low oxygen tension experienced by the developing embryo. EMT is also controlled by Transforming Growth Factor- β (TGF-β) that respond to ECM signals (e.g. collagen, hyaluronic acid and integrin) (Misra et al. 2012; Zheng 2017).

The cellular remodelling of EMT includes the degradation of underlying basement membrane and epithelial cell-cell junctions, loss of cell polarity and reorganisation of the cytoskeletal architecture and acquiring a mesenchymal phenotype. This includes enhanced motility capacity, invasiveness, and increased production of ECM proteins (Z Kalluri & Weinberg 2009; eisberg & Neilson 2009) (Figure 1.4). This switch in cell differentiation and behaviour is mediated by key transcription factors such as SNAIL, SLUG, zinc-finger E-box-binding (ZEB) and TWIST, which modulate the expression of epithelial and mesenchymal markers at both transcriptional and translational levels (Eastham et al. 2007; Yang et al. 2008; Gheldof & Berx 2013). These regulators down-regulate epithelial markers expression (e.g. E-cadherin, Collagen type IV, and Laminin 1), rearrange the cytoskeleton architecture and promote the expression of mesenchymal markers (e.g. N-cadherin, Integrin, Vimentin, Fibronectin, and Collagen type I) (Vićovac & Aplin 1996; Eastham et al. 2007; Zheng et al. 2009; Yeo et al. 2017). Hypoxia (low O_2) is an important factor that regulates SNAIL expression as well as other EMT regulators (TWIST, SLUG, and ZEB1). In addition, the production of Matrix Metalloproteinases (MMPs) was found to be through the activation of SLUG (Medici et al. 2008). Hypoxia also activate TWIST expression during development and tumorigenesis (Peinado et al. 2007; Xu et al. 2009) through the activation of Hypoxia Inducible Factors (HIFs) (mediator of physiological response to hypoxia, as will be discussed below), thus promoting the acquisition of EMT process (Yang et al. 2008).

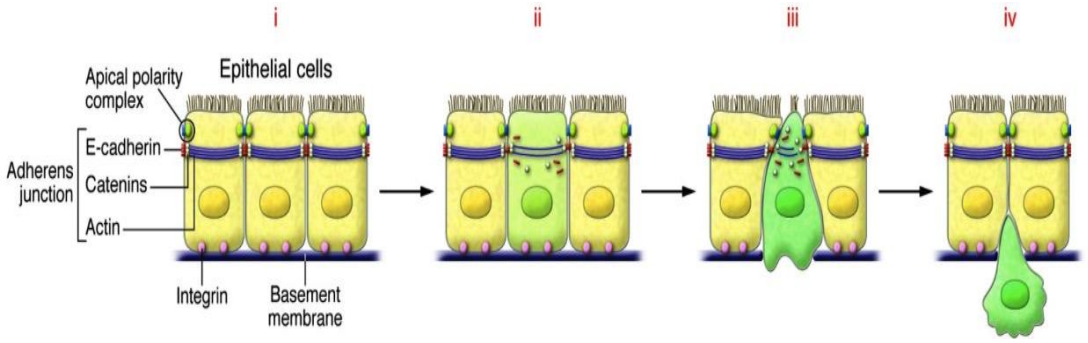

Figure 1.4 Cellular aspects of EMT
(i) Normal Epithelial cells (yellow) contain adherens junctions including of E-cadherin (CDH1), Catenin and Actin. Tight junctions are responsible for the apical polarity complexes, while integrin interacts with basal membrane components. **(ii)** Loss of cell-cell adhesion by E-cadherin degradation. EMT characterised by the down-regulation of genes encoding the components of adherens and tight junctions, and loss of cell polarity. **(iii)** degradation of the basal membrane and apical constriction that is associated with profound cytoskeletal remodelling **(iv)** activation of MMPs to facilitate mesenchymal cell (green) migration and invasion through the ECM (Acloque et al. 2009).

1.3.1.3 Vasculature development

Low oxygen microenvironment is necessary for the patterning of the embryonic vascular system, in which existing vessels would sprout into regions containing O_2-starved cells. Several angiogenic growth factors, produced by theses O_2-starved cells, regulate vasculature morphogenesis including Vascular Endothelial Growth Factor (VEGF) (A–D), the VEGF receptors (VEGFR1-3), the angiopoietin growth factors (Ang1, Ang2, Ang3/4), and their receptors (Tie1, Tie2) (Shweiki et al. 1992; Flamme et al. 1997; Augustin et al. 2009), which are direct transcriptional targets of HIFs. These molecules are involved in regulating several steps of vascular morphogenesis including vasculogenesis, angiogenesis, vessels remodelling and stabilisation (Ferrara et al. 2003) (Figure 1.5A). The initial remodelling of the vasculature requires VEGF, and its receptors, where embryonic blood vessels develop through vasculogenesis, a process by which angioblasts differentiate into endothelial cells that assemble into a primary capillary plexus, this process occurs under low oxygen tension. Additional blood vessels are formed by both sprouting and non-sprouting angiogenesis and are progressively remodelled to complete the vasculature wall. Final stages of vascular remodelling and stabilization require Ang-Tie system, when the vessels remodel and acquire their pericyte (pct) and smooth muscle cell (smc) coating, this occurs under increased oxygen condition after the

establishment of fetal-placental circulation (van Tuyl et al. 2005; Hirota & Semenza 2006; Hickey & Simon 2006; Sriram et al. 2015).

Gain- and loss-of-function approaches revealed the role of oxygen gradient in embryonic vascular development. For example, HIF-1β (-/-) embryos showed lethality by embryonic day (E)10.5, due to inhibition of both vasculogenesis and angiogenesis (Ryan et al. 1998; Iyer et al. 1998; Ryan et al. 2005). Also, HIF-1β-deficient mice exhibit reduced levels of VEGF and increased numbers of apoptotic HSCs. Consistent with these findings, HIF-1A- deficient embryos show similar phenotypes to HIF-1β (-/-) mice, with defects in blood vessel formation and neural fold closure (Kozak et al. 1997; Iyer et al. 1998). These studies indicate that VEGF secretion is modulated by low oxygen microenvironment in the early embryo (Ferrara & Davis-Smyth 1997; Risau 1997; Mahon et al. 2001; Rey & Semenza 2010).

1.3.1.4 Bone formation

Bone formation occurs through two different mechanisms: intramembranous (formation of the flat skull bones) and endochondral ossification (development of other skeletal bones) (Kronenberg 2003). Intramembranous ossification involves the differentiation of Mesenchymal Stem Cells (MSCs) directly into Osteoblasts. Other skeletal bones are derived from the differentiation of MSCs into highly proliferative chondrocytes (primary cell type of cartilage) via condensation (Figure 1.5B). These later processes form an avascular and highly hypoxic fetal growth plate, an environment that favours the chondrocytes proliferation. During bone vascularisation stage, chondrocytes stop proliferating and differentiate into hypertrophic chondrocytes where they produce cartilage matrix proteins (collagen type X), and then they undergo apoptosis. Then, cartilaginous matrix degrades and replaced by highly vascularized bone tissue in a VEGF-dependant mechanism (Kronenberg 2003), which eventually causes an elevation in the oxygen level within the bone. The fetal bone formed according to a defined temporal and spatial pattern. For example, while hypertrophic chondrocytes undergo apoptosis to facilities vascularisation in the upper hypertrophic zone, in other regions of the growth plate, where it is hypoxic, chondrocytes continue to proliferate lengthening the bone. This balance between chondrocytes proliferating and differentiation is an O_2-dependent process, with

proliferation is induced by low oxygen level while higher oxygen levels drive differentiation (Karsenty 2003; Provot & Schipani 2005; Lefebvre & Smits 2005).

Several studies have shown that the HIF signalling pathway regulates endochondral bone formation by coupling angiogenesis to osteogenesis and controlling the spatial and temporal onset of angiogenesis in the fetal growth plate (Rankin et al. 2011). Moreover, deletion of HIF-1A gene in chondrocytes resulted in massive cell death in the centre of the cartilaginous fetal growth plate and delayed differentiation at its periphery (Schipani et al. 2001). As the fetal growth plate is hypoxic it characterised by anaerobic glycolysis; studies showed that HIF-1A null growth plate exhibited deficient levels of phosphoglycerate kinase (PGK-1), a key enzyme in anaerobic glycolysis and a classical downstream target of HIF-1A (G. Yang et al. 2008). Further, VEGF-A deletion in chondrocytes causes cell death in the center of fetal growth plate, similar to that observed chondrocytes lacking HIF-1A (Schipani et al. 2001), which suggest that VEGF-A is essential for chondrocyte survival and that HIF-1A and VEGF-A are part of an important signalling pathway that promotes chondrocyte survival in endochondral bone formation (Zelzer et al. 2004).

A

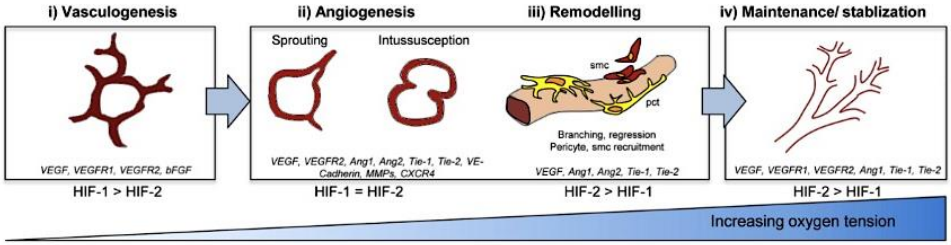

B

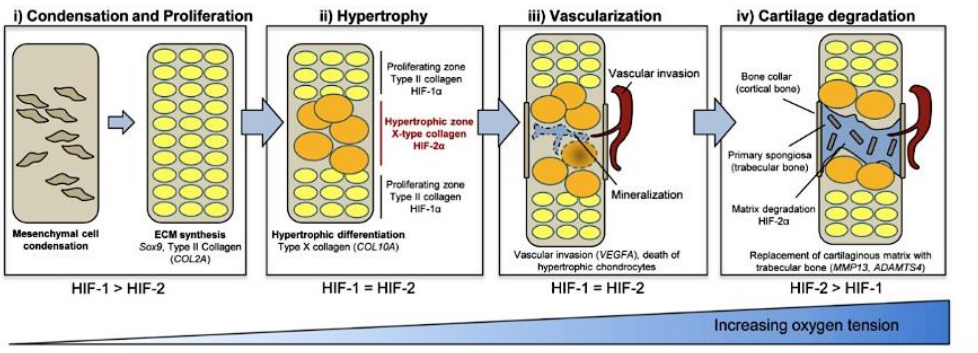

Figure 1.5 The role of oxygen gradient in the formation of vascular system and bone during early embryogenesis.

(A) vasculogenesis (i) and angiogenesis (ii) occur under intense hypoxia, the final stages of vascular remodelling and stabilisation (iii, iv), such as pct and smc recruitment, occur under less hypoxic conditions. **(B)** During the initial stage of bone development, mesenchymal cell condensation, chondrocyte proliferation, and synthesis of the cartilaginous ECM (i) Next, proliferation continues to be promoted by the hypoxia pathway, cells within the hypertrophic zone undergo hypertrophic differentiation (ii), (i) and (ii) occur under low oxygen tension environment. This is followed by the vascular invasion of the hypertrophic zone (iii) cause an elevation in oxygen levels. Finally, degradation of cartilage and its eventual replacement with bone is promoted under higher oxygen condition (iv) (Koh & Powis 2012).

1.3.2 Adult Tissues

Various Adult Stem Cells (ASCs) including HSCs, MSCs and Neural Stem Cells (NSCs), reside in hypoxic niches (Figure 1.6). The stem cells niche refer to a specialised microenvironment that includes cellular and acellular components that interact with stem cells to regulate their fates (Li & Xie 2005; Jones & Wagers 2008). Contact and communication of stem cells niches elements such as cell-cell interactions, adhesion molecules, ECM glycoproteins, the oxygen tension, metabolites (e.g. ATP) and cytokinesis critical to regulating stem-cell characteristics within the niche.

One of the most well-studied niches is that of the HSCs (Moore & Lemischka 2006; Yin & Li 2006). In the early 1990s, it was hypothesised that oxygen tension of Bone Marrow (BM) is lower than other tissues (Dello Sbarba et al. 1987; Cipolleschi et al. 1993). This hypothesis was based on the observation that quiescent HSCs physically reside away from blood vessels and that several cells (e.g. stromal cells and progenitor cells) were localised to the closest blood vessel (Figure 1.6). Animal studies showed that oxygen tension in BM could be as low as 1% O_2 (Chow et al. 2001). These observations have led to widely accepted notion that gradients of oxygen from ~ 1 to 6% O_2 is experienced by sinusoidal cavity exist within the human BM (Eliasson & Jönsson 2010). Supporting this concept, different studies have shown that slow-cycling HSCs localise in the low oxygen areas of the BM, away from the vasculature, whereas fast-cycling early hematopoietic progenitors with limited capacity for self-renewal reside in areas much closer to blood vessels (Kubota et al. 2008).

MSCs are present in perivascular niches in proximity to the vasculature in almost all tissues (Miura et al. 2003; Shi & Gronthos 2003; Crisan et al. 2008; Zannettino et al. 2008). Despite their adjacency to blood vessels, the different tissues where MSCs reside exhibit low oxygen tensions (Harrison et al. 2002; Matsumoto et al. 2005; Pasarica et al. 2009). It is suggested that hypoxic microenvironment may be critical to maintaining the undifferentiated state of MSCs. Several studies have supported this, for example, the differentiation capacities of BM-derived MSCs were decreased under low oxygen tensions compared to normoxic (D'Ippolito et al. 2006; Fehrer et

al. 2007). MSCs from different sources (e.g. adipose tissue) showed similar behaviours when cultured under low oxygen conditions, confirming the role of the hypoxic condition in maintaining the undifferentiated state of these cells (Malladi et al. 2006).

Mouse brain exhibited a considerably low oxygen level; it ranges from 0.55% O_2 in the mesencephalon to 8%O_2 at the surface of the brain (Erecińska & Silver 2001). The oxygen tension in the human brain is also low (3% - 4% O_2) as measured by partial pressure catheter electrodes (Dings et al. 1998). Given this, it is conceivable that NSCs are also located in a low oxygen microenvironment. Neurogenic niches in the brain have the ability to support the undifferentiated state of NSCs. This is supported by close contact of type B1 astrocytes with the cerebrospinal fluid and blood vessels (Doetsch et al. 1999; Mirzadeh et al. 2008; Shen et al. 2008). This is also supported by other neurogenic niches elements such as intercellular signals, soluble factors, and the ECM proteins (Alvarez-Buylla & Garcia-Verdugo 2002). Oxygen tension may be an additional critical element of NSCs niche. The main neurogenic niche in the adult mammalian brain is the subventricular zone (SVZ), where NSCs reside (Alvarez-Buylla and Garcia-Verdugo, 2002; Lim et al. 2007). NSCs can respond to hypoxic/ischemic injury in other regions of the brain (Miles & Kernie 2008; Jin-qiao et al. 2009). When NSCs transplanted into hypoxic areas of the brain, they promoted neuronal survival through HIF-1A mediated secretion of VEGF (Roitbak et al. 2008; Harms et al. 2010). Several *in vitro* studies supported this notion, for instance, hypoxic conditions have promoted survival, the proliferation of NSCs, multi-potentiality and maintained the undifferentiated state of NSCs and Neural Crest Stem Cells (NCSCs) (Morrison et al. 2000; Chen et al. 2007; Santilli et al. 2010).

It was found that residing in these hypoxic niches is beneficial for ASCs population, as it maintains slow-cycling proliferation rates while avoiding the deleterious effects of O_2 on proteins and DNA, through the production of reactive oxygen species (ROS), that is usually associated with more well-oxygenated tissues (Cipolleschi et al. 1993; Busuttil et al. 2003; Eliasson & Jönsson 2010). HIF-1A has emerged as a significant mediator for this regulatory mechanism, as several studies have shown that HIF-1A promotes cell-cycle arrest in several cell lines (Koshiji et al. 2004).

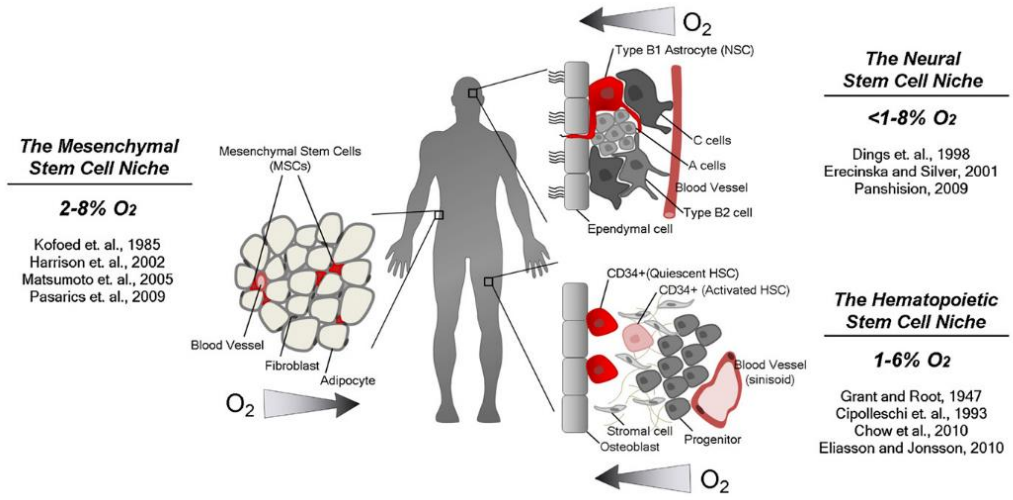

Figure 1.6 Schematic models of low oxygen tension measurements in various stem cell niches and their relationship with the local vasculature network.
Oxygen levels were measured in the BM, adipose tissue, and the SVZ, where HSCs, MSCs, and NSCs reside, respectively. (Mohyeldin et al. 2010).

1.4 HYPOXIA AND HIFs

Physiological oxygen tensions are significantly lower than atmospheric oxygen tensions (20% O_2), as a result of the dramatic decrease in blood oxygen content as it travels from the respiratory system throughout the body following inhalation (Table 1-1). Hypoxia can be defined as a reduction in the ambient O_2 concentration. In mammals, HIF-A is the master regulator for any hypoxic response (Semenza 1999; Ke & Costa 2006; Chuang et al. 2011). When activated during hypoxia, it switches on a vast array of hypoxia-induced cell signalling pathways resulting in promotion or inhibition of several genes expression. Particularly when HIF is up-regulated, it induces the expression of Hypoxia Responsive Genes (HRGs) such as VEGF, Glucose transporter 1 (GLUT1), Lactate dehydrogenase A (LDHA) and Erythropoietin (EPO) (van Tuyl et al. 2005; Fryer & Simon 2006; Provot et al. 2007; Chen et al. 2009; Dunwoodie 2009; Patterson & Zhang 2010; Heinis et al. 2010) which in turn coordinate many biological processes such as cell differentiation (Mohyeldin et al. 2010), metabolism (Takubo et al. 2013) angiogenesis and erythropoiesis (Rey & Semenza 2010) and tumorigenesis (Ratcliffe 2013).

Table 1-1 Contextual oxygen and terminology expressed in percentage of oxygen

	Percentage (%)	**Scientific Term**	**Common Term**
Air	20%	Atmospheric	Normoxic (Hyperoxic)
Organ			
Trachea	19.7 %		
Alveoli	14.5 %		Mild hypoxia
Arterial blood	13.2 %		
Brain	4.45 %	Physiologic	Hypoxia
Muscle	3.85 %		
Bone Marrow	6.45 %		
Placenta	1.5 – 8%		

1.4.1 Hypoxia Signalling Pathway

HIFs are heterodimeric transcription factors consisting of two subunits; HIF-A (HIF-A1, HIF-2A or HIF-3A) and an HIF-β (ARNT [HIF-1β], ARNT2 [HIF-2β] (Tian et al. 1998; Gu et al. 1998; O'Rourke et al. 1999). These subunits interact via two Per-Arnt-Sim (PAS) domains, bind DNA via N-terminal basic helix-loop-helix (bHLH)

domains, and activate transcription with C-terminal transcriptional transactivation domains (TADs). In mammals, HIF-β is constitutively expressed, but the expression and activity of HIF-A is highly dependent on the cellular oxygen concentration.

Under normoxic conditions (Figure 1.7), HIF-1A and HIF-2A (HIF-1A/2A) are hydroxylated at two conserved Proline residues by specific Prolyl Hydroxylases (PHDs) that are located within the Oxygen-dependent Degradation Domain (ODD) in a reaction requiring oxygen. HIF-1A/2A hydroxylation enables the binding of von Hippel-Lindau protein (pVHL) to the HIF-1A/2A ODD (Jaakkola et al. 2001). PVHL forms the substrate recognition module of an E3 ubiquitin ligase complex, which targets HIF-1A/2A poly-ubiquitylation and proteasomal degradation (Ohh et al. 2000). Additionally, Factor Inhibiting HIF-1 (FIH-1) inhibits HIF-1A by hydroxylating an asparagine residue in the TAD-C of human HIF-1A, blocking interaction with the transcriptional co-activator p300/CBP(Mahon et al. 2001). HIF-2A is also hydroxylated the corresponding Asn by FIH-1, but at a much lower efficiency than HIF-1A (Koivunen et al. 2004). As with the PHDs, Asn hydroxylation is repressed under hypoxic conditions, which promote the binding of the p300/CBP complex to HIF-1A/2A, thus allowing HIF activation. Under hypoxic conditions (Figure 1.7), the activity of PHD is inhibited, pVHL binding is reduced, and HIF-1A/2A are stabilised. HIF-1A/2A translocate into the nucleus, where they dimerise with HIF-1β and bind to Hypoxia Responsive Element (HRE), to up-regulate a variety of HRGs (Maxwell et al. 2001).

Different HIF regulatory pathways, other than pVHL, have been identified. These pathways can be independent to oxygen availability also they can be HIF-1A isoform-selective or affect both HIF-1A/2A. Examples on oxygen independent pathways are the receptor of activated protein kinase C (RACK1), and human double minute 2 (Hdm2), which degrade HIF-1A by binding into heat shock protein 90 (Hsp90) and p53, respectively (Ravi et al. 2000; Liu & Semenza 2007). Other regulatory pathways that degrade HIF-1A are selective; Hypoxia-Associated Factor (HAF), which degrades HIF-1A by ubiquitylation, however, it promotes HIF-2A activation under sustained hypoxia. Additionally, Hsp70/CHIP complex, which degrades HIF-1A under prolonged hypoxia or high glucose conditions (Koh et al. 2008; Luo et al. 2010).

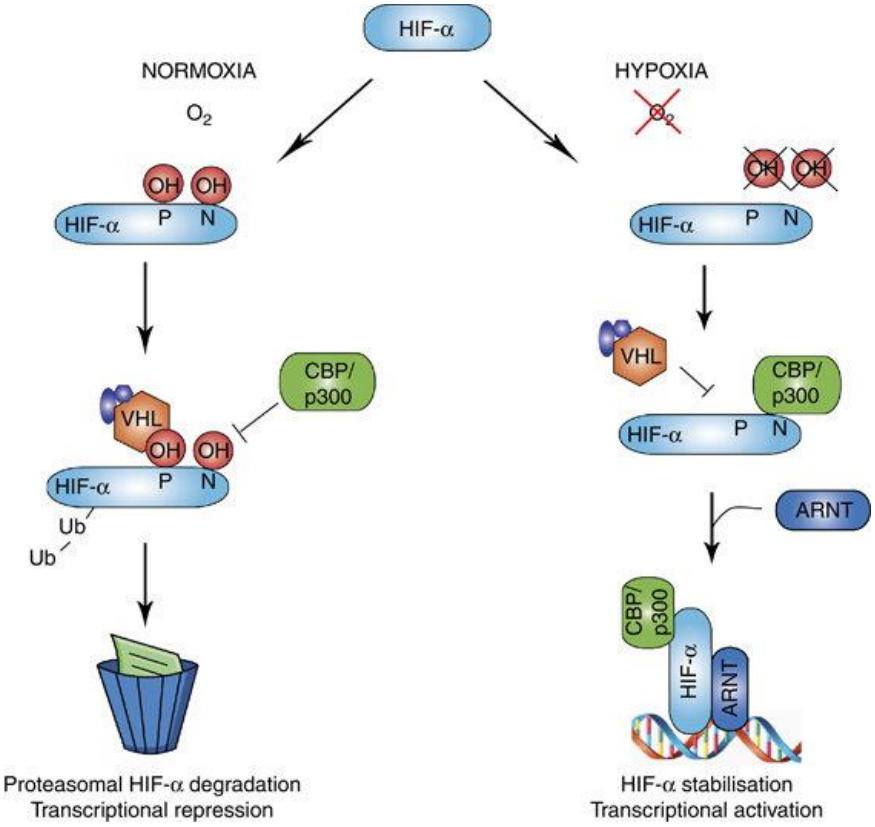

Figure 1.7 Regulation of hypoxia-inducible factor HIF-1A/2A by physiological oxygen tension (Hypoxia) and atmospheric oxygen tension (Normoxia).
Under normoxia level, HIF-A is hydroxylated by prolyl hydroxylase domain (PHD), which increases the recognition, binding and ubiquitylation by Von Hippel-Lindau (VHL) tumour suppressor protein. Consequently, this complex is targeted for proteasomal degradation. Under Hypoxia, HIF-A is stabilised and translocate to the nucleus to bind with HIF-1β (ARNT), this heterodimer initiates the transcription of HRGs that are essential for many bioprocesses in the body (Maes et al. 2012).

1.4.2 Different Temporal and Functional Roles of HIF-1A versus HIF-2A

HIF-1A was first discovered in studies of hypoxia-induced erythropoiesis (Semenza et al. 1991), since that time, HIF-1A has been identified as a universal regulator in response to hypoxia (Wang et al. 1995). HIF-2A was initially described as a transcription factor that is selectively expressed in endothelial cells; therefore it was considered to have a more limited role than HIF-1A (Tian et al. 1997). However, HIF-2A was also found to be expressed in distinct cell populations of different organs such as the liver, kidney, and brain, indicating its widespread function (Wiesener et al. 2003). Other studies have shown that both HIF-1A and HIF-2A participate in hypoxia-dependent gene regulation through complex and sometimes antagonistic interactions, such as that observed in renal cell carcinoma (Raval et al. 2005). Despite the large degree of overlap in binding sites of HIF-1A and HIF-2A, there were intriguing differences in regulatory regions of target genes with HIF-2A contributed very little to the overall HIF response (Mole et al. 2009). Emerging studies have demonstrated that HIF-1A and HIF-2*A* regulate different target genes that are involved in various biological functions. For example, endothelial cell proliferation, migration and vessel sprouting are mainly governed by HIF-1A, while vascular morphogenesis, integrity and assembly are regulated by HIF-2A (Fraisl et al. 2009). Moreover, HIF-1A selectively up-regulates genes encoding glycolytic enzymes (e.g. LDHA), genes that are involved in pH regulation (e.g. CA-IX) and genes that induce apoptosis (e.g. BNIP3L). In contrast, HIF-2A induces genes that are involved in invasion (e.g. MMP), and that regulate pluripotency (e.g. OCT4) (Keith et al. 2012). Interestingly, it was found that both HIF-1A and HIF-2A could each substitute for the other's isoform-specific functions. For example, HIF-2A has been shown to regulate glycolytic enzymes, in the absence of HIF1A. Also, HIF-1A activates MMPs when HIF-2A was deleted (Warnecke et al. 2004). HIF-1A and HIF-2A have some common target genes, including VEGF and GLUT1 (Keith et al. 2012).

HIF-1A and HIF-2A also contribute to distinct temporal responses to hypoxia (Figure 1.8). For example, HIF-A1 adapts the initial response to hypoxia, while HIF-A2 involves in long-term response to hypoxia (Forristal et al. 2010; Hawkins et al.

2013). The temporal regulation of HIF-1A and HIF-2A is primarily mediated by two oxygen-dependent hydroxylation events (PHDs and FIH) that regulate HIF-1A and HIF-2A stability and activity. Additionally, PHDs differentially regulate HIF-1A and HIF-2A; in which PHD2 influences the activity of HIF-1A while PHD3 has more influence on HIF-2A (Appelhoff et al. 2004). Also, HIF-A2 is hydroxylated at a much lower efficiency than HIF-1A by both hydroxylation events, which causes HIF-2A stabilisation at higher oxygen levels but not HIF-1A (Koivunen et al. 2004). In addition to post-translational mechanisms of HIF-1A, the mRNA stability of HIF-1A is repressed during sustained hypoxia (chronic response), due to negative feedback regulation of HIF-1A antisense RNA (aHIF-1A) (Uchida et al. 2004).

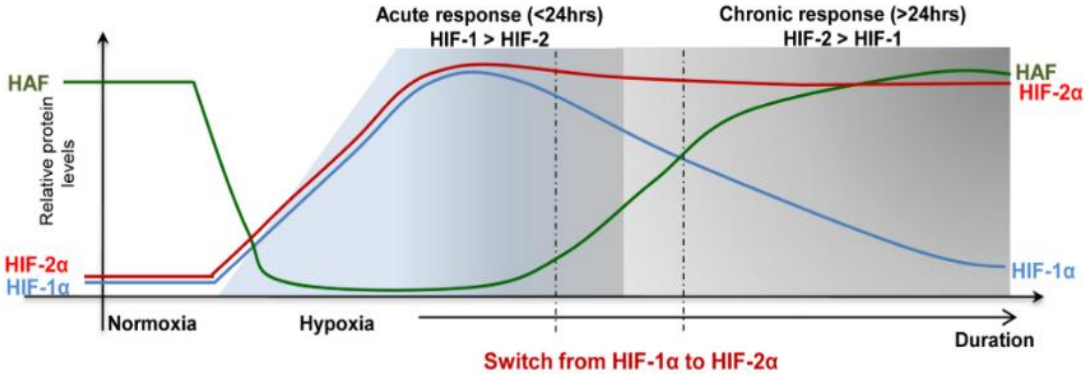

Figure 1.8 The interplay of HIF-1A and HIF-2A regulation during hypoxia responses. The temporal regulation of HIF-1A (blue line), HIF-2A (green line) and HAF (red line) in response to prolonged hypoxic exposure. Hypoxia-Associated Factor (HAF) degrades HIF-1A by ubiquitylation and promotes HIF-2A activation under prolonged hypoxia. The window in which HIF-1A switch to HIF-2A is indicated by broken vertical lines (Koh & Powis 2012).

1.5 METABOLIC PROPERTIES OF STEM CELLS

In contrary to differentiated cells, hESCs rely on a greater extent on glycolysis than on Oxidative Phosphorylation (OXPHOS) to generate adenosine-59-triphosphate (ATP) to meet their energy needs (Zhang et al. 2011; Zhou et al. 2012) (Figure 1.9). This consistency with immature morphology of mitochondria (e.g. few defined cristae and limited oxidative capacity) and their presence in less number in hESCs than in their differentiated progenies (Cho et al. 2006; Facucho-Oliveira et al. 2007).

A switch from OXPHOS to glycolysis is also observed during somatic cells reprogramming into iPSCs (Folmes et al. 2011; Shyh-Chang et al. 2013). One of the reprogramming factors that used to enhance reprogramming efficiency is LIN28A. This factor is highly expressed in both mESCs and hESCs, and it has a role in maintaining self-renewal capacity. Also, LIN28A binds to a large number of mRNAs encoding mitochondrial and glycolytic enzymes in hESCs (Balzer & Moss 2007; Viswanathan et al. 2008; Peng et al. 2011). In iPSCs, LIN28A was shown to block the production of mature let-7 microRNAs (miRNAs) through binding to let-7 pre-miRNA, which in turns regulates glycolysis by modulating the insulin–PI3K–mTOR signalling pathway (Zhu et al. 2011).

Owing to the hypoxic niches in which ASCs reside *in vivo*. Studies on mitochondrial respiration, glycolytic flux or proteomic profiles have revealed that ASCs rely primarily on anaerobic glycolysis, rather than mitochondrial OXPHOS (Unwin et al. 2006; Simsek et al. 2010; Miharada et al. 2011). For example, hMSCs express higher levels of glycolytic enzymes and lower levels of OXPHOS proteins, which indicates their reliance on glycolysis for their energy supply (Chen et al. 2008). In addition, when MSCs cultured under the atmospheric condition they switch into OXPHOS; as a result, their stemness function is attenuated due to increased senescence (Pattappa et al. 2013). This suggests that hypoxia-induced glycolysis reduces the proliferative rate of MSCs to prevent oxidative stress-induced senescence and to maintain long-term self-renewal property *in vitro*. Furthermore, self-renewing HSCs limit mitochondrial respiration to maintain cell cycle quiescence under hypoxic conditions (Warr & Passegué 2013; Takubo et al. 2013). In contrast to OXPHOS, glycolysis can proceed anaerobically, which raises the possibility that the

dependency of hPSCs and ASCs on glycolysis is an adaptation to the low oxygen conditions that are experienced *in vivo*.

HIF-A is a master regulator of cellular energy metabolism. HIF-1A$^{-/-}$ knockout-HSCs exhibited reduced glycolytic rates and increased mitochondrial metabolism, which caused HSC exhaustion. This indicates that HIF-1A has a critical role in maintaining HSCs function. Additionally, HIF-1A promotes the expression of Pyruvate Dehydrogenase Kinase 2 (PDK2) and PDK4, which together inhibit pyruvate from entering the Krebs cycle, therefore, blocking mitochondrial OXPHOS (Ito & Suda 2014).

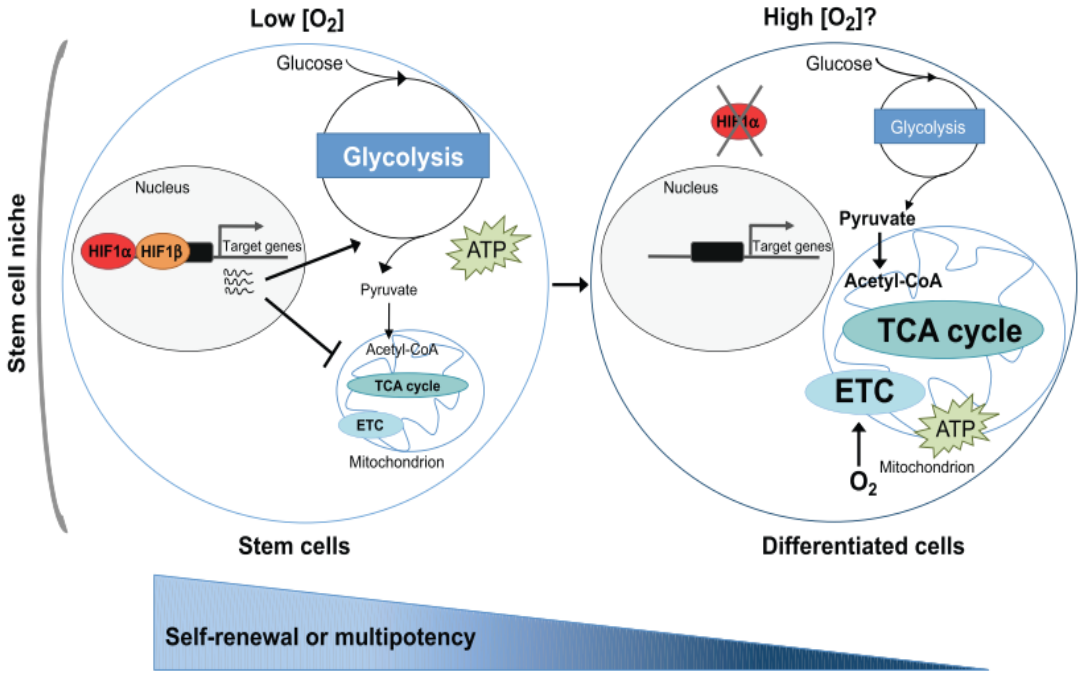

Figure 1.9 Energy sources in stem cells and differentiated cells.
Under low oxygen tension, HIF-1A is stabilised and dimerise with HIF-1B. The HIF1 heterodimer binds to HREs to transactivate target genes involved in glucose metabolism and transport. HIF-1A has a significant role in the regulation of stem cells metabolism, as it can induce stem cells to shift towards anaerobic glycolysis. In contrast, differentiated cells generate ATP through mitochondrial OXPHOS, which requires oxygen. Abbreviations; ETC, Electron Transport Chain; TCA, Tricarboxylic Acid. Image from (Rafalski et al. 2012).

1.6 HUMAN PLURIPOTENT STEM CELLS CULTURE

1.6.1 In Vitro Growth and Maintenance of Human Pluripotent Stem Cells (hPSCs)

The unlimited self-renewal capacity of hPSCs (including hESCs and hiPSCs) is a fundamental hallmark of successful *in vitro* culture. Since the discovery of the first hESCs line, MEF feeder layers have been used to support the undifferentiated phenotype of hPSCs (Pera et al. 2000; Reubinoff et al. 2000). Feeder cells generate specific cytokines, adhesion molecules and ECM to support the growth and survival of hPSCs (Saxena et al. 2008). However, these animal-derived cells pose a high possibility of transferring unknown viruses and zoonotic pathogens into the culture system (Martin et al. 2005). Therefore, different approaches have been established to move away from animal source feeder cells. For example, human fibroblast feeder cells derived from fallopian tube epithelium (Bongso et al. 1994), fetal foreskin (Amit et al. 2003), muscle (Richards et al. 2002) and bone marrow (Cheng et al. 2003). Although these feeder cells support the growth of hPSCs, they suffer from the drawbacks of being not immortal; which necessitate the derivation of new feeder cells, the thing that causes variability in culture systems.

In recent years, scientists have established more standardised and better-defined culture conditions to replace the feeder-dependant system, for large-scale and safe production of hPSCs for future clinical applications. Human PSCs depend on cooperation between different signalling pathways that are related to basic-Fibroblast Growth Factor (b-FGF), inhibition of Bone Morphogenetic Protein (BMP) signalling via Noggin, Activin/Nodal, and TGF-β pathways, leading to the activation of SMAD2/3. These exogenous growth factors have been added in high concentrations to maintain self-renewal of hPSCs in serum-free and xeno-free culture system (Pera & Trounson 2004; Beattie et al. 2005; Vallier et al. 2005; Wang et al. 2005; Armstrong et al. 2006; Singh et al. 2012). Feeder- and serum-free culture systems using medium that contains only human-sourced recombinant proteins have been developed to propagate hPSCs, and are commercially available, such as E8 (Ludwig et al. 2006), TeSR1 (Chen et al. 2011) and KORS supplemented with Activin A and

FGF-2 (Xiao et al., 2006). However, these conditions may not be optimal for a wide range of hPSCs lines (Rajala et al., 2007; Van Hoof et al. 2008; Ding et al. 2015). Therefore, even though feeder-free and serum-free defined conditions for maintenance of hPSCs have been developed, further investigations are needed to determine the factors responsible for maintenance of the pluripotent phenotype and stability of hPSCs lines in general.

1.6.2 Characterization of hPSCs

Human PSCs grow in tightly packed colonies and maintain defined borders at the periphery. High nucleus to cytoplasm (N/C) ratio and prominent nucleoli are typical features of individual cells (Wakui et al. 2017). Self-renewal capacity is regulated by an intrinsic regulatory network of core transcription factors, including OCT4, NANOG and SOX2 (Chambers & Tomlinson 2009). Additionally, hPSCs can be also characterized by the expression of cell surface markers including Stage-Specific Embryonic Antigen-4 (SSEA-4), SSEA-3, Keratan sulfate– Related Antigens (TRA-1-60 and TRA-1-81), and the absence of early differentiation marker, such as SSEA-1 (Carpenter et al. 2003; Chambers et al. 2003; Heins et al. 2004; Jonathan S. Draper et al. 2004). Analysis of self-renewal properties of hPSCs are also evaluated by measuring telomere length and telomerase activity after prolonged culture *in vitro* (Brandenberger et al. 2004; Carpenter et al. 2004). Several reports studying long-term stability of several hPSCs lines have shown that the expression of pluripotency markers is maintained following prolonged cultivation *in vitro*. This has been demonstrated in cell lines grown on feeder-dependant culture systems, on Matrigel with conditioned media, andon feeder- and serum-free culture containing a combination of growth factors including TGF-β1, b-FGF and Leukemia Inhibitory Factor (LIF) (Amit et al. 2000; Richards et al. 2002; Amit et al. 2004; Rosler et al. 2004). These indicate that hPSCs retain ‘stemness’ characteristic over long-term culture periods in different conditions. However, cells can acquire karyotypic abnormalities during prolonged culture period, which may be correlated to tumorigenic events that occur *in vivo* (Draper et al. 2002; Jonathan S Draper et al. 2004; Baker et al. 2007). Chromosomal aberrations are thought to be a result of abnormal cell growth and division that is gradually predominate and eventually take over the entire diploid culture (Baker et al. 2007).

1.6.3 In Vitro Differentiation of hPSCs

Human PSCs can be differentiated into derivatives from all three germ layers (Thomson et al. 1998), raising promising prospects for the development of new therapeutic strategies. Many of the diseases are originated from the absence of one or more critical cells populations that the body couldn't regenerate. For example, heart failure, stroke, spinal injury, haematological disorders, diabetes, neurodegenerative disorders, and kidney failure. Having the ability to produce clinically relevant cells population set the stage for tissue regeneration. Although hPSCs exhibit this capacity, the challenge remains, as the same plasticity that permits hPSCs to generate various cell types also makes them difficult to control.

In vivo, the capacity of hPSCs to differentiate into all cell types was observed through teratoma formation (Prokhorova et al. 2009) and chimaera (Bradley et al. 1984). *In vitro*, three basic approaches, that demonstrate hPSCs multipotency, have been developed to induce the differentiation of hPSCs: (1) the formation of EBs, (2) the culture of hPSCs as monolayers on ECM proteins, and (3) the direct culture of hPSCs on supportive stromal layers (Murry & Keller 2008) (Itskovitz-Eldor et al. 2000; Buta et al. 2013).

Manipulation of the BMP, Wnt, and Nodal pathways in hPSCs cultures reveals that they are involved in the regulation of three germ layers formation *in vitro* (Murry & Keller 2008). Differentiation protocols rely on the addition of specific inducers to direct differentiation and the development of reporter hPSCs to monitor and access early differentiation stages (Wiles and Johansson, 1999; Fehling et al., 2003; Kubo et al., 2004; Ng et al., 2005; Tada et al., 2005; Yasunaga et al., 2005; Gadue et al., 2006). It is also acknowledged, however, that certain hPSC lines have different differentiation tendencies towards specific lineages (Osafune et al. 2008).

Generally, monolayer differentiation culture (2D) favour the spontaneous differentiation of hPSCs. Nonetheless, differentiation can be directed to specific lineages by controlling the composition and organisation of growth factors, ECM proteins and attachment substrates (Guilak et al. 2009). Both hESCs and hiPSCs can be differentiated using the same *in vitro* protocols; however, iPSCs demonstrate

higher variability due to the nature of somatic cells and the approach used for generating these iPSCs (Batalov & Feinberg 2015). Human PSCs have been directed to differentiate into ectodermal, mesodermal, and endodermal lineages, including mature neurons and glial cells (Trounson 2002) Osteocytes (Duplomb et al. 2006) Cardiomyocytes (Laflamme et al. 2007) and Hepatocytes (Mater et al. 2016). The advantage of using monolayer culture is that it allows for uniform treatment for differentiating cells (Ishii et al. 2008). As such, 2D culture has been improved by using synthetic substrates and step-wise strategies for controlled differentiation of hPSCs (Batalov & Feinberg 2015) (Laflamme et al. 2007). For example, the efficiency of hESCs differentiation into Cardiomyocytes was increased about 30% when using monolayer culture with MEF conditioned medium, followed by treatment of Activin A and BMP4 (Laflamme et al. 2007). Also, step-wise 2D protocols have been applied to differentiate hPSCs into hepatic progenitors (Mater et al. 2016).

Despite the great results achieved using the 2D system, it often results in heterogeneous populations of differentiated cells (Pineda et al. 2013). Therefore, several attempts have been made to perform 3D culture (e.g. EBs) methods to better mimic native microenvironments *in vivo* (Itskovitz-Eldor et al. 2000; Buta et al. 2013). This approach allows 3D interactions with cells and the ECM in the absence of additional exogenous substrates (Baraniak & McDevitt 2012). Different cell types were generated from hPSCs using this system such as Cardiomyocytes (Burridge et al. 2007) and HSCs (Hong et al. 2010). Differentiation of hPSCs using 3D approach into endothelial cell tube (Kachamakova-Trojanowska et al. 2016) and functional bile ductal differentiation (Tian et al. 2016) were improved. These EBs contain different cell types including highly proliferative, non- proliferative, and apoptotic cells in the centre of the EBs, due to limited diffusion of oxygen and nutrients (Edmondson et al. 2014). This inherent heterogeneity, however, complicates the reproducibility of directed differentiation and high-throughput screening techniques of EBs (Hong et al. 2010). Additionally, this system often results in agglomeration of cells, leading to necrotic centres due to limit the diffusion of nutrients and oxygen into EBs and the waste out (Edmondson et al. 2014).

1.7 HYPOXIA IN VITRO

1.7.1 Effect of Hypoxia on Stem Cells Growth and Self-Renewal

Knowing that hypoxic conditions are the physiological norms for various stem cells niches, more research has considered hypoxia into cell culture protocols (Table 1-2). Several studies have demonstrated a significant benefit of using hypoxia in maintaining the undifferentiated state of hPSCs (Ivanović et al. 2000; Studer et al. 2000; Simon & Keith 2008). Studies showed that hPSCs appear to grow more efficiently under hypoxic conditions when compared to normoxia. For instance, bovine blastocysts demonstrate significantly more ICM when maintained under hypoxia (Harvey et al. 2004), similar benefits observed in hESCs (Catt & Henman 2000; Ma et al. 2009). Additionally, hypoxia contributes to the maintenance of hPSCs in an undifferentiated state, increase the proliferation rate, reduce chromosomal aberrations and enhance the cell recovery (Millman et al. 2009; Ji et al. 2009; Serra et al. 2010; Forristal et al. 2010; Sato et al. 2014; Correia et al. 2014). The proliferation rate and the expression of OCT4, SOX2 and NANOG, were increased when PSCs cultivated under hypoxia condition (Forsyth et al. 2006; Gibbons et aI. 2006). A study showed that culturing hESCs in hypoxia has prevented hESCs spontaneous differentiation, based on the expression of OCT4 and SSEA-4 (Ezashi et al. 2005). Further support of the benefits of hypoxic culturing arises from research on ASCs. For instance, culturing BM-MSCs under hypoxia condition resulted in a 30-fold increase in cells expansion when compared to normoxic conditions (Grayson et al. 2007).

1.7.2 Hypoxia as a Stimulus for Stem Cells Differentiation

As hypoxia has a beneficial role in maintaining an undifferentiated hPSCs, other studies also showed the role of hypoxia in inducing the differentiation toward different lineages (Table 1-2). For instance, the generation of hESCs-derived vascular lineage cells was achieved more efficiently when cultured under the hypoxic condition without the addition of any exogenous factor (Shin et al. 2011). Furthermore, the production of clinically relevant numbers of Cardiomyocytes has

been reported through combining hypoxia microenvironment and bioreactor system (Correia et al. 2014). Moreover, the same number of cells was maintained in hypoxic and normoxic conditions to examine their ability to form EBs, a higher number of EBs were formed from those maintained under hypoxic conditions and were able to attach to the substratum and developed outgrowths more efficiently than normoxic EBs (Ezashi et al. 2005). Similarly, various progenitors' cells have been derived from hPSCs such as endothelial (Ramírez-Bergeron et al. 2004), Chondrogenic (Koay & Athanasiou 2008) and Retinal Progenitor Cells (RPCs) (Bae et al. 2012; Garita-Hernández et al. 2013). A comparative study concluded that more RPCs were co-expressing PAX6 and CHX10, key early retinal markers, in hypoxia compared to normoxia culture (Bae et al. 2012). These data highlight the significance of considering hypoxia in the routine culture of hPSCs, as one of the highly specialised stem cells niche cues, also indicating that the hPSCs retain a 'memory' of their previous microenvironment. Although there are many studies exploring the role of hypoxia on hPSCs behaviour *in vitro* using microfluidic devices or chambers to permit single oxygen level (Oppegard et al. 2009; Polinkovsky et al. 2009; Chen et al. 2011), defining different and stage-specific hypoxic level on a tentative manner during an expansion and/or differentiation protocol is still requisite. Taken together these studies have revealed that mimicking *in vivo* oxygen tensions can be used to enhance the undifferentiated state and to direct the differentiation of both hPSCs and ASCs.

Table 1-2 Effect of hypoxic condition on the proliferation and differentiation properties of stem cells

Cell Type	Cell line	Oxygen Tension (%O_2)	Cultivation Conditions	Expansion (compared to 20% O_2)	Differentiation (compared to 20% O_2)	Reference
ESCs	WA15 & WA16	5%	Monolayer on Matrigel / a combination of collagen IV, laminin, and Vitronectin	Highest proliferation rate at 5%		(Ludwig et al. 2006)
	H1, RH1, and H9	2%	Monolayer on Matrigel	Reduced heterogeneity in transcriptome at 2%; no change in expression of OCT4, NANOG, and SOX2		(Forsyth et al. 2008)
	H1 & H9	4%	Monolayer on MEFs or Matrigel	No change in expression of OCT4, NANOG and SOX2 increased expression of LEFTY2		(Westfall et al. 2008)
	CLS1 & CLS2	1%, 5% and 10%, 15%	A monolayer of γ - irradiated HFF	No change in OCT4 expression, some increase in NANOG and NOTCH1 expression at 5% in culture for 4 weeks, but after 18 weeks no difference observed compared with 20 %, reduced proliferation rates at 5%		(Prasad et al. 2009)
	H1	1%, 3%, 5%	Monolayer on MEFs or Matrigel and EBs	Reduction of differentiated areas around colonies, increase expression of SSEA-4 and OCT4; no change in proliferation rate at 3% and 5% and slight reduction at 1%; increased EBs formation at 1%		(Ezashi et al. 2005)
	H1, H9, and RH1	2%	Monolayer on Matrigel	No changes in SSEA-1, SSEA-4, TRA-1-60/TRA-1-81expression; increased clonal recovery; decreased chromosomal abnormalities		(Forsyth et al. 2006)

Cell Type	Cell line	Oxygen Tension ($\%O_2$)	Cultivation Conditions	Expansion (compared to 20% O_2)	Differentiation (compared to 20% O_2)	Reference
	H9	2%	Monolayer on Matrigel	Increased clonal recovery		(Hewitt et al. 2006)
	H9 & HES2	4%	3D complex bioreactor approach		Differentiation to Cardiomyocytes, cell number increased 30–47%, some cardiac markers increased	(Niebruegge et al. 2009)
	H9	2%	Cells were cultured in alginate beads		Differentiation to chondrocytes; collagen I and II,tensile modulus, and compressive properties increased	(Koay & Athanasiou 2008)
	H9, HS401 and HS360	4%		Hypoxia Enriches SSEA-3 +ve cells and reduces Levels of TRA-2-54		
	NTU1 & NTU3	5%	Monolayer culture on MEFs	No change in OCT4, NANOG and CRIPTO expression		(Chen et al. 2009).
	H9	3%	Feeder-free\ chemically defined conditions on laminin		High yields of Oligodendrocyte precursor cells expressing related markers (98% NG2, PDGF-RA and OLIG2)	(Stacpoole et al. 2013)
	MEL-2	5%		No change in the expression of pluripotency and differentiation markers No difference in proliferation Increased apoptosis under 5%		(Harvey et al. 2016)
	HSF6, Miz4 and H9	3% & 12%	Feeder-free on laminin \ EBs in suspension culture	Increased OCT4 & NANOG expressing and reduced BrdU incorporation at 12% EBs subjected to 3% exhibited well-differentiated microvilli on their surface, secreted high levels of collagen, and showed enhanced differentiation into primitive endoderm. Increased expression of FOXA2, SOX17, AFP, and GATA4		(Lim et al. 2011)

Cell Type	Cell line	Oxygen Tension (%O_2)	Cultivation Conditions	Expansion (compared to 20% O_2)	Differentiation (compared to 20% O_2)	Reference
ESCs& iPSCs	H1, H7 and OSLN6-iPSCs	2%	Monolayer culture on MEFs	hESC- or iPSC-derived differentiated cells reverted to a stem cell-like state as revealed by re-activation of an OCT4-promoter reporter increased expression of TRA1-60 and SSEA4		(Mathieu et al. 2013)
iPSCs		1% & 5%	Monolayer culture on MEFs	Increased the number of colonies with a positive alkaline phosphatase activity at 5% enhances reprogramming efficiency to iPSCs using only two factors (OCT4 & KLF4)		(Yoshida et al. 2009)
Stem cells derived from the infrapatellar fat pad (IPFP)		5%	Monolayer culture in basic medium		Increased matrix accumulation of proteoglycan during chondrogenesis; Increase HIF-2A	(Khan et al. 2007)
hMSCs		2%	3D constructs		Increase in expansion and prolonged maintenance hMSC expressed higher levels of Osteoblastic and Adipocytic differentiation markers	(Grayson et al. 2006)

Abbreviations. HFF, human foreskin fibroblasts; SSEA, stage-specific embryonic antigen; SSEA, stage-specific embryonic antigen; NG2, proteoglycan markers; PDGF-RA, platelet-derived growth factor receptor A; OLIG2, Oligodendrocyte transcription factor; OCT4, octamer-binding transcription factor 4; KLF4, Kruppel-like factor 4; FOXA2, forkhead box protein A2; Cripto, a member of the epidermal growth factor-Cripto-FRL-Criptic (EGF-CFC); LEFTY2, Left-right determination factor 2 is a protein; SOX2, SRY (sex determining region Y)-box 2; AFP, alpha-fetoprotein.

1.8 RESEARCH QUESTIONS

Although it is well established that (i) hypoxic conditions are the physiological norms for a variety of stem cells niches including hPSCs and ASCs, and that (ii) stem cells populations, as discussed here and elsewhere, self-renew under hypoxia while undergoing differentiation under relatively higher oxygen levels (still hypoxia), some questions remain to be addressed;

1- What is the optimum hypoxic level for maintaining the self-renewal capacity of hPSCs?
2- What is the optimum hypoxic level for inducing the *in vitro* differentiation of hPSCs into different lineages?
3- Is there an optimum hypoxic level to promote the differentiation of hPSCs into specific lineage?
4- How the cells sense and respond to small changes in oxygen tensions, for instance, do they respond similarly to 2% and 5% O_2? If not, how these small changes affect the hPSCs decisions; whether to self-renew, differentiate or undergo quiescent?

As an attempt to address these questions, we have explored the effect of a wide range of oxygen tensions (0%, 2%, 5%, 8%, and 12% O_2) on the behaviour of hPSCs, including the standard culture condition at 20% O_2 to be used as a control throughout this project.

1.9 HYPOTHESIS

We have two hypotheses in this project;

- That the pluripotency feature of hPSCs, including hESCs and hiPSCs, will be enhanced by lower oxygen conditions ≤5%O_2, while higher oxygen levels >5%O_2, favour the differentiation of hPSCs
- That distinct oxygen level modulates the formation of specific germ layer in hPSCs by up-regulating coordinated genes through HIF-mediated response.

2 CHAPTER 2: MATERIALS AND METHODS

All the methodological approaches used to culture all cell types will be described in this chapter. These include Mouse Embryonic Fibroblasts (MEFs), human embryonic stem cells (hESCs) and human induced pluripotent stem cells (hiPSCs). Then, all the techniques used to analyse these cells will be summarised.

Cell culture techniques were carried out in a Walker Class II Safety Cabinet (Manchester, UK). Laboratory coat and latex gloves were worn at all the times. Furthermore, all items introduced into the safety cabinet were wiped out with 70% Ethanol to avoid contamination. Additional care was taken not to pass objects over an open container.

Where Dulbecco's Phosphate Buffered Saline (DPBS) has been used, this corresponds to a 1x solution of DPBS containing no calcium or magnesium (Thermo Fischer Scientific Inc. USA). All solutions used for cell culture were first warmed in a 37°C water bath or incubator for at least 30 minutes before contact was made with cells.

Cells were routinely cultured under sterile conditions in a humidified incubator at 37°C, supplemented with 5% CO_2 (inCusaFe IR Sensor CO_2 incubator, Panasonic, Leicestershire, UK), and grown in either Nunc™ EasYFlask™ Cell Culture Flasks with filter caps or Thermo Scientific™ Nunc™ Cell-Culture Treated Multidishes (Thermo Fischer Scientific Inc. USA).

2.1 HUMAN PLURIPOTENT STEM CELL CULTURE

2.1.1 Isolation, Maintenance and Preparation of Mouse Embryonic Feeder Cells (MEFs)

2.1.1.1 Isolation of MEFs

MEFs were obtained from post coitus day 12.5–13.5 CD1 mice, following local animal welfare guidelines and regulations. Embryos were placed in a petri dish containing PBS supplemented with 50µg/ml penicillin and 50µg/ml streptomycin (pen/strep). Each embryo was separated from the embryonic sac and the placenta using sterile dissection tools. The brain and the dark organs were discarded, and the remaining tissues were collected in PBS containing pen/strep. Then, the tissues from around 10 to 15 embryos were pooled and incubated in 0.05 % (w/w) Trypsin-EDTA (Invitrogen, UK) at 37°C for 10 to 15 minutes. The solution was vortexed and re-suspended in 2ml MEF medium comprised of Dulbecco's Modified Eagle's Medium (DMEM) with Glutamax^{TM} (high glucose formula with no pyruvate), 10% (v/v) Fetal Bovine Serum (FBS), 1% (v/v) Non-Essential Amino Acid (NEAA) stock, and 0.1mM 2-mercaptoethanol (all from Thermo Fischer Scientific Inc. USA). The partially digested tissue was then subjected to centrifugation at 1200rpm for 3 minutes. The supernatant was discarded, and the pellet was re-suspended in 2ml MEF medium per embryo. The 2ml suspension was then transferred to a pre-coated T75 flask with 0.1% Gelatin (StemCell Technologies, UK), containing 8ml MEF medium and 1% (w/v) pen/strep solution. These flasks were incubated for 2 to 3 days until cells reached approximately 90% confluence. These ‘P0’ MEFs were then cryopreserved as described below.

2.1.1.2 Cryopreservation of MEFs

MEFs were Trypsinised (Sigma-Aldrich Company Ltd. UK) and collected as outlined above. The cell pellet was re-suspended at a ratio equivalent to a passage split ratio (1:3) in cryopreservation media (40% (v/v) MEF media,

50% (v/v) FBS (Gibco, Life Technologies), 10% (v/v) dimethyl sulphoxide (DMSO) (Sigma-Aldrich Company Ltd. UK), and the cell suspension was aliquoted into Cryogenic vials (Thermo Fischer Scientific Inc. USA). MEF stocks were frozen immediately overnight at a rate of -1°C/min by storage at -80°C in a Cryo 1°C Freezing Container, insulated with foam soaked in 100% isopropyl alcohol (Nalgene). After 24 hours storage in the containers, Cryogenic vials were transferred to liquid nitrogen for long-term maintenance.

2.1.1.3 Thawing of MEFs

A vial of the stock ‘P0' MEFs was taken from liquid nitrogen storage and immediately thawed at 37°C. MEFs were then transferred from the cryovial into a centrifuge tube containing 9ml of fresh MEF medium and gently re-suspended and centrifuged at 1200 rpm for 5 minutes; then the cell pellet was re-suspended in 2ml fresh MEF medium. Then, the 2ml MEF suspension was added to 8ml MEF medium in pre-gelatinised T75 flasks as described above. The cells were incubated until 80-90% confluent and then passaged as described below.

2.1.1.4 Expansion of MEFs

Confluent MEFs were washed with pre-warmed PBS before the addition of 0.25% (w/v) Trypsin/EDTA, and then incubated at 37°C until the cells detached. Quench trypsin by adding 5ml of MEF media and the cell suspension centrifuged at 1200 rpm for 5 minutes, the supernatant removed and the cell pellet was re-suspended in 3ml MEF medium. Subsequently, 1ml of the cell suspension was inoculated per T75 tissue culture flask, pre-coated with 0.1% Gelatin containing 9mL MEF medium. Split ratios were determined according to the confluence of cells observed microscopically. The cells were incubated until 80-90% confluent, and then subsequently cryopreserved to create a working cell bank for future use. All MEFs used in this project were within 6 passages (P6).

2.1.1.5 Preparation of MEFs as a feeder layer for hPSCs culture

The day before hPSCs passaging, MEFs were inactivated with highly toxic Mitomycin-C (Sigma-Aldrich). Briefly, MEF media was replaced with 7ml of Mitomycin C medium (0.01mg/ml of filtered Mitomycin C in MEF media) and incubated for 2 hours. Inactivated MEFs were then washed thoroughly with PBS three times and trypsinised as described above. After washing the cells, cell count was done using a haemocytometer, then, inactivated MEFs were plated at a density of 25,000 cells/cm2 in complete MEF media onto tissue culture surface pre-coated with 0.1% Gelatin.

2.1.2 Human PSCs Culture

At the beginning of this project, mitotically inactivated MEFs were used as a feeder layer for MSUH001-hiPSCs line, which was then adapted to a feeder-free culture system (Khalife & Mason 2015). From now on, all cell lines were cultured in the feeder-free system. The following section describes the steps involved in culturing human cell lines including thawing, passaging and banking.

2.1.2.1 Cryopreservation and cell banking of hPSCs lines.

Human PSCs were cultivated in T25 flasks until 80-90% confluent. Cells were then dissociated using EDTA and frozen in mFreSR™, a defined, serum-free cryopreservation medium (STEMCELL Technologies Ltd. UK). One ml was re-distributed per sterile cryovial (Nalgene, Nunc, New York, USA). Cells were frozen at a rate of -1°C/min by storage at -80°C in a Cryo 1°C Freezing Container, insulated with foam soaked in 100% isopropyl alcohol (Nalgene, Labware, New York, USA). After 24 hours storage in the containers, vials were transferred to liquid nitrogen for long-term maintenance as a master cell bank (MCB), or at -80°C freezer for a working cell bank (WCB).

2.1.2.2 Thawing hPSCs lines.

The cryopreserved hPSCs were thawed by placing in a 37°C water bath. Cells were transferred to a 15ml Falcon tube and re-suspended with 10ml of

fresh growth media. The cell suspension was centrifuged at 1200 rpm for 3 minutes. After discarding the supernatant, the cells were re-suspended in 5ml of fresh growth media and transferred to Vitronectin (VTN-N) Recombinant Human Protein (Thermo Fisher Scientific) coated flasks and placed in the incubator for routine culturing.

2.1.2.3 Maintenance of hPSCs lines

Human PSCs were cultured in Essential 8™ Basal Medium (Thermo Fischer Scientific Inc. USA) on serum and feeder-free culture condition. When hPSCs colonies cover approximately 85% of the surface area of the T25 flask, the cells are dissociated by 0.5mM EDTA in DPBS for 5 minutes. Then, EDTA was discarded, and the cells were washed with Essential 8™ Basal Medium and transferred into a VTN pre-coated T25 flask (coated for 1 hour), with a final coating concentration of 0.1–1.0 µg/cm2 on the culture surface. Media was changed daily.

2.1.2.4 Maintaining hPSCs under different oxygen Tensions

When cells were confluent, they were dissociated using TrypLE^{TM} Express for 5 minutes at 37^{o}C. Then, fresh Essential 8™ Basal Medium was added to quench the effect of TrypLE^{TM}, and the cell suspension was centrifuged at 1200 rpm for 5 minutes. Cells were plated at a density of 0.6 x 10^{6} cells/well of 6-well plate that was pre-coated with VTN for 1 hour at room temperature. Cell were then maintained under different oxygen tensions (0%, 2%, 5%, 8%, 12% and 20% O_2) and harvested on different time points (30 minutes, 2hrs, 8hrs, 24hrs, 48hrs, 72hrs) for downstream analysis (see Chapter 5).

2.1.3 Differentiation Of hPSCs lines

2.1.3.1 EBs Spontaneous Differentiation

To examine whether hPSCs can differentiate spontaneously into the three germ layers (endoderm, mesoderm and ectoderm), EBs were formed by force aggregation using AggreWell^{TM}800 plates (STEMCELL Technologies Ltd. UK)

in Spontaneous Differentiation (SP.D) medium containing DMEM/F12, 20% (v/v) Knockout Serum Replacement (KOSR), 1% NEAA, 0.1% 2-Mercaptoethanol (all from Gibco, Life Technologies) and 10μM ROCKi Y-27632 (STEMCELL Technologies Ltd. UK) was added to promote single cell survival. The cells were incubated with TrypLE™ Express (Gibco, Life Technologies) for 5 minutes at 37°C to form a single cell suspension. To form 3000 cells size EBs, $9.0X10^5$ cells were inoculated to each microwell of AggreWell™800 plates (D0). The EBs were harvested from AggreWell™800 plates after 24 hours by firmly pipetting medium in the well up and down two to three times with micro pipettors outfitted with 1 μl disposable tip to dislodge the EBs. Then, EBs were transferred to suspension culture in 30mm non-adherent bacterial grade culture dishes (Sterilin) containing 3mL of fresh medium for one day (D1). On D2, around 25–35 EBs were selected under the dissecting microscope by using micro pipettors outfitted with 1 μl disposable tip and plated in each well of a 6-well plate coated with Matrigel (Corning Incorporated, Life Sciences, Germany) and cultured for five days and the media was changed every two days. On D7 of EBs formation protocol, EBs were fixed or harvested for further downstream analysis.

2.1.3.2 Monolayer spontaneous differentiation of hPSCs under different oxygen Tensions

Human PSCs were routinely cultured on Essential 8™ Basal Medium. To initiate monolayer SP.D protocol, hPSCs were dissociated with TrypLE™ Express for 5 minutes at 37°C, put through a cell strainer (BD, NJ, USA) to ensure single cell suspension, and seeded at $0.8X10^5$ cells/well on a Matrigel pre-coated plates for 4 days in SP.D media supplemented with 10μM ROCKi Y-27632 under different oxygen tensions (0%, 2%, 5%, 8%, 12%, and 20% O_2). Cells were collected on D2, and D4 for downstream analysis and media was changed every two days.

2.1.3.3 Directed differentiation of hPSCs into early mesodermal lineage.

Human PSCs cultured in T25 flasks coated with VTN were grown to 80-90% confluence and treated with TrypLE™ to a single-cell state to initiate the

differentiation into mesoderm. Then, TrypLE™ was inactivated by the addition of a DMEM/F12 medium. After centrifugation at 1200 rpm for 5 minutes, cells were re-suspended with SP.D medium supplemented with 10µM ROCKi Y-27632 and plated at a seeding density of 0.5 x 10^5 cells/well of 6-well plate onto Matrigel pre-coated plates. Then, cells were incubated at 37°C for 24 hours. On D1, SP.D media were aspirated from the well and replaced with 3ml of pre-warmed STEMdiff™ Mesoderm Induction Medium (MIM) (STEMCELL Technologies Ltd. UK). Media was changed every other day and cells were harvested on D2 and D4 to be assayed for the formation of early mesoderm lineage.

2.2 ANALYTICAL METHODS

2.2.1 Cell Number

Cell number counts were analysed in triplicate before plate inoculation and growth kinetics experiments, using Beckman Coulter Vi-CELL® Cell Viability Analyser (Beckman Coulter, UK), according to manufacturer's instructions. This machine is a video imaging system that provides a fully automated means to perform the traditional Trypan Blue Dye Exclusion method.

2.2.2 Metabolites Analysis

2.2.2.1 Specific metabolite consumption and productions rates

The exhausted media was recovered from cell cultures; sampling was performed by gently shaking the well followed by carefully pipetting of 10-15µL of media for analysis. Samples can be centrifuged to remove dead cells and debris. Fresh medium was also assessed, and the results were used for the determination of glucose consumption and lactate production rates (GCR and LPR, respectively). Glucose and lactate concentrations in the media were measured every 24hrs using a handheld blood glucose analyser, the Accutrend® Plus system (Roche Diagnostics, USA) for immediate readings. These measurements were taken in triplicates and were used to calculate

GCR and LPR. These values were then used to assume the yield of lactose from glucose ($Y'_{Lactate/Glucose}$) as a result of glycolysis bioprocess. ViCell automated cell counter was used to determine total viable cells counts, which in combination with the glucose/lactate concentrations were used to calculate specific metabolic rates (q_{Met}. = mmol.hr-1.cell-1) using the equation:

$$qMet = \frac{\Delta Met}{\Delta t.\Delta Xv}$$

Where ∆Met (mmol/L) is the variation in metabolite concentration during the time period ∆t (hours) and ∆Xv (cells) the average of viable cells during the same time period.

2.2.2.2 Yield Calculations

The overall yield of lactate from glucose ($Y'_{Lactate/Glucose}$) was calculated as the ratio between lactate and glucose. This gives an estimation of glucose converted into lactate via glycolysis.

2.2.3 Counting cell migration/foci event

The numbers of events/foci were counted in a minimum of three images (under the 10X magnification) per experiment, performed for three independent experiments. The average number of events/foci plotted against undifferentiated cells cultured at the normoxic condition as a negative control (value=0). Images were taken using a digital fluorescence microscope EVOS FL Cell Imaging System (Life Technologies, Thermo Fischer Scientific Inc. USA).

2.2.4 Immunostaining

Cells were fixed with 4% (w/v) paraformaldehyde (PFA) for 20 min before being permeabilized with 0.25% (v/v) Triton X-100 in DPBS for 10 min at 37^{o}C (Sigma- Aldrich). Then, samples were washed twice with DPBS and incubated in blocking solution (2% (v/v) goat serum in X-100 in DPBS) (Sigma-Aldrich) for 20-40 minutes. No permeabilisation step was performed

for cell surface marker detection. Samples were incubated with primary antibodies diluted in blocking solution for 2hrs. The primary antibodies used are shown in **Table 2-1** The cells were washed twice with DPBS and incubated with Alexa Flour 488 goat anti-mouse, Alexa Flour 488 goat anti-rabbit IgM, Alexa Flour 555 goat anti-mouse (Invitrogen; 1:400) and Alexa Fluor 594 Donkey Anti-Goat IgG (Thermo Fischer Scientific Inc. USA) in blocking solution for 30 minutes in a dark room at room temperature. The cells were washed twice with DPBS and incubated with 4, 6-diamidino-2-phenylindole (DAPI; Invitrogen, 1:3,000) in DPBS for 5 minutes. Fluorescence images were taken using a digital fluorescence microscope EVOS FL Cell Imaging System (Life Technologies, Thermo Fischer Scientific Inc. USA).

2.2.4.1 Hypoxia-inducible factors-specific immunostaining protocol

For HIF protein analysis (HIF-1A and HIF-2A), cells were cultured on VTN-pre-coated glass-bottom dishes (FluoroDish Sterile Culture Dish, World Precision Instruments, WPI), for 30minutes, 2hrs and 8hrs under different O_2 tensions (0%, 2%, 5% 8%, 12% and 20% O_2). Due to the short half-life of HIF proteins after re-oxygenation (Chilov et al. 1999a), adherent cells were transferred immediately into ice followed by fixation with ice-cold 4% (w/v) PFA for 20minutes, washed three times with ice-cold DPBS, and permeabilized with ice-cold 0.5% Triton X-100 in DPBS for 5 minutes and rinsed again three times with ice-cold DPBS. After blocking nonspecific binding by adding ice-cold (2% (v/v) goat serum in X-100 in DPBS) (Sigma-Aldrich) for 20-40 minutes, cells were incubated with Mouse anti-hypoxia inducible factor-1alpha monoclonal antibody (Millipore) diluted in blocking solution overnight at 4^oC. Primary antibodies were detected by incubation with Alexa Flour 488 goat anti-mouse at dark at room temperature for 30 minutes. Following extensive washing in DPBS and counterstained with DAPI for 3 minutes. Fluorescence images were acquired at ×40 magnification using an Olympus FV1000 confocal microscope (Olympus America, Inc.) and analysed with FV10-ASW 4.2 confocal image acquisition software.

2.2.4.2 DMOG treatment to induce HIF1- as a positive control.

Its well-known that the half-life *of* HIF-1A protein is extremely short (<5min, after reoxygenation), which poses a technical difficulty to detect it *in vitro* by the mean of immunostaining It was decided to use dimethyloxalylglycine (DMOG), commonly used drug to stabilize of HIF-1A at normoxic condition (20%O_2) (Elks et al. 2011). DMOG was prepared following the manufacturer's instructions; hPSCs were cultured in 12-well plates in a low density, until 60-70% confluent. DMOG was added to the wells at different concentrations (0.5, 1, 1.5, 2 µM) each performed in triplicate) and the cells incubated for 24hrs at 37^{o}C under normoxic condition (Figure 2.1). Cells were then fixed and stained for HIF-1A as described previously. The optimal concentration was then established and can be used as positive control for HIF-1A staining/localisation pattern.

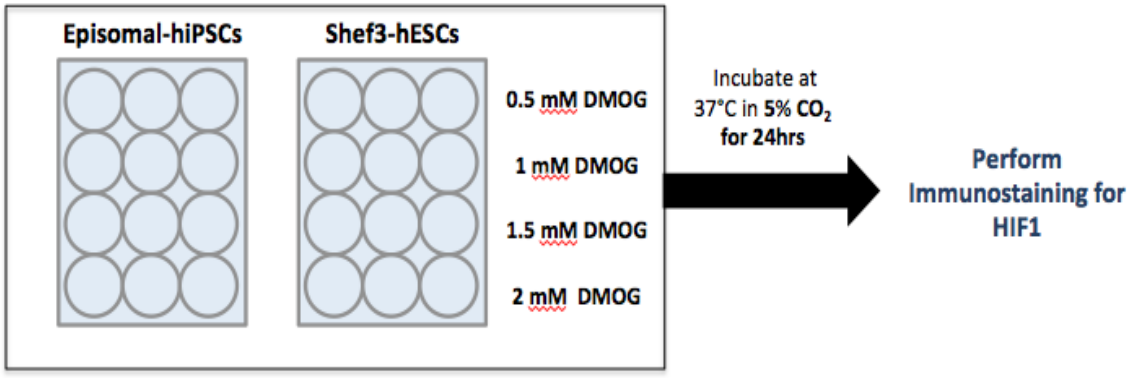

Figure 2.1 Schematic representation of the experimental design to establish and validate the staining and localisation pattern of HIF-1A using DMOG (PHD inhibitor).

Table 2-1 Primary antibodies that were used in Immunostaining

Primary Antibodies	**Catalogue Number**	**Dilution**
Monoclonal mouse anti-OCT4 IgM (Millipore)	MAB4419	1:200
Monoclonal mouse anti-TRA-1-60 IgM (Millipore)	MAB4360	1:200
Polyclonal rabbit anti-NESTIN (Millipore)	ABD69	1:300
Monoclonal mouse anti-PAX6 IgG (Millipore)	MAB5552	1:300
Monoclonal mouse anti-SEEA-4 IgG (Millipore)	MAB4303	1:200
Monoclonal mouse anti-TRA-1-81 IgM (Millipore)	MAB4381	1:200
Polyclonal rabbit anti-SOX17 (Thermo Fisher)	PA5-23352	1:200
Monoclonal mouse anti-BRACHYURY IgG (Thermo Fisher)	04-135	1:200
Mouse anti-hypoxia inducible factor-1alpha monoclonal antibody (Millipore)	MAB5382	1:200
Mouse Anti-Vimentin (Invitrogen)	MA5-11883	
Polyclonal rabbit Anti-FSP1/S100A4	07-2274	
Anti-ARNTL, clone 1C5 (HIF-β) (Millipore)	MABN673	1:200
Anti-Hypoxia Inducible Factor-2 alpha (Millipore)	MAB5382	1:200
Mouse Anti-HIF-2, Human Antibody	MAB3472	
Mouse Anti-FIH-1, Human Antibody	MABE102	
Secondary Antibodies	Catalogue Number	Dilution
Alexa Fluor® 488 Goat Anti-mouse IgG (Invitrogen)	A11001	1:300
Alexa Fluor® 555 Goat Anti-mouse IgG (Invitrogen)	A28180	1:300
Alexa Fluor® 555 Goat Anti-mouse IgM (Invitrogen)	A-21426	1:300
Alexa Fluor® 488 Goat Anti-rabbit IgG (Invitrogen)	A11008	1:300
Alexa Fluor® 555 Goat Anti-rabbit IgG (Invitrogen)	1252795	1:300
Alexa Fluor®594 Goat Anti-rabbit IgG (LifeTechnologies)	1745478	
Alexa Fluor® 488 Rabbit Anti-Goat IgG (Invitrogen)	A11078	1:300
Alexa Fluor® 555 Rabbit Anti-Goat IgG (Invitrogen)	A27017	1:300

2.2.5 Cell Proliferation Analysis

Cells were passaged at a confluence of 80%. Briefly, cultured cells were dissociated using TrypLE™, incubated for 5 minutes at 37 °C, harvested and washed using DPBS followed by at centrifugation at 1200 rpm for 5 minutes. Cell numbers were determined every 24hrs for three days as described previously. The growth kinetics was evaluated to determine the proliferation ability of hPSCs at different O_2 conditions. This was determined by population doubling time (PDT), the time required for a culture to double in number. The number of cells was determined at the beginning (24hrs) and the end of the culture (72hrs). PDT was calculated based on the formula

PDT= (TXLOG (2))/(LOG(NH)-LOG(NI))

Where T is the time is taken (in hours); (NH) is the total number of harvested cells and (NI) is the number of cells at the lag phase (24hrs).

2.2.6 Flow Cytometry

After removing media from the wells, adherent cells were washed twice with 2ml of ice-cold DPBS followed by incubating the cells with TrypLE™ for 5-10 minutes at 37^{o}C, depending on cell density, to obtain a single cell suspension. Fresh media was added to deactivate TrypLE™ action, and the cell suspension was transferred to 15-ml falcon tube filled with 10ml of DPBS. The cell suspension was centrifuged at 1200 rpm for 5 minutes. The supernatant was then removed, and the pellet was re-suspended in 5ml of ice-cold DPBS and put through a cell strainer (BD, NJ, USA) to ensure single- cell suspension, and centrifuged again at 1200 rpm for 5 minutes. The supernatant was removed, and the cells were fixed with BD Cytofix™ Fixation Buffer (BD Bioscience, San Diego, CA) for 20 minutes on ice. Cells were then washed with BD 1X Perm/Wash buffer twice (BD Bioscience, San Diego, CA) and incubated for permeabilisation with the same buffer for 10 minutes at room temperature followed by two washing steps with DPBS. Cells were re-suspended in 1ml of 1X BD Perm/Wash buffer and split into 250µl per

Eppendorf tubes (Eppendorf, Hamburg, Germany). Cells were stained with FITC, Mouse, anti-Human, Anti-Ki-67 for 30 minutes at 4°C, in the dark followed by two washing steps with DPBS and re-suspend in 1X BD Perm/Wash buffer for analysis. Flow Cytometry analysis was performed using BD Accuri™ C6 Plus Flow Cytometer (BD Bioscience, San Diego, CA). Debris and dead cells were excluded using forward, and side scatters parameters, and only a single cell population was selected using the pulse width parameter. Samples were incubated with the FITC Mouse IgG1, □ isotype control and gated as a negative population (BD Bioscience, San Diego, CA). The data were analysed with FlowJo® software (FlowJo, LLC, Tree Star Inc, Ashland, OR).

2.2.7 Gene Expression Analysis.

The relative gene expression was analysed by real-time quantitative polymerase chain reaction (RT-qPCR). Human PSCs pellets were harvested using TrypLE^{TM} dissociation at 37^{o}C and stored at -80 ºC until RNA is extracted.

2.2.7.1 RNA extraction.

Total RNA was extracted by using the Qiagen RNeasy kit (Qiagen, Crawley, UK). Cell pellets were placed on ice for thawing and re-suspended with RLT buffer provided in the kit. The cell lysate was put into a QIAshredder spin column and centrifuged for 2 minutes at full speed. This is a critical step because incomplete homogenization leads to a reduced RNA yield. Samples were processed according to the manufacturer's instructions. To prevent genomic DNA (gDNA) contamination, RNAse-free DNAse (Qiagen) was used. Finally, the extracted RNA was eluted with 40µL of RNase-free water by centrifuging for 1minute at 10,000rpm. The RNA concentration was determined by measuring the absorbance at 260nm using a spectrophotometer (NanoDrop ND-1000; Thermo Scientific, Epson, UK). For complementary DNA (cDNA) synthesis, a QuantiTect® Reverse Transcription kit was used. A ratio of about 2.0 is accepted as ‘pure' for RNA. A lower rate

indicates the presence of phenol, protein, or other contaminants that absorb at 280 nm. The isolated RNA was held on ice for immediate use or stored at -80°C for future use.

2.2.7.2 Complementary DNA synthesis.

cDNA was synthesised from a mass of 500ng to 1µg of the total RNA using QuantiTect® Reverse Transcription kit. A total reaction volume was 25µl. After thawing RNA samples on ice, RNA is incubated in genomic DNA (gDNA) Wipeout Buffer and RNase-free water at 42°C for 2 minutes to remove contaminating gDNA. After eliminating the DNA, samples were ready for reverse transcription which was carried out using a master mix of 1µl Quantiscript Reverse Transcriptase, which has a high affinity for RNA and is optimized for efficient and sensitive cDNA synthesis from 10 pg to 1 µg of RNA. 4 µl Quantiscript RT Buffer, and 1 µl RT Primer Mix was also added to ensure cDNA synthesis from all regions of RNA transcripts. A 14 µl RNA template was added to each tube containing the reverse transcription master mix. The synthesis reaction was held at 42°C for 15 minutes and then at 95°C for 3 minutes to inactivate the reverse transcriptase. The mixture was cooled to 4 °C and samples were kept on ice to proceed with qPCR using QuantiTect Kit (Qiagen). All samples were diluted at a ratio of 1:3 to 1:5 with RNase free water to dilute out any buffers in the RT reaction that might inhibit the PCR reaction. No Reverse Transcription control (NRT), although the genomic DNA was eliminated as mentioned previously, all reverse-transcription experiments must include a negative control to detect any gDNA contamination. In which the NRT contains template RNA, and all reverse transcription components except for Quantiscript Reverse Transcriptase, the volume of which was replaced with RNase-free water. Therefore, reverse transcription cannot take place, and the available template will be the contaminating gDNA.No Template Control (NTC), which contains all the components of the reaction except for the template. This enables detection of carryover contamination from previous experiments.

2.2.7.3 PCR amplification of the cDNA

The synthesised cDNA was amplified in 20 µl volumes using the 2x MESA BLUE qPCR MasterMix Plus for SYBR® Assay (Eurogentec, Hampshire, UK) following the manufacturer's instructions. Primers that were used are shown in Table 2-2**.**

Table 2-2 Primers used in RT-qPCR and their catalogue codes (all from Qiagen)

Primers	Catalogue Code
Hs_SLC2A1_1_SG	QT00100709
Hs_LDHA_1_SG	QT02059764
Hs_FOXA1_1_SG	QT00212828
Hs_DNMT3L_1_SG	QT00081305
Hs_FGF5_1_SG	QT00008848
Hs_BMP4_1_SG	QT00012033
Hs_GDF3_1_SG	QT00014952
Hs_ACTB_2_SG	QT01680476
Hs_HIF1A_1_SG	QT00083664
Hs_EPAS1_1_SG (HIF2)	QT00069587
Hs_HIF3A_1_SG	QT00059157
Hs_VEGFA_1_SG	QT01010184
Hs_SOX17_1_SG	QT00204099
Hs_NES_2_SG	QT01015301
Hs_T_1_SG (BRACHYURY)	QT00062314
Hs_UBC_1_SG	QT00234430
Hs_NANOG_1_SG	QT01025850
Hs_POU5F1_1_SG (OCT4)	QT00210840
Hs_CDH1_1_SG (E-cadherin)	QT00080143
Hs_CDH2_1_SG (N-cadherin)	QT00063196
Hs_PAX6_1_SG	QT00071169
Hs_SNAI1_1_SG	QT00010010
Hs_CDH15_1_SG (M-cadherin)	QT00024703

All primers were diluted with TE buffer. The master mix was prepared by mixing MESA Blue Master-mix, primers and RNAse-free water for each of House Keeping Genes (HKGs) and Genes of Interest (GOI). Mini master mixes containing 5 µl of cDNA were then made for each sample, and triplicate reactions carried out in a 96-well skirted PCR plate (BioRad Laboratories, Hemel Hempstead, UK). NTC was used for each primer master mix and NRT for each sample. The plate was sealed with a Micro-seal 'B' adhesive seal (Bio-Rad) and was centrifuged for few seconds before carrying out RT-qPCR analysis on a CFX Connect Real-Time PCR Detection System (Bio-Rad). The

PCR mix was activated for 5 minutes at 95°C and denatured at 95°C for 15 seconds, followed by annealing and extension at 60°C for 60 seconds, for 40 cycles.

The ratio between the amount of HKGs and GOI, which is known as ΔCt, was used to calculate relative gene expression levels. This ratio was calculated for controls and samples, and the difference between them is known as the normalised relative quantity (NRQ) (Livak & Schmittgen 2001). However, ΔCt value assumes 100% efficiency (E) for PCR reaction and allows normalisation to only one HKG. Another method was established that considered PCR efficiency, known as the Pfaffl equation' (Pfaffl 2001), and allows for normalisation to one HKG. The further adjustment that allows normalisation to the mean of two or more HKGs and takes into account gene-specific amplification efficiencies has been considered (Hellemans et al. 2007), using the following formula to calculate NRQs.

$$NRQ = \frac{E_{goi}^{\Delta Ct,goi}}{\sqrt[n]{\prod_{i}^{n} E_{ref_i}^{\Delta Ct,ref_i}}}$$

2.2.8 Statistical Analysis

All experiments were conducted in triplicate (n=3) and error bars represent the standard deviation of the mean (SD). The statistical methods used in this project include unpaired two-tailed Student's t-test, one-way ANOVA with Dunnett's multiple comparisons test, and two-way ANOVA with Dunnett's multiple comparisons test. The application of each statistics method was specified in figure legends. GraphPad Prism 7.0 (GraphPad Software, La Jolla USA) was used for the statistical analysis. Data with $P \leq 0.05$ was considered statistically significant.

2.3 OXYGEN CONTROL

Two platforms have been used to control oxygen level during hypoxic experiments; airtight chambers fabricated in-house and C-Shuttle Glove Box (BioSpherix, Ltd). In the following sections; fabrication, validation and installation procedures are described.

2.3.1 In-house Hypoxic Chambers

At the beginning of this project, all hypoxic experiments were carried out using in-house manufactured acrylic chambers and placed inside a standard incubator to control the temperature at 37°C during the culture period (Mondragon-Teran et al. 2009). A previously available chamber as the (Figure 2.2A) shows, allowed for liquid-phase measurements by using fabricated platforms that comprising a polystyrene surface with small holes drilled in for the optical sensors to be screwed into from above or below and aluminium legs, as shown in (Figure 2.2A). Then, culture flasks were placed above the platforms that have already the oxygen spots glued inside their inner surface. These platforms need to be sterilised with 70% Ethanol for use during cell culture in the incubator. However, the platforms required more space in the incubator and the culture flasks were not fixed on the top of these platforms, which caused in most cases instability in oxygen tension readings. This prototype was improved, herein and after described as the first prototype. In this prototype, space was re-considered so that more culture flasks could fit (Figure 2.2B). However, only air-phase oxygen measurement was possible, due to the rounded bottom that handicapped the liquid-phase measurements. Optical sensors were glued on the outer polystyrene surface of the chamber, and the oxygen spot was fixed on the inner surface. The optical cables were aligned with the sensors to allow oxygen measurements. The second prototype has overcome some of the limitations, shown in (Figure 2.2C) In which, the rounded bottom surface was changed into a flat bottom that has small holes drilled in for the optical sensors to be screwed into for liquid-phase measurements. This prototype was more ergonomic in regard to its capacity.

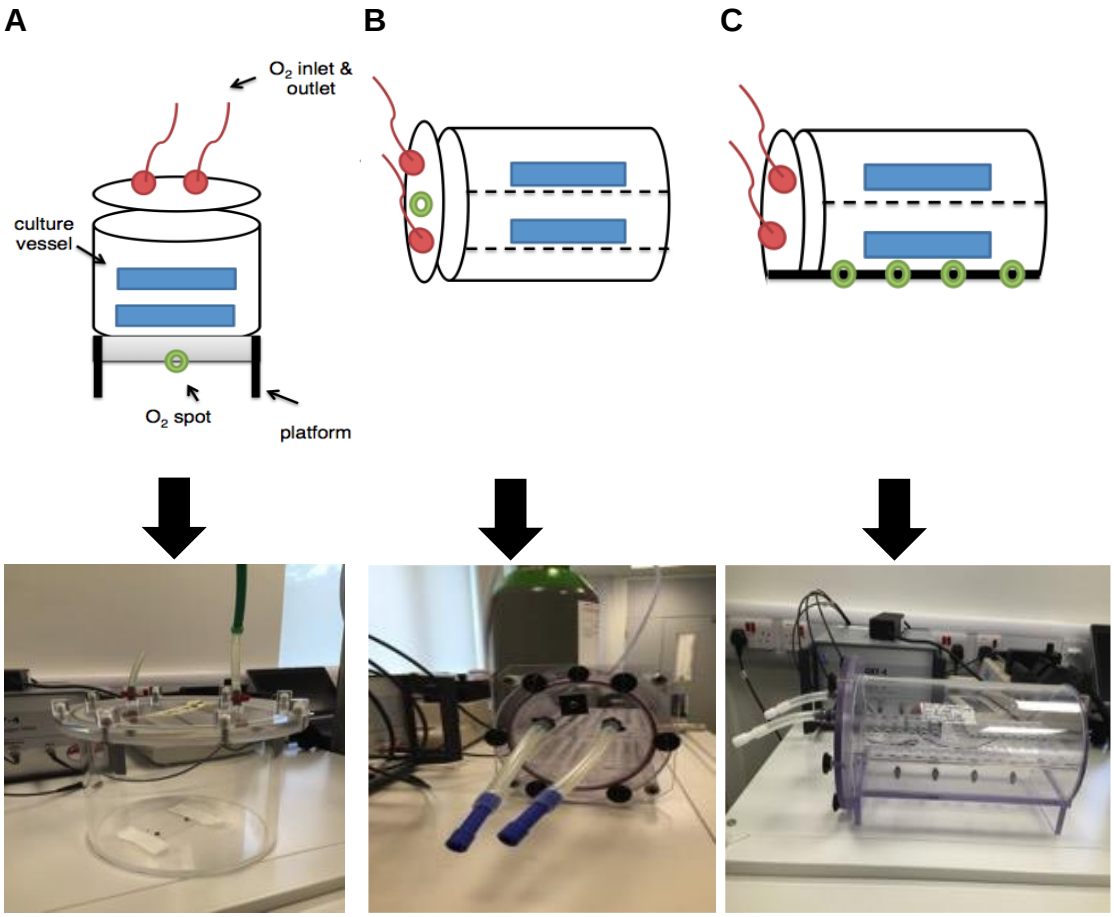

Figure 2.2 Prototypes of hypoxic chambers manufactured in-house.
(A) Previous fabricated chamber. **(B)** The first prototype of hypoxic champers, space was improved by including two shelves, but it has rounded bottom that handicapped the liquid-phase measurements. **(C)** Second prototype, showing the flat bottom, two shelves and 4 oxygen sensors screwed in in the bottom surface

These chambers were able to hold up to three to six of 6-well plates and a 10-cm diameter Petri dish (SLS) containing 3 ml of sterile H_2O for humidification. Once the 6-well plates and Petri dish were placed inside the chamber, a removable cover was attached, tightly sealed and flushed with the gas mixture containing 2% O_2 supplemented with 5% CO_2 and balanced with 93% N_2 (BOC, UK). The top of the chamber was removable and contained filter-inlet of gas to allow sterile gassing of the system performed for 5 min at a flow rate of 7.5 l/min and an outlet to allow the excessive gas to be released. Then, the top was then tightly sealed using an O-ring sealing mechanism and eight clamping screws. The Oxygen tension was measured continually by PreSens

OXY4 System (Presens, Regensburg, Germany). Oxygen level is recorded every 30 seconds by the optical oxygen sensors that attached to the bottom of the chamber. These optic sensors work in a dynamic fluorescence quenching principle. The optical oxygen sensors contain a fluorescent dye that is excited by a specific wavelength. The luminescence response of the optical sensor changes depending upon some oxygen molecules present. Then, an optical fibre transmits the excitation wavelength light of the sensor and transmits the PreSens OXY4 System measures the fluorescence response at the same time. Measurements were taken over 48 hours and re-set after media changed. The PreSens OXY4 System and sensor spots were calibrated weekly and before each experiment following the manufacturer's instructions, which can be found at www.presens.de.

Despite some improvements, these chambers suffered from some drawbacks. For instance, precise O_2 tension was difficult to achieve, as the duration of gas purging affects the final oxygen tension inside the chamber, which gave a fluctuating in O_2 tension. Also, these chambers were found to be prone to leakage. Additionally, their size and their surface area (15 cm width) could not accommodate the large volume of cell culture plates required for big or parallel hypoxic experiments. Most significantly, all hypoxic experiments were subjected to a sudden shift in oxygen tension during cells manipulation in normal room air, which havocs HIF genes.

For all these limitations, it was decided that all hypoxic experiments in the future will be undertaken with a new system; C-Shuttle Glove Box system (Biospherix, Canada). C-Shuttle is a complete closed system, so the cells will not be exposed to sub-optimal conditions during cell culturing and manipulation.

2.3.2 C-Shuttle Glove Box - BioSpherix

2.3.2.1 System overview

The C-Shuttle Glove Box from BioSpherix is a comprehensive Xvivo System that has a full range of oxygen control (0.1% - 99.9%O_2). The system consists of the Glove Box (Figure 2.3A), the O_2/CO_2 controllers (Figure 2.3B), and the gas supply, and the C-Chamber (Figure 2.3C). Access to the Glove Box for manual cell manipulation or equipment control can be done through the soft glove front panel. The glove sleeves are fused into a clear vinyl front window providing optical clarity. The pass-through chamber has an internal door that swings up out of the workspace and external door (Figure 2.3D). The C-Chambers; provide a semi-sealed gas-controlled transport mechanism for cell cultures to travel back and forth to the C-Shuttle Glove Box from remote incubators without disturbing in O_2 levels. The pass-through chamber of the C-Shuttle Glove Box is designed to fit C-Chambers. C-Chamber cab be left in the pass-through chamber and cells can be removed and manipulated inside the C-Shuttle Glove Box without disturbance. Cells are then can be transferred back inside the C-Chambers and shuttled back to the host incubator for incubation, for full-time optimization (Figure 2.3E). Moreover, tools and instruments that require electricity can be moved in and out of the C-Shuttle Glove Box. The C-Shuttle Glove Box has two control Options; oxygen controllers (ProOx model 360) and carbon dioxide sensor (ProOx model 110), while the C-Chambers has one control option; oxygen sensor (ProOx model 120).

2.3.2.2 C-Shuttle Glove Box Operation

Detailed standard operating procedure (SOP) is illustrated in BioSpherix manual (Figure 2.3E). Briefly, when conducting a hypoxic experiment, different quality control steps were considered including cleaning and decontamination procedure, sensor calibration and validation, establishing operating gas levels, moving cells in and out. The results of these quality control assessment processes are described in section 3.3.

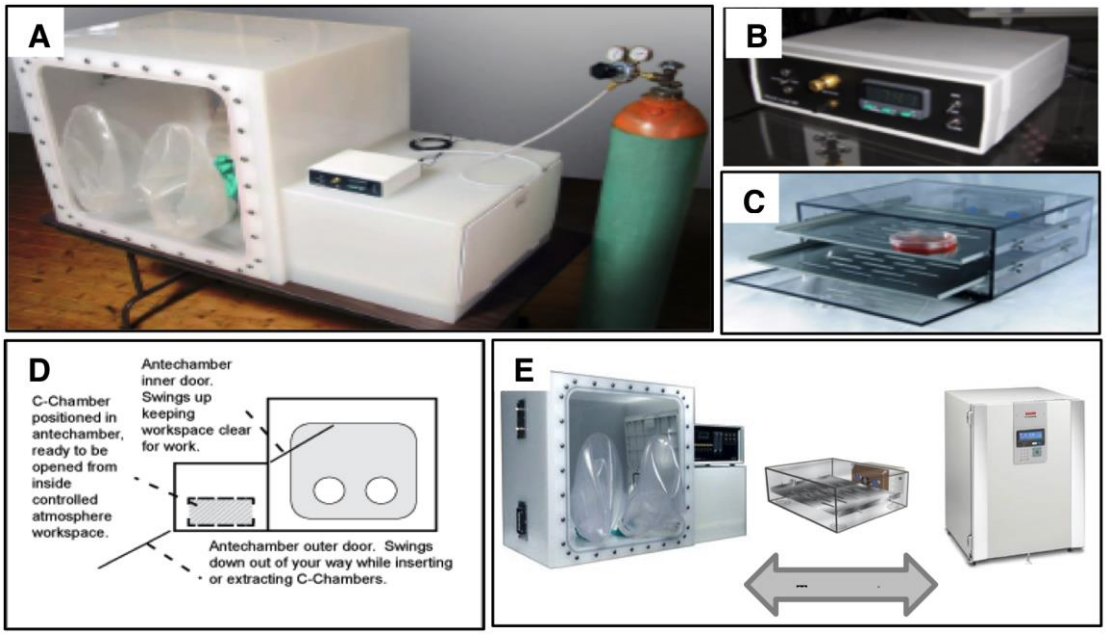

Figure 2.3 C-Shuttle Glove Box with O_2/CO_2 control atmosphere
(A) The whole system **(B)** O_2/CO_2 Controllers **(C)** C- Chamber **(D)** Descriptive image for the internal and external doors. **(E)** Overview of system operation. C-Shuttle Glove Box used to culture and process cells under hypoxic conditions. Cells are grown under hypoxic conditions in the C-Chamber, which is placed inside an incubator. Upon processing of the cells, the C-Chamber is transported into the C-Shuttle Glove Box, which contains the same oxygen level as inside the C-Chamber (BioSpherix) (www.biospherix.com).

2.3.2.3 Gas supply set-up

Certified research grade pre-mixed gas was used to purge the C-Chamber with the desired oxygen levels that were used in this project (Table 2-3).

Table 2-3 Gas mixture composition of experimental oxygen levels in this project.

Desired Concentration of Oxygen (O_2%)	Air displace to %	%Mix required	Desired % CO_2	%CO_2 Concentration in N_2
0%	0	100	5	5
2%	9.615384615	90.38461538	5	5.531914894
5%	24.03846154	75.96153846	5	6.582278481
8%	38.46153846	61.53846154	5	8.125
12%	57.69230769	42.30769231	5	11.81818182

3 CHAPTER 3: OXYGEN CONTROL

3.1 INTRODUCTION

The following section will summarize the relevant literature, which was previously discussed in Chapter 1.

Oxygen levels range from 1.5–13% *in vivo* (Giaccia et al. 2004; Simon & Keith 2008). However, the majority of *in vitro* culture protocols are carried out under normoxic condition (20% O_2), due to the convenience of traditional procedures and absence of suitable methods and instruments that provide precise oxygen control. Oxidative stress due to the generation of Reactive Oxygen Species (ROS) in cells cultured under the normoxic condition is implicated in many harmful effects, such as DNA damage, genomic instability and senescence (Halliwell 2003; Burhans & Weinberger 2007; Cieślar-Pobuda et al. 2017). Also, increases in ROS levels were noticeable when the cells were exposed to re-oxygenation during hypoxic culture (Therade-Matharan et al., 2004). In contrast, cells processed under sustained hypoxic conditions exhibited a decrease in ROS levels (Jagannathan et al. 2016). Most importantly, due to the short half-life of HIF-1A protein (<5 min) in the well-oxygenated atmosphere, changes in oxygen concentrations have a profound impact on HIF-1A stabilisation and its downstream mechanism (Kong et al. 2007; Wenger et al. 2015; Yazdani 2016).

Several technologies have been developed to provide low oxygen environment *in vitro* — for example, airtight chambers that are flushed with a specific gas mixture (Wu & Yotnda 2011; Gille & Joenje 1992; Kaneko & Takamatsu 2012). Although these chambers are efficient and portable (Kaneko & Takamatsu 2012; Mondragon-Teran et al. 2013) they don't provide real-time oxygen monitoring; especially during cell handling, which usually takes place under normoxic conditions. Gas-controlled incubators are also used for controlling oxygen level during cell culture. However, incubators suffer from the drawbacks of being less portable than airtight boxes and more

susceptible to fluctuations in internal gas composition due to the repeated opening and closing of the doors, it takes up to 30 minutes for the oxygen level to recover (Lim et al. 2011; Cicione et al. 2013; Garita-HernÁndez et al. 2013). This intermittent disruption in O_2 levels during cell manipulation may be the cause of the discrepancies reported in the literature. Therefore, precise oxygen control is very crucial for reproducible and consistent outcomes, especially in studies that focus on hypoxia signalling pathways.

In this project, two platforms were used to control oxygen levels during hypoxic experiments. The first platform used was an in-house fabricated airtight chamber. However, due to the limitations mentioned here and in section 2.3.1, it was decided to use the C-Shuttle Glove Box, which is the focus of the results that follow.

3.2 AIM

This work aimed to validate the efficiency of the C-Shuttle Glove Box system to maintain a precise O_2 level during all hypoxic experiments.

Several tasks were performed to accomplish the aim of this chapter;

I. Establish a sterile working environment within the C-Shuttle Glove Box system.
II. Provide evidence that the system serves the overall purpose of this project by establishing the full range of experimental O_2 levels, as low as 0.1% O_2.
III. Assess the C-Chamber efficiency in maintaining stable O_2 level, especially during transportation.
IV. Show evidence that the cells were handled in undisrupted O_2/CO_2 conditions throughout the following states; (i) cell incubation, (ii) manual manipulation (cell seeding, cell harvesting and media change (iii) transportation from the C-Shuttle Glove Box to the incubator.
V. Show that the O_2/CO_2 controllers are stable and accurate.

3.3 RESULTS AND DISCUSSION

All cell culture procedures including initial seeding, splitting and media change were performed in sterile C-Shuttle Glove Box. Cells were transported using C-Chambers. The levels of O_2/CO_2 were maintained using feedback controllers; ProOx Model 360, ProCO2 Model 120 (in C-Shuttle) and ProOx Model 110 (in C-Chambers) (BioSpherix, Ltd.). The steps involved in conducting a hypoxic experiment using the C-Shuttle and C-Chambers are illustrated in (Figure 3.1); each step is discussed in detail below.

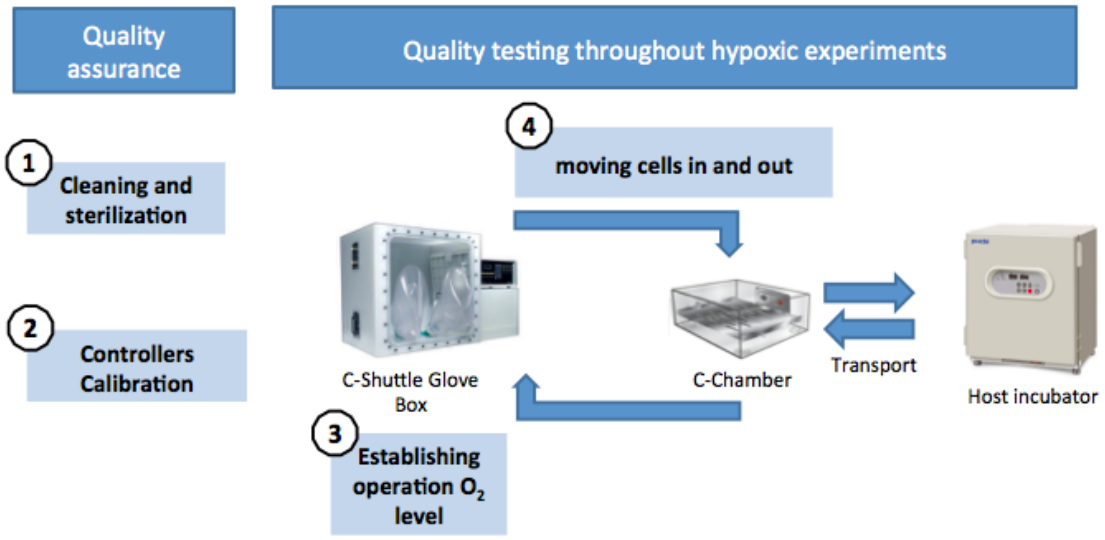

Figure 3.1 Flowchart of the steps needed for conducting hypoxic experiments.

3.3.1 Validation of Cleaning and Decontamination Processes of C-Shuttle Glove Box (Figure 3.1, Step1)

Cleaning and decontamination procedures (described in the operations manual, BioSpherix, Ltd.) were performed before carrying out a hypoxic experiment. Following decontamination, several strategies were employed to maintain a sterile environment inside the system. For example, media and buffers were prepared under sterile/aseptic conditions and filter sterilised. Additionally, the C-Shuttle Glove Box and C-Chambers were purged with streams of sterile-filtered gas mixtures. No signs of contamination were observed visually in the culture vessels when culturing cells in the C-Shuttle Glove Box throughout this project (Figure 3.2). Also, this was confirmed by the negative Mycoplasma testing.

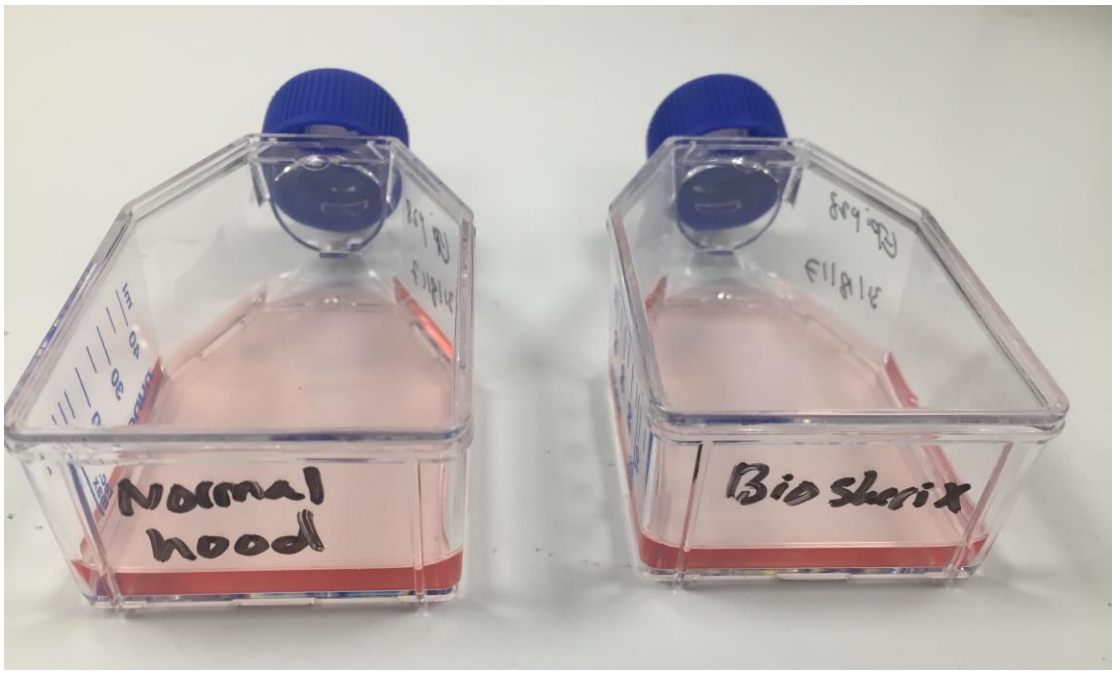

Figure 3.2 Visual observation of contamination signs in the hPSCs during Cell culute.
The media did not turn yellow or became cloudy when hPSCs were maintained at Walker Class II Safety Cabinet (normal hood) on the right hand, and at C-Shuttle Glove Box (BioSpherix) on the left side.

3.3.2 Calibration Procedures Validation (Figure 3.1, Step2)

Calibration of sensors was performed at least once every two weeks or before conducting hypoxia experiments. ProOx Model360 and ProOx Model110 (control O_2% inside C-Shuttle Glove Box and C-Chamber, respectively) were calibrated using a mixture of 100% N_2 and normal air (20% O_2), and the ProCO2 Model120 (controls CO_2%) was calibrated using a mixture of 90% N_2 and 10% CO_2 (described in the operations manual, BioSpherix, Ltd). Based on the R^2 values, the results indicate that the controllers provided accurate means of sensing O_2 levels over the set ranges of O_2 levels (0%, 2%, 5%, 8% and 12%O_2) (Figure 3.3) and they could provide efficient control of desired gas levels within few minutes in the C-Shuttle Glove Box and C-Chambers. The same validation procedure was undertaken for the CO_2 sensor to establish the physiological value of 5% CO_2. The measured value achieved was 4.98 ± 0.2% CO_2; the results are included in Appendix 8.1

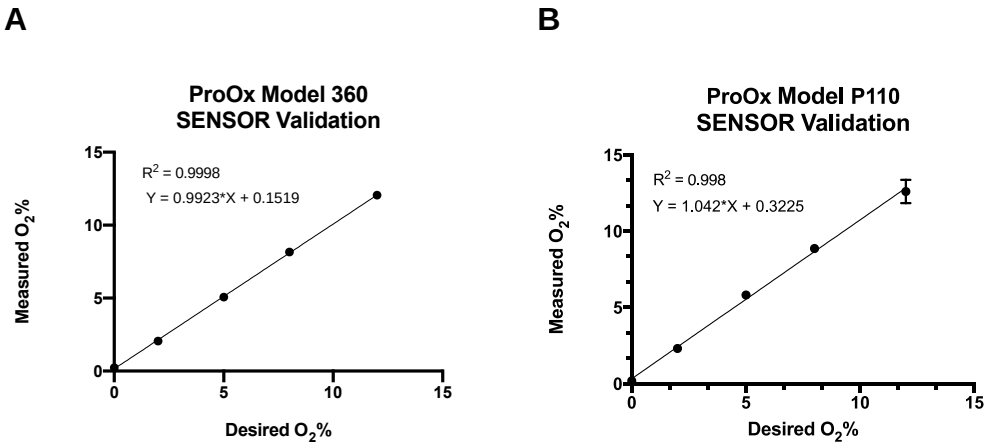

Figure 3.3 Validation plots for O_2 controllers
The experimental O_2 levels (0%, 2%, 5%, 8% and 12% O_2) were used after each calibration procedure to validate O_2 controllers. After ~5 minutes, steady state was reached and average O_2 concentrations were recorded (from 5 consecutive readings) over a period of 24 hours by **(A)** ProOx Model360 and **(B)** ProOx Model110. Error bars represent the standard deviation (SD) for 8 calibration repetitions.

3.3.3 Establishing Operating Gas Levels (Figure 3.1, Step3)

To conduct a hypoxic experiment, the O_2 and CO_2 levels in the C-Shuttle Glove Box and the C-Chamber should be the same for the cells to be handled without disruption. First, the O_2 and CO_2 levels should be established in the C-Shuttle Glove Box using ProOx P360 and ProCO2 P120 controllers, respectively. The results showed that the controllers were accurate and established all operational O_2 levels as low as 0.1% O_2 (Figure 3.4A). The data also showed that the time required to establish operation gas levels increased when the set point was lowered (Figure 3.4). The controllers required a maximum of 90 minutes to establish the lowest O_2 level (0.1% O_2) (Figure 3.4A, Horizontal yellow line) within the C-Shuttle Glove Box. In contrast, establishing the operation O_2 level inside the C-Chamber was relatively quicker (<5 minutes), primarily due to differences in unit size. By verifying the time required to establish steady states for the operating O_2 levels inside the C-Shuttle Glove Box, it was possible to determine precisely when to move in the C-Chamber containing the cells for optimised use of the unit, when either changing media or harvesting cells, without any disturbance in the O_2 and CO_2 levels.

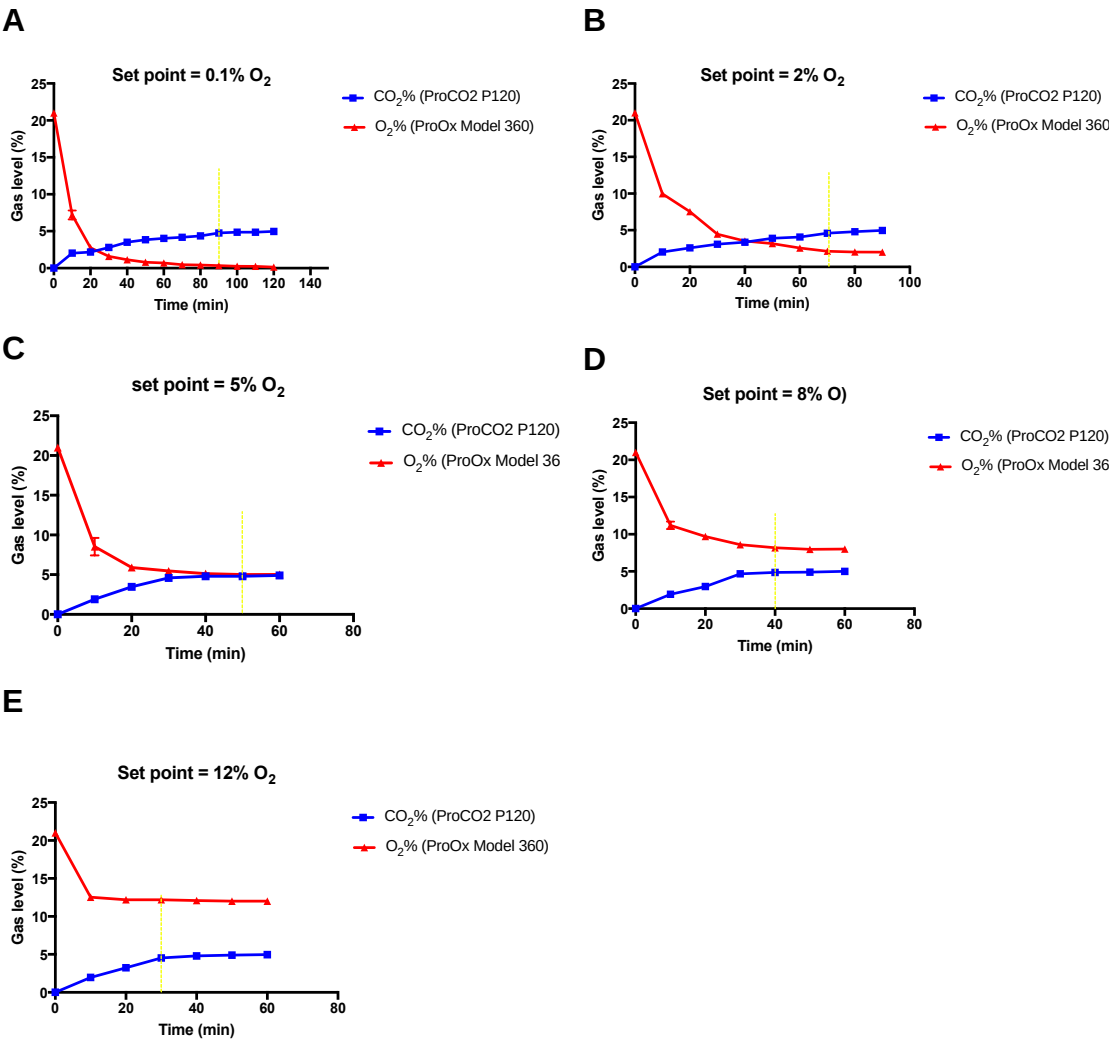

Figure 3.4 Establishing operating O_2 and CO_2 levels in the C-Shuttle Glove Box using the ProOx P360 and ProCO2 P120 controllers. Set points 0.1%O_2 (A), 2%O_2 (B), 5% O_2 (C), 8%O_2 (D), and 12% O_2 (E) were establised, yellow lines reprent the time needed for each set point to be established inside the Glove Box C-shuttle. n=1

3.3.4 Moving Cells from the Incubator to C-Shuttle Glove Box and Back to the Incubator (Figure 3.1, Step4)

After establishing the gas level in the C-Shuttle Glove Box as described previously, the cells were transferred using a transport vessel; C-Chamber for further manipulation. In this experiment, we sought to investigate the effects of routine cell culture procedures -when opening the outer door of the unit- on O_2 and CO_2 levels inside the C-Shuttle Glove Box as well as the C-Chamber throughout 6 different stages (Table 3-1). For the purpose of this experiment, another O_2 sensor (ProOx P110*) was integrated into the C-Shuttle Glove Box unit (Figure 3.5, red sensor) to investigate the spatial variation of O_2 levels within the larger compartment compared to the factory integrated sensor in the pass-through chamber (ProOx P360). The ProOx P110* sensor was also used to investigate how much the C-Chambers leaked gas during transportation before moving it inside the C-Shuttle Glove Box unit. The disturbance in O_2 and CO_2 levels were monitored for 30 minutes, which was the maximum time needed for cellular manipulation within the larger compartment of the C-Shuttle Glove Box. The procedure used here was specifically implemented to study the after-effects of cell transportation and manipulation on O_2 level post establishment of a given O_2 level inside the C-Chamber and C-Shuttle Glove Box; 5%O_2 was tested as an example.

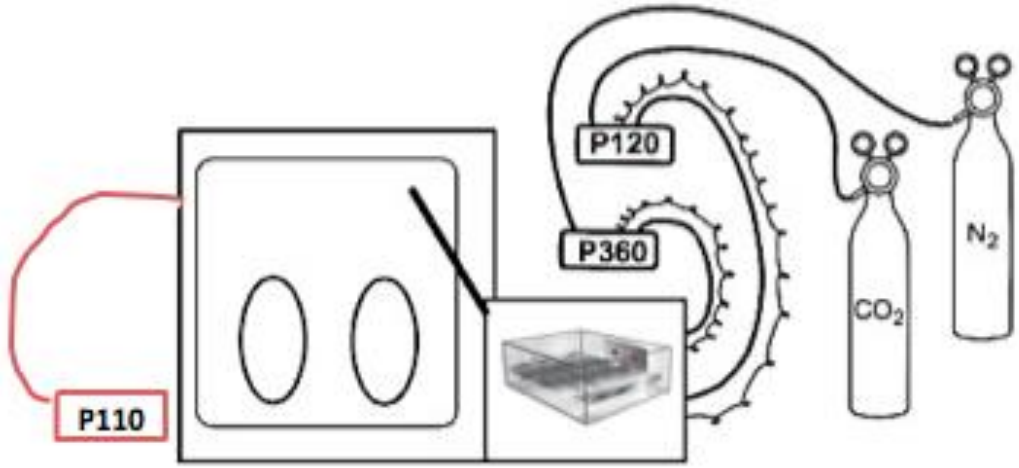

Figure 3.5 Illustration for the integrated ProOx model 110 sensor (shown in red) in the C-Shuttle Glove Box to control the changes in O_2 levels inside the C-Shuttle Glove Box system.

During stage1 (Table 3-1), when the C-Chamber was inside the incubator, the oxygen level remained stable (5%O_2, by ProOx P110). Similarly, the O_2 level inside the C-Shuttle was 5% O_2 as measured by ProOx P360 and the concentration of CO_2 was also stable (5% CO_2, by ProCO2 P120) (Table 3-1). However, the level of O_2 was higher than the set point on the other side of the unit (6.47% O_2) as measured by ProOx P110*. This was undoubtedly due to the large size of the unit, as the gas inlet port is next to the outer door, which indicates that more time is required to reach 5% O_2 inside the whole unit. By establishing similar O_2 levels inside the C-Shuttle, it was possible at this stage to bring the cells inside the unit. When the C-Chamber was disconnected from the gas supply and transported to the C-Shuttle (Table 3-1, stage2), the level of O_2 inside the C-Chamber was 5.8% O_2 as measured by the integrated ProOx P110*, which indicates that some gas escaped during transportation. The leakage is because this C-Chamber is semi-sealed, and it will leak gas slightly from around the edge of the door. This leakage is important to some extent to vent out the build-up of gas within the C-Chamber as well as to allow some outside air to enter the system passively (D Henn 2016). When the outer door of C-Shuttle was opened to transfer the C-Chamber containing the cells inside the unit (Table 3-1, stage3), the results showed that there was some disturbance in the gas level (7.33%O_2 and 3.76%CO_2) due to the door

opening. However, the recovery to pre-set levels was quick when the outer door was closed (Table 3-1, stages4&5), the O_2 levels were restored to 5.17% and 5.1% O_2 by the ProOxP360 within a few minutes. Comparable results were obtained for CO_2; as the controller re-established the gas level quickly (within two minutes) (4.37% and 4.53%CO_2). When the C-Chamber was moved out of the C-Shuttle Glove Box (Table 3-1, stage6), there was a minor disturbance in the gas level. The results showed that the O_2 level inside the C-Chamber was 6.6% O_2 (measured by integrated ProOx P110*) and the gas level inside the C-Shuttle Glove Box was 7.63% O_2 and 2.83% CO_2, this was due to the second opening of the door. The O_2 and CO_2 levels recovered to the pre-set values (5%O_2 and 4.53%CO_2) quickly when the outer door was closed (Table 3-1, stage7). When the C-Chamber was transported back to the host incubator (Table 3-1, stage7), the level of O_2 inside C-Chamber was 7.3% O_2 as measured by ProOx P110; however, the O_2 level recovered quickly (within 2 to 5 min) to 5% O.

Table 3-1 Oxygen level measurements during moving cells in and out of the C-Shuttle Glove Box.

Stages		C-Chamber		C-Shuttle Glove Box				
		ProOx P110 O_2 %	ProOx P110* O_2 %	ProOx P360 O_2 %	ProOx P110* O_2 %	ProCO2 P120 CO_2 %	**INNER DOOR**	**OUTER DOOR**
1	Before transport (in incubator)	5		5	6.47	5	O	C
2	After transport - before moving to C-Shuttle		5.8				O	C
3	After transport to C-Shuttle			7.33	6.43	3.67	C	O/C
4	After removing cells from C-Chamber			5.17	6.7	4.37	O	C
5	After placing cells back into C-Chamber			5.1	6.7	4.57	O	C
6	Removing the C-Chamber from C-Shuttle		6.6	7.63	6.97	2.83	C	O/C
7	After transport back to the incubator	7.3		5	6.5	4.53	O	C

*The ProOx P110 sensor that was integrated into the C-Shuttle Glove Box was removed to measure the O_2 level in the C-Chamber, which was transported into proximity to the C-Shuttle Glove Box, before moving it to the inside. Then it was connected back to the C-Shuttle Glove Box to measure the O_2 level in the big unit of the C-Shuttle Glove Box to assess O_2 level changes when the doors were opened (outer and inner). The grey highlights represent the O_2 and CO_2 levels inside the C-Shuttle Glove Box only. C; Closed. O; Open (n=3).

3.3.5 Leaking During Cells Transportation from the Host Incubator to the C-Shuttle Glove Box (Figure 3.1, Step4)

It was essential to evaluate the effectiveness of the C-Chamber to maintain the desired oxygen tension during transportation of the cells from the incubator to the C-Shuttle Glove Box for media change and cell harvesting. Oxygen measurements were taken while the C-Chamber was disconnected from the gas supply over a time period of 30 minutes. As expected, there were small differences observed in O_2 % levels while transporting the C-Chamber. However, the deviation of the various tested oxygen level was minimal (not more than 1.5% O_2), maintaining levels relatively close to the O_2 set points; 0.1%, 2%, 5%, 8% and 12% (Figure 3.6). This indicates that the C-Chamber provides an efficient mode of transport while maintaining the desired gas levels within a tolerable range during transportation and manipulation.

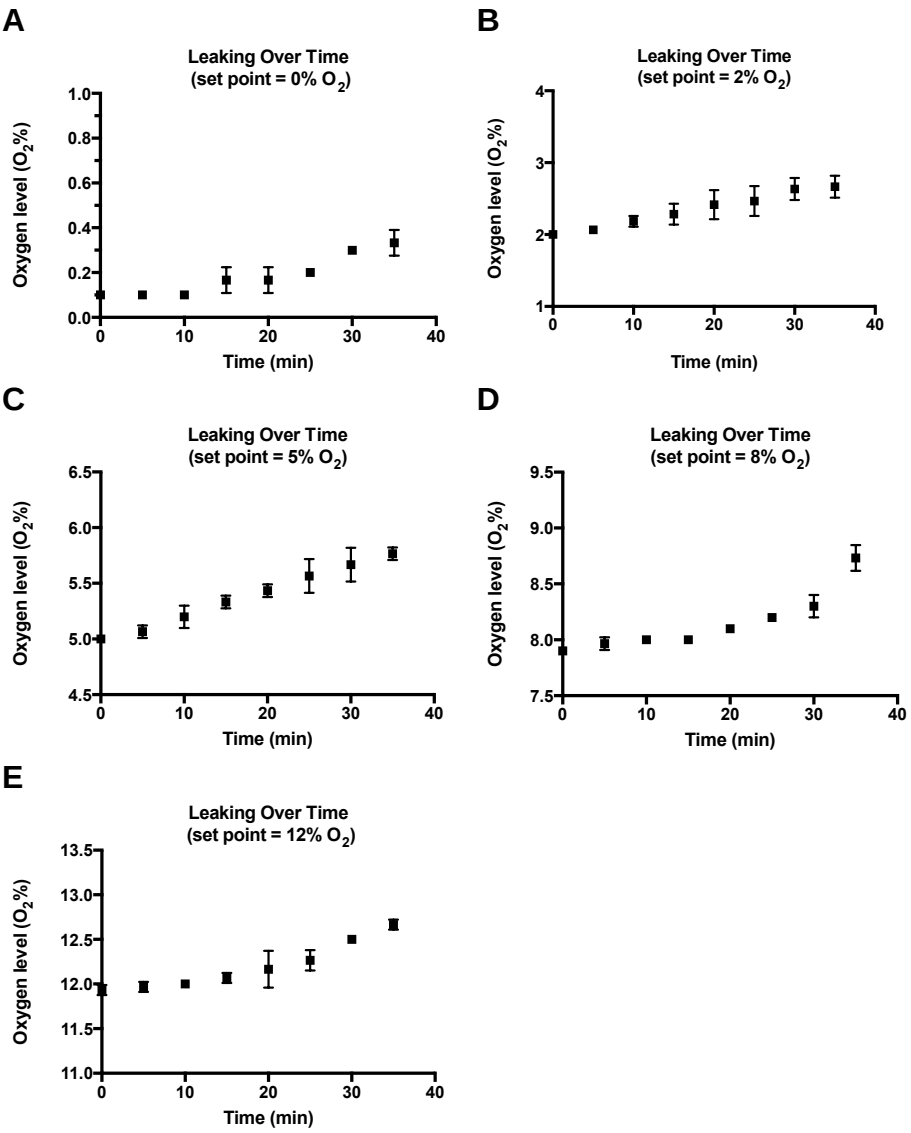

Figure 3.6 Leaking measurements in C-Chambers during transportation from the host Incubator to the C-Shuttle Glove Box for downstream manipulation.
During hypoxia experiments, cells were incubated inside the C-Chamber within the host incubator. During transportation into the C-Shuttle Glove Box, the O_2 values were monitored over 30 minutes, and values were recorded every 10 minutes. This experiment was repeated three times (n=3) for each O_2 level; 0%O_2 **(A),** 2%O_2 **(B),** 5% O_2 **(C),** 8%O_2 **(D),** and 12% O_2 **(E).**

3.4 CONCLUSION

Cells *in vivo* experience much lower O_2 level than atmospheric level (20% O_2). Therefore, handling and culturing cells in conventional clean benches under normoxic condition may cause cellular shock. With increasing interest in the performance of cell culture experiments under lower O_2 levels, various technologies and instruments (e.g. gas-tight boxes and gas-controlled incubators) have been utilised. However, some of these technologies and instruments have drawbacks and require further optimisation. This chapter described and validated the use of a complete closed system capable of maintaining a precise oxygen tension during both the incubation and cells handling steps. This work has provided evidence of the efficiency of C-Shuttle Glove Box and C-Chambers in establishing all experimental hypoxia levels. Although there was some disturbance (not more than 1.5% O_2 increase in the desired level) during door opening, the gas level re-established quickly within a few minutes. The number of experiments that would benefit from enhanced spatial and temporal control over oxygen concentration offered by the hypoxia system is substantial and is likely extend to new areas of research that were either too difficult to conduct with the current technologies or were just not possible.

4 CHAPTER 4: CHARACTERISATION OF MSUH001- and Episomal-hiPSCs AND SHEF3-hESCs

4.1 INTRODUCTION

The following section will summarize the relevant literature, which was previously discussed in Chapter 1.

Human PSCs can proliferate indefinitely and yet maintain the potential to form derivatives of all three germ layers (mesoderm, endoderm and ectoderm). These features make them useful to study developmental biology, for drug discovery, toxicological screening and transplantation therapies (Thomson et al. 1998; Pera et al. 2000; Takahashi et al. 2007). The culture system used to support the derivation and expansion of the first hESCs line was based on co-culturing with MEFs (Evans and Kaufman 1981; Martin 1981). However, MEFs have proven to be unsuitable, as these animal-derived cells pose a high possibility of transferring zoonotic pathogens into the culture system (Martin et al. 2005), which compromises safe production of hPSCs for future therapeutic applications. Additionally, it was found that prolonged culture of hPSCs with cells from animal sources have resulted in genetic changes as the cells adapt to grow under conditions to which they are exposed (Draper et al. 2004). Therefore, moving toward a xeno-free culture system represents a significant improvement in the field of regenerative medicine (Takahashi et al. 2009; Rodríguez-Pizà et al. 2009). Currently, different matrices are widely used to replace feeder cells from animal sources for the maintenance as well as differentiation of hPSCs, including recombinant human proteins (e.g. Vitronectin) (Xu et al. 2001; Chen et al. 2011). Also, various xeno-free media are available commercially such as Essential E8 medium (Chen et al. 2011).
Multiple criteria have been used to evaluate the pluripotent state of hPSCs (Thomson et al., 1998). One key criterion is the routine morphological evaluation of hPSCs for the presence of high nuclear-cytoplasmic ratio cells

and the formation of compact colonies. Moreover, expression of the classic cell surface pluripotent markers such as SSEA-3, SSEA-4, TRA-1-60, TRA-1-81, and core transcription factors including OCT4 and NANOG as well as demonstration of differentiation capacities of hPSCs into derivatives from the three germ layers by assessing the expression of related markers including NESTING/ectoderm, SOX17/endoderm and BRACHYURY/mesoderm (Kannagi et al. 1983; Andrews et al., 1984; Carpenter et al. 2003; Hoffman & Carpenter 2005; Hoffman and Carpenter, 2005 ; Josephson et al. 2007; Prokhorova et al. 2009; Valamehr et al. 2011; Quintanilla 2013). The functional assays of hPSCs differentiation capacities compromise *in vitro* differentiation (EBs formation), teratoma formation in immune-deficient mice and chimaera development *in vivo* (Jaenisch & Young 2008). Recently, a wide range of laboratory techniques has been used to assess whether hPSCs fulfill the criteria mentioned above to be considered as pluripotent cells, including Immunostaining, Flow Cytometry and RT-qPCR for the detection of pluripotency- and differentiation-related markers (Loh et al., 2006).

There are many similarities between ESCs and iPSCs, as both cell types possess the same proliferation and differentiation capacities *in vitro*; forming EBs, teratoma, and chimaera. These cells also share relatively similar gene expression profiles (Ying et al. 2003).

Three human cell lines were used in this work; MSUH001-hiPSCs line that was gifted from Dr Cibelli (Cellular Reprogramming Laboratory, Michigan State University) that it was derived by transfecting four factors (OCT4, SOX2, LIN28 and NANOG), Episomal-hiPSCs line is Nonviral, non-integrated human cell line that was generated using cord blood-derived CD34+ progenitors with seven episomal expressed factors (OCT4, SOX2, KLF4, MYC, NANOG, LIN28 and SV40T) (purchased from Life Technologies) and Shef3-hESC line (Draper et al. 2004) was obtained from the UK Stem Cell Bank. Hereinafter abbreviated as hPSCs, unless otherwise stated.

In this chapter, hPSCs were assessed using traditional characterization methods including morphological appearance, Immunostaining and RT-qPCR

for the expression of the pluripotent- and germ layer-specific markers through the formation of EBs. All characterization protocols used in this chapter were applicable for all the cell lines including Shef3-hESCs, MSUH001-hiPSCs- and Episomal-hiPSCs. All cells lines were used between passages 64-72 (MSUH001-hiPSCs), 39-51 (Episomal-hiPSCs) and 41-49 (Shef3-hESCs).

4.2 AIM

Work in this chapter aimed to examine whether hPSCs fulfill the criteria to be considered as PSCs. All cell lines were assessed for (i) their undifferentiated state under standard xeno-free culture conditions by analyzing the expression of pluripotent-specific markers (e.g. OCT4, NANOG, SSEA4, SSEA3, TRA-1-81 and TRA-1-60); and (ii) their multipotent differentiation capacities into three germ layers, using EBs approach, based on the expression of mesoderm (BRACHYURY), endoderm (NESTIN &PAX6) and ectoderm (SOX1) markers. The results obtained in this chapter are crucial to ensure the quality of these cells as starting materials to carry on the experiments in chapters 5 and 6.

4.3 RESULTS

At the beginning of this project, mitotically inactivated MEFs were used as a feeder layer to support the growth of MSUH001-hiPSCs line (Figure 4.1A). However, given the drawbacks of using animal derived-cells to support human cell growth; MSUH00H-hiPSCs were then adapted to feeder-free culture system (Khalife & Mason 2015). From now on, hPSCs lines including MSUH001-hiPSCs, Episomal-hiPSCs and Shef3-hESCs were cultured in feeder-free and chemically defined conditions using Essential 8™ Medium (Figure 4.1B). Cells were typically passaged every 4 to 5 days at a ratio of 1:3. To maintain the undifferentiated hPSCs colonies, cells were plated on human Vitronectin-coated T25 flasks and passaged before reaching the 90% confluence.

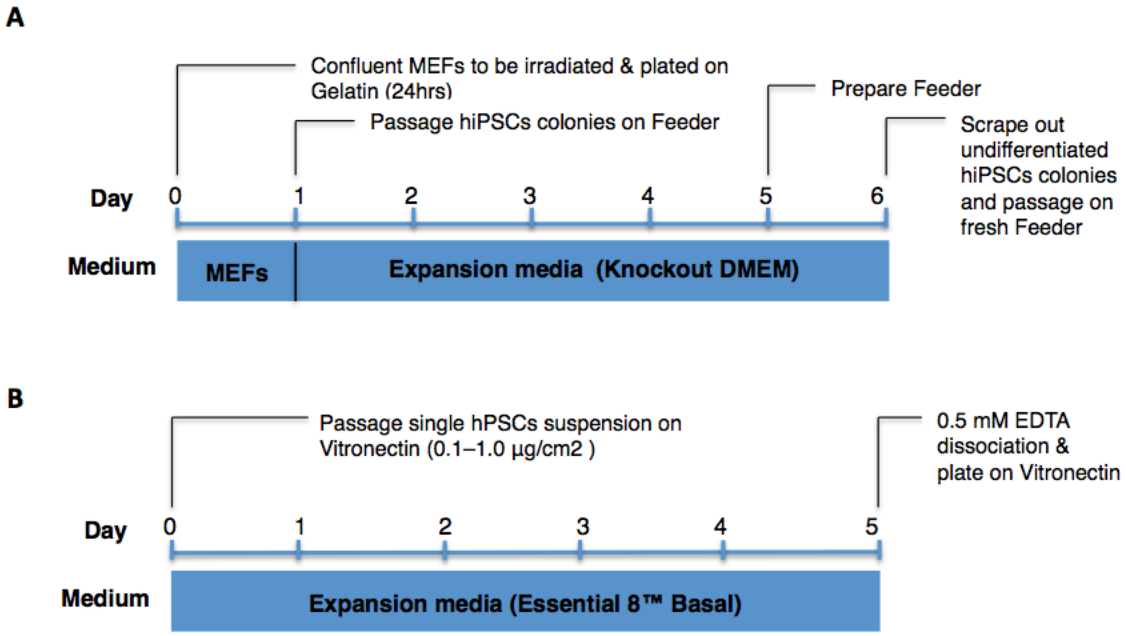

Figure 4.1 Overview of the maintenance protocol for culturing hPSCs.
(A) Feeder-dependent culture of MSUH001-hiPSCs. **(B)** The feeder-free culture of MSUH001-hiPSCs, Episomal hiPSCs and Shef3-hESCs.

4.3.1 Morphological Analysis and Undifferentiated State of hPSCs

Human PSC colonies retained a compact undifferentiated morphology during the expansion in culture. The colonies of the first cell line, MSUH001-hiPSCs that grew on the feeder exhibited a round morphology and well-defined sharp edges separating the hiPSCs from surrounding feeder cells (Figure 4.2A).

Feeder-free cell lines; (i) adapted MSUH001-hiPSCs (ii) Episomal-hiPSCs and (iii) Shef3-hESCs were maintained on Vitronectin-coated T25 flasks in chemically defined E8 media. The morphologies of the feeder-free cell lines were different from the traditional feeder-dependent cell line. As (Figure 4.2B-C-D) shows, the individual colony was expanded and often tended not to be round but rather partly with sharp edges, a feature previously encountered with feeder-free cell lines (Brouwer et al. 2016). However, the overall cells from all the lines exhibited high nucleus/cytoplasm ratio with multi nucleoli cells (Figure 4.2B-C-D), which indicates the undifferentiated state of stem cells (Wakui et al. 2017).

The undifferentiated state was also characterized by Immunostaining. The results reveal that the pluripotent markers OCT4, as well as the surface markers TRA-1-60 and SSEA4, were strongly and uniformly expressed at the protein level in undifferentiated colonies from all cell lines (Figure 4.3).

All the observations suggest that the cells remained undifferentiated while they propagated in culture and showed distinct stem cell-like morphologies, which is consistent with previous reports (Pera et al. 2000; Reubinoff et al. 2001; Tavakoli et al. 2009; Steiner et al. 2010).

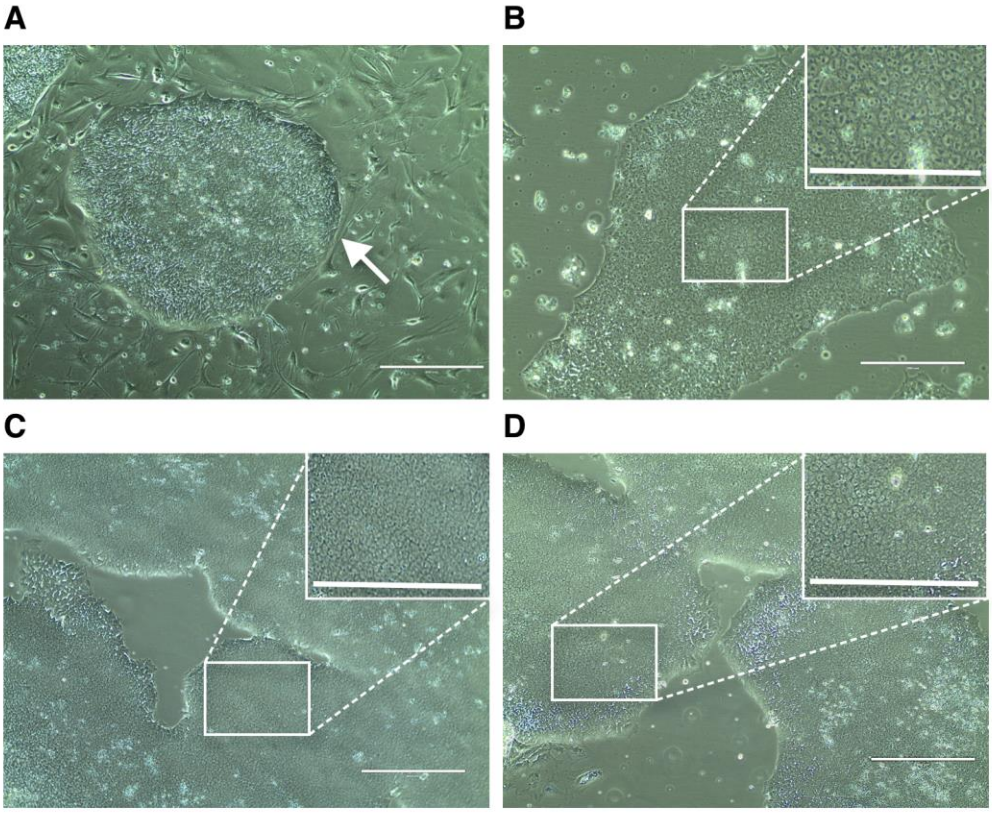

Figure 4.2 Phase contrast images of undifferentiated hPSCs
(A) MSUH001-hiPSCs (P72) growing on MEFs for 4 days, cells grew in tightly packed colonies with well-defined edges (white arrow). Feeder-free cell lines; **(B)** MSUH001-hiPSCs (P71) after adaptation **(C)** Episomal-hiPSCs (P43) and **(D)** Shef3-hESCs (P49), cells exhibited spherical cell morphology with a high N/C ratio and prominent nuclei (magnified images). (Magnification 10X, bar= 400µm).

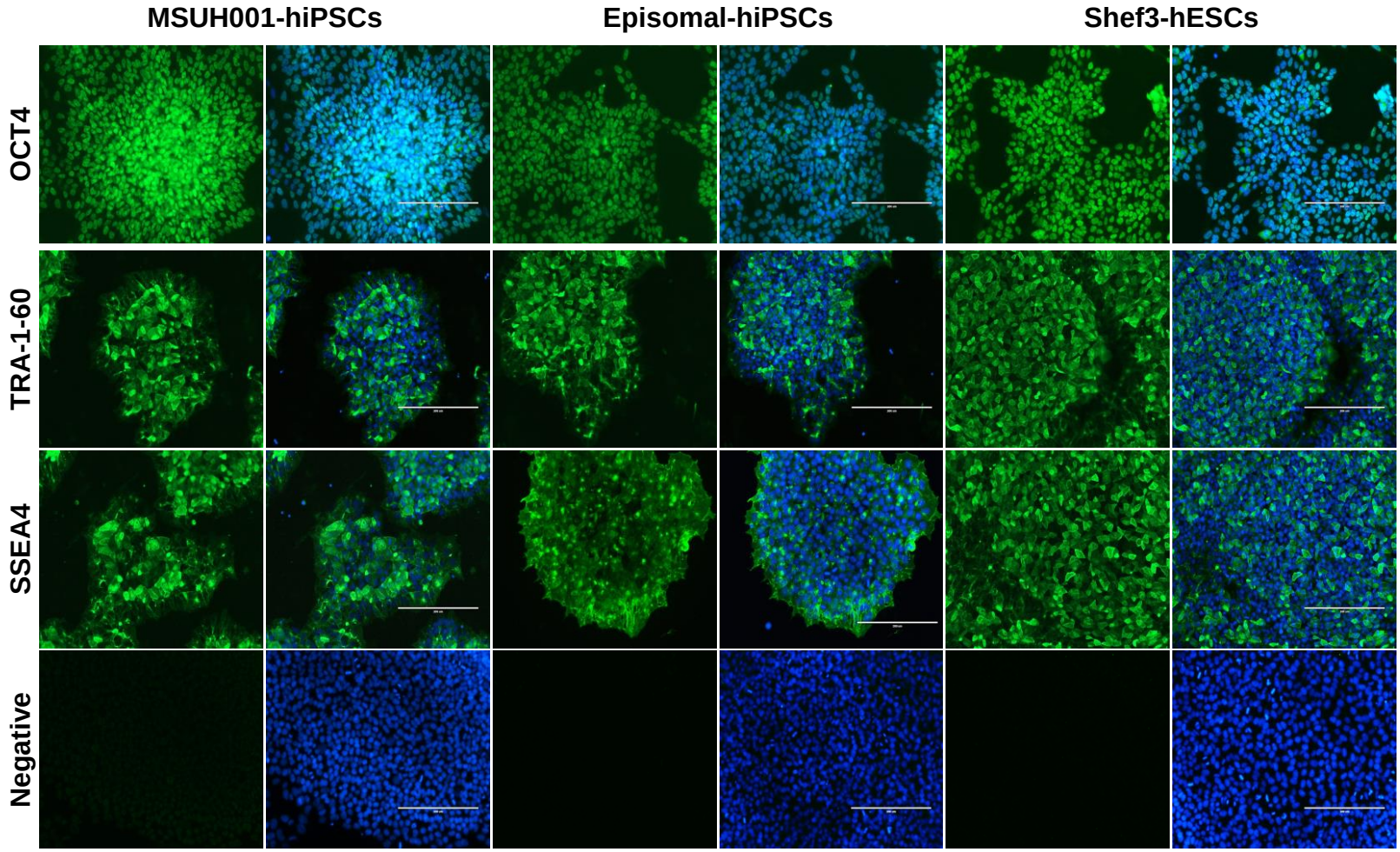

Figure 4.3 Immunostaining analysis of pluripotent markers in MSUH001-hiPSCs, Episomal-hiPSCs and Shef3-hESCs.
High level of nuclear OCT4 protein and surface TRA1-60 & SSEA-4 proteins were detected in all cell lines (green). Nuclei were stained by DAPI (blue), and the corresponding merged image is represented in the right-hand panel for each marker. The negative control is with secondary antibody instead of primary antibody. (Magnification 20X, bar = 200µm).

4.3.2 Morphological Analysis and Differentiation Potentials of hPSCs

In vitro EBs formation provides an important alternative method to the teratoma assay *in vivo*. The EBs approach was used (Figure 4.4A) to investigate the potential of hPSCs to differentiate into derivatives of all three germ layers. Human PSCs successfully formed EBs, as demonstrated visually by the phase contrast images (Figure 4.4B). The expression of three germ layers markers, at the protein level, was assessed by Immunostaining analysis at D7 after EB formation. The results show strong immunoreactivity to NESTIN (ectoderm), BRACHYURY (mesoderm) and SOX17 (endoderm) (Figure 4.5), while the expression of these markers was absent in the undifferentiated hPSCs (used as a negative control) (Figure 4.5).

The RT-qPCR analyses were performed to acquire molecular information respecting the key transcription factors of self-renewal as well as early differentiation markers. The results show that MSUH001-hiPSCS, Episomal-hiPSCs and Shef3-hESCs were maintained under feeder-free culture system expressed pluripotency markers, including OCT4 and NANOG, at higher levels than their counterparts EBs (Figure 4.6A-B-C). In contrast, similar trends of germ layer gene expression (BRACHYURY, SOX17 and PAX6) were observed in EBs at D7 of differentiation. However, the expression was absent in the undifferentiated cells or only slightly expressed (Figure 4.6A-B-C).

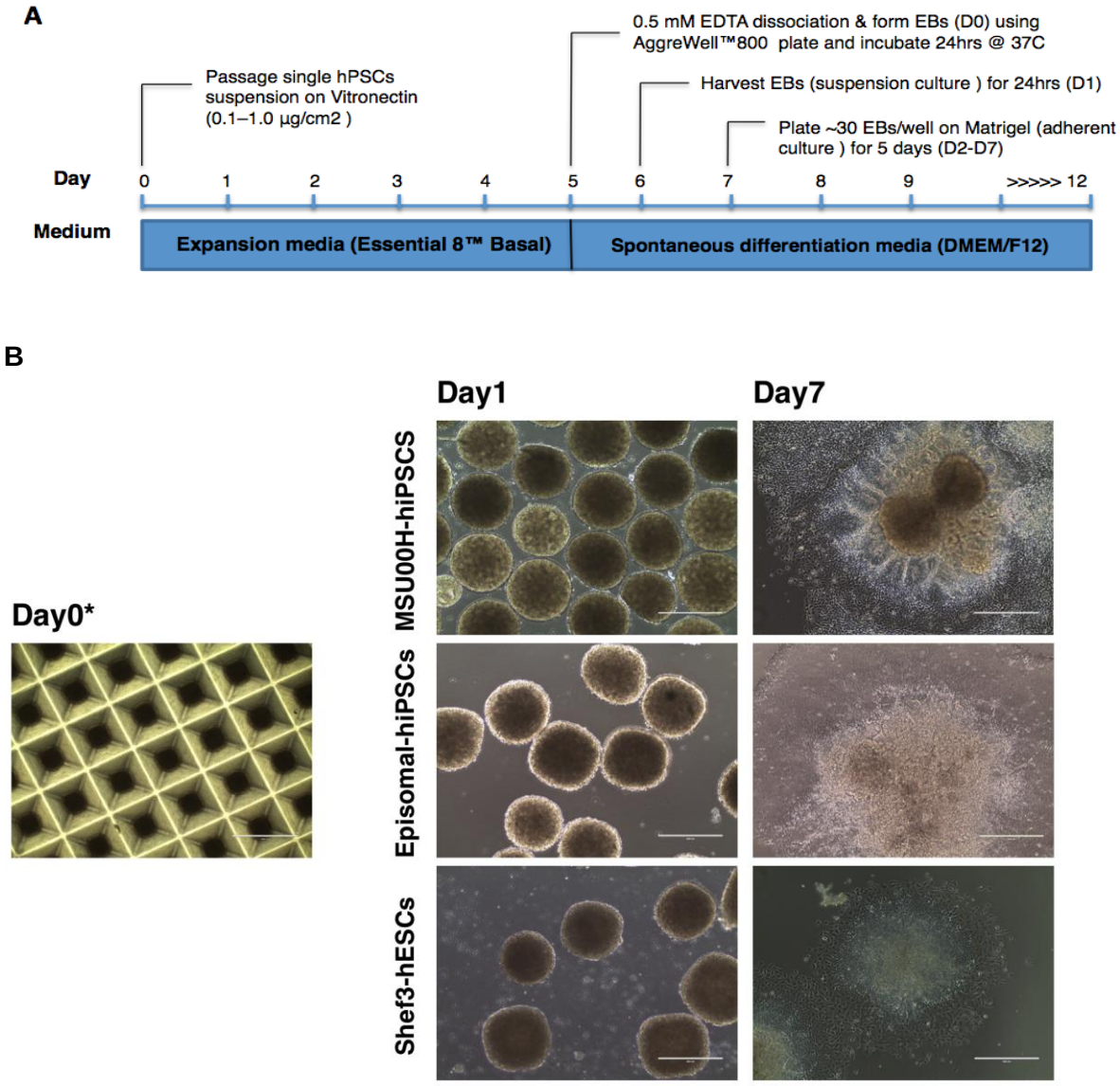

Figure 4.4 Differentiation potentials of hPSCs

(A) Timeline schematic for the spontaneous EBs differentiation protocol using AggreWellTM800 Plates. **(B)** Bright-field microscopy images showing morphological changes during spontaneous differentiation of hPSCs into three germ layers, at the earliest time-point; Day0 EBs formation by using AggreWell^{TM} 800 plates (Magnification 4X, bar=1000µm). At Day1, EBs were harvested and kept in suspension for 24hrs. Then, around 30 EBs were collected under a dissecting microscope and plated on Matrigel-coated plates for 5 days (Magnification 10X, bar= 400µm). Day7 EBs, heterogeneous population of differentiated cells (Magnification X10, bar= 400µm). Day0* Presented image is for one cell line; a similar procedure was applied for all cell lines.

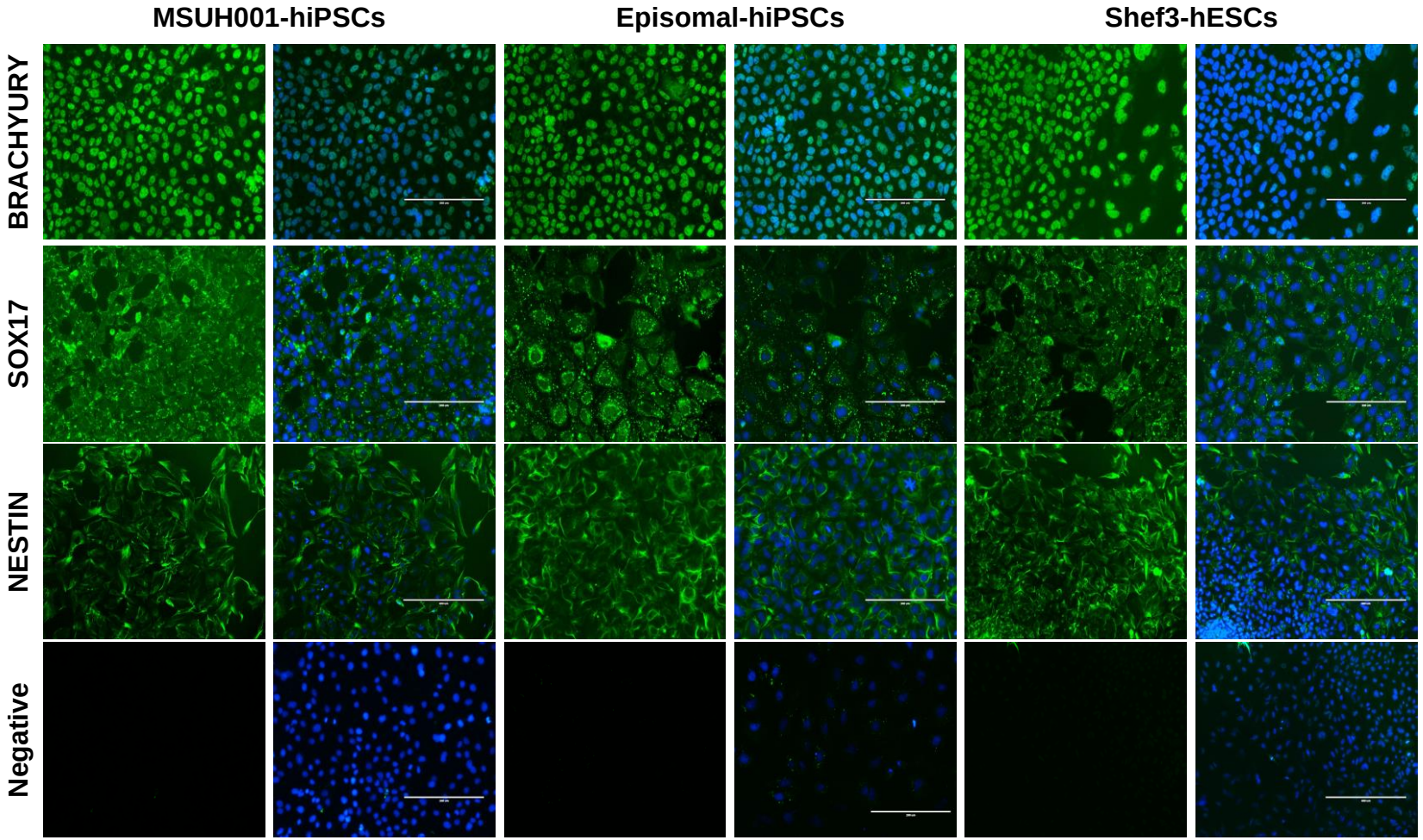

Figure 4.5 Immunostaining analysis of differentiation markers in MSUH001-hiPSCs, Episomal-hiPSCs and Shef3-hESCs.

BRACHYURY (mesodermal marker), SOX17 (endodermal marker), and NESTIN (ectodermal marker) in green. Nuclei were stained by DAPI (blue), and the corresponding merged image is represented in the right-hand panel for each marker. The negative control is undifferentiated hPSCs. (Magnification 20X, bar = 200μm)

A

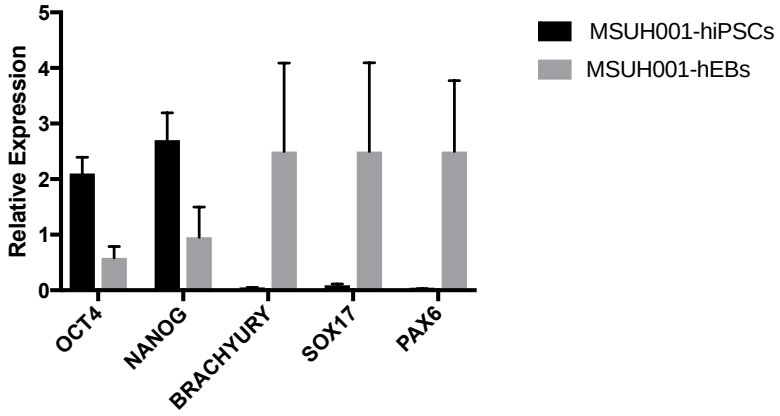

B

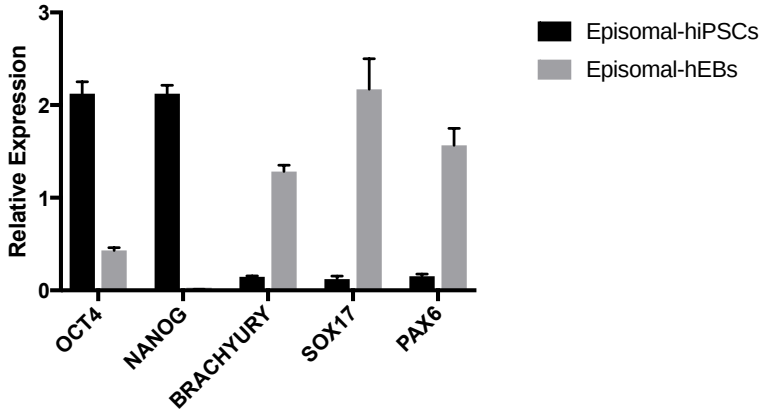

C

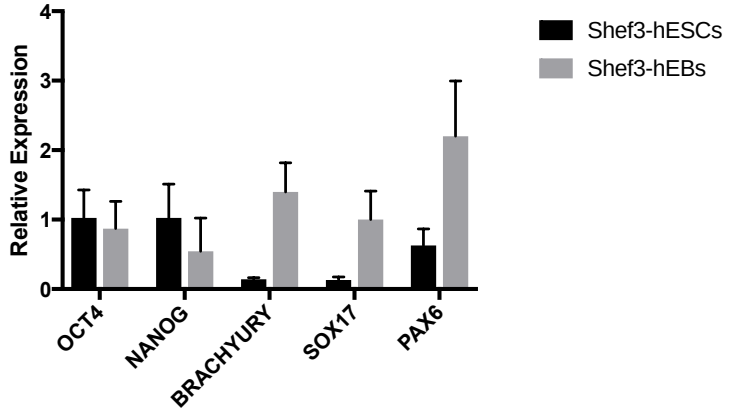

Figure 4.6 Quantification of pluripotency and differentiation gene expression by RT-qPCR.

The expression of OCT4 & NANOG (pluripotent markers) and BRACHYURY, SOX17 and PAX6 (differentiation markers) in **(A)** MSUH001-hiPSCs and their differentiating counterparts MSUH001-hEBs **(B)** Episomal-hiPSCs and Episomal-hEBs **(C)** Shef3-hESCs and Shef3-hEBs. All data have been normalised to β-actin. Data are shown as mean ± SD, unpaired two-tailed Student's t-test was used for statistical analysis (n = 3).

4.4 DISCUSSION AND CONCLUSION

It has become clear that different stem cell lines (derived from various sources) have similar 'stemness' profile, but with inherent differences in gene expression, the rate of proliferation, and differentiation capacity (Skottman et al. 2005; Hoffman & Carpenter 2005). Therefore, comparative analysis of individual stem cell line that focuses on assessing the expression of pluripotency and the differentiation markers is crucial (Ware et al. 2006; International Stem Cell Initiative et al. 2007; Feng et al. 2009; Crook et al. 2010; Needed 2012; Chen et al. 2014).

In this chapter, we have given a comparative investigation among three human stem cell lines; MSUH001-hiPSCs, Episomal-hiPSCs and Shef3-hESCs. The overall profiles of the hPSCs lines were relatively similar, despite small variations in the relative abundance of germ layers gene expression. In fact, all cell lines retained standard stem cell-like morphology and maintained their ability to self-renew, based on the persisted expression of OCT4, NANOG, SSEA-4 and TRA1-60. Additionally, the data show that undifferentiated hPSCs did not express any of the germ layers markers when they were maintained under feeder-free culture system (Figure 4.5).

Furthermore, the results show that hPSCs lines gave rise to the progeny of all three germ layers, as revealed by the expression of BRACHYURY (mesoderm), SOX17 (endoderm) and PAX6 & NESTIN (ectoderm), which indicates that the multilineage differentiation potential of hPSCs observed mimics the human embryonic development in terms of expressing endoderm, ectoderm and mesoderm markers (Poh et al. 2014).

Given all the drawbacks of feeder-dependent cultures system (e.g. introduction of animal-derived pathogens to the human stem cells), it was decided to use xeno-free culture in combination with chemically defined Essential 8™ Medium and Vitronectin. Our data confirmed that switching to this system did not break the main hPSCs features during *in vitro* cultivation

but instead supported scalable hPSCs expansion, which substantiated the results of previous studies (Chen et al. 2011; Badenes et al. 2016).

Collectively, the data indicate that all human stem cell lines provide a good candidate for examining the effect of a wide range of oxygen tensions on the proliferation characteristics and the early differentiation potentials of hPSCs (see chapter 5 and 6, respectively).

5 CHAPTER 5: STUDY THE EFFECT OF DIFFERENT OXYGEN TENSIONS ON THE BEHAVIOUR OF UNDIFFERENTIATED HPSCS

5.1 INTRODUCTION

The following section will summarize the relevant literature, which was previously discussed in Chapter 1.

Human ESCs are derived from ICM of the pre-implantation embryo, in a relatively low oxygen microenvironment (~1.5% O_2) (Rodesch et al. 1992; Jauniaux et al. 1999; Burton & Jaunaiux 2001). An environment that has been shown to improve the *in vitro* embryos culture of several species including human (Dumoulin et al. 1999; Petersen et al. 2005), mouse (Orsi & Leese 2001) and bovine (Olson & Seidel 2000). Also, *in vitro* hypoxic culture conditions (2% - 5% O_2) have been shown to maintain pluripotency of hPSCs, prevent spontaneous differentiation and reduce chromosomal abnormalities (Ezashi et al. 2005; Forsyth et al. 2008; Forristal et al. 2010). However, another study has suggested that culturing under 5% O_2 was not beneficial for maintaining hESCs in the undifferentiated state (Chen et al. 2009). Therefore, the effect of hypoxia on hPSCs properties remains controversial, requiring further research.

The majority of *in vitro* maintenance protocols to date compare atmospheric conditions (20% O_2) with one or two hypoxic conditions, ranging from 1%-5% O_2. As a result, there is a lack of information on how intermediate oxygen tensions (e.g. 0.1%, 8% and 12% O_2) regulate the behaviour of hPSCs. There is also limited information on the response of hPSCs to small changes in oxygen levels, and whether this has a role in stem cell fate decisions.

5.2 AIM

The work in this chapter aimed to test the effect of a full spectrum of oxygen tensions (0%, 2%, 5%, 8%, 12% and 20% O_2) on the short-term maintenance of hPSCs. Morphological changes of hPSCs under different O_2 tensions were examined using phase contrast microscopy, and the proliferation rate was studied using KI67 labelling. Additionally, the expression of markers associated with pluripotency, metabolism and hypoxia was analysed using RT-qPCR, and immunostaining. All experimental conditions were compared to standard culture condition at 20% O_2. Due to the higher passage number of MSUH001-hiPSCs (P72-77), it was decided from this chapter and onward that Episomal-hiPSCs and Shef3-hESCs will be used to test our hypothesis in chapters 5 and 6.

5.3 RESULTS

5.3.1 Pluripotency Analysis of hPSCs Maintained under Different Oxygen Tensions

To investigate the effects of different oxygen tensions on the self-renewal and proliferation properties of Episomal-hiPSCs and Shef3-hESCs, cells were passaged as a single cell suspension using TrypLE^{TM}, instead of the traditional manual techniques (e.g. manually scraping of the undifferentiated colonies). This seeding protocol resulted in better control over cell number and allowed for uniform and consistent initial seeding density (0.6X10^5 cells/cm^2). Then, cells were maintained in parallel under normoxic (20% O_2) and hypoxic (0%, 2%, 5%, 8% and 12% O_2) conditions for three days. All incubations and daily changes of culture medium were performed under strictly controlled oxygen conditions, which means that cells were not expose to ambient air at any stage of the experiment (Figure 5.1) (using C-Shuttle Glove Box and C-Chambers for transportation).

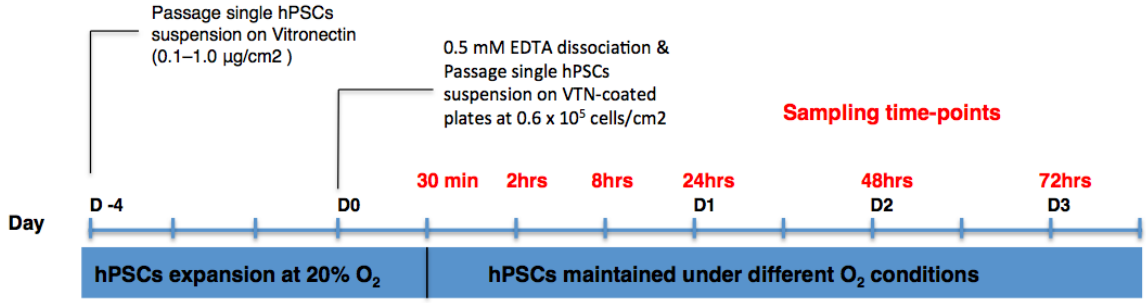

Figure 5.1 Schematic representation of the maintenance protocol of hPSCs under different oxygen conditions.
D0 indicates the initiation of hPSCs culture under different oxygen conditions (0%, 2%, 5%, 8%, 12% and 20% O_2). Red text represents the sampling time-points where the samples are collected for the downstream analysis.

5.3.1.1 Morphology of hPSCs

In this experiment we looked into two aspects; (i) the morphology of the cells and (ii) the time needed for cells to recover and adhere after initial seeding stress under all oxygen tensions.

Phase contrast images reveal that Episomal-hiPSCs attached to culture plates and expanded under all oxygen tensions following 24hrs. Episomal-hiPSCs exhibited a typical stem cell-like morphology with a high N/C ratio (Figure 5.2-magnified images) and formed relatively small and flat colonies (Figure 5.2). After 24hrs, it became apparent that the cells were proliferating and grew closer together leaving less space between the adjacent colonies. This observation was accompanied by a decrease in the number of floating cells over the culture period as evident visually. However, some floating cells remained in some culture conditions; this is a common phenomenon in hPSCs cultures (Krishna Dasa SS et al. 2014), which indicates that the cells were still recovering from the shear stress following initial seeding (Figure 5.2, red arrows). Interestingly, after 72hrs, colonies under 2% and 20% O_2 conditions were more abundant in size and denser in cell number than the other oxygen conditions (Figure 5.2, white arrows).

Having observed the effects of different oxygen tensions on Episomal-hiPSCs morphology, this experiment was performed to establish if similar morphological changes would be found in Shef3-hESCs. Phase contrast images show that cells attached to culture plates under all oxygen tension cultures. During the earlier time point of culture (24hrs), cells exhibited stem cell-like morphology with a high N/C ratio (Figure 5.3, magnified images), and expanding to form relatively small and flat colonies (Figure 5.3). However, there was a noticeable transition from rounded colonies to more pointy-edge colonies formed by Shef3-hESCs (Figure 5.3, red arrow). Following 24hrs and 48hrs of culture, colonies became considerably larger under 8%, 12% and 20% O_2 conditions than those observed under 0%, 2% and 5% O_2 conditions (Figure 5.3, white lines). By culture period of 72hrs, colonies became more ‘spiky’ with less spherical morphology. Interestingly, Shef3-hESCs maintained

under 5%, and 20% O_2 began to show signs of spontaneous differentiation as evident by the emergence of flattened cells with translucent cytoplasm forming colonies with a white space in an intercellular area (Figure 5.3, white arrows), the data are on agreement with (Forristal et al. 2010; Wakui et al. 2017).

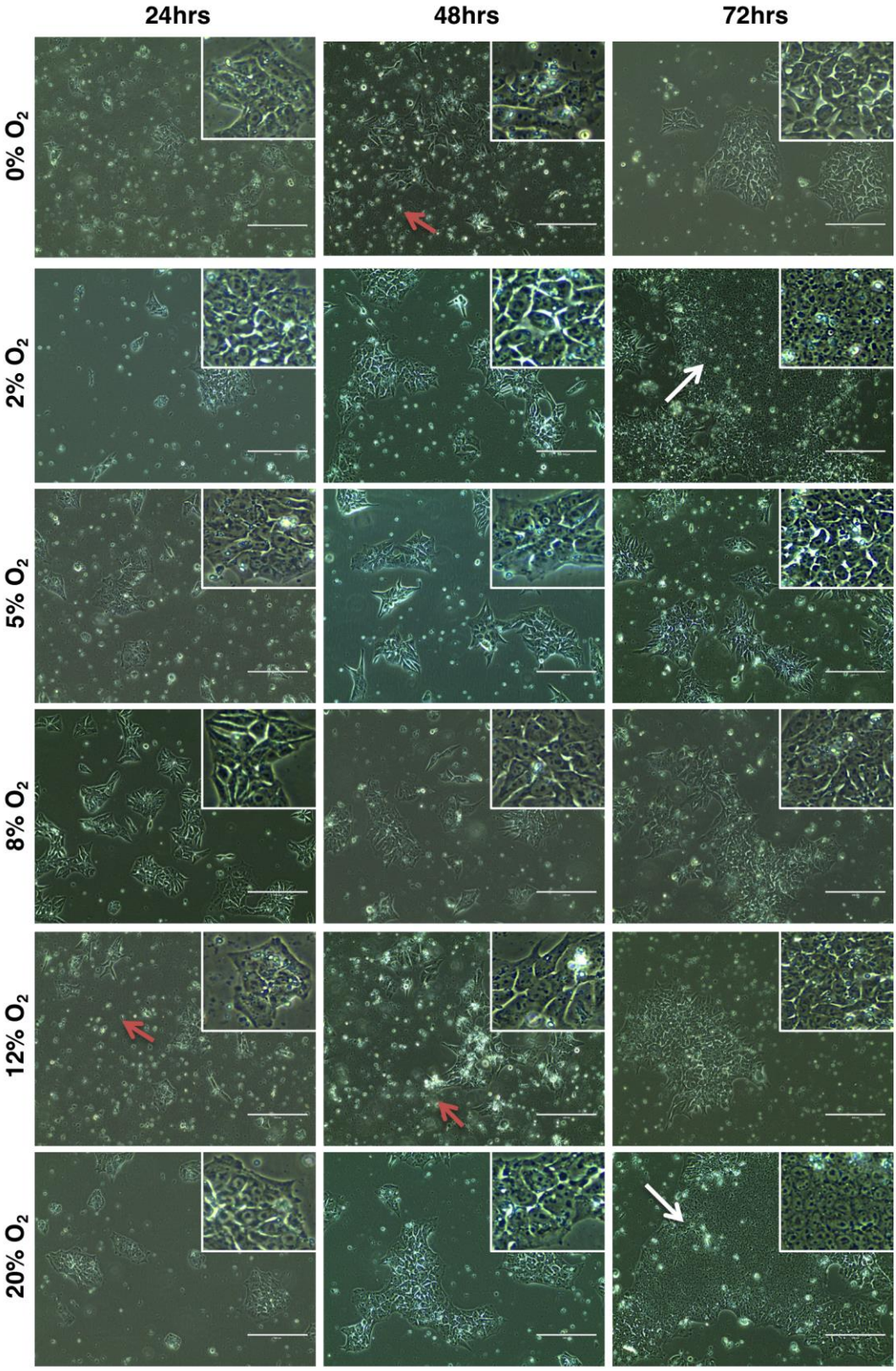

Figure 5.2 Phase contrast images show the spatial distribution of Episomal-hiPSCs cultured under different oxygen conditions at 24hrs, 48hrs and 72hrs. Cells exhibited stem cell-like morphology with high N/C ratios and large condensed nuclei (Magnified images). Episomal-hiPSCs formed dense colonies at 2% and 20% O_2 (white arrows). Floating cells (red arrows) (Magnification 20X bar=200µm).

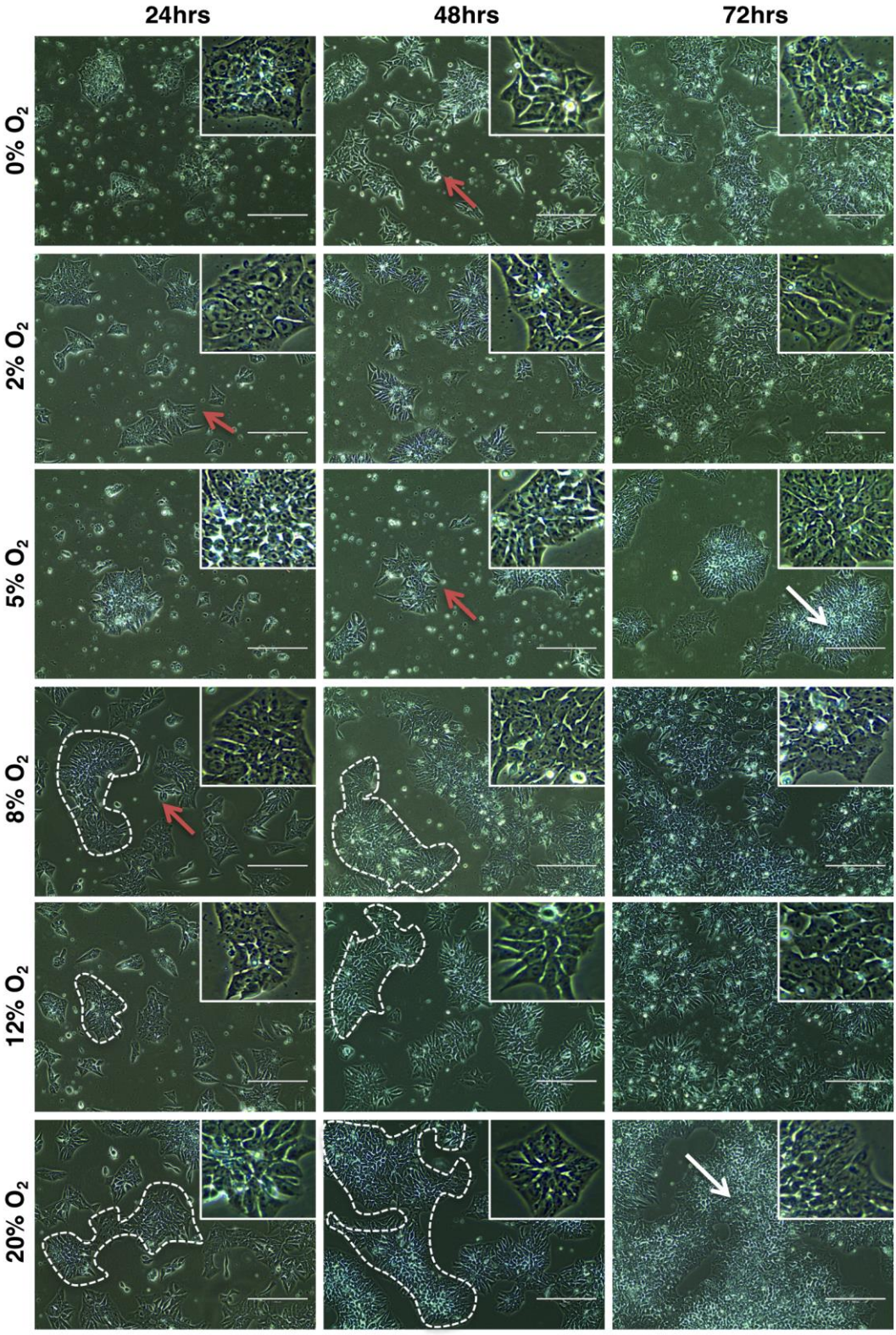

Figure 5.3 Phase contrast images show the spatial distribution of Shef3-hESCs cultured under different oxygen conditions at 24hrs, 48hrs and 72hrs.
Cells exhibited stem cell-like morphology with high N/C ratios (Magnified images). Shef3-hESCs formed large colonies at 8%, 12% and 20% O_2 (white dash lines). Colonies with a white space in an intercellular space under 5% and 20% O_2 (White arrows). Pointy-edge colonies (red arrows) (Magnification 20X bar=200µm).

5.3.1.2 Proliferative response of hPSCs under different oxygen conditions

To determine the effect of different oxygen tensions on the proliferative capacity of hPSCs, cells were cultured at 0%, 2%, 5%, 8%, 12% and 20% O_2 for three days, as described in (Figure 5.1) and Population Doubling Time (PDT) was calculated. The data show that Episomal-hiPSCs cultured under 0%, 2% and 5% O_2 displayed a higher PDT, the difference was significant under 2% O_2 compared to 20% O_2 (Figure 5.4A). A similar profile was observed in Shef3-hESCs where PDT was significantly higher under 0% and 2% O_2, compared to 20% O_2 (Figure 5.4B). In contrast to the general trend, Shef3-hESCs cultured under 5% O_2 displayed low PDT but the difference was not significant, compared to 20%O_2. Additionally, Episomal-hiPSCs and Shef3-hESCs cultured under 8%, 12% and 20% O_2 yielded higher total cell numbers at 72hrs as shown in Appendices 8.2A and B. Together, these results indicate a higher proliferation rate of Episomal-hiPSCs and Shef3-hESCs under 8%, 12% and 20% O_2. While cells maintained under 0%, 2% and 5% O_2 grew at slower rates.

We also investigated whether changes in oxygen tensions influence the proportion of cells that are actively committed to cell division. Episomal-hiPSCs and Shef3-hESCs were stained for the proliferation biomarker KI67 at the end of the culture period (72hrs). The KI67 antigen is expressed in the nucleus of dividing cells that are in the G1, S, G2, and M phases of the cell cycle, but not those in the G0 phase (Schwarting et al. 1986). Although the growth profile was different between conditions as evident by PDT results, Episomal-hiPSCs and Shef3-hESCs under all oxygen tensions had a high expression of KI67 (Figure 5.4C and D). However, a significant reduction in the percentage of KI67 positive cells was observed in Episomal-hiPSCs and Shef3-hESCs cultured under 0% O_2 in comparison to those cultured under normoxic conditions (20% O_2) (Figure 5.4C and D). These might suggest that a proportion of these cells experienced cell cycle arrest and cells were undergoing apoptosis, which may have been due to oxygen deprivation. Indeed, this culture condition generated high numbers of floating cells when

compared to other O_2 conditions at the end of culture period (72hrs) in both cell lines (Appendices 8.2C and D). We also noticed that there was a significant reduction of KI67 in Episomal-hiPSCs cultured at 12% O_2 in comparison to those cultured under normoxic conditions (20% O_2) (Figure 5.4C). Cells under this condition detached and final cell number was very low which might affect the reduction in KI67 staining. The results also suggest that sustained proliferation capacity observed in Episomal-hiPSCs and Shef3-hESCs throughout the culture period (72hrs) indicates that these cells did not enter the post-mitotic state required for differentiation, which further suggests the undifferentiated phenotype of these cells.

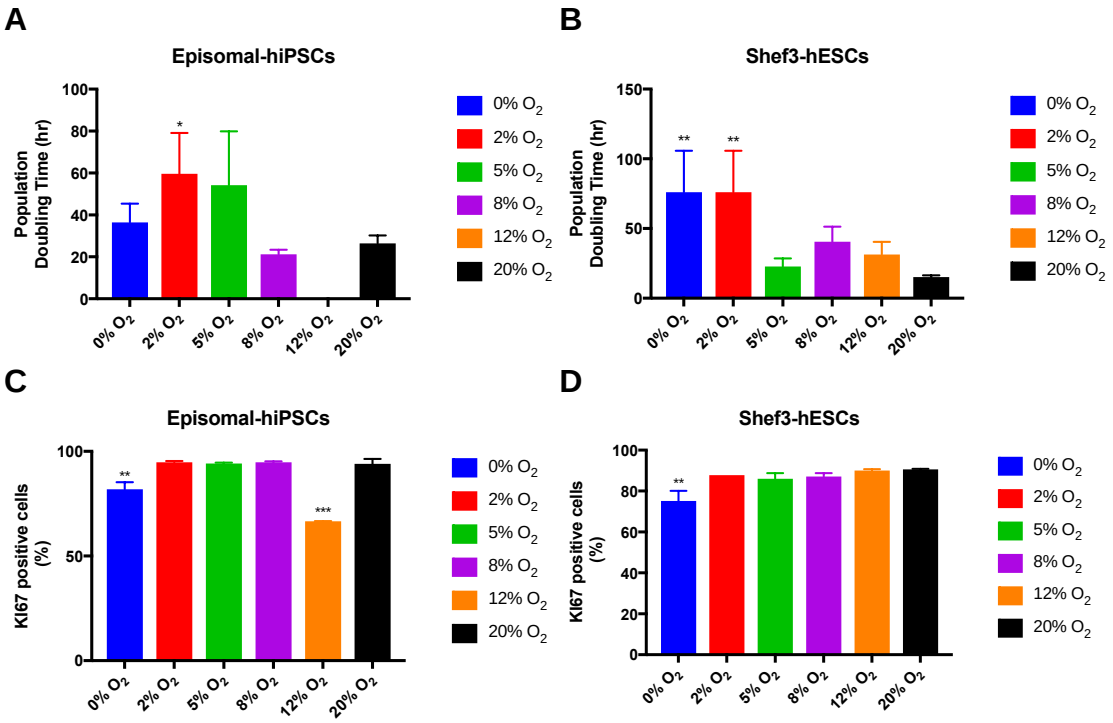

Figure 5.4 Proliferation responses of Episomal-hiPSCs and Shef3-hESCs cultured under different oxygen tensions (0%, 2%, 5%, 8%, 12% and 20% O_2). PDT analysis in hour of **(A)** Episomal-hiPSCs and **(B)** Shef3-hESCs. Data are shown as mean ± SD, (n = 3). Data points from Episomal-hiPSCs cultured under 12% O_2 were excluded from the graph, as the cells were detaching, and the final cell number was lower than the initial cell number. Detection of KI67 in hPSCs by Flow Cytometry in **(C)** Episomal-hiPSCs and **(D)** Shef3-hESCs. Cells were stained with proliferation marker KI67 at 72hrs. Positive KI67 expression was gated on unstained cells, and FITC-conjugated antibody of isotype was used as a negative control. Data are shown as mean ± SD, (n=2). One-way ANOVA with Dunnett's multiple comparisons test was used for statistics analysis *($p \leq 0.05$), **($p \leq 0.01$), ***($p \leq 0.001$), ****($p \leq 0.0001$), relative to 20% O_2.

5.3.1.3 Influence on pluripotency genes expression

OCT4 Fand NANOG are the core transcription factors governing hPSCs self-renewal and differentiation (Boyer et al. 2005; Närvä et al. 2013). To study whether OCT4 and NANOG gene regulation is influenced by changes in oxygen tensions, gene expression was analysed with RT-qPCR. Cells were cultured under 0%, 2%, 5%, 8%, 12% and 20% O_2 and the gene expression was analysed at 72hrs in both cell lines.

The data show that changes in oxygen tensions did not alter the expression pattern of OCT4 and NANOG genes in Episomal-hiPSCs and Shef3-hESCs, compared to the normoxic culture (20% O_2) (Figure 5.5A and B). Suggesting that OCT4 and NANOG expression is not solely governed by hypoxia, our results are on an agreement with others (Närvä et al. 2013). It is interesting to note that OCT4 and NANOG were differentially expressed between cell lines; this is apparently due to the inherent variability between specific iPSCs and ESCs lines (Chin et al. 2009; Bar-Nur et al. 2011).

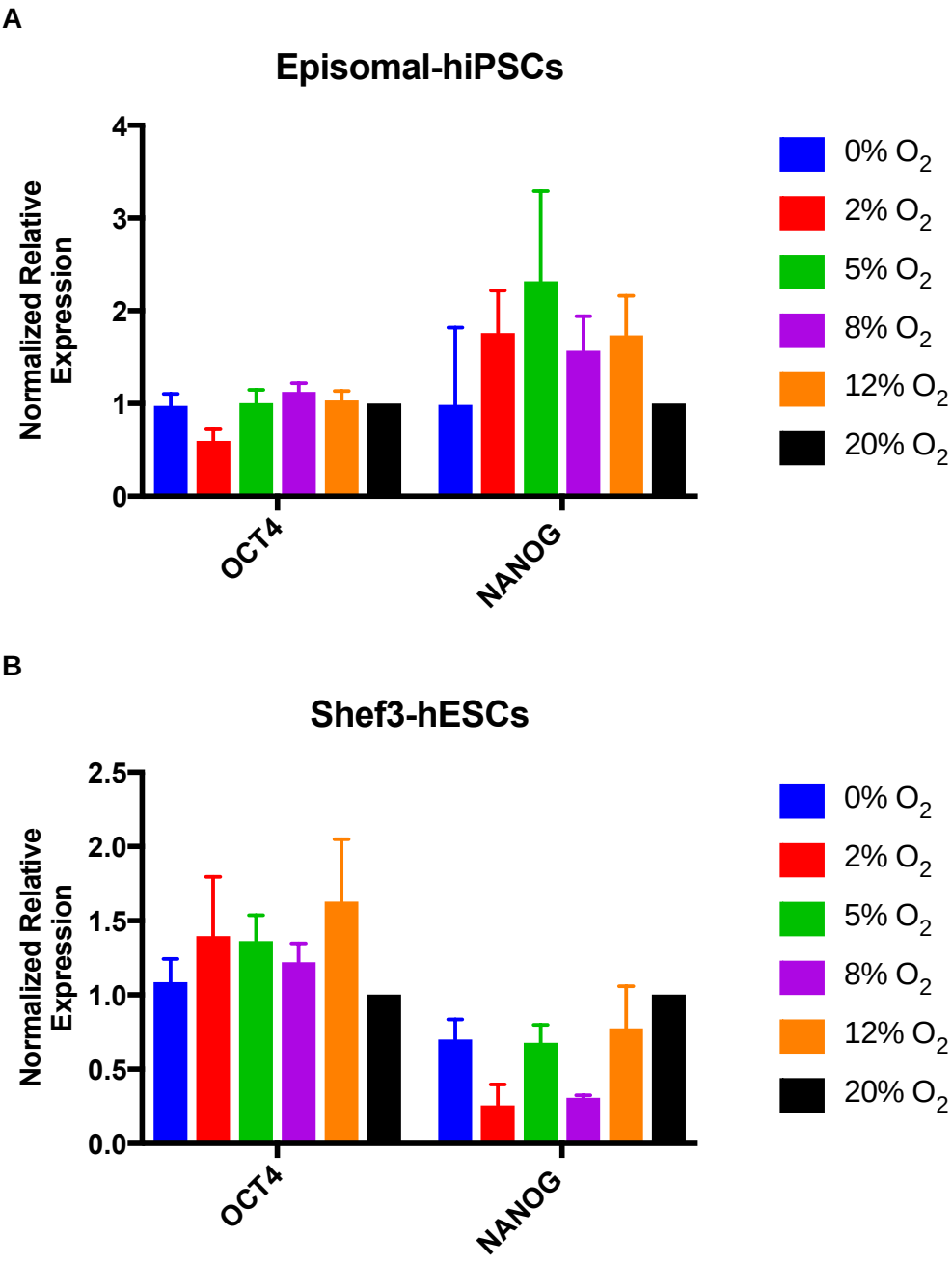

Figure 5.5 Quantification of OCT4 and NANOG gene expression by RT-qPCR
(A) Episomal-hiPSCs and **(B)** Shef3-hESCs cultured under 0%, 2%, 5%, 8%, 12% and 20% O_2. All data have been normalised to β-actin and 1 for cells cultured at 20% O_2. Data are shown as mean ± SD, Two-way ANOVA with Dunnett's multiple comparisons test was used for statistical analysis (n = 3).

5.3.2 Hypoxia Responses of hPSCs maintained under Different Oxygen Tensions

5.3.2.1 HIF-1A orchestrates universal oxygen response, while HIF-2A has more limited oxygen sensing feature

In response to reduced oxygen tensions, HIF-A subunits (HIF-1A and HIF-2A) accumulate in the cytosol in the cytoplasm and translocate into the nucleus where it dimerises with HIF-1B. Activated HIF-1A/B dimer plays a crucial role in adaptive responses to changes in oxygen tensions through transactivating over 200 downstream genes involved in cell metabolism, angiogenesis and erythropoiesis (Gassmann & Wenger 1997; Wenger et al. 1997; Chilov et al. 1999b). HIF-1A plays a role in the initial adaptation to hypoxia (acute <24hrs) while HIF-2A is responsible for maintaining the hypoxic response (chronic ≥24hrs) (Forristal et al. 2010; Kumar & Choi 2015).

Here, we sought to investigate whether different oxygen tensions differentially regulate acute and chronic responses in Episomal-hiPSCs and Shef3-hESCs. Cells were analysed for HIF-1A and HIF-2A expression at time points equals to 30 min, 2hrs, 8hrs, 24hrs, 48hrs and 72hrs, to assess acute and chronic responses qualitatively (protein stabilisation by Immunostaining) and quantitatively (gene expression by RT-qPCR).

HIF-1A can be tricky to detect in the nucleus, as it has a very short half-life after reoxygenation (<5min) (Semenza 2014), which can be troublesome. Also, because this was the first time these cell lines were analysed for HIF-1A protein. It was necessary to establish a positive control data for HIF-1A staining/localisation pattern, to which HIF-1A protein in the Episomal-hiPSCs and Shef3-hESCs can be compared. As mentioned in (Chapter 2), cells were incubated with DMOG, a commonly used drug to stabilise of HIF-1A protein at 20% O_2 (Jaakkola et al. 2001; Elks et al. 2011).

In this experiment, different concentrations of DMOG were used to find a detectable level of HIF-1A protein in the nucleus. The results show that after 24hrs of incubation, DOMG induced HIF-1A stabilisation in a concentration-dependent manner (Figure 5.6), highest staining intensity was detected at a concentration of 2mM. This was then used as a positive control when analysing staining/localisation pattern of HIF-1A protein under different oxygen tensions in Episomal-hiPSCs and Shef3-hESCs.

Immunostaining analyses reveal discrete dot-like structures of HIF-1A protein throughout the nucleus in both cell lines, which is consistent with (Berchner-Pfannschmidt et al. 2004). The data also show that hypoxia levels of 0%, 2%, 5%, 8% and 12% O_2 caused a concentration- and time-dependent increase in HIF-1A nuclear accumulation in Episomal-hiPSCs and Shef3-hESCs (Figure 5.7A and B) and (Figure 5.8A and B). As the more severe the hypoxic exposure, the faster it will take for HIF-1A to translocate into the nucleus. No protein was detected under 20% O_2 in both cell lines at all-time points tested (data are shown for one-time point, as the pattern was negative for the rest of time points) (Figure 5.7B) and (Figure 5.8B). The level of HIF-1A protein was almost undetectable after prolonged 24hrs culture under all oxygen conditions in both cell lines; the results are included in Appendix 8.3A and B. These results (i) imply the role of HIF-1A in acute hypoxic response and (ii) provide a further evidence on the fact that HIF-1A protein is transiently expressed in the nucleus, which is consistent with previous studies (Hu et al. 2003; Cameron et al. 2008; Forristal et al. 2010; Bagnall et al. 2014; Pimton et al. 2014; Xie et al. 2014).

To further assess the chronic response to changes in oxygen tensions, Episomal-hiPSCs and Shef3-hESCs were analysed for the expression pattern of HIF-2A protein in time points equal to 30 min, 2hrs and 24hrs. Early time points were chosen to see if HIF-2A protein also induced in concentration- and time-dependent manner similar to those observed with HIF-1A protein. Interestingly, during the early exposure (30min and 2hrs), immunostaining of HIF-2A protein shows positive nuclear staining under 2% and 5% O_2

(Figure 5.9A) and (Figure 5.10A) in both cell lines, while the protein was found in the cytoplasm at 0%, 8%, 12%, and 20% O2 (Figure 5.9A and B) and (Figure 5.10A and B), in both cell lines. Following chronic exposure (≥24hrs), Episomal-hiPSCs and Shef3-hESCs displayed a predominantly cytoplasmic expression under all oxygen conditions (Figure 5.9) and (Figure 5.10), respectively. These data suggest that HIF-2A has more restrict ability to sense changes in oxygen tension than HIF-1A, which could be an indication for its limited function. These data give further evidence that HIF-1A and HIF-2A have different regulatory roles; these results are in good agreement with other reports (Loboda et al. 2010; Dengler et al. 2014).

Given the fact that HIF-1B protein expression is independent of oxygen availability as it constitutively expressed in all cells (Forristal et al. 2010). Additionally, considering that fact that HIF-A subunits accumulation in the nucleus is independent of the presence of HIF-1B (Chilov et al. 1999). It was therefore not necessary to investigate the localisation of HIF-1B protein in Episomal-hiPSCs and Shef3-hESCs.

The data presented here reveal for the first time that HIF-1A could be detected, on a cellular level, in Episomal-hiPSCs and Shef3-hESCs by the mean of Immunostaining. However, this requires careful sample collection and manipulation (described in section 2.2.4.1).

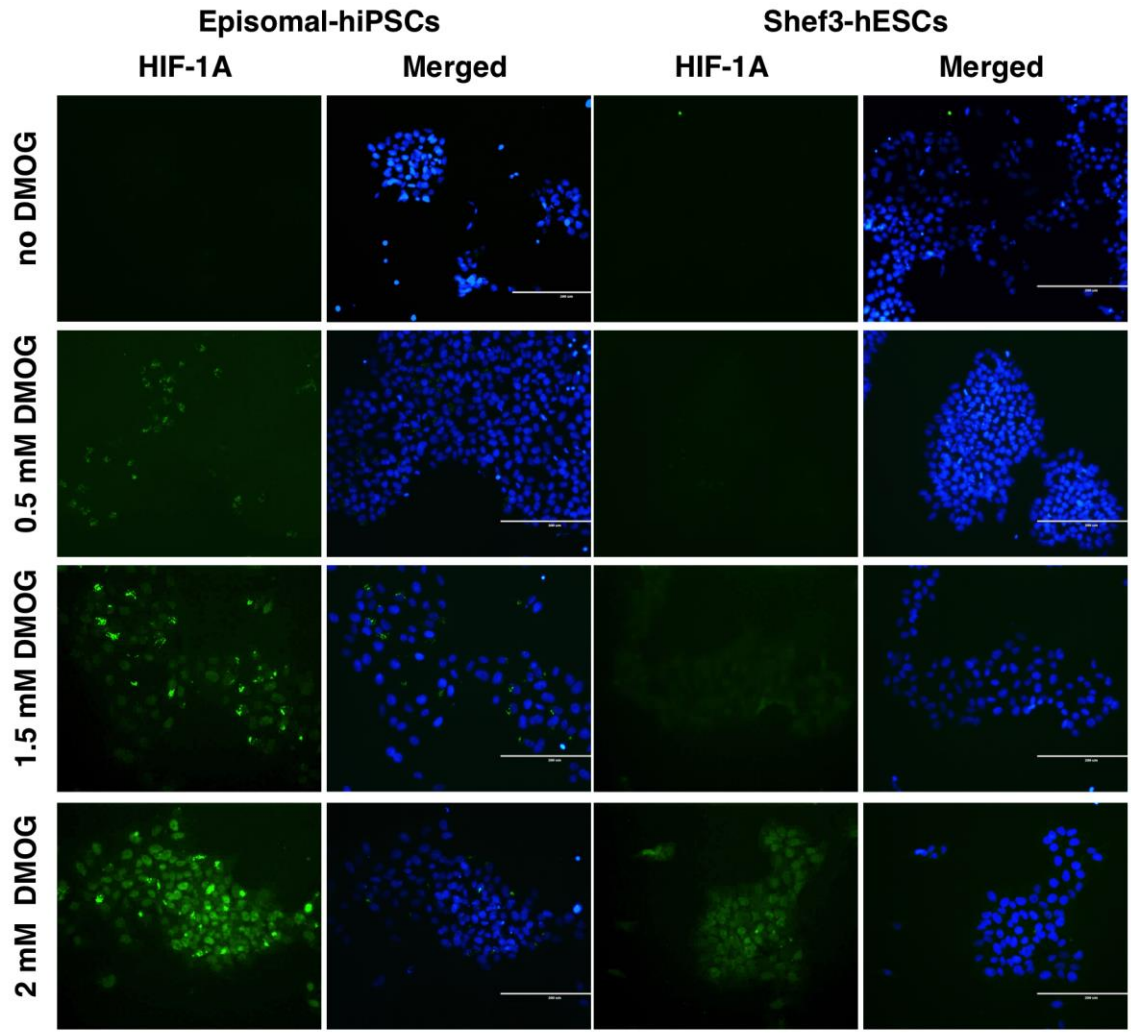

Figure 5.6 Establishing the localisation pattern of HIF-1A protein (green) in Episomal-hiPSCs and Shef3-hESCs.

Cells were treated with DMOG drug (PHD inhibitor) for 24hrs on different concentrations to assess the detectable protein expression and to validate the localisation pattern of HIF-1A protein in tested cell lines. Immunofluorescence microscopy was used to analyse HIF-1A protein expression (green) on a cellular level, Nuclei were stained by DAPI (blue), and the corresponding merged image is represented in the right-hand panel for each cell line (Magnification X20, Bar= 200µm).

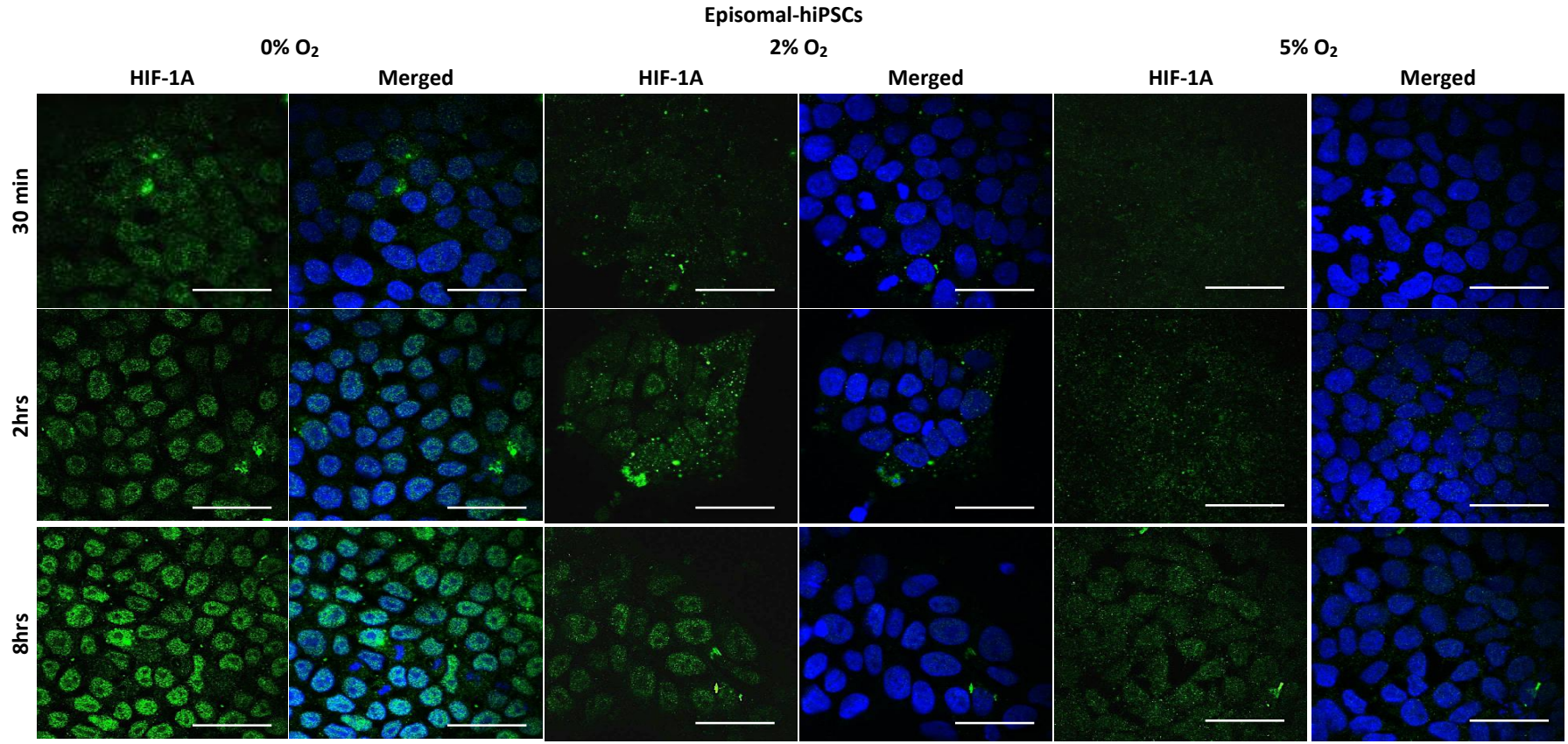

Figure 5.7 Confocal images show the time course analysis of HIF-1A protein expression (green) in Episomal-hiPSCs during the acute response to different oxygen tensions.

Different patterns of HIF-1A nuclear localisation under different oxygen tensions. Nuclei were counterstained with DAPI (blue), and the corresponding merged image is represented in the right-hand panel (Magnification X100, bar = 40μm).

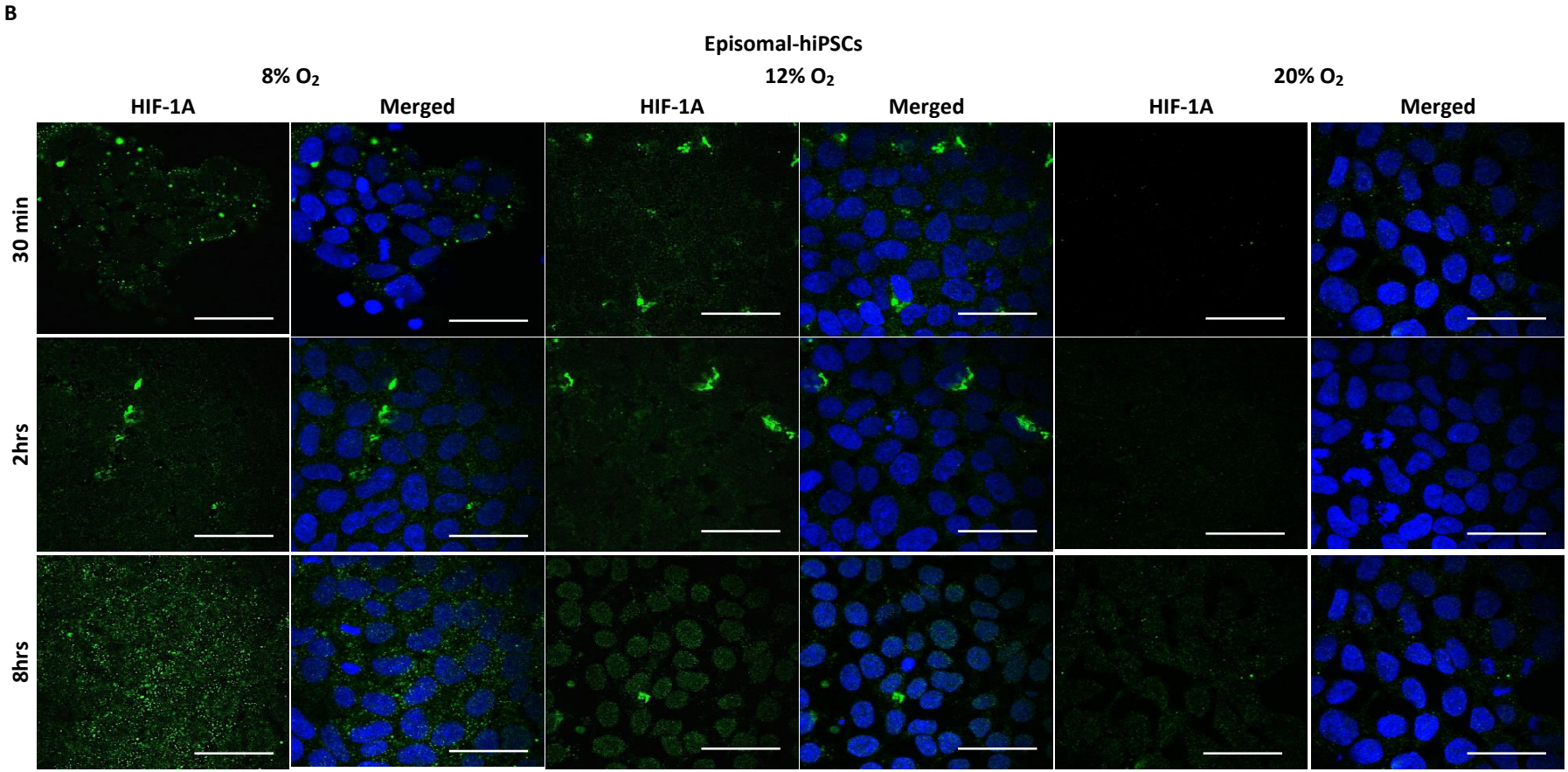

Figure 5.7 Confocal images show the time course analysis of HIF-1A protein expression (green) in Episomal-hiPSCs during the acute response to different oxygen tensions.

Different patterns of HIF-1A nuclear localisation under different oxygen tensions. Nuclei were stained by DAPI (blue), and the image is represented in the right-hand panel (Magnification X100, bar = 40µm).

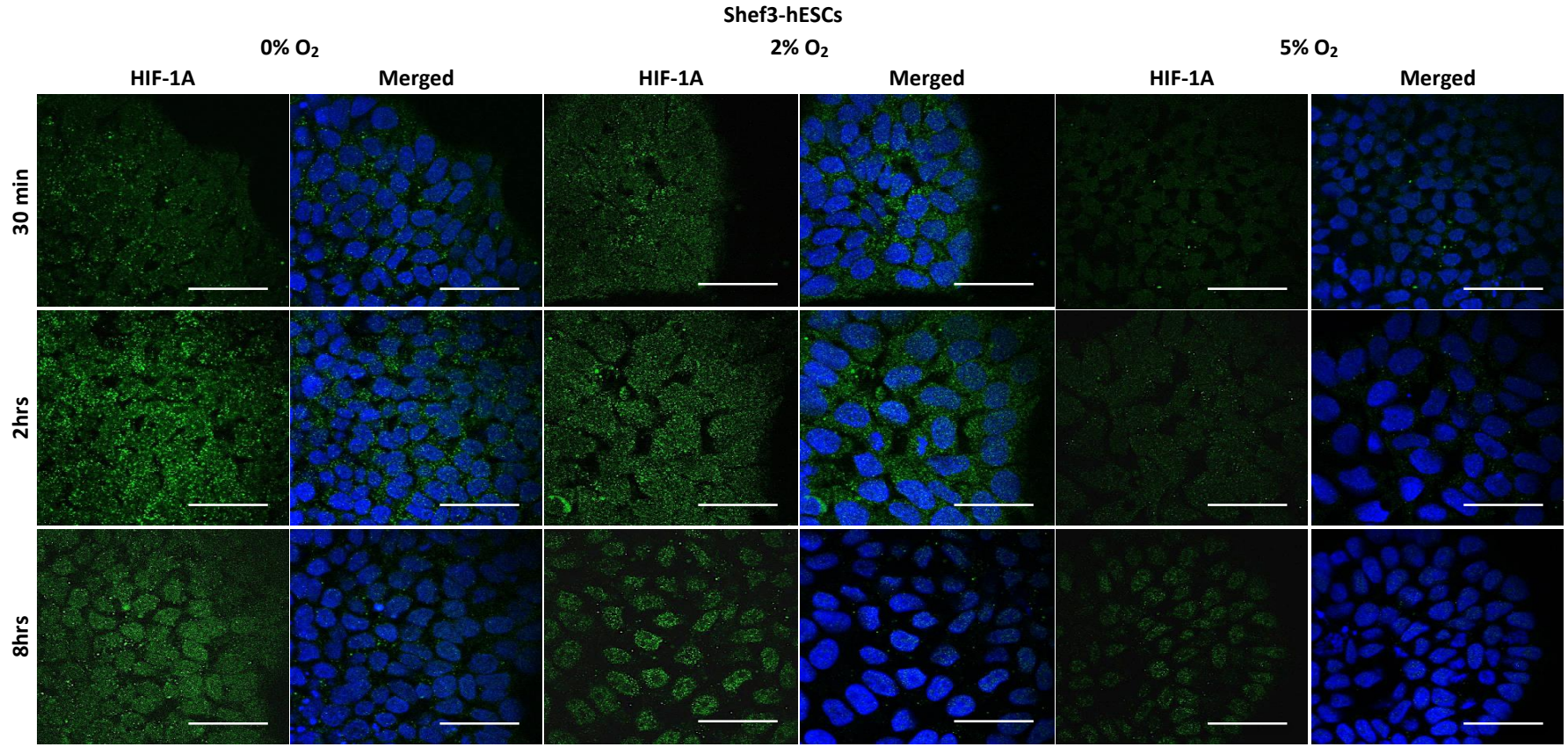

Figure 5.8 Confocal images show the time course analysis of HIF-1A protein expression (green) in Shef3-hESCs during the acute response to different oxygen tensions.

Different patterns of HIF-1A nuclear localisation under different oxygen tensions. Nuclei were stained by DAPI (blue), and the image is represented in the right-hand panel (Magnification X100, bar = 40μm).

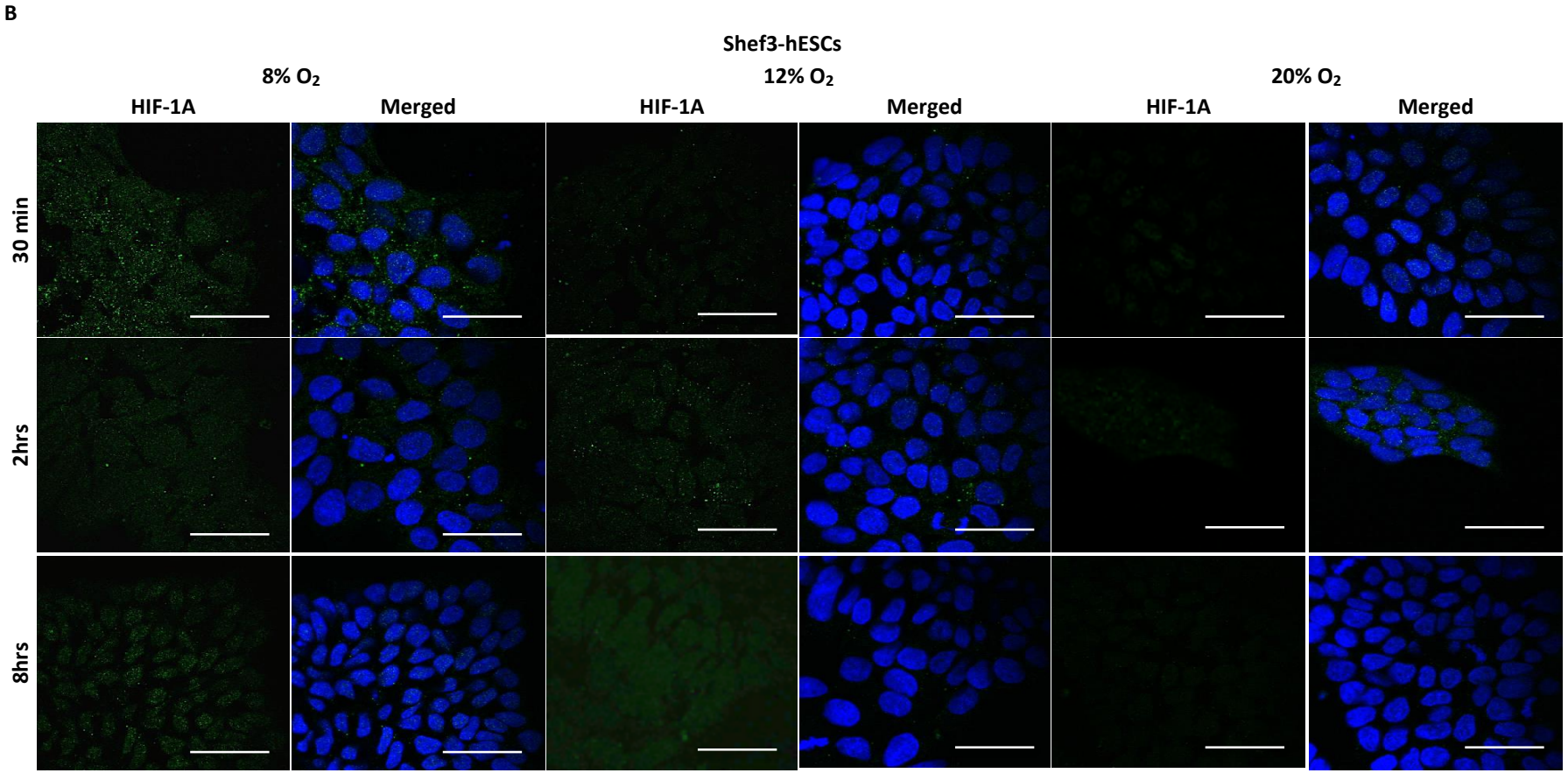

Figure 5.8 Confocal images show the time course analysis of HIF-1A protein expression (green) in Shef3-hESCs during the acute response to different oxygen tensions.

Different patterns of HIF-1A nuclear localisation under different oxygen tensions. Nuclei were stained by DAPI (blue), and the image is represented in the right-hand panel (Magnification X100, bar = 40μm).

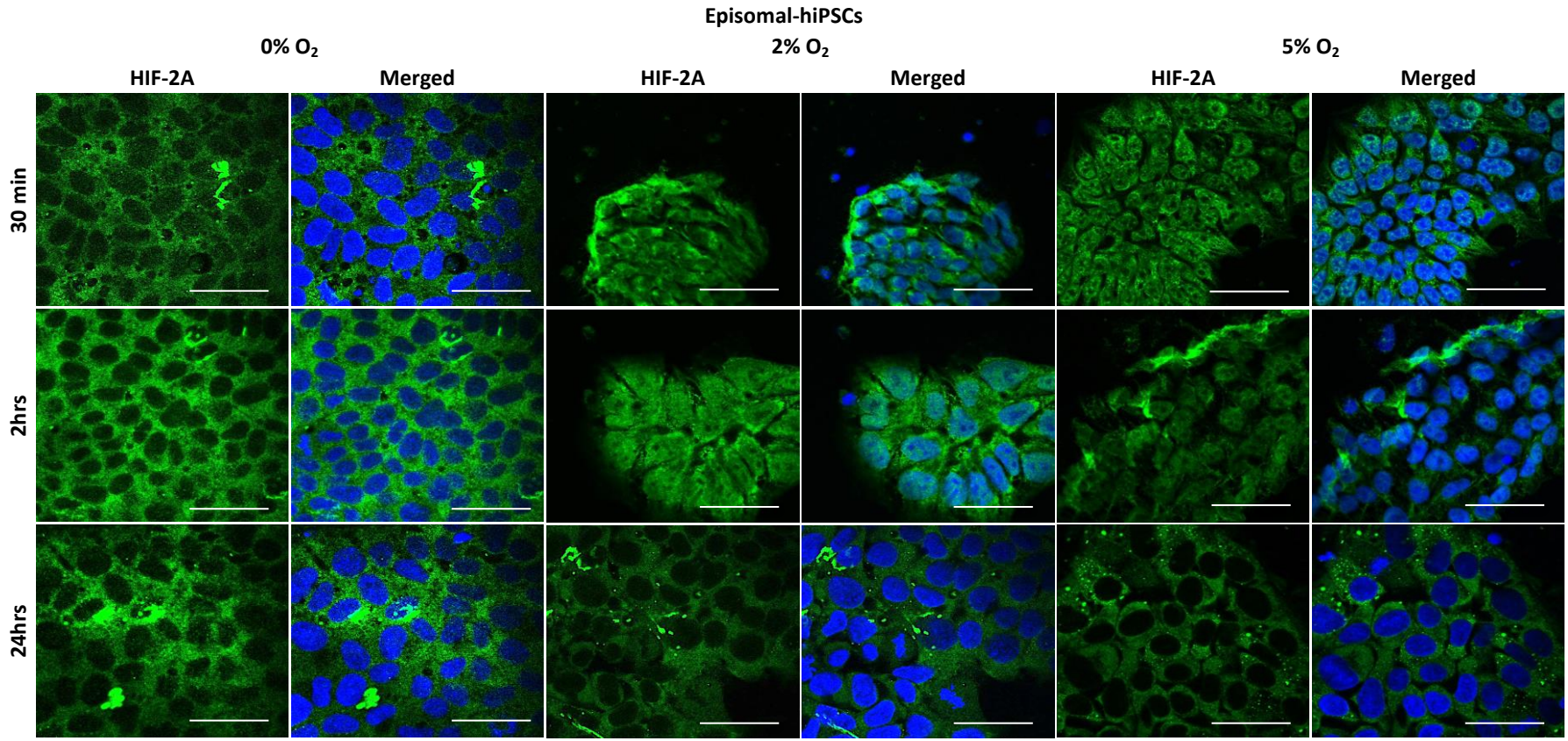

Figure 5.9 Protein expression of HIF-2A (green) by immunostaining in Episomal-hiPSCs maintained under different oxygen conditions for 30min and 2hrs (acute response) and 24hrs (chronic response).
Nuclei were counterstained with DAPI (blue), and the corresponding merged image is represented in the right-hand panel (Magnification X40, bar 100μm).

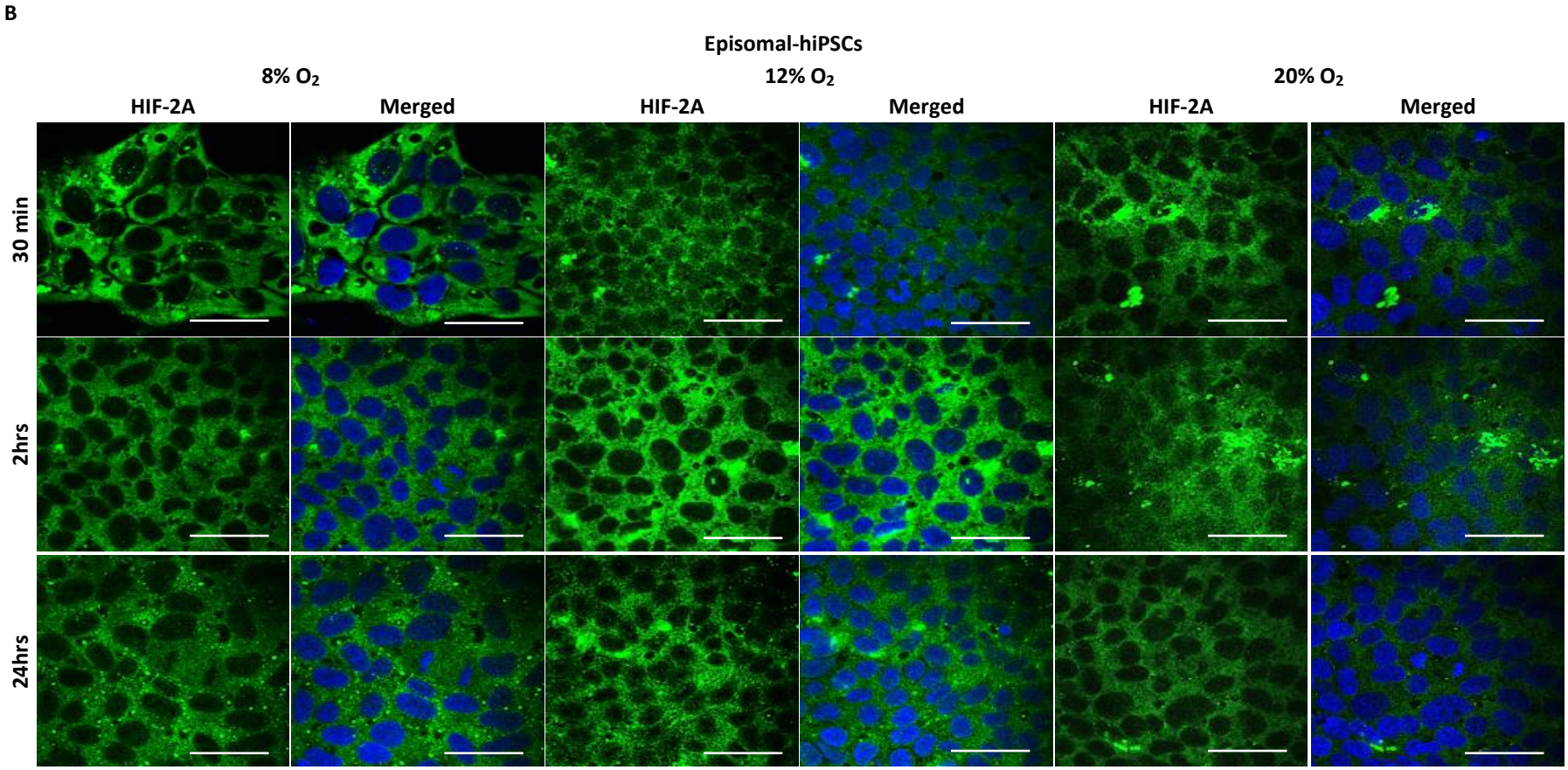

Figure 5.9 Protein expression of HIF-2A (green) by immunostaining in Episomal-hiPSCs maintained under different oxygen conditions for 30min and 2hrs (acute response) and 24hrs (chronic response).
Nuclei were counterstained with DAPI (blue), and the corresponding merged image is represented in the right-hand panel (Magnification X40, bar 100µm).

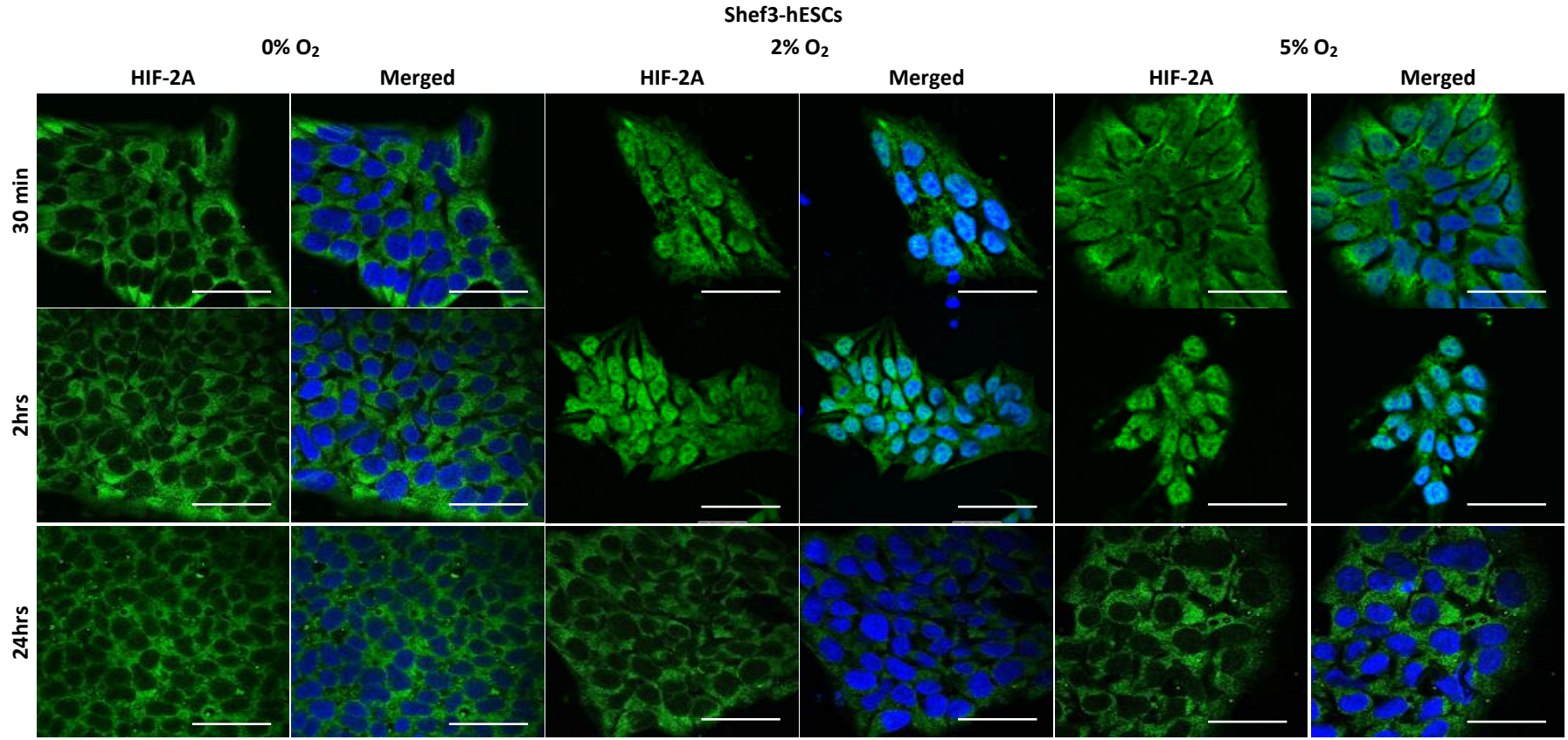

Figure 5.10 Protein expression of HIF-2A (green) by immunostaining in Shef3-hESCs maintained under different oxygen conditions for 30min and 2hrs (acute response) and 24hrs (chronic response).
Nuclei were counterstained with DAPI (blue), and the corresponding merged image is represented in the right-hand panel (Magnification X40, bar 100μm).

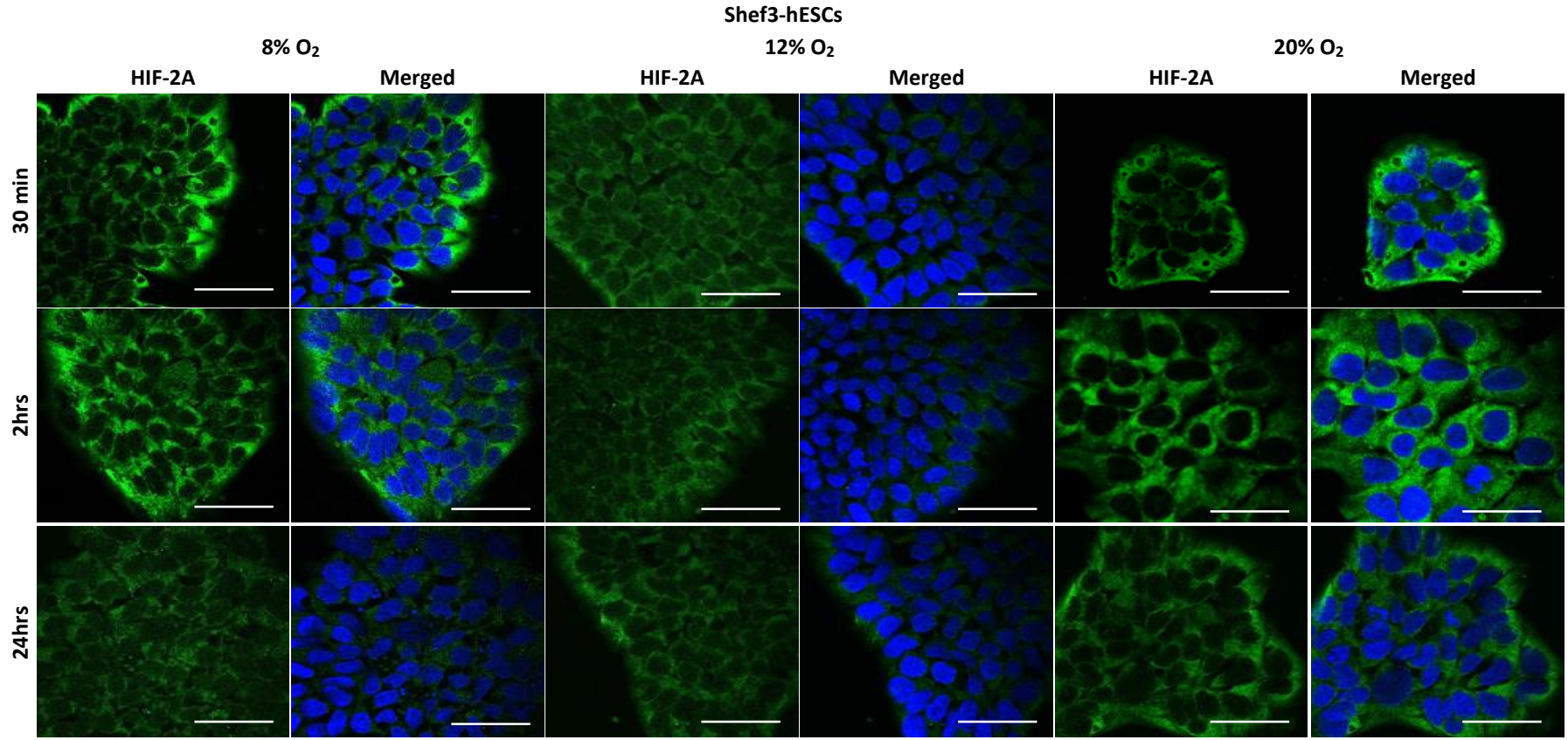

Figure 5.10 Protein expression of HIF-2A (green) by immunostaining in Shef3-hESCs maintained under different oxygen conditions for 30min and 2hrs (acute response) and 24hrs (chronic response).
Nuclei were counterstained with DAPI (blue), and the corresponding merged image is represented in the right-hand panel (Magnification X40, bar 100μm).

5.3.2.2 Transcriptional regulation of HIF-1A and HIF-2A under different oxygen tensions

We further studied the gene expression profile of HIF-1A and HIF-2A during acute and chronic responses to different oxygen tensions. Quantitative RT-PCR analysis in Episomal-hiPSCs show a trend of decreasing HIF-1A gene expression under 0%, 2%, 5%, 8%, and 12% O_2 relative to normoxic cultures (Figure 5.11). However, there was a significant increase in HIF-1A expression under 5% O_2 at 8hrs and under 12% O_2 at 24hrs relative to normoxic cultures (Figure 5.11C and E, respectively). Additionally, RT-qPCR data show that HIF-2A gene expression was not considerably altered by changes in oxygen tensions. However, HIF-2A expression increased following 24hrs and 48hrs under some oxygen tensions; the difference was only significant under 8% O_2 at 24hrs and 12% O_2 at 48hrs and 72hrs relative to 20% O_2 (Figure 5.11D and E, respectively).

Shef3-hESCs were also analysed for HIF-1A and HIF-2A expression profile. The results show that HIF-1A expression was down-regulated under all oxygen conditions at all-time points, compared to the normoxic condition (20% O_2) (Figure 5.12). However, HIF-1A expression was significantly increased under 2% O_2 at 48hrs, relative to 20% O_2 (Figure 5.12B). A significant increase in HIF-2A expression was observed under 0% O_2 following late time points; 24hrs and 48hrs relative to 20% O_2 (Figure 5.12A).

Taken together, our data showed further evidence that post-transcriptional mechanisms are involved in HIF-1A activation, as HIF-1A protein was detected in the nucleolus, but mRNA was down-regulated at almost all time points. HIF-2A expression slightly increased after ~ 8hrs to 24hrs under all oxygen conditions in Episomal-hiPSCs, while in Shef3-hESCs; HIF-2A increased after ~24hrs under 0% and 2% O_2 only. Although this was not expected somehow, it confirms that HIF-2A is not involved in early adaptation to O_2.

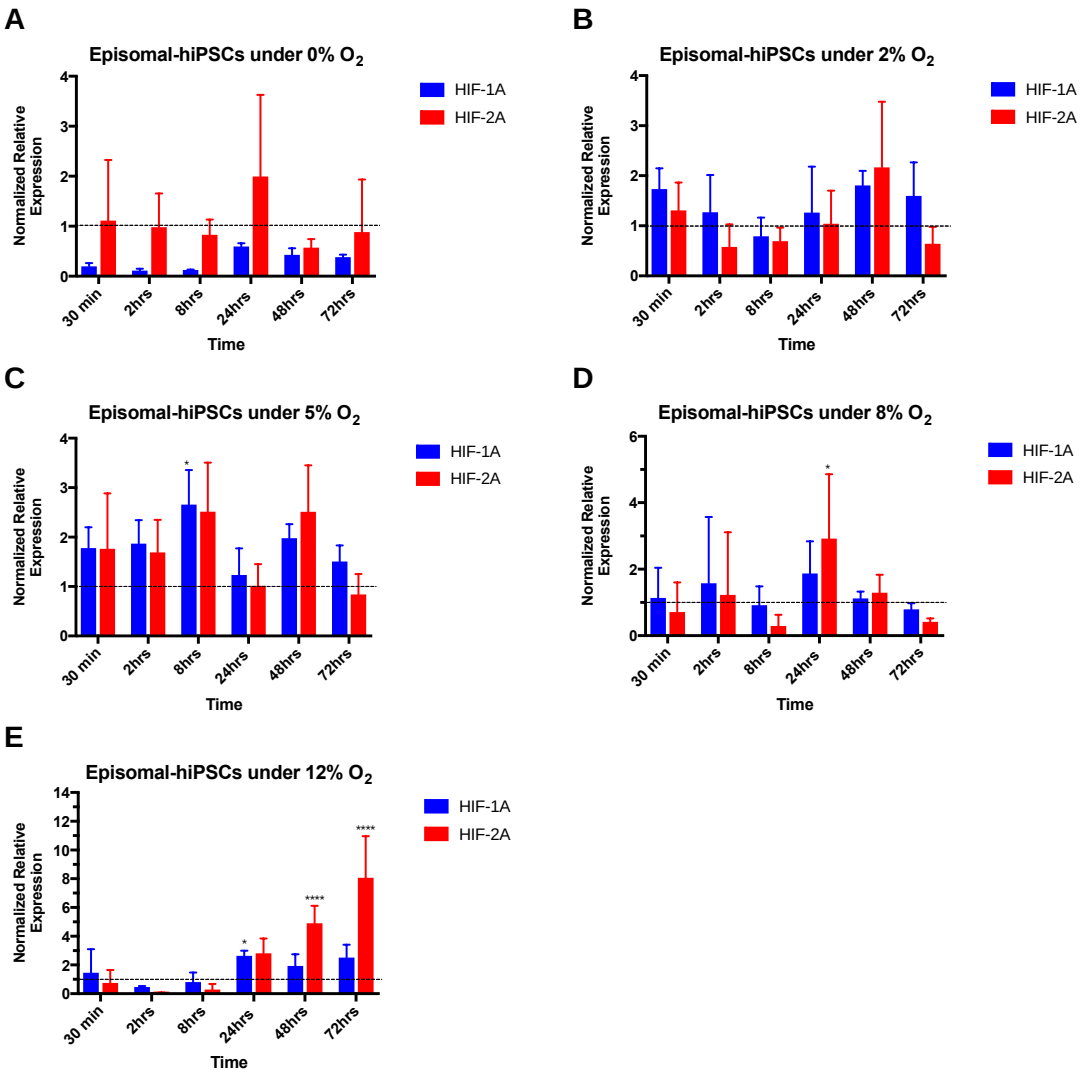

Figure 5.11 Quantification of HIF-1A and HIF-2A gene expression in Episomal-hiPSCs by RT-qPCR.

Cells were maintained under 0% O_2 **(A),** 2% O_2 **(B),** 5% O_2 **(C),** 8% O_2 **(D)** and 12% O_2 **(E)** for 30min, 2hrs, 8hrs, 24hrs, 48hrs, 72hrs and acute and chronic hypoxic responses were evaluated by quantifying the gene expression of HIF-1A and HIF-2A, respectively. All data have been normalised to β-actin and 1 for Episomal-hiPSCs cultured at 20% O_2. Data are shown as mean ± SD, Two-way ANOVA with Dunnett's multiple comparisons test was used for statistical analysis *(p≤ 0.05), **(p≤0.01), ***(p≤0.001), ****(p≤0.0001) (n = 3).

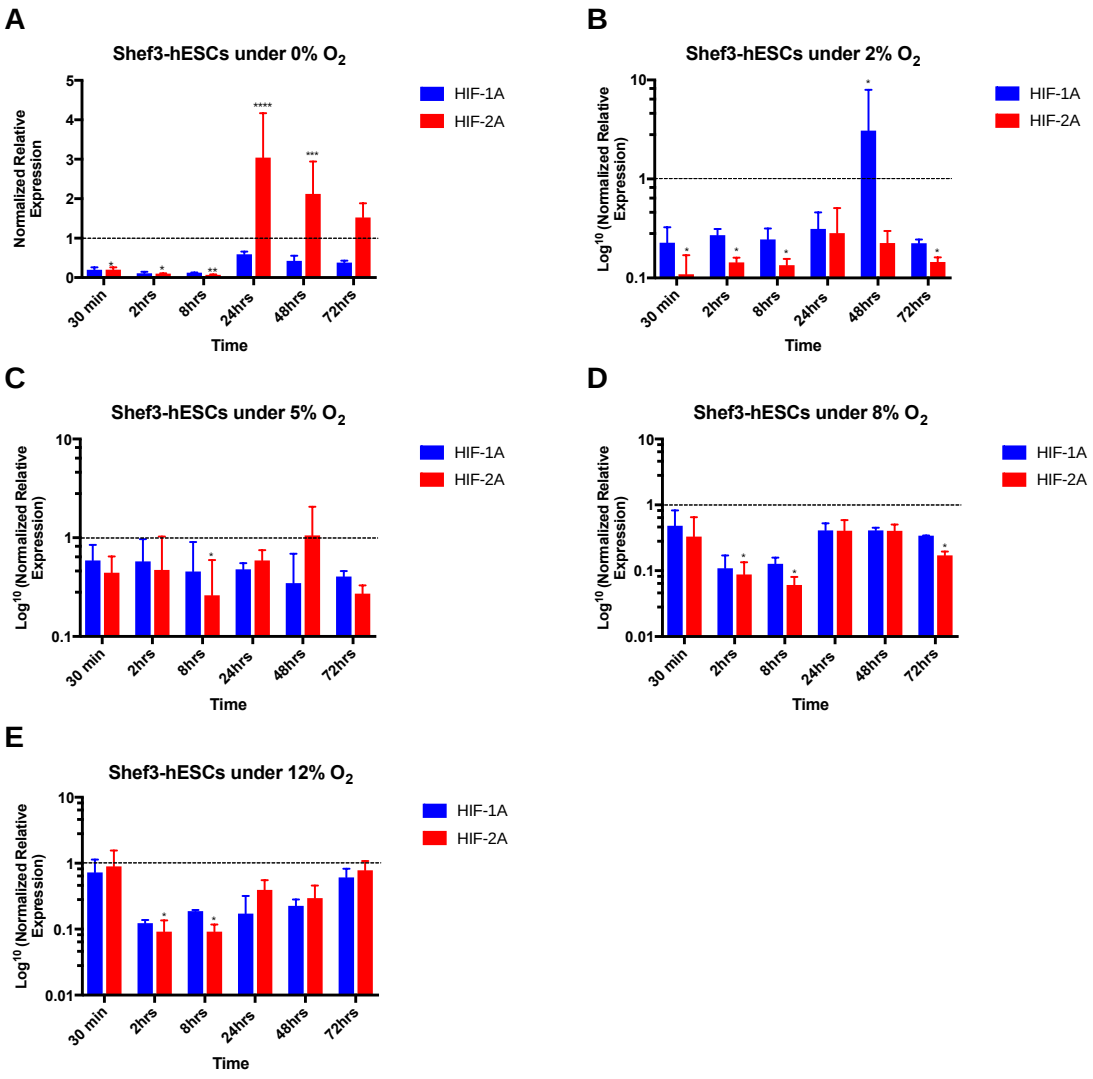

Figure 5.12 Quantification of HIF-1A and HIF-2A gene expression in Shef3-hESCs by RT-qPCR.

Cells were maintained under 0% O_2 **(A),** 2% O_2 **(B),** 5% O_2 **(C),** 8% O_2 **(D)** and 12% O_2 **(E)** for 30min, 2hrs, 8hrs, 24rs, 48hrs, 72hrs and acute and chronic hypoxic responses were evaluated by quantifying the gene expression of HIF-1A and HIF-2A, respectively. All data have been normalised to β-actin and 1 for Shef3-hESCs cultured at 20% O_2. Data are shown as mean ± SD, Two-way ANOVA with Dunnett's multiple comparisons test was used for statistical analysis *($p \leq 0.05$), **($p \leq 0.01$), ***($p \leq 0.001$), ****($p \leq 0.0001$) ($n = 3$).

5.3.2.3 Different oxygen tensions induce changes in energy metabolism of hPSCs

HIF-1A plays a significant role in the adaptive regulation of energy metabolism, by initiating a switch from mitochondrial OXPHOS to anaerobic glycolysis (Heilig et al. 2003; Jose & Bellance 2011; Saito et al. 2015; Lange et al. 2016). Anaerobic glycolysis and the aerobic OXPHOS are the two means for cells to consume energy. The relative metabolic state of the cells -whether aerobic or anaerobic- can be determined by measuring specific glucose consumption and lactate production rates (GCR and LPR, respectively); the higher the amount of lactate produced, the more likely that the relative metabolic state is anaerobic. Increase glucose uptake is regulated by the increased expression of GLUT1 (Barthel et al. 1999; Vander Heiden et al. 2001; Frauwirth et al. 2002). Glucose is converted to lactate by LDHA as a dead-end product. LDHA is considered to be a key checkpoint of anaerobic glycolysis (Lunt & Vander Heiden 2011; Panopoulos et al. 2012).

To understand how different oxygen conditions affect cellular metabolism; concentration profiles of glucose and lactate were used in conjunction with viable cell numbers to determine GCR and LPR for the time interval (24hrs -72hrs) to give an estimation of glycolysis rate in both cell lines at different O_2.

The results show that Episomal-hiPSCs exhibited higher rates of GCR and LPR when cultured under 2% and 5% O_2, however, the difference was not statistically significant, compared to 20% O_2 (Figure 5.13A and B). In contrary, Episomal-hiPSCs cultured under 8% and 20% O_2 exhibited low levels of GCR and LPR (Figure 5.13A and B). This indicates a reliance on glycolysis under low O_2 (≤5% O_2). Distinct profile observed under 0% O_2, although there was less glucose consumption, cells had relatively high LPRs and yielded higher lactate from glucose ($Y'_{Lactate/Glucose}$) than other conditions (Figure 5.13C). It is important to mention that few cells remained attached under 12% O_2 as mentioned previously causing calculation of the GCR and LPR to become impossible, therefore metabolic profile could not be concluded (Figure 5.13).

Shef3-hESCs were also analysed, the data show that 0% O_2 caused a significant increase in GCR and LPR, compared to 20% O_2 (Figure 5.14A and B). Additionally, GCR was also high under 2% and 5% O_2, the difference was significant under 5% relative to 20% O_2 (Figure 5.14A). Lactate production mirrored the glucose consumption under 2% and 5% O_2, but the difference was not significant relative to 20% O_2 (Figure 5.14B). This result indicates that Shef3-hESCs relied more on glycolysis for energy production at low oxygen tension (≤5% O_2), based on the higher consumption of glucose. In contrast, Shef3-hESCs cultured under 8% and 12% O_2 consumed less glucose but produced more lactate (Figure 5.14B). We observed a significant increase in the yield of lactate from glucose ($Y'_{Lactate/Glucose}$) under 8% and 12% O_2 (Figure 5.14C).

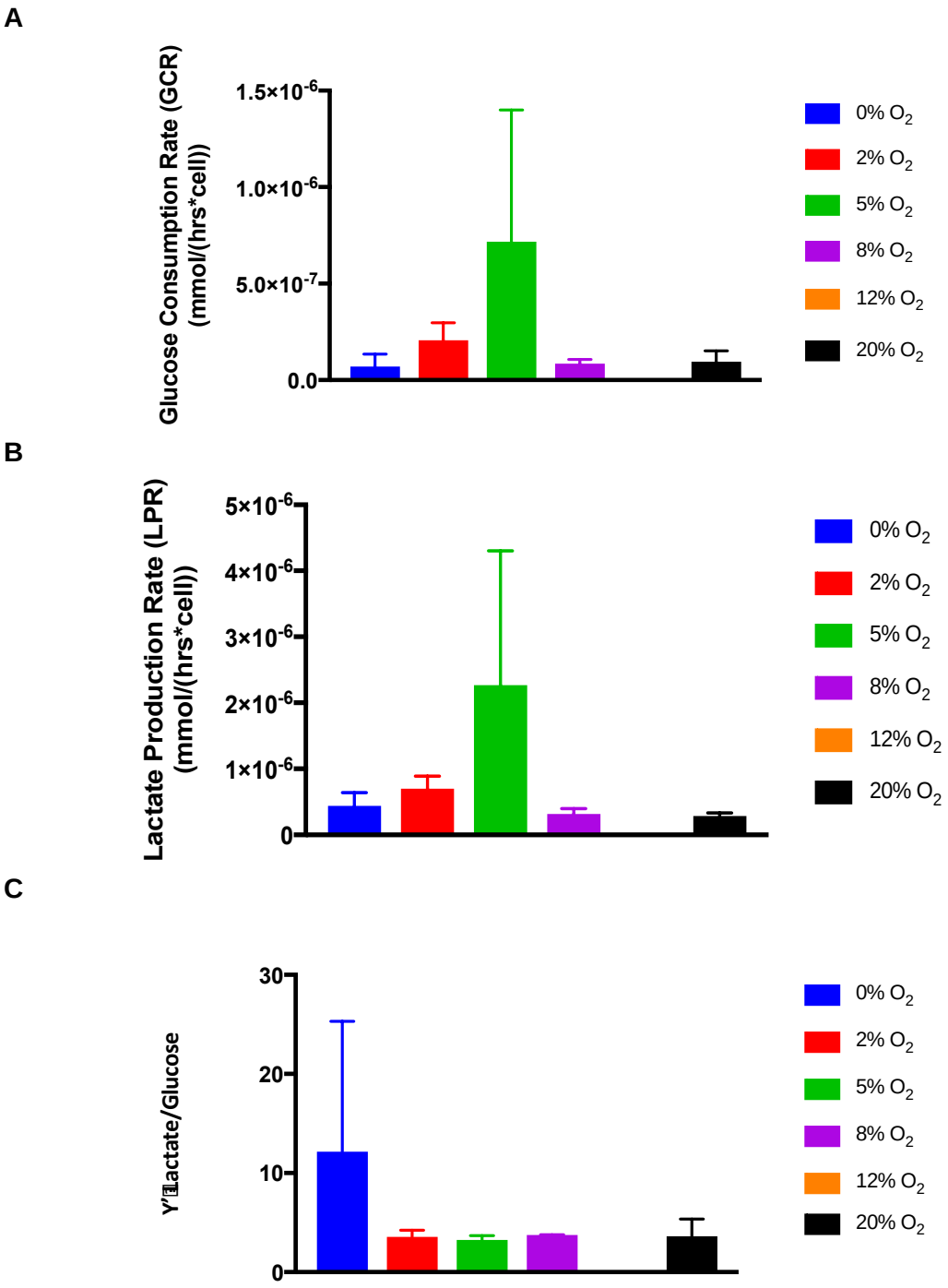

Figure 5.13 The effects of different oxygen conditions on the metabolic profiles of Episomal-hiPSCs.

Cells were maintained in parallel under 0%, 2%, 5%, 8%, 12%, and 20% O_2 for 72hrs. Viable cell number, and glucose and lactate concentration were measured every 24 hours over 72hrs using the VI-Cell Cell and Accutrend® Plus analysers, respectively. These values were used to calculate the GCR **(A)** and LPR **(B),** as well as the lactate from glucose yield **(C).** Data are shown as mean ± SD, One-ANOVA with Dunnett's multiple comparisons test was used for statistical analysis *(p≤ 0.05), **(p≤0.01), ***(p≤0.001), ****(p≤0.0001) (n = 3).

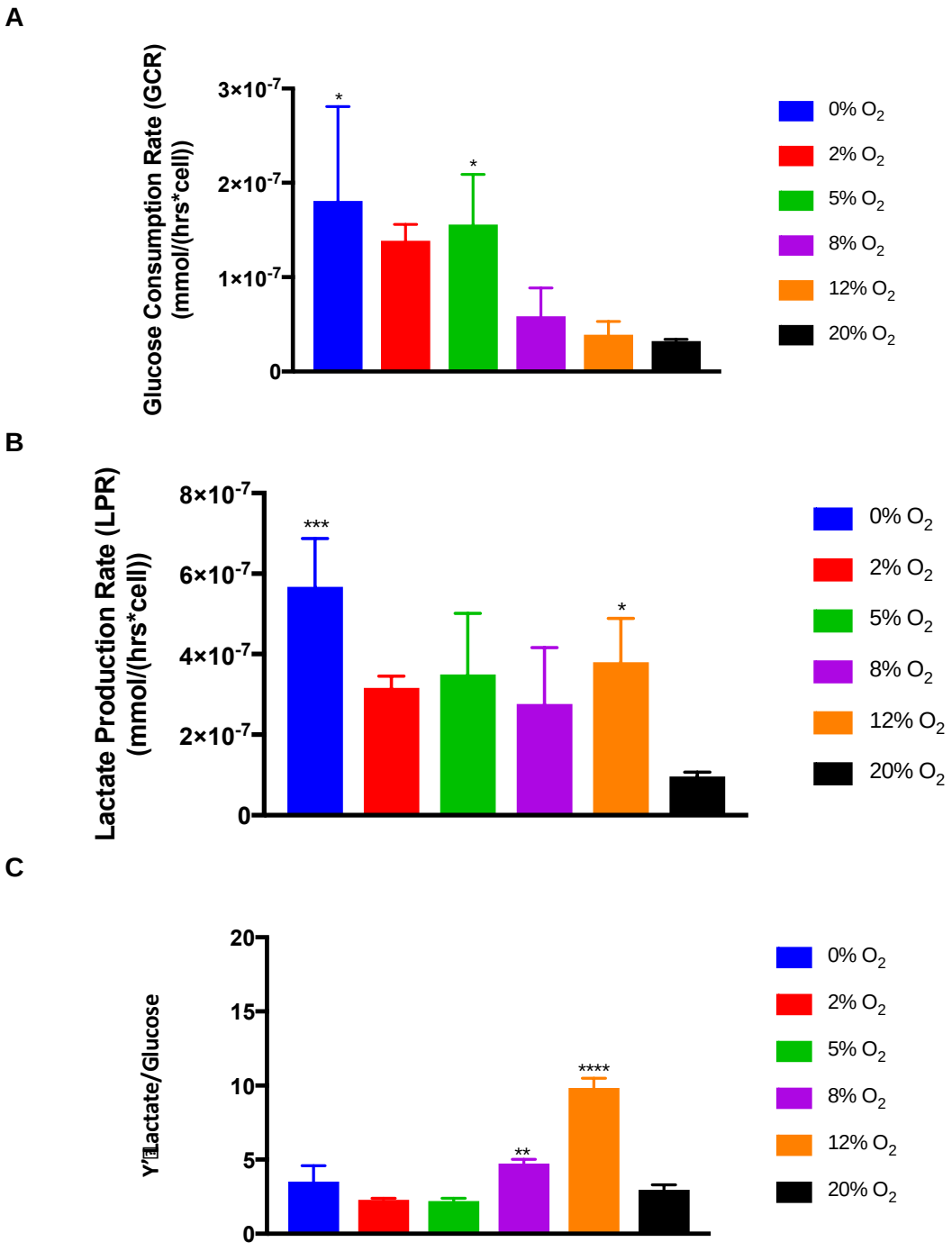

Figure 5.14 The effects of different oxygen conditions on the metabolic profiles of Shef3-hESCs.

Cells were maintained in parallel under 0%, 2%, 5%, 8%, 12%, and 20% O_2 for 72hrs. Viable cell number, and glucose and lactate concentration were measured every 24 hours over 72hrs using the VI-Cell Cell and Accutrend® Plus analysers, respectively. These values were used to calculate the GCR **(A)** and LPR **(B),** as well as the lactate from glucose yield **(C).** Data are shown as mean ± SD, One-ANOVA with Dunnett's multiple comparisons test was used for statistical analysis *($p \leq 0.05$), **($p \leq 0.01$), ***($p \leq 0.001$), ****($p \leq 0.0001$) ($n = 3$).

5.3.2.4 Quantification of metabolic related genes expression

To examine whether differences in glucose transport, that is regulated by GLUT1, may be responsible for the increased glucose consumption observed in both cell lines under low oxygen conditions (2% and 5% O_2 in Episomal-hiPSCs) and (0%, 2% and 5% O_2 in Shef3-hESCs), compared to 20% O_2, the mRNA expression of GLUT1 was investigated. We also investigated the mRNA level of LDHA to confirm the reliance of cells on anaerobic glycolysis.

We observed an oxygen-dependent regulation of GLUT1 and LDHA expression. In particular, 0% O_2 significantly up-regulated GLUT1 expression in Episomal-hiPSCs and Shef3-hESCs compared to those cultured under 20% O_2 (Figure 5.15A and B, respectively). Also, culturing Episomal-hiPSCs and Shef3-hESCs under 0% O_2 resulted in a significant increase in LDHA expression, compared to 20% O_2 (Figure 5.15A and B). Episomal-hiPSCs exposed to 2% exhibited a significant increase in LDHA, relative to 20% O_2 (Figure 5.15A).

Overall these data show a general increase in expression of glycolytic enzymes in both cell lines during the culture period under different oxygen tensions. This implies that hPSCs are highly sensitive to even small changes in oxygen tensions. Taken together, our results suggest that under lower oxygen tensions (0%, 2% and 5% O_2) there was an increased dependence on anaerobic glycolysis rather than on OXPHOS in both cell lines. These findings are in agreement with many studies (Hu et al. 2003; Lunt & Vander Heiden 2011; Shyh-Chang & Daley 2015; Hu et al. 2016).

A

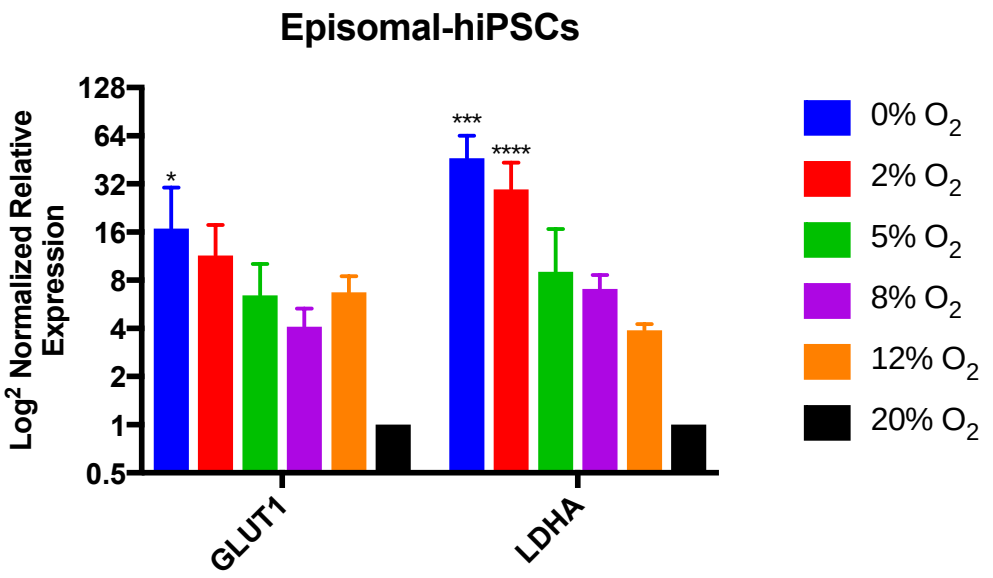

B

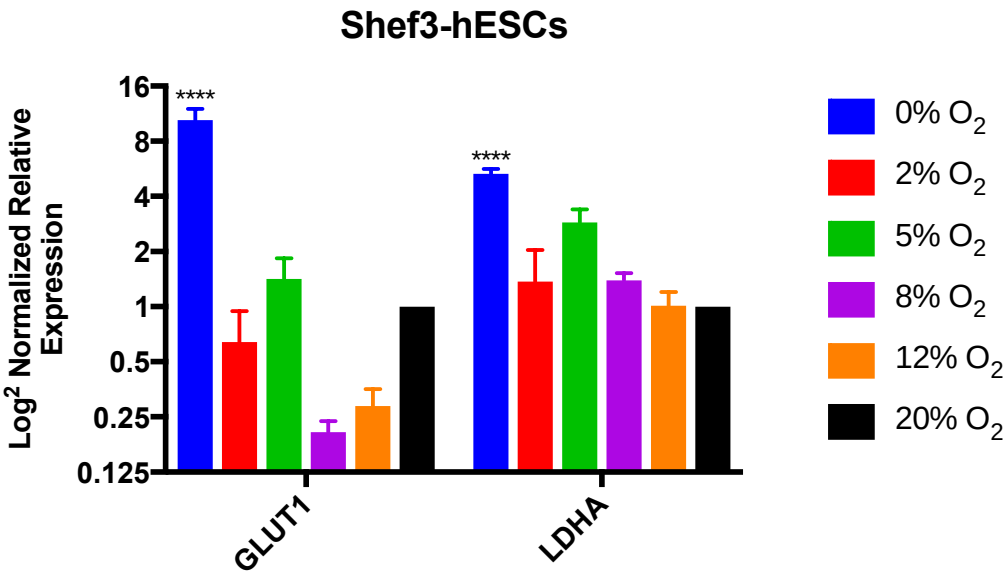

Figure 5.15 The Influence of different oxygen tensions on the glycolytic-related gene expression by RT-qPCR

The expression of GLUT1 and LDHA in **(A)** Episomal-hiPSCs and **(B)** Shef3-hESCs that were grown in parallel under 0%, 2%, 5%, 8%, 12%, and 20% O_2 for 72hrs. All data have been normalised to β-actin and 1 for cells maintained at 20% O_2. Data are shown as mean ± SD, Two-way ANOVA with Dunnett's multiple comparisons test was used for statistical analysis *($p \leq 0.05$), **($p \leq 0.01$), ***($p \leq 0.001$), ****($p \leq 0.0001$) ($n = 3$).

5.4 DISCUSSION AND CONCLUSION

Hypoxia is known to be involved in stemness preservation, proliferation and metabolism. However, little is known on how stem cells respond to small changes in oxygen levels. In this work, we investigated the effect of the full range of oxygen tensions on the behaviours of hPSCs. We found that the cells exhibited a distinct profile regarding morphological changes, proliferation, metabolism and hypoxia response when cultured at different oxygen conditions (≥8% O_2 and ≤5% O_2).

The results show that Episomal-hiPSCs and Shef3-hESCs exhibited accelerated proliferation rate when cultured under higher oxygen conditions (≥8% O_2) as evident by the lower PDT values. Additionally, the KI67 analysis showed that Episomal-hiPSCs and Shef3-hESCs were highly proliferative under oxygen conditions (≥8% O_2). Our findings agree with Zhi et al. (2018), as culturing under 10% O_2 induced the proliferation ability of Induced hepatic stem cells (iHepSCs) by accelerating the G1/S transition. Although different oxygen tensions did not change the morphology of Episomal-hiPSCs, some changes were observed in Shef3-hESCs. The cells under higher oxygen tensions (≥8% O_2) formed larger and less-cohesive colonies than those seen under lower oxygen tensions (≤5% O_2). Also, early signs of differentiation were observed as indicated by the emergence of flattened cells with a white intercellular space between cells in Shef3-hESCs maintained under 20% O_2. As based on (Wakui et al. 2017), when stem cells deviate from pluripotency toward a differentiated state, they develop a white intercellular space. Nonetheless, there weren't any significant differences in the expression of OCT4 and NANOG under these conditions. Several studies have shown similar observations, as hypoxia did not change the gene expression of pluripotency markers in hESCs (Forsyth et al. 2008; Westfall et al. 2008).

Culturing hPSCs under 0% and 2% O_2, showed a different profile. The data show that Episomal-hiPSCs exposed to 0% and 2% O_2 showed higher PDT, with a more pronounce increase at 2% O_2. This indicates that these cells grew at slower rates than those exposed to higher oxygen tensions (≥8%O_2). Also, these cells exhibited homogenous morphology as indicated by high N/C ratio. Shef3-hESCs showed similar characteristics at 2% O_2 but not at 5% O_2, as morphological analysis reveals

some signs of differentiation under 5% O_2, these cells also exhibited significant down-regulation in OCT4 at some time points (at 8hrs, data not shown), which might explain the deviation from undifferentiated into a differentiated state. A study by Prasad et al. (2009) supported our observations; when ESCs maintained under 5% O_2, persisted level of differentiation was observed. Moreover, Shef3-hESCs cultured under 5% O_2 proliferate at higher rates as evident by the lower PDT. These data confirm that hPSCs respond differentially to small changes in oxygen tensions (from 2% to 5% O_2), especially in Shef3-hESCs. We suggest, based on this finding, that cells cultured under 5% O_2 were in transitions with the dual mechanism between pluripotency and differentiation, identified as "clock model" (Akberdin et al. 2018). Our data have also shown that culturing under the highest level of hypoxia (0% O_2) have caused a reduction in KI67 expression. This suggests that 0% O_2 might have caused cell cycle arrest and increased cell apoptosis as evident by the increasing number of floating cells (especially in Shef3-hESCs, Appendix 8.2D) due to oxygen deprivation. Several studies supported this notion, for example, Ezashi et al. (2005) have found that culturing under 1% O_2 reduced the growth of hESCs which was accompanied by cells differentiation. Also, apoptosis was induced in reduced oxygen cultures (Carmeliet et al. 1998).

Acute and chronic responses to different oxygen tensions were evaluated by analysing HIF-1A and HIF-2A. Our data show that HIF-1A and HIF-2A were differentially regulated in response to varying oxygen tensions. During the early response (<24hrs), HIF-1A translocate into the nucleus under all hypoxia levels, but not normoxia (20% O_2) in a concentration- and time-dependent manner. However, HIF-2A protein translocated to the nucleus under 'only' 2% and 5% O_2 conditions during the early exposure. Pahlman and colleagues first showed in HeLa and neuroblastoma cells that HIF-2A protein stabilised at 2% to 5% O_2, but not at lower oxygen tensions (1% O_2) (Nilsson et al. 2005; Holmquist-Mengelbier et al. 2006).

It was found that under hypoxic condition, expression of HIF-2A protein was confined to the cells in an undifferentiated state, while HIF-1A protein was expressed in all cells independent on their state (Westfall et al. 2008). Also, a study has found that HIF-2A, but not HIF-1A, binds to the Oct4 promoter and induces its expression in hypoxic cells (Petruzzelli et al. 2014). Taking this together with our data that show a

homogenous morphological profile of hPSCs under 2% O_2, we strongly suggest that this restricted nuclear translocation of HIF-2A protein under lower oxygen conditions (≤5% O_2) might be related to the role of HIF-2A in maintaining pluripotency feature. The nuclear translocation of HIF-1A protein was detected under all hypoxia conditions (from 0% to 12% O_2), which implies that HIF-1A is highly sensitive to small changes in oxygen conditions. HIF-1A was found to be more sensitive to FIH-1-mediated inhibition than HIF-2A (Khan et al. 2011). Factor Inhibiting HIF-1A (FIH) is an asparaginyl hydroxylase enzyme that blocks association of HIF-1A/1B and thus inhibiting transcriptional activation. Moreover, other studies have demonstrated that HIF-1A, but not HIF-2A, induces the expression of many genes in various cell types, while HIF-2A has unique target genes that seemed to be cell-type specific (Hu et al. 2003; Raval et al. 2005). Also, a study used genome-wide chromatin immunoprecipitation approach suggested that HIF-2A found to contribute very little in compare to HIF-1A to the transcriptional changes during hypoxia (Mole et al. 2009). Together, these results strongly suggest that; (i) HIF-1A has a universal role in a hypoxia-signalling pathway, and that (ii) HIF-2A plays a critical role in the maintenance of hPSCs pluripotency. Although oxygen changes have a drastic impact on HIF-1A and HIF-2A proteins stability, HIF-1A mRNA expression were not changed dramatically following exposure to different oxygen conditions, especially in Shef3-hESCs. This is might due to the regulation of HIF by oxygen primarily at the post-transcriptional level. We however found that HIF-2A was upregulated after ~8-24hrs under 0%, 2%, 5%, 8% and 12% O_2, which shows that HIF-2A is taking over long hypoxic response.

Changes in oxygen tensions had an impact on the metabolic profile of Episomal-hiPSCs and Shef3-hESCs. Our data show that glucose was the predominant substrate utilised by Episomal-hiPSCs and Shef3-hESCs under 2% and 5% O_2 as evident by the increasing level of GCR which was associated with a higher LPR compared to 20% O_2. Cells maintained under 2% O_2 exhibited higher expression levels of GLUT1 and LDHA. Collectively, these data indicate an increase in anaerobic metabolism (glycolysis). Comparable results have been reported with different cell types such as MSCs and mESCs (Follmar et al. 2006; Santos et al. 2010). Shef3-hESCs cultured under 0% O_2 exhibited similar metabolic profile to those observed at 2% and 5% O_2. Whereas Episomal-hiPSCs cultured under 0% O_2

showed a different pattern; despite the significant increase in GLUT1expression relative to 20% O_2, glucose consumption was low as evident by the lower level of GCR. These data suggest an intriguing switch from glycolysis, however, this calculation is only an estimate, and calculating other energy sources would give a better idea on the on the energy metabolism profile. Episomal-hiPSCs and Shef3-hESCs respond differently to higher oxygen conditions. This is expected, as a recent study has reported that some aspects of iPSCs metabolism differ from ESCs, which may reflect a parental cell memory, or be a consequence of the reprogramming process of iPSCs (Harvey et al. 2018). The results also show that Episomal-hiPSCs maintained under 8% and 12% O_2 exhibited low rates of glucose uptake and lactate production, which was further confirmed by the down-regulation of the GLUT1 and LDHA expression, compared to 20% O_2. This suggests that the conversion of lactate from pyruvate was absent or reduced, which implies a shift away from glycolytic toward oxidative metabolism; these results are consistent with (Gu et al. 2016). Metabolites analysis in Shef3-hESCs showed different profile; cells under 8% and 12% O_2 exhibited high LPR and significantly yielded higher lactate from glucose, compared to 20% O_2, despite the low level of glucose being consumed. This might be explained by the presence of other metabolic pathways than glycolysis (e.g. glutaminolysis), which might have an effect to some extent on this yield. Indeed, several studies have demonstrated the role of glutaminolysis as a critical energy source for proliferating cells (Wise & Thompson 2010; Fernandes et al. 2010; Son et al. 2013; Ito & Suda 2014). Another study by Moussaieff et al. (2015) demonstrated that ESCs utilise OXPHOS to fuel high rates of cytosolic acetyl-CoA synthesis to maintain the histone acetylation required for pluripotency. In addition, a study has measured the contribution of OXPHOS to the cellular ATP supply and found that mitochondria generate about 79% of the cellular ATP in HeLa cells and that upon hypoxia this contribution is reduced to around 30% (Jose & Bellance 2011). Collectively, our results with others, suggest a potential interplay between glycolysis and OXPHOS in hPSCs, especially, under higher oxygen conditions (≥8% O_2). This metabolic flexibility is used to meet the higher demand of proliferating cells (Catherine E. Forristal et al. 2013; Shyh-Chang et al. 2013; Prigione et al. 2015; Shyh-Chang & Daley 2015; Gu et al. 2016; Lees et al. 2017; Dahan et al. 2018). As we have shown that these culture conditions (≥8% O_2) induced rapid growth, as

evident by (i) the lower PDT, (ii) high KI67 and (iii) the formation of larger colonies when compared to standard culture condition (20% O_2).

In conclusion, this study has provided further evidence that culturing within a threshold of 2 to 5% O_2, seems to be more beneficial for maintaining the self-renewal capacity of hPSCs. Although the expression pattern of pluripotency genes was not significantly altered, low oxygen tension renders the hPSCs with a more uniform phenotypic profile. Additionally, the slow mitotic division that occurred under 2% O_2 might allow the cells to segregate chromosomes accurately. As consequent, decreasing the number of abnormal cells that need to be eliminated by apoptosis. In contrast, growing hPSCs under higher oxygen tensions (≥8% O_2) increased the growth rate, which could be responsible for the increased occurrence of genetic instability and differentiation potential commonly encountered with traditional culture condition under 20% O_2. See **(**Table 5-1**)** for concluding remarks. Nonetheless, this conclusion was based only on the experimental criteria used to assess the cells, and the potential impact of different oxygen tensions on other cellular features such as telomerase activity can be further studied. Taken together from the present work with the previous studies (Ludwig et al. 2006; Forsyth et al. 2006; Hewitt et al. 2006; Koay & Athanasiou 2008; Westfall et al. 2008; Forsyth et al. 2008; Chen et al. 2009; Prasad et al. 2009; Niebruegge et al. 2009; Lim et al. 2011; Stacpoole et al. 2013) it is strongly suggested that different constituents of culture, duration and purposes of hPSCs maintenance probably need different oxygen tensions for optimal performance. Since these issues are not addressed thoroughly, further exploration will be required before the implementation of hypoxia protocols for hPSCs can be universally recommended. Moreover, oxygen tension should be maintained within a certain range, because concentrations of oxygen that are too low or too high negatively influence the self-renewal capacity of hPSCs.

Table 5-1 Concluding Remarks.

O_2 level (%)	Cell behaviour (Cell number/ PDT/KI67)			Pluripotency		Hypoxic response		Metabolic state				
	Cells adapting	Cells responding to different O_2	Cells making different decisions	OCT4	NANOG	HIF-1A	HIF-2A	GCR	LPR	Yield	GLUT1	LDHA
	24hrs	48hrs	72hrs									
0%	Cell recovered in a comparable rate	Decrease cell number/remaining floating cells	Increase cell number/ slow growth/increase floating cells	No change (NC)	NC	Nuclear translocation at acute phase +++	Cytoplasmic	High	High	Higher yields	Significant up regulation (8hrs-72hrs)	
2%		Slight increase cell number	Slight increase cell number/homogenous morphology/ slow growth	NC	NC	Nuclear translocation at acute phase +++	Nuclear translocation at acute phase	Lactate production mirrored glucose utilization			Up regulation	
5%		Increase cell number	Slight decrease in cell number /sign of differentiation/rapid growth	Down regulated	Increase at 8hrs	Nuclear translocation at acute phase ++	Nuclear translocation at acute phase	High	High	Low	Down regulation at 24hrs	
8%		Increase cell number	Pronounced increase cell number/+floating cells/ rapid growth	NC	NC	Nuclear translocation at acute phase +	Cytoplasmic	Low	Low	Low	Change is not Significant	
12%		-	Pronounced increase cell number/+floating cells/ rapid growth	NC	NC	Faint nuclear translocation at acute phase	Cytoplasmic	-	-	-		
20%		Increase cell Number	Pronounced increase cell number/+floating cells/ rapid growth	NC	NC	Absent	Cytoplasmic	Low	Low	Low		

Concluding remarks	0% O_2	Stressful condition indicated by higher number of floating (cell cycle arrest) & accelerated lactate production (San-Millán & Brooks 2017).
	2% O_2	"Stemness" optimal condition indicted by slow mitotic division, homogenous morphology, nuclear HIF-2A correlates to pluripotency & reliance on glycolysis
	5% O_2	Cells seemed to be at unstable transition stage (between pluripotency and differentiation) – clock model (Akberdin et al. 2018)
	8% -20% O_2	Unhealthy condition indicated by high growth rate, tendency to differentiate, absent or reduced HIF-1A, cytoplasmic HIF-2A and flexible energy metabolism (OXPOHS and glycolysis)

6 CHAPTER 6: EFFECT OF A WIDE RANGE OF OXYGEN LEVELS ON THE EARLY DIFFERENTIATION OF HPSCS

6.1 INTRODUCTION

The following section will summarize the relevant literature, which was previously discussed in Chapter 1.

Mammalian development occurs in low oxygen microenvironment (1.5- 3% O_2), before the development of the vasculature system (Okazaki and Maltepe, 2006; Dunwoodie 2009). Sequence of cellular division events lead to blastocyst attachment and implantation into the uterine wall at days 5 – 7 after fertilization (Vigano et al. 2003). This critical event establishes the maternal-fetal blood circulation to begin where oxygen and nutrient delivery are permitted to the embryo during the first two weeks of gestation. The gradient of oxygen levels at these stages has profound roles in stem cells fate determinations (Burton & Jaunaiux 2001; Staun-Ram & Shalev 2005; M Celeste Simon & Keith 2008; Zhu et al. 2012), as discussed in section 1.3.

Similar effects were obtained when considering hypoxia during in vitro differentiation protocols. For example, placental trophoblastic stem cells (TSCs) adopt a spongiotrophoblast cell fate as opposed to a trophoblastic giant cells (TGCs) fate when cultured under 3% O_2 instead of 20% O_2 (Adelman et al. 2000). Additionally, MSCs cultured under 5% O_2 produced more osteocytes when subsequently implanted into a host animal compared to 20% O_2 (Lennon et al. 2001). Considering hypoxia in vitro has also increased the differentiation efficiency of stem cells into different cell types. For instance, hypoxia has increased the differentiation efficiency to ~94% of EBs beating from several hPSCs lines (Elliott et al. 2011). Further, hypoxic culture conditions efficiently directed the differentiation into vascular-lineage

cells, based on increased expression of the related marks in mESCs (Lee et al. 2012) and hESCs (Shin et al. 2011). Using this approach, various progenitors' cells have been derived from PSCs such as endothelial (Ramírez-Bergeron et al. 2004), Chondrogenic (Koay & Athanasiou 2008) and RPCs & Photoreceptors (Bae et al. 2012; Garita-Hernández et al. 2013), hepatic progenitors (Zhi et al. 2018), MSCs (Akira et al. 2015). These data highlight the significance of considering hypoxia in the routine culture of PSCs, as one of the highly specialized microenvironment cues. Also indicates that PSCs retain a 'memory' of their previous microenvironment. Although there are many studies have explored the role of hypoxia on PSCs behaviour in vitro using microfluidic devices or chambers to permit single oxygen level (Oppegard et al. 2009; Polinkovsky et al. 2009; Chen et al. 2011), defining different and stage-specific hypoxic level on a tentative manner during an expansion and/or differentiation protocol is still a requisite.

As we have demonstrated in chapter 5 the role of a wide range of oxygen tensions on the self-renewal and proliferation capacities of hPSCs, we sought next to explore how different oxygen tensions, without the addition of exogenous factors, regulate hPSCs fate determination into three germ layers.

Human hPSCs were allowed to differentiate spontaneously to assess the role of oxygen factor only as a regulator of stem cell fate. Simple, rapid, well-controlled monolayer system was used to avoid multiplicity and to study single cell phenotypic changes. Moreover, hPSCs were cultured for short period (4 days) to mimic the early O_2-dependent events (blastocyst implantation and the initiation of feto-maternal circulation) at which the progenitors of germ layers are formed (endoderm, mesoderm, and ectoderm).Full range of oxygen tensions (0%, 2%, 5%, 8%, 12% and 20% O_2) was explored to find the optimum level for generating each germ layer progenitor as hypothesized, and to study the involvement of HIF-A signalling pathway during the early differentiation.

6.2 AIM

The work in this chapter aimed to test the effect of a full spectrum of oxygen tensions (0%, 2%, 5%, 8%, 12% and 20% O_2) on the early differentiation potentials of hPSCs. Morphological changes were examined using phase contrast microscopy. Additionally, the expression of markers associated with hypoxia, EMT and early differentiation was analysed using RT-qPCR, and immunostaining. All experimental conditions were compared to undifferentiated cells cultured at standard condition at 20% O_2.

6.3 RESULTS

6.3.1 The Effect of Different Oxygen Tensions on the Early Differentiation Of hPSCs

Hypoxic microenvironment plays a critical role in regulating stem cell fates. However, it is controversial to which direction between self-renewal and differentiation hypoxia drives stem cells. Here, we investigated whether a short exposure (4 days) to different oxygen tensions differentially regulates the specification of Episomal-hiPSCs and Shef3-hESCs into three germ layers.

Before the start of SP.D, undifferentiated Episomal-hiPSCs and Shef3-hESCs cultures were characterized. All cultures regardless of passage number showed typical morphology of both cell lines and expressed pluripotency markers as expected (see chapter 4).

To initiate the SP.D protocol (Figure 6.1), Episomal-hiPSCs and Shef3-hESCs were seeded at $0.8X10^5$ cells/well on Matrigel pre-coted well of 6-well plates and allowed to differentiate spontaneously as a monolayer, keeping cell morphology intact with minimal cellular stress. Cells were cultured in parallel under normoxic (20% O_2) and hypoxic levels of (0%, 2%, 5%, 8% and 12% O_2) for 4 days. Cells were harvested at different time points (D2 and D4) to check the expression of genes marking pluripotency (OCT4, NANOG, and GDF3), differentiation (PAX6, SOX17, and BRACHYURY), hypoxia genes (HIF-1A, HIF-2A) and their downstream target genes (VEGF, LDHA and GLUT1). All incubations and daily changes of culture medium were performed under strictly controlled oxygen conditions. Therefore, the cells did not expose to ambient air at any stage of the experiment (using C-Shuttle Glove Box and C-Chambers for transportation).

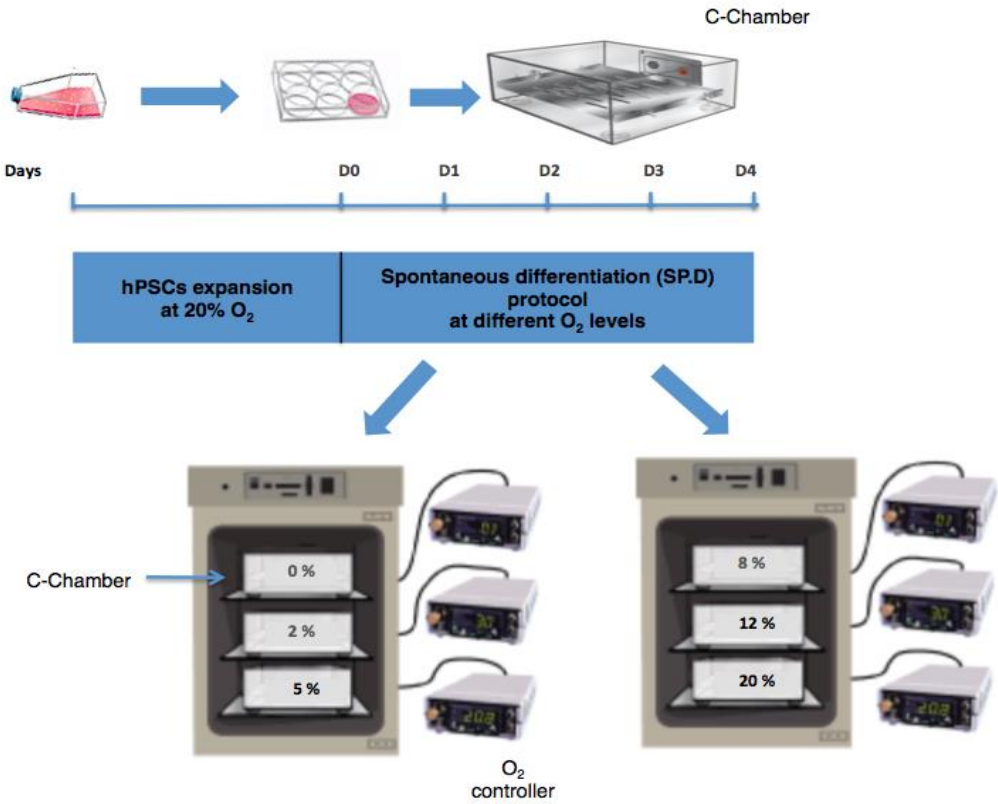

Figure 6.1Experimental setup of the SP.D protocol of hPSCs under different oxygen conditions and installation option of C-Shuttle System.
Initially cells were maintained in T75 flask until they reached confluency, and then seeded at a density of $0.8X10^5$ cells/well on Matrigel-coated 6 well plates and incubated for four days under different oxygen conditions (0%, 2%, 5%, 8%, 12% and 20% O_2) in parallel using C-Chambers, oxygen levels were monitored throughout the culture period by O_2 controllers.

6.3.1.1 Morphological characteristics of hPSCs during short-term culture protocol

Morphological properties of a cell depend on cytoskeleton organization, cell adhesion and activated signalling pathways. Accordingly, a cell shape can be considered to be an indicator of cell fate and differentiation (Settleman 2004). Morphological evaluation of both cell lines on D2 and D4 of SP.D protocol exhibited different patterns of different cell types (Figure 6.2). Overall, four subpopulations were distinguished under all conditions in both cell lines; small and triangular cells, star-shaped with accentuated membrane regions cells, large mesenchymal-like cells and elongated spindle-shaped cells. These subpopulations were observed similarly in both cell lines; thus, results for only one representative line (Episomal-hiPSCs) are shown in (Figure 6.3).

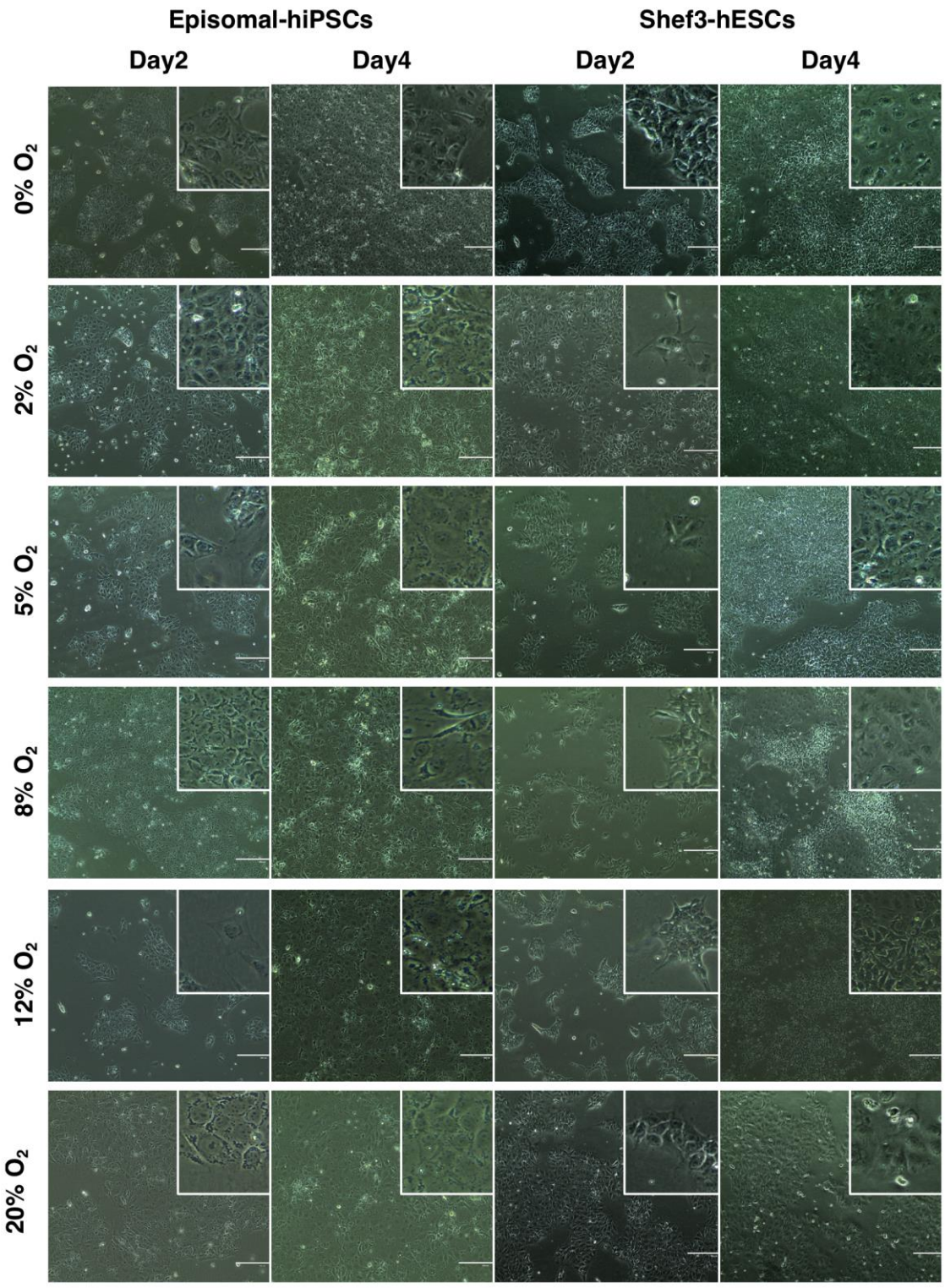

Figure 6.2 Morphological changes of hPSCs cultured under different oxygen concentrations.

Colonies, in both cell lines, displayed heterogeneous morphology of cells within the population, with larger nuclei and a greater cytoplasmic-to-nuclear ratio (magnified images) (Magnification 10X, bar = 400μm).

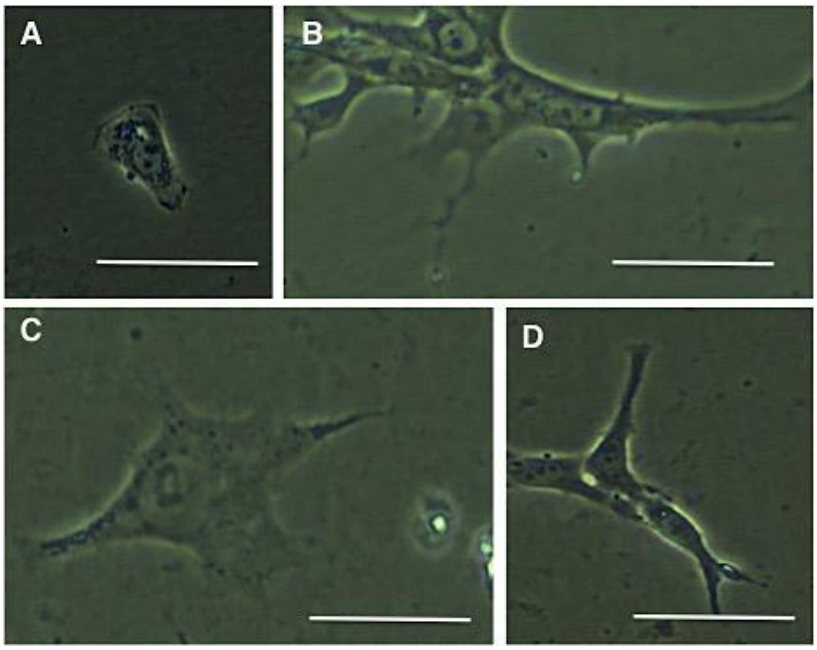

Figure 6.3 Phase contrast images of Episomal-hiPSCs and Shef3-hESCs culture containing distinct subpopulations.
(A) Small and triangular **(B)** star-shaped with accentuated membrane regions **(C)** large mesenchymal-like cells and **(D)** elongated and fibroblastic-like. Magnified images from 20X image in Figure 6.2 (bar = 20µm). Images were taken from Episomal-hiPSCs.

6.3.1.2 Protein expression analysis of germ layers–specific markers

To further characterize Episomal-hiPSCs and Shef3-hESCs, cells were stained with antibodies against BRACHYURY (Mesoderm), SOX17 (Endoderm) and NESTIN (Ectoderm) at D4 of SP.D. Episomal-hiPSCs and Shef3-hESCs stained positive for all markers (Figure 6.4) and (Figure 6.5), respectively. These observations suggest that the heterogeneity of Episomal-hiPSCs and Shef3-hESCs cultures is due to the presence of different progenitors of three germ layers and that the cells were able to differentiate in spite of the absence of any exogenous molecules by only manipulating the oxygen level. Which implies the role of oxygen tension on the regulation of stem cell fate as previously shown (Smith et al. 2004).

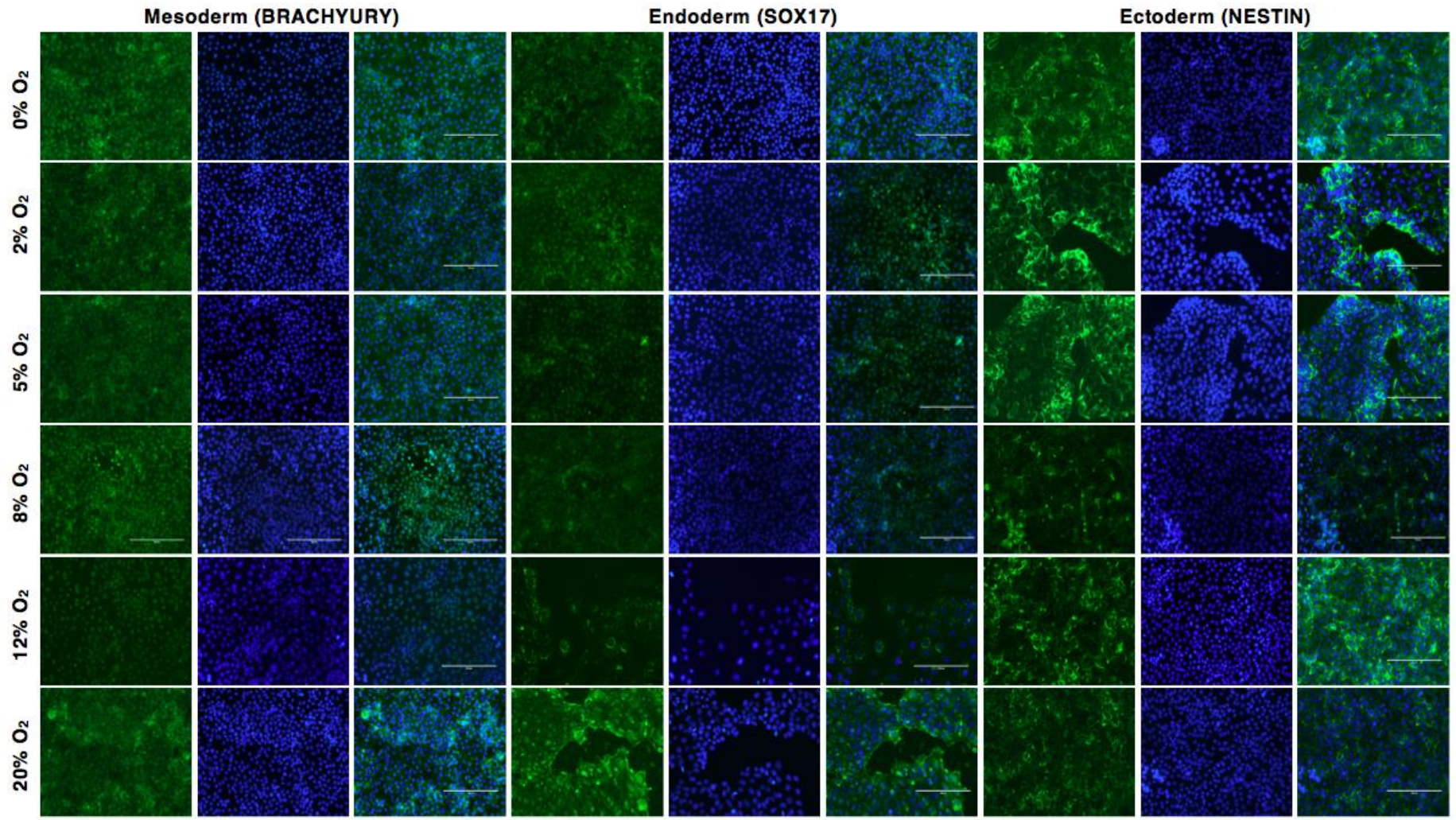

Figure 6.4 The effect of different oxygen tensions on the early differentiation of Episomal-hiPSCs.
Immunostaining analysis was performed to detect protein expression of three germ layers markers; BRACHYURY, SOX17, and NESTIN (green). Nuclei were stained by DAPI (blue), and the corresponding merged image is represented in the right-hand panel for each marker (Magnification 20X, bar= 200µm).

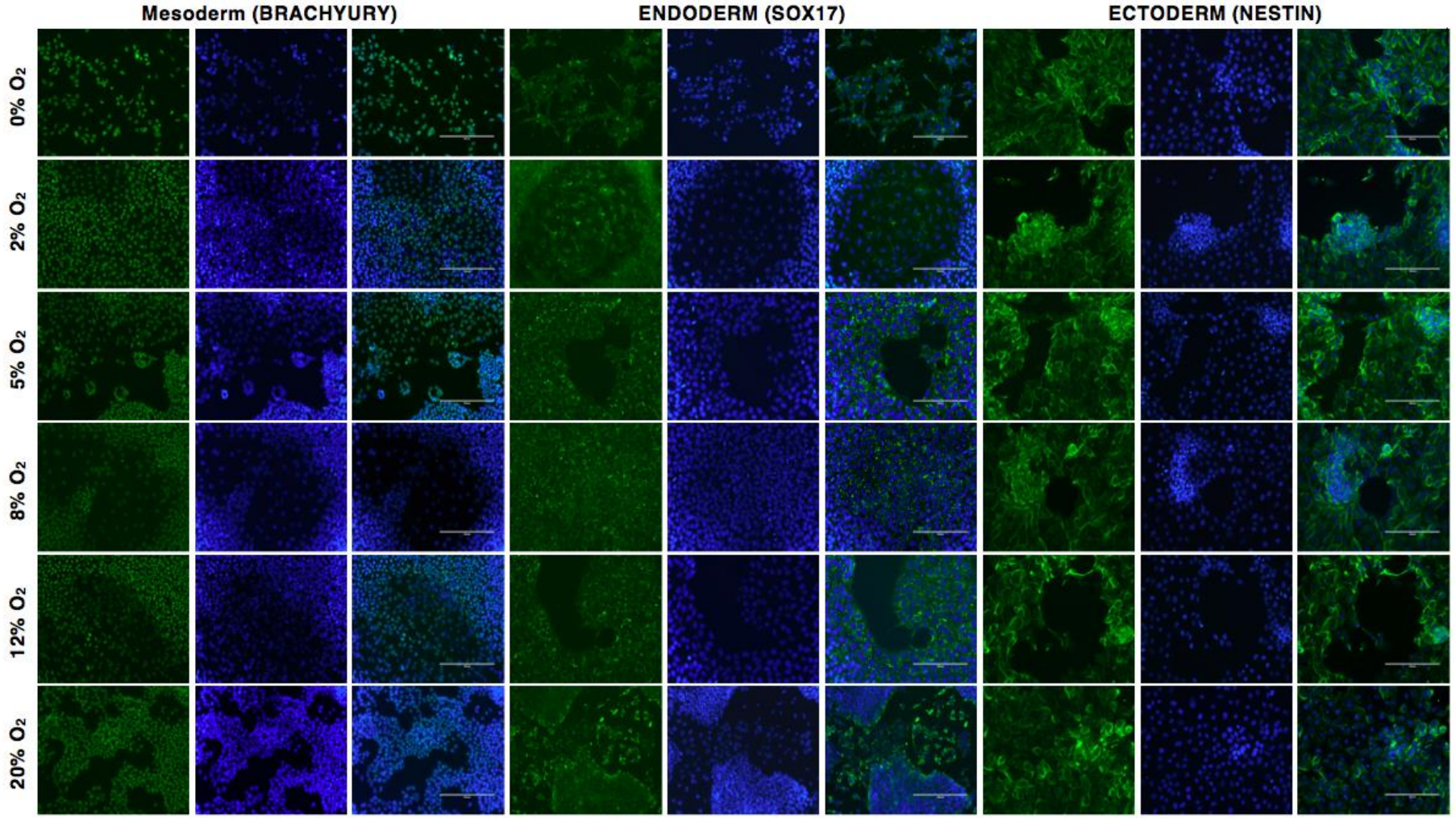

Figure 6.5 The effect of different oxygen tensions on the early differentiation of Shef3-hESCs.
Immunostaining analysis was performed to detect protein expression of the three germ layers markers; BRACHYURY, SOX17, and NESTIN (green). Nuclei were stained by DAPI (blue), and the corresponding merged image is represented in the right-hand panel for each marker (Magnification 20X, bar= 200μm).

6.3.1.3 Temporal expression pattern of pluripotency- and germ layer-specific markers

Initiation of SP.D in Episomal-hiPSCs resulted in a significant down-regulation of OCT4 and NANOG expression under all oxygen conditions at both time points, compared to the control (undifferentiated Episomal-hiPSCs cultured at 20% O_2) (Figure 6.6A and B). It was thought to analyse the expression of Growth Differentiation Factor-3 (GDF3) as it plays a vital role in the earliest stem cells fate decisions during gastrulation, GDF3 declines dramatically when the cells are allowed to differentiate (Sato et al. 2003; Levine et al. 2006). Interestingly, our data demonstrated that different oxygen levels differentially regulated GDF3 expression. As under lower oxygen conditions (0% and 2% O_2), the expression was significantly increased at D2 and remained at high levels until D4, compared to the control (Figure 6.6C). In contrast, culturing under higher oxygen conditions (5%, 8%, 12% and 20% O_2) resulted in a significant down-regulation of GDF3 at D4, relative to the control (Figure 6.6C). These data suggest that the cells cultured under higher oxygen tensions (≥5% O_2) were primed to differentiate faster than those cultured under lower oxygen tensions (≤2% O_2).

In Shef3-hESCs, the expression of OCT4 was down-regulated under all oxygen conditions at both time points, the difference was significant at D2 under 5%, 8% and 12% O_2, compared to the control (undifferentiated Shef3-hESCs cultured at 20% O_2) (Figure 6.7A). Similarly, an overall decrease in NANOG expression under all oxygen conditions at all-time points was observed, and the difference was significant at D2 under 2%, 5%, and 8% O_2 and at D4 under 0% and 20% O_2, compared to the control (Figure 6.7B). The expression of GDF3 was down-regulated under all conditions at D2, while at D4 a significant increase was observed under 20% O_2, relative to the control (Figure 6.7C). In contrast to the general trend, OCT4, NANOG and GDF3 significantly increased at D4 in Shef3-hESCs cultured under 12% O_2, compared to the control (Figure 6.7A, B and C, respectively). This result suggests that these fluctuations may have evolved to allow stem cells to self-renew while also offering 'windows of opportunity' to respond to environmental signals that can trigger specific differentiation (Graf & Stadtfeld 2008).

Together, the results suggest that Episomal-hiPSCs and Shef3-hESCs lose their pluripotency in order to differentiate into the three germ layers under 0%, 2%, 5%, 8%, and 20% conditions, which mimic ESCs behaviour during gastrulation initialization *in vivo*, as down-regulation of OCT4 and NANOG is essential for proper differentiation (Guo et al. 2002).

The stepwise cell fate transition during embryo development is orchestrated by sequential activation and inactivation of lineage-determining transcription factors such as BRACHYURY (mesoderm), SOX17 (endoderm) and PAX6 (ectoderm) (Yamanaka et al. 2006).

To confirm the commitment of hPSCs into three germ layers, and further, compare the differentiation potency among cell lines, lineage-specific genes (SOX17, BRACHYURY, and PAX6) were quantified at D2 and D4 using RT-qPCR. The results demonstrated that Episomal-hiPSCs differentiation towards endodermal lineage was accelerated in response to oxygen tensions (0%, 2% and 8% O_2), based on the significant up-regulation of SOX17 expression at D2 which remained at significant levels until D4 under 0% and 2% O_2, relative to the control (Figure 6.6D).

The differentiation into endodermal lineage was also induced at higher oxygen tensions (12% and 20% O_2); however, the increase in gene expression was observed at the later time point (D4); the difference was significant relative to the control (Figure 6.6D). The results also showed that mild hypoxia (8% O_2) promoted the differentiation into mesodermal lineage as evident by the significant increase in BRACHYURY expression at both time points (Figure 6.6E). Additionally, there was a significant up-regulation under 0% O_2 at both time points, compared to the control (Figure 6.6E). The differentiation into ectodermal was transient in Episomal-hiPSCs under all oxygen tensions, as the expression of PAX6 increased significantly at D2 and became undetectable at the later time points (D4) (Figure 6.6F). However, it has been shown that the transcription factors PAX6 is expressed sequentially during early embryonic neurogenesis (Suter et al. 2009), which might explain the transient expression of PAX6 in our results.

In Shef3-hESCs, first to note that the differentiation into three germ layers was delayed when compared to Episomal-hiPSCs. Hence, the onset of almost all germ layer-specific genes appeared at D4 of SP.D. While in Episomal-hiPSCs, germ layer-specific genes were up-regulated at the earlier time point (D2). The results showed that the differentiation toward endodermal lineages was delayed until Day 4 under all oxygen tensions, SOX17 expression was significantly higher under 5%, 12% and 20% O_2, compared to the control (Figure 6.7D). A similar trend in BRACHYURY expression was observed with a significant increase in gene expression under 20% O_2, compared to the control (Figure 6.7E). In contrast to Episomal-hiPSCs, Shef3-hESCs seemed to behave differently regarding their specification into the ectodermal lineage; the results showed a gradual increase in PAX6 expression throughout the culture period, the expression increased significantly at D4 under 0%, 2% and 5% O_2, compared to the control (Figure 6.7F). These results suggest that hypoxia levels of 0%, 2% and 5% O_2 shifted the cells into the ectodermal lineage, while Shef3-hESCs preferentially differentiated along the mesoendoderm lineage under 5%, 12%, and 20% O_2.

These data suggest that lineage-determining transcription factors heterogeneity is linked to the existence of various functional states in both cell lines. They are also linked to the fact that individual cells in a heterogeneous population have a propensity either to self-renew or commit to differentiation.

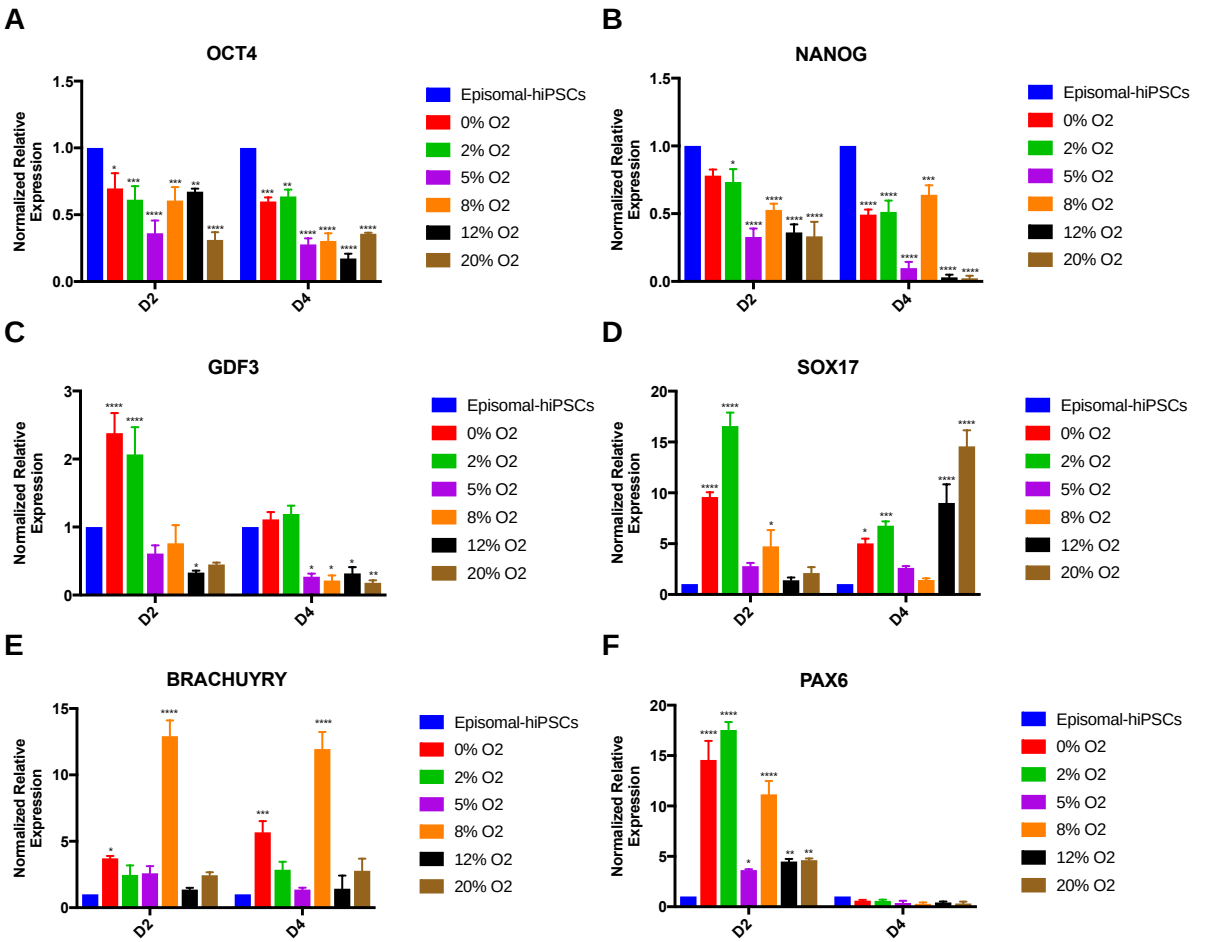

Figure 6.6 Loss of pluripotency and germ layers specification of Episomal-hiPSCs during SP.D protocol.

Time-course analysis of the relative mRNA expression levels of pluripotency genes **(A-C)** OCT4, NANOG and GDF and **(D-F)** early germ layers markers SOX17 (Endoderm), BRACHYURY (Mesoderm) and PAX6 (Ectoderm) in Episomal-hiPSCs cultured under 0%, 2%, 5%, 8%, 12% and 20% O_2 for 4 days. All data have been normalized to β-actin and 1 for undifferentiated Episomal-hiPSCs cultured at 20% O_2. Data are shown as mean ± SD, Two-way ANOVA with Dunnett's multiple comparisons test was used for statistical analysis *($p \leq 0.05$), **($p \leq 0.01$), ***($p \leq 0.001$), ****($p \leq 0.0001$) ($n = 3$).

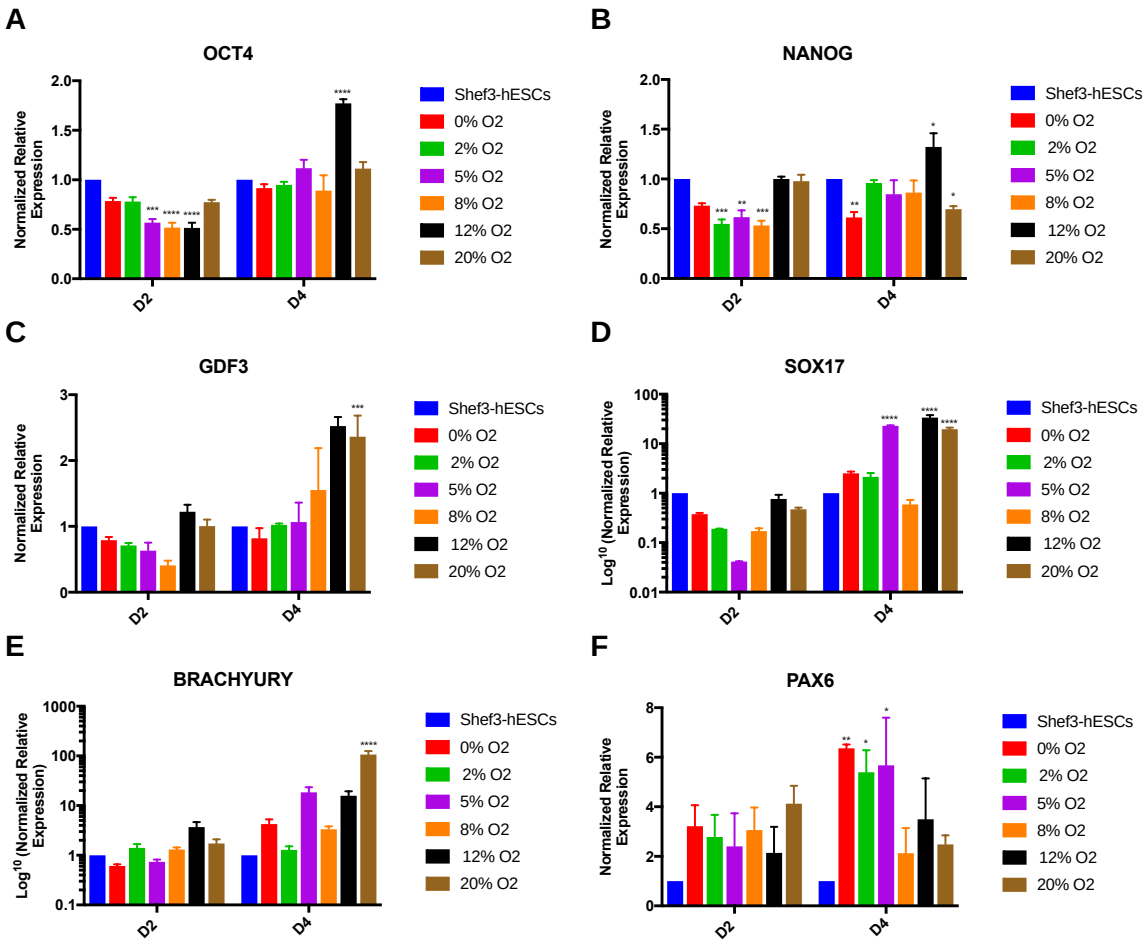

Figure 6.7 Loss of pluripotency and germ layers specification of Shef3-hESCs during SP.D protocol.

Time-course analysis of the relative mRNA expression levels of pluripotency genes **(A-C)** OCT4, NANOG and GDF and **(D-F)** the early germ layers markers SOX17 (Endoderm), BRACHYURY (Mesoderm) and PAX6 (Ectoderm) in Episomal-hiPSCs cultured under 0%, 2%, 5%, 8%, 12% and 20% O_2 for 4 days. All data have been normalized to β-actin and 1 for undifferentiated cells cultured at 20% O_2. Data are shown as mean ± SD, Two-way ANOVA with Dunnett's multiple comparisons test was used for statistical analysis *($p \leq 0.05$), **($p \leq 0.01$), ***($p \leq 0.001$), ****($p \leq 0.0001$) ($n = 3$).

6.3.2 Adaptation Responses Of hPSCs To Different Oxygen Conditions

During early embryogenesis, hypoxia induces rapid cellular proliferation that resulted in the formation of three germ layers. This complex morphogenesis is regulated by HIFs through the up-regulation of several genes including, but is not limiting to, VEGF, GLUT1, and LDHA. Each of these genes plays an important role during *in vivo* gastrulation: VEGF mediates vascularization, LDHA, and GLUT1 increase anaerobic glycolysis to meet increased energy demands (Flamme et al. 1997; Augustin et al. 2009; Fraisl et al. 2009; Pringle et al. 2010). The interplay between these genes during *in vitro* differentiation into germ layers will be examined next.

6.3.2.1 HIF-1A and HIF-2A play non-overlapping roles during the early differentiation of hPSCs into three germ layers

The data reported in chapter5 showed that the up-regulation of HIF-1A mediated hypoxic response in the undifferentiated cells in the acute phase and HIF-2A in the chronic phase; however, their roles in differentiation are still unclear. The rationale of the present experiment was to explore (i) whether the hypoxic response in the differentiated cells regulated in a similar manner that were observed in the undifferentiated cells and (ii) whether the signalling cascades act synergistically within the differentiation into the three germ layers.

RT-qPCR analysis in Episomal-hiPSCs show that HIF-1A expression was a significantly increased under 0% O_2 at both time points and under 5% O_2 at D4, compared to the control (Figure 6.8A). A slight increase in HIF-1A expression was also observed at D4 under 8% and 12% O_2 (Figure 6.8A). HIF-2A expression was up-regulated under all oxygen conditions, and reached significant levels at D4, compared to the control (Figure 6.8B), which indicates a chronic response due to the sustained hypoxic condition.

The expression of HIF-1A in Shef3-hESCs was not considerably changed in response to different oxygen tensions (Figure 6.9A). On the other hand, a gradual up-regulation of HIF-2A was observed throughout the culture period in Shef3-hESCs

under all oxygen levels, reaching significant levels at D4 under 20% O_2, compared to the control (Figure 6.9B). Our data has observed that the mRNA expression profile of HIF-1A and HIF-2A during early differentiation is temporally correlated with germ layers formation from hPSCs, which mimics the behaviour of ESCs in vivo during early stages of embryo development (see Figure 1.8). Our findings are in agreement with previous studies (Appelhoff et al. 2004; Holmquist-Mengelbier et al. 2006).

6.3.2.2 Changes in hypoxia-related genes expression

HIF-1A and HIF-2A mediate the adaptation of hPSCs to hypoxic conditions by switching the energy metabolism or avoiding the oxidative stress (Rafalski et al. 2012; Prigione et al. 2015). Given the critical role of VEGF in early germ layers formation as a main downstream factor that is transcriptionally regulated by hypoxia (Semenza 1998; Ferrara et al. 2003). The next objective was to study whether different oxygen tensions differentially regulate VEGF, LDHA, and GLUT1 during SP.D of hPSCs.

RT-qPCR analysis reveals that Episomal-hiPSCs cultured under all oxygen tensions exhibited a significant increase in VEGF gene expression in an O_2-dependent manner at both time points (Figure 6.8C). However, VEGF expression was relatively reduced at 12% O_2 at both time points and under 5% at (Figure 6.8C). Episomal-hiPSCs exhibited significant increases in GLUT1 expression at D2 under 2% O_2 and at D4 under 0% O_2 relative to the control (Figure 6.8D). Following the same trend, LDHA gene expression was increased significantly under 0% and 2% O_2 at all-time points, and at D4 under 5% O_2, compared to the control (Figure 6.8E).

In Shef3-hESCs, VEGF expression behaved in a manner that is consistent with the delayed onset of differentiation observed with this cell line previously. The results showed that VEGF expression was induced at the later time point (D4) in an O_2-dependent manner; the difference was significant under lower oxygen tensions (≤ 5% O_2), compared to the control (Figure 6.9C). However, induction of VEGF expression at early time points was only observed at 0% O_2, which indicates an accelerated response (Figure 6.9C). A significant increase in GLUT1 expression was observed under 0% and 2% O_2 at both time points, and at D4 under 5% O_2, relative

to the control (Figure 6.9D). LDHA was also expressed at significant levels at both time points under 0% and 2 O_2, compared to the control (Figure 6.9E).

It was interesting to note that VEGF, LDHA, and GLUT1 were all found to be expressed in an O_2-dependent manner at both time points in all cell lines. Our results are in agreement with previous studies (Gibbons et al. 2006; Sun et al. 2007; Lee et al. 2012; Bae et al. 2012; Forristal et al. 2013; Jung et al. 2016).

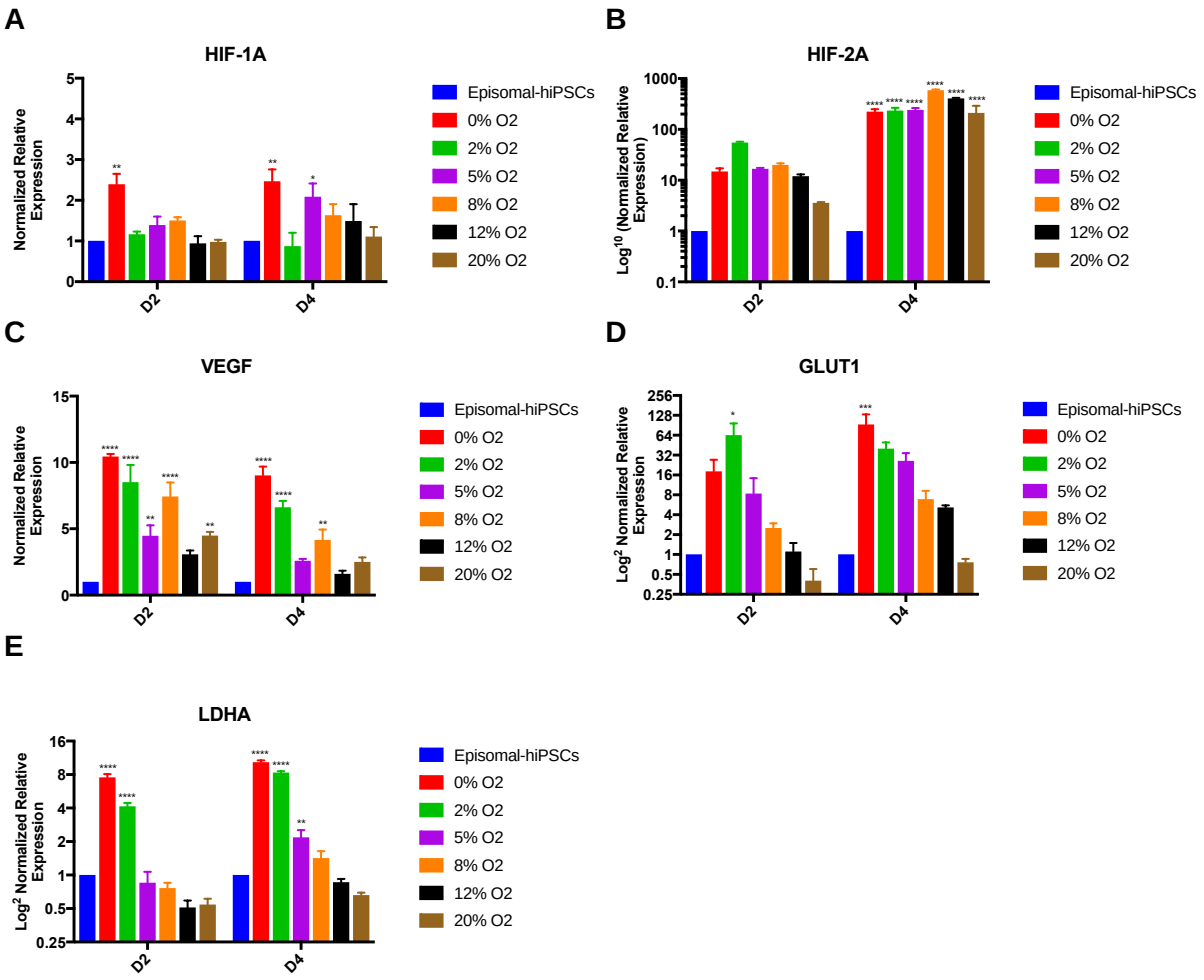

Figure 6.8 Changes in hypoxia-related gene expression in response to different oxygen tensions Episomal-hiPSCs.

Cells were grown in parallel under 0%, 2%, 5%, 8%, 12% and 20% O_2 for 4 days. RT-qPCR was used to analyze the expression of hypoxia-related genes **(A)** HIF-1A and **(B)** HIF-2A and the HIF-responsive genes **(C)** VEGF, **(D)** GLUT1 and **(E)** LDHA. Expression levels are normalized to housekeeping gene β-actin and relative to 1 for undifferentiated Episomal-hiPSCs cultured at 20% O_2. Data are shown as mean ± SD, Two-way ANOVA with Dunnett's multiple comparisons test was used for statistical analysis *($p \leq 0.05$), **($p \leq 0.01$), ***($p \leq 0.001$), ****($p \leq 0.0001$) ($n = 3$).

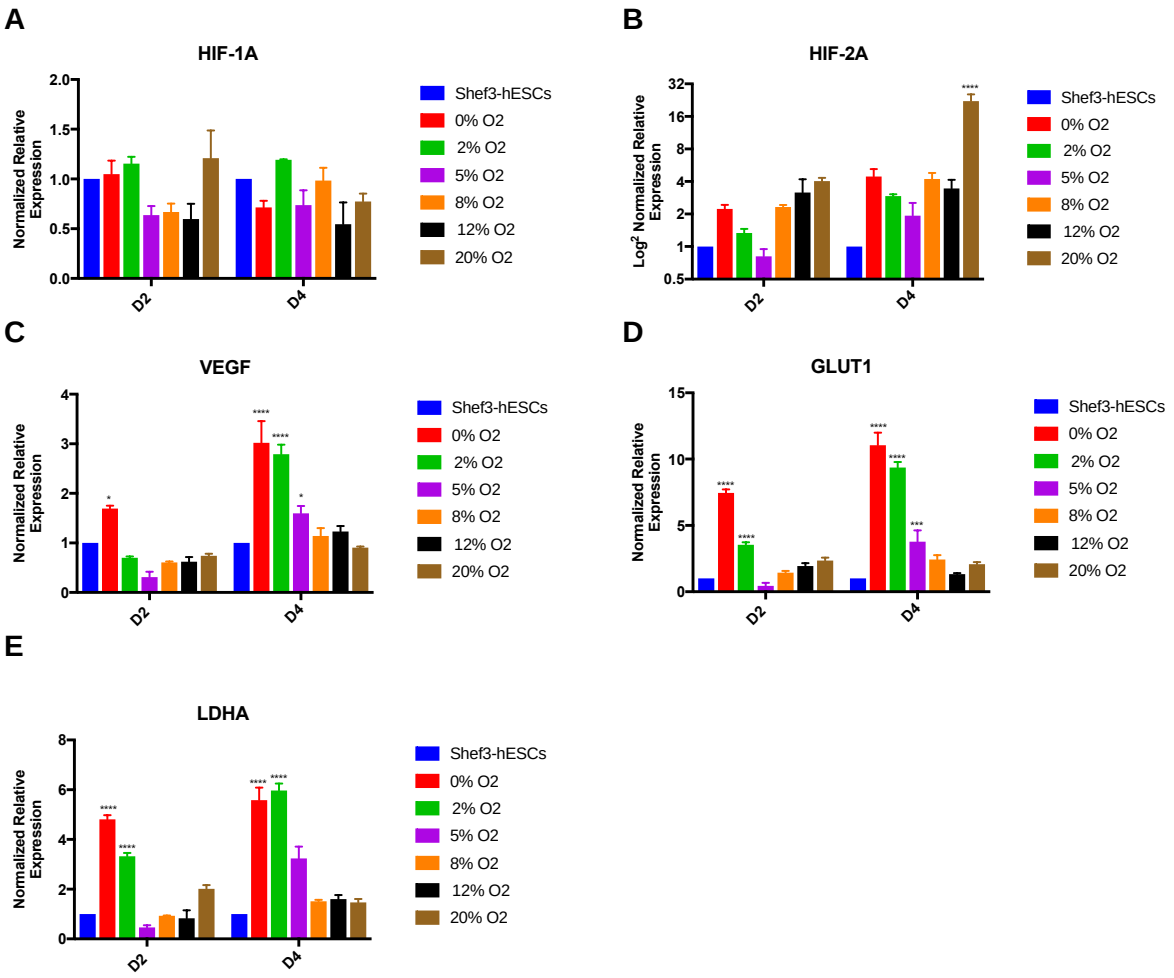

Figure 6.9 Changes in hypoxia-related gene expression in response to different oxygen tensions in Shef3-hESCs.

Cells were grown in parallel under 0%, 2%, 5%, 8%, 12% and 20% O_2 for 4 days. RT-qPCR was used to analyze the expression of hypoxia-related genes **(A)** HIF-1A and **(B)** HIF-2A and the HIF-responsive genes **(C)** VEGF, **(D)** GLUT1 and **(E)** LDHA. Expression levels are normalized to housekeeping gene β-actin and relative to 1 for undifferentiated cells cultured at 20% O_2. Data are shown as mean ± SD, Two-way ANOVA with Dunnett's multiple comparisons test was used for statistical analysis *($p \leq 0.05$), **($p \leq 0.01$), ***($p \leq 0.001$), ****($p \leq 0.0001$) ($n = 3$).

6.3.3 Mild hypoxia induced EMT and Promoted the Differentiation of hPSCs into Mesodermal Lineage

6.3.3.1 Mild hypoxia induced changes in cell architecture in hPSCs

During embryo development, the formation of the three germ layers arises from a series of conversions of epithelial cells to mesenchymal cells, through EMT, where changes in tissue architecture, cell morphology, adhesion, and migratory capacity of ESCs occur (Hay 1995; Pijnenborg et al. 1980; Tam & Behringer 1997).

As the results previously showed that mild hypoxia (8% and 12% O_2) induced the differentiation of Episomal-hiPSCs and Shef3-hESCs into mesoendoderm lineages. We sought next to examine whether mesoendoderm commitment evolved through EMT process, especially, hypoxia is considered to be a key inducer of this process (Fujiwara et al. 2007; Kalluri & Weinberg 2009; Daly et al. 2017). Noticeable morphological features were observed during SP.D of both cell lines cultured under 8% O_2; Episomal-hiPSCs seemed to migrate directionally forming characteristic chains of cells aligned in circles (Figure 6.10A. white arrow), which indicates cell migration (hereinafter referred to as cell migration event) (Thiery et al. 2009; Yeo et al. 2017). While Shef3-hESCs formed epithelial foci that grew as circular and expanded until mesenchymal phenotype formed (Figure 6.10B, white dashed circle). Similar observations have been reported when mesenchymal precursors were derived from hESCs and underwent EMT (Boyd et al. 2009).

These morphological features in both cell lines were observed at a very low rate under other oxygen conditions; to investigate this phenomenon further, we quantified the number of cell migration events formed by Episomal-hiPSCs and the number of epithelial foci that were formed by Shef3-hESCs under all oxygen tensions. The results reveal significantly higher numbers of cell migration events as well as epithelial foci in Episomal-hiPSCs and Shef3-hESCs cultured under 8% O_2, compared to the control (Figure 6.11A and B, respectively). These results reflect the situation *in vivo* during mesoendoderm formation under low oxygen microenvironment. In addition, the results strongly suggest that these cells have a

different cytoskeleton, hence, distinct phenotype; our findings strongly suggest that it was a mesenchymal phenotype.

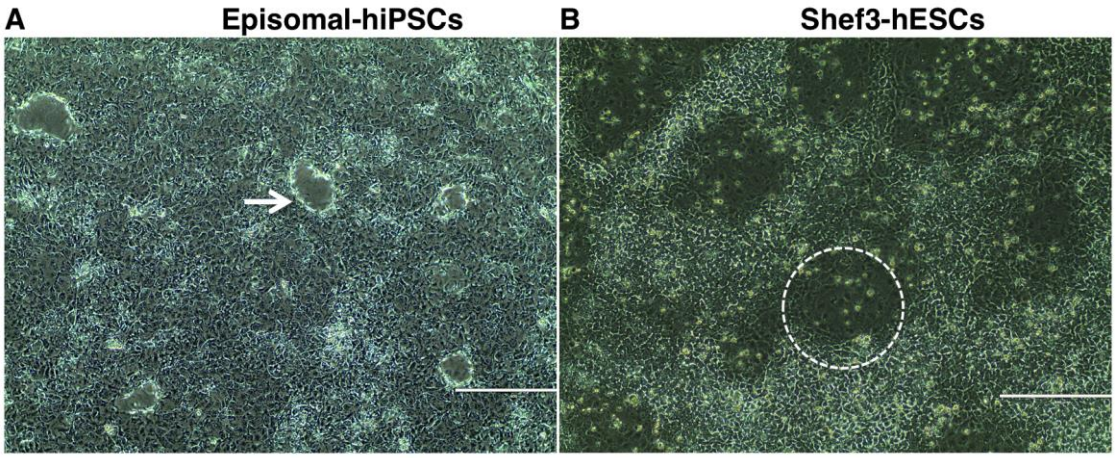

Figure 6.10 Mild hypoxia induces morphologic changes that are characteristic of EMT in both cell lines.
(A) Episomal-hiPSCs polarization at D4 of SP.D (white arrows) and **(B)** epithelial foci formed by Shef3-hESCs (white dashed circle) due to the acquisition of EMT phase. (Magnification 10X, bar= 400µm).

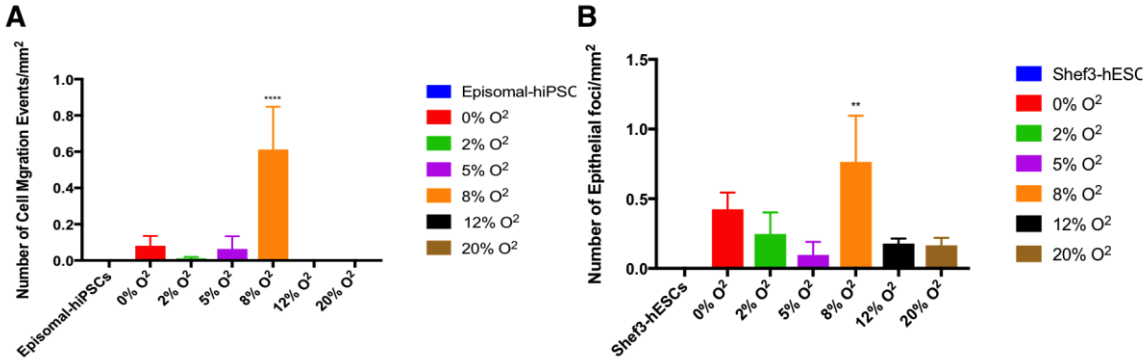

Figure 6.11 Quantification of cell architecture changes at D4 of SP.D
Number of **(A)** cell migration events formed by Episomal-hiPSCs and **(B)** Epithelial foci formed by Shef3-hESCs under all oxygen tensions. The numbers of events/foci were counted in a minimum of three (X10) images per experiment, performed for three independent experiments. The average number of events/foci plotted against undifferentiated cells cultured at the normoxic condition as a negative control (value=0). Data are shown as mean ± SD, Two-way ANOVA with Dunnett's multiple comparisons test was used for statistical analysis *($p \leq 0.05$), **($p \leq 0.01$), ***($p \leq 0.001$), ****($p \leq 0.0001$) ($n = 3$).

6.3.3.2 Analysis of EMT-related protein expression

In light of our morphological observations, we performed immunostaining analysis for the cytoskeletal markers; α-SMA, S100A4, and VIMENTIN. These markers were chosen as specific markers that are used to identify populations generated during early mesodermal differentiation through EMT (Guarino 1995; Eastham et al. 2007; Kim et al. 2014; Liu et al. 2015; Daly et al. 2017; Totonchi et al. 2017).

In Episomal-hiPSCs, α-SMA, S100A4, and VIMENTIN were found to be strongly expressed under 8% O_2 condition (Figure 6.12), suggesting that an EMT event had occurred. Moreover, weak to moderate staining of α-SMA was found in Episomal-hiPSCs cultured under 0%, 2% and 5% O_2, S100A4 was detected under 0%, and 5% O_2, and VIMENTIN was detected under 5% O_2 (Figure 6.12).

Differentiating Shef3-hESCs cultured under 0%, 8% and 12% O_2 conditions exhibited high levels of α-SMA and S100A4 proteins as shown in (Figure 6.13). In contrast, low protein expression patterns of these markers were observed under 2%, 5% and 20% O_2 conditions (Figure 6.13). However, VIMENTIN was expressed at low detectable levels in Shef3-hESCs cultured under 0%, 5%, 8% and 12% O_2, and the protein level was much lower in 20% O_2 (Figure 6.13). Together, these findings suggest that mild hypoxia (range between 5% to 12% O_2) induced Shef3-hESCs differentiation to mesodermal lineage through EMT event.

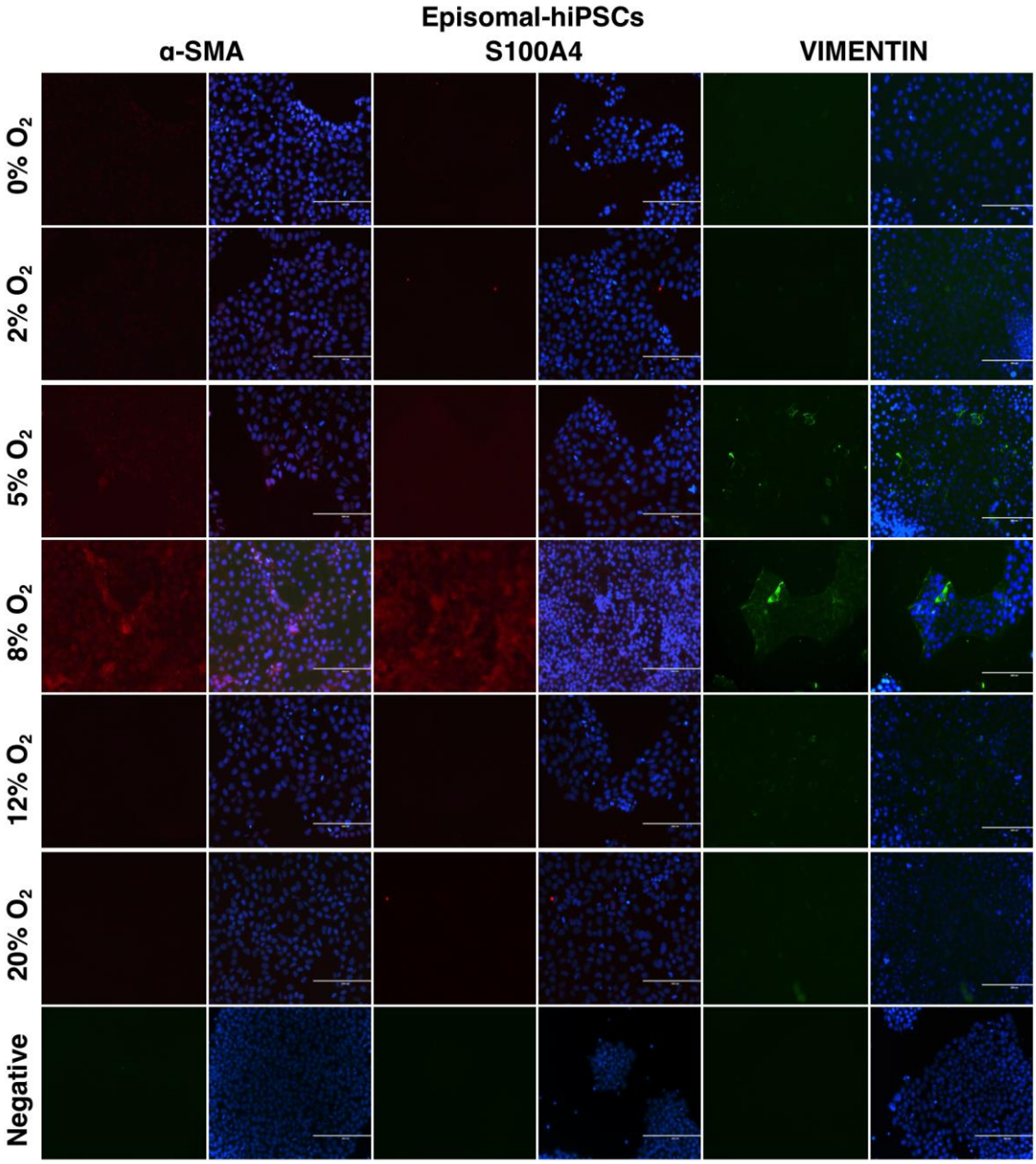

Figure 6.12 Immunostaining analysis of EMT-related markers in Episomal-hiPSCs.
α-SMA & S100A4 (red) and VIMENTIN (green) in Episomal-hiPSCs differentiated spontaneously for 4 days under 0%, 2%, 5%, 8%, 12%, and 20% O_2 conditions. Staining patterns of EMT markers were compared to the negative control of undifferentiated Episomal-hiPSCs cultured under 20% O_2. Nuclei were stained by DAPI (blue), and the corresponding merged image is represented in the right-hand panel for each marker (Magnification 20X, bar= 200μm).

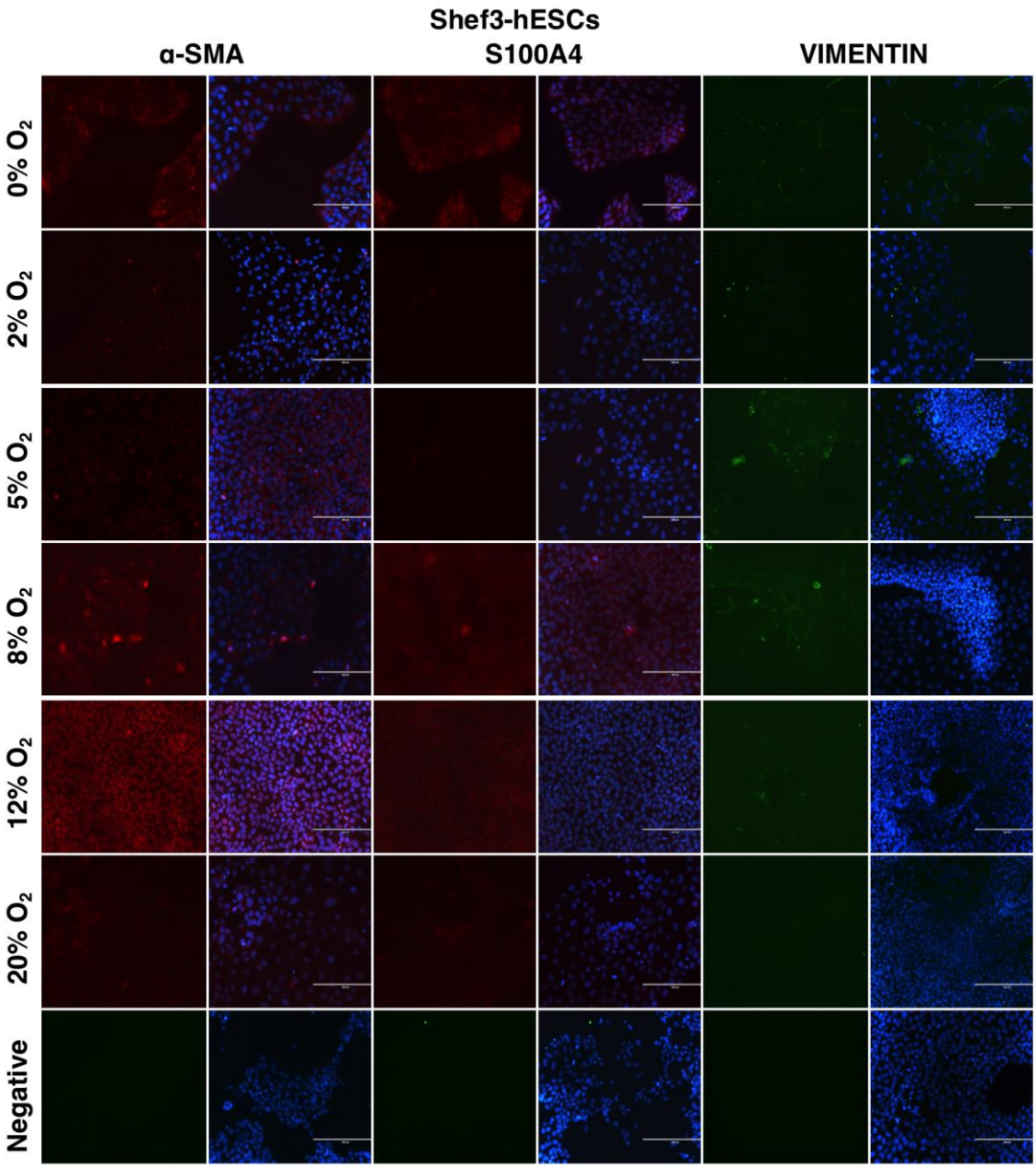

Figure 6.13 Immunostaining analysis of EMT-related markers in Shef3-hESCs.
α-SMA & S100A4 (red) and VIMENTIN (green) in Shef3-hESCs differentiated spontaneously for 4 days under 0%, 2%, 5%, 8%, 12%, and 20% O_2 conditions. Staining patterns of EMT markers were compared to the negative control of undifferentiated Shef3-hESCs cultured under 20% O_2. Nuclei were stained by DAPI (blue), and the corresponding merged image is represented in the right-hand panel for each marker (Magnification 20X, bar= 200μm).

6.3.3.3 Mild hypoxia regulated EMT via SNAIL pathway in hPSCs and induced Cadherin switch

The hallmark of EMT *in vivo* is the down-regulation of E-cadherin (CDH1), an important trans-membrane protein for stable adherence junctions that coincides with the up-regulation of mesenchymal marker N-cadherin (CDH2) and increasing migration ability (Thiery et al. 2009). SNAIL is a transcription factor that regulates EMT during mesoderm formation *in vivo* during gastrulation (Ciruna & Rossant 2001; Hajra et al. 2002; Spencer et al. 2007; Gheldof & Berx 2013). *In vitro* differentiation of hESCs into mesoderm has been shown to be associated with a membranous E- to N-cadherin switch (Behr et al. 2005; Angela M Eastham et al. 2007; Spencer et al. 2007; Boyd et al. 2009).

The changes in E-cadherin and N-cadherin expression were investigated in Episomal-hiPSCs and Shef3-hESCs cultured under all oxygen conditions. The data reveal that no significant differences were observed in the expression of E-cadherin between oxygen conditions in both cell lines (Figure 6.14A and D).

Our results show that mild hypoxia (8% O_2) accelerated the induction of N-cadherin in Episomal-hiPSCs (Figure 6.14B), which was followed by significant up-regulation in SNAIL expression at D4, relative to the control (Figure 6.14C). This suggests that the cells were in a transition stage into a mesenchymal phenotype through EMT. The expression of N-cadherin was reduced in Episomal-hiPSCs cultured under 0%, 2%, 5%, 12% and 20% O_2 conditions at all-time points, and the difference was significant at D4 under 2%, 5%, 8%, 12% and 20% O_2 relative to the control (Figure 6.14B). These results indicate that Episomal-hiPSCs did not acquire a mesenchymal phenotype especially under 0%, 5%, 12, and 20% O_2 as cells under these conditions expressed lower levels of SNAIL at both time (Figure 6.14C). Episomal-hiPSCs unexpectedly expressed SNAIL at D4 under 2% O_2 relative to the control (Figure 6.14C).

In Shef3-hESCs, N-cadherin expression was significantly increased under 0%, 8%, and 20% O_2 at D2, but the expression of N-cadherin remained significant until D4 under 0% O_2, compared to the control (Figure 6.14E). N-cadherin also increased

significantly at D4 under 12% O_2, compared to the control (Figure 6.14E). The expression of SNAIL was increased considerably under 5%, 12% and 20% O_2 conditions, compared to the control (Figure 6.14F). It is important to note that there was a slight increase in mRNA expression of N-cadherin and SNAIL at D4 under 8% O_2 in Shef3-hESCs; however, the difference was not statistically significant, compared to the control (Figure 6.14E and F).

Although some of the oxygen conditions induced EMT-like changes in both cell lines, the aspect of EMT events including E- to N-cadherin switch and a significant up-regulation in SNAIL expression were more pronounced in Episomal-hiPSCs and Shef3-hESCs cultured under 8% and 12% O_2 conditions, respectively, as these conditions induced multiple aspects of EMT.

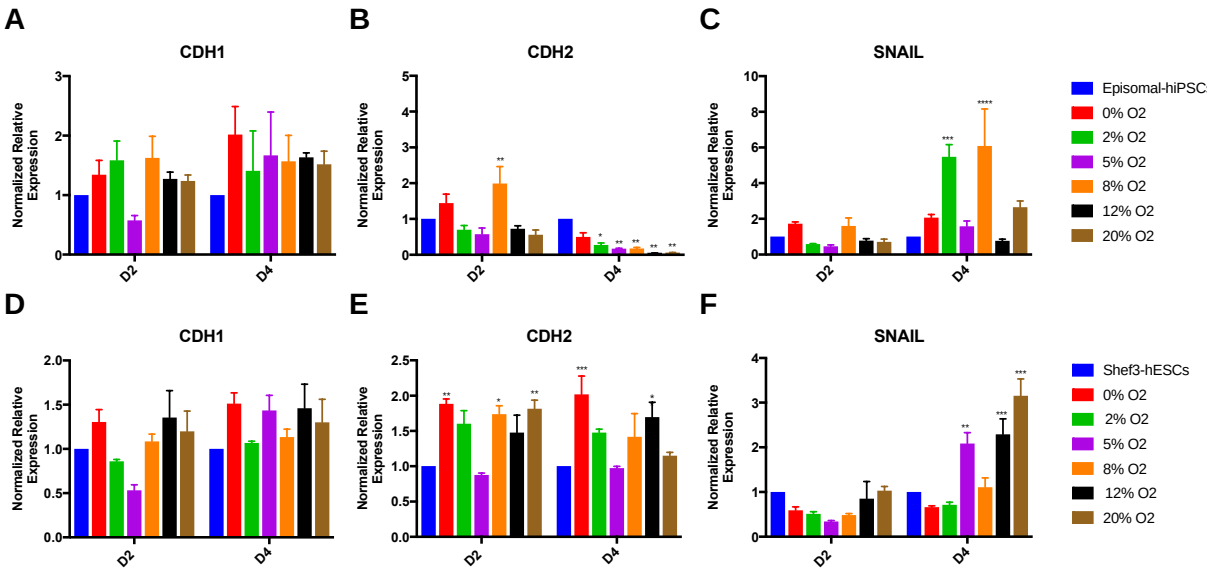

Figure 6.14 Relative quantification of CDH1, CDH2 and SNAIL mRNA expression levels during SP.D under different oxygen tensions.

Epithelial marker CDH1, mesenchymal marker CDH2 and EMT regulator SNAIL (CDH1 suppressor) in Episomal-hiPSCs **(A-C)** and Shef3-hESCs **(D-F).** Expression levels were normalized to housekeeping gene β-actin, and relative to 1 for undifferentiated cells cultured at 20% O_2 Data are shown as mean ± SD, Two-way ANOVA with Dunnett's multiple comparisons test was used for statistical analysis *($p \leq 0.05$), **($p \leq 0.01$), ***($p \leq 0.001$), ****($p \leq 0.0001$) ($n = 3$). Abbreviation: CDH1: E-cadherin, CDH2: N-cadherin.

6.3.4 The Effect of Combining Mild Hypoxia with STEMDIFF™ Mesoderm Induction Medium (MIM)

The experimental work discussed previously investigated the effect of a full range of oxygen tensions on the SP.D of hPSCs into the three germ layers. The results demonstrated how manipulation of the oxygen level could be used to influence stem cells fate. Specifically, mild hypoxia (8% and 12% O_2) was shown to drive Episomal-hiPSCs and Shef3-hESCs towards mesoendoderm lineage through EMT based on the increased expression of candidate markers. By establishing this outcome, it was important to investigate whether combining this optimum oxygen level, as hypothesized, would improve the efficiency of directed the mesoderm differentiation through EMT by analysing the related markers.

Using a monolayer differentiation protocol, under chemically defined conditions without additional growth factors and cytokines, Episomal-hiPSCs and Shef3-hESCs were plated on 6-well plates coated with Matrigel and cultured under normoxic or mild hypoxic conditions (8% and 12% O_2). On the following day, the culture medium (DMEM/F12+10um Y27632) was replaced with STEMdiff™ Mesoderm Induction Medium (MIM), and cells were further incubated up to 4 days and collected on (D2 and D4) for analysis (Figure 6.15).

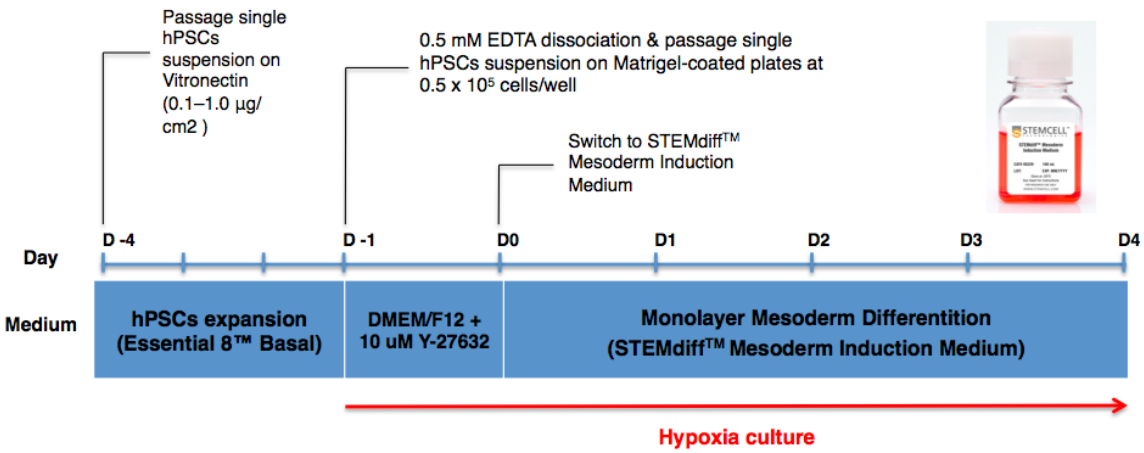

Figure 6.15 Timeline of mesoderm induction medium differentiation protocol.
On D-1, hPSCs were harvested and seeded as single cells at $0.5x10^5$ cells/well in DMEM/F12 medium supplemented with 10 µM Y-27632. On D0, initiation of mesoderm differentiation, when cells were at approximately 20 - 40% confluency, DMEM/F12 medium was replaced with STEMdiff™ Mesoderm Induction Medium (MIM). Cells were then fed daily and collected on D2 and D4 for downstream analysis. Red arrow represents the initiation of hypoxic culture at 8% and 12% O_2.

6.3.4.1 Morphological analysis.

Within 2 to 4 days of changing into STEMdiff™ MIM, confluent Episomal-hiPSCs and Shef3-hESCs began to differentiate and exhibited changes in cytoskeletal architecture and cell-cell interaction under all conditions (Figure 6.16). They grew as compact colonies; adjacent cells are connected by tight junctions (Krtolica et al. 2007), gap junctions (Huettner et al. 2006), and adherens junctions (U. Ullmann et al. 2007). Interestingly, at D2, Shef3-hESCs formed epithelial foci similar to those seen previously with the SP.D culture of Shef3-hESCs under 8% O_2 (Figure 6.10B, white dashed circle). This morphological characteristic is commonly observed in ESCs differentiated into mesoderm through EMT (Gheldof & Berx 2013; Kim et al. 2014; Liu et al. 2017). On D4, Episomal-hiPSCs and Shef3-hESCs became elongated, junction complexes started to disrupt, and some cells migrated individually, which indicates loss of cell polarity, and mesenchymal-like cells were emerging (Figure 6.16, black arrows)

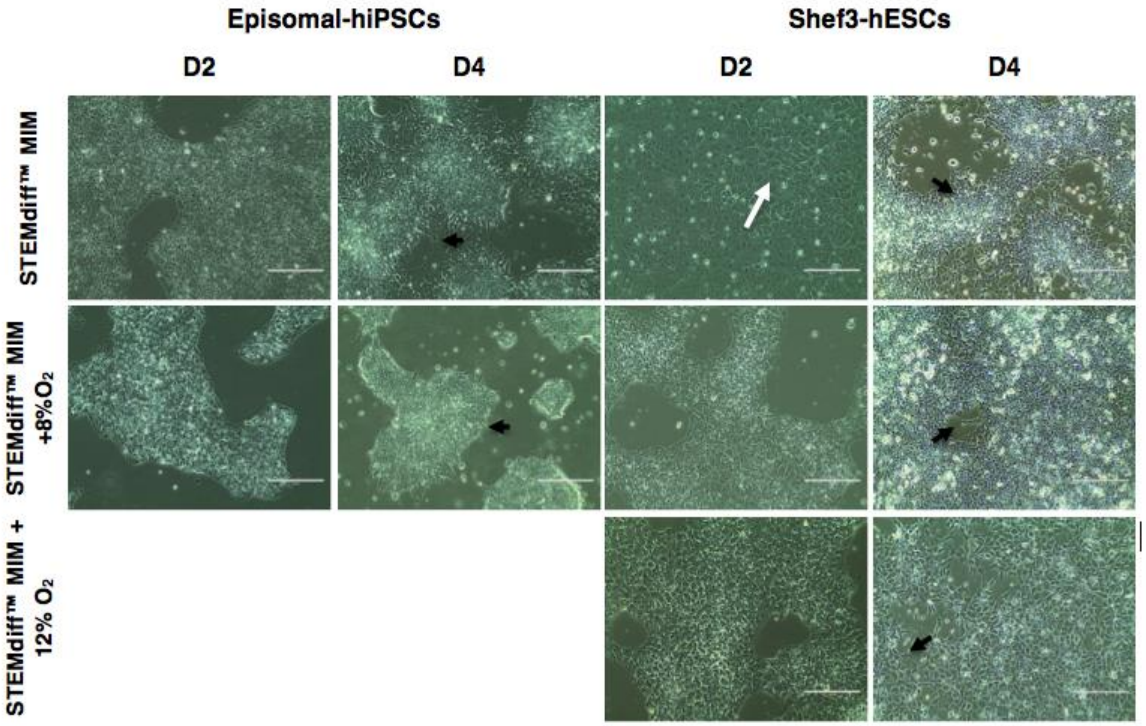

Figure 6.16 Phase contrast images of Episomal-hiPSCs and Shef3-hESCs cultured under STEMdiff™ MIM directed protocol.

Cells were differentiated in STEMdiff™ MIM media for 4 days under normoxic or mild hypoxic conditions (8% O_2 for Episomal-hiPSCs) and (8% and 12% O_2 for Shef3-hESCs). At D2, cells are organized in one layer of flattened cells, and the entire culture presented an epithelial phenotype, Shef3-hESCs began forming epithelial foci expanded in a circular pattern (white arrow). At D4, cells underwent EMT, and mesenchymal-like cells are emerging (black arrows). (Magnification 20X, bar= 200µm).

6.3.4.2 Influence on the pluripotency- and mesoderm-related markers

Immunostaining analysis showed that there was an up-regulation of BRACHYURY in both cell lines under all conditions (Figure 6.17). It is interesting to note that more intense staining of BRACHYURY was detected under STEMdiff™MIM+8% O_2 as well as STEMdiff™MIM+12%O_2 than those cultured under STEMdiff™MIM alone (Figure 6.17).

RT-qPCR results showed profound changes in gene expression during the time course of STEMdiff™ MIM treatment under all conditions. Pluripotency marker OCT4 significantly down-regulated in both cell lines at all-time points tested relative to the control (Figure 6.18A and C).

Early mesoderm population was characterized by BRACHYURY expression. The results show that combining mild hypoxia (8% O_2) with STEMdiff™MIM significantly induced BRACHYURY expression in Episomal-hiPSCs at D2, compared to the control (Figure 6.18B). BRACHYURY remained expressed at significant levels at D4 in STEMdiff™MIM and in STEMdiff™MIM+8%O_2 conditions, compared to the control (Figure 6.18B).

Similar gene expression trend was observed in Shef3-hESCs. The results show that at D2, STEMdiff™MIM+8% O_2 and STEMdiff™MIM+12% O_2 significantly increased BRACHYURY expression, compared to the control (Figure 6.18D), the expression was higher than that observed under STEMdiff™MIM alone. At D4, the expression significantly increased under STEMdiff™MIM and STEMdiff™MIM+8% O_2 conditions compared to the control (Figure 6.18D). There was also a relative up-regulation of BRACHYURY expression under STEMdiff™MIM+12% O_2; however, the difference was not significant, compared to the control (Figure 6.18D).

It was interesting to note that, under STEMdiff™MIM condition, the expression level of BRACHYURY was significantly induced but at a later time point (D4) in Episomal-hiPSCs and Shef3-hESCs, relative to control (Figure 6.18B and D). Our results revealed that combining mild hypoxia (8% and 12% O_2) enables the differentiation of

Episomal-hiPSCs and Shef3-hESCs towards mesodermal precursors at faster kinetics and more efficiently.

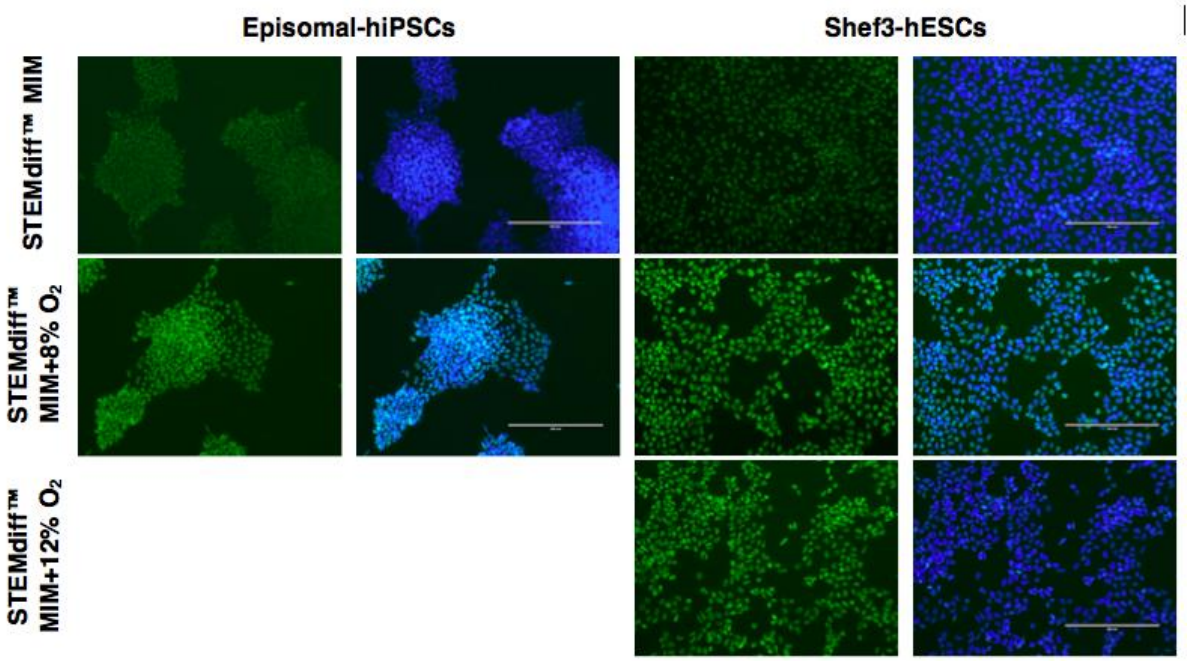

Figure 6.17 Immunostaining analysis of mesoderm marker during STEMdiff™MIM protocol.
BRACHYURY (green) was detected in Episomal-hiPSCs and Shef3-hESCs cultured under STEMdiff™MIM, STEMdiff™MIM + 8% O_2 and STEMdiff™MIM +12% O_2 for 4 days. Nuclei were stained by DAPI (blue), and the corresponding merged image is represented in the right-hand panel for each cell line (Magnification 20X, bar= 200µm).

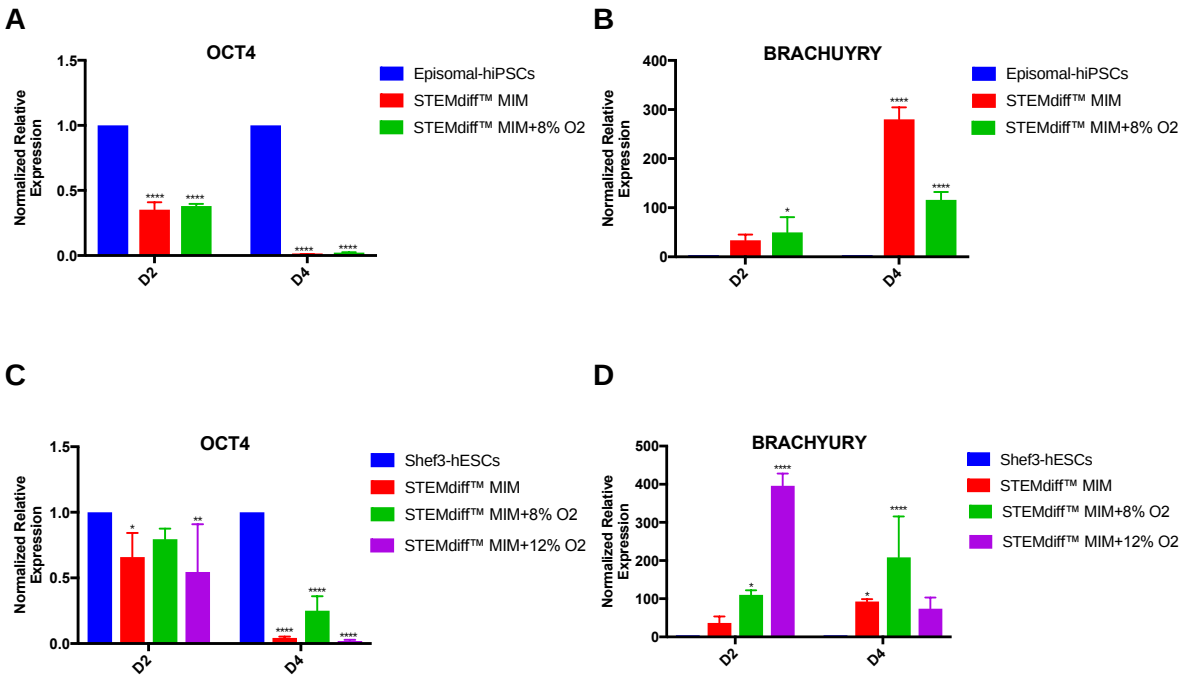

Figure 6.18 Gene expression of OCT4 and BRACHYURY over time during STEMdiff™MIM protocol combined with mild hypoxia in Episomal-hiPSCs and Shef3-hESCs.

Data showed significant down-regulation of OCT4 **(A & C)** and up-regulation of BRACHYURY **(B & D)** expression and on D4 of the protocol. All data have been normalized to β-actin and 1 for undifferentiated cells cultured at 20% O_2. Data are shown as mean ± SD, Two-way ANOVA with Dunnett's multiple comparisons test was used for statistical analysis *($p \leq 0.05$), **($p \leq 0.01$), ***($p \leq 0.001$), ****($p \leq 0.0001$) ($n = 3$).

6.3.4.3 Human PSCs undergo EMT during directed mesoderm differentiation

We further analysed the expression of EMT-associated markers to investigate whether combining mild hypoxia with STEMdiff™ MIM differentially regulate EMT mechanism *in vitro*.

Immunostaining analysis showed a significant re-organization of cytoskeletal proteins on the basis of α-SMA, S100A4 and VIMENTIN up-regulation under all conditions in both cell lines (Figure 6.19.A and B). Interestingly, the staining intensity of cytoskeletal proteins were more pronounced under STEMdiff™ MIM+8%O_2 and STEMdiff™MIM+12%O_2 than STEMdiff™ MIM alone.

Quantitative analysis by RT-qPCR showed a significant down-regulation of E-cadherin expression under all conditions at D2 and D4 in both cell lines, compared to the control (Figure 6.20A and D). E-cadherin down-regulation was followed by a gradual up-regulation in N-cadherin expression under all conditions in both cell lines, reaching significant levels at D4 in Episomal-hiPSCs and Shef3-hESCs, compared to the control (Figure 6.20B and E), respectively. The cadherin switch observed in both cell lines was associated with an elevation in SNAIL expression at D4 under all conditions; the difference was significant under STEMdiff™ MIM in both cell lines relative to the control (Figure 6.20C and F). Also, combining mild hypoxia (8%O_2) with STEMdiff™ MIM increased the expression of SNAIL in Episomal-hiPSCs and Shef3-hESCs, relative to the control (Figure 6.20C and F).

These results strongly suggest that (i) the population of cells formed under all conditions had undergone EMT during mesodermal commitment and (ii) combining mild hypoxia accelerates the acquisition of EMT phenotypes in hPSCs.

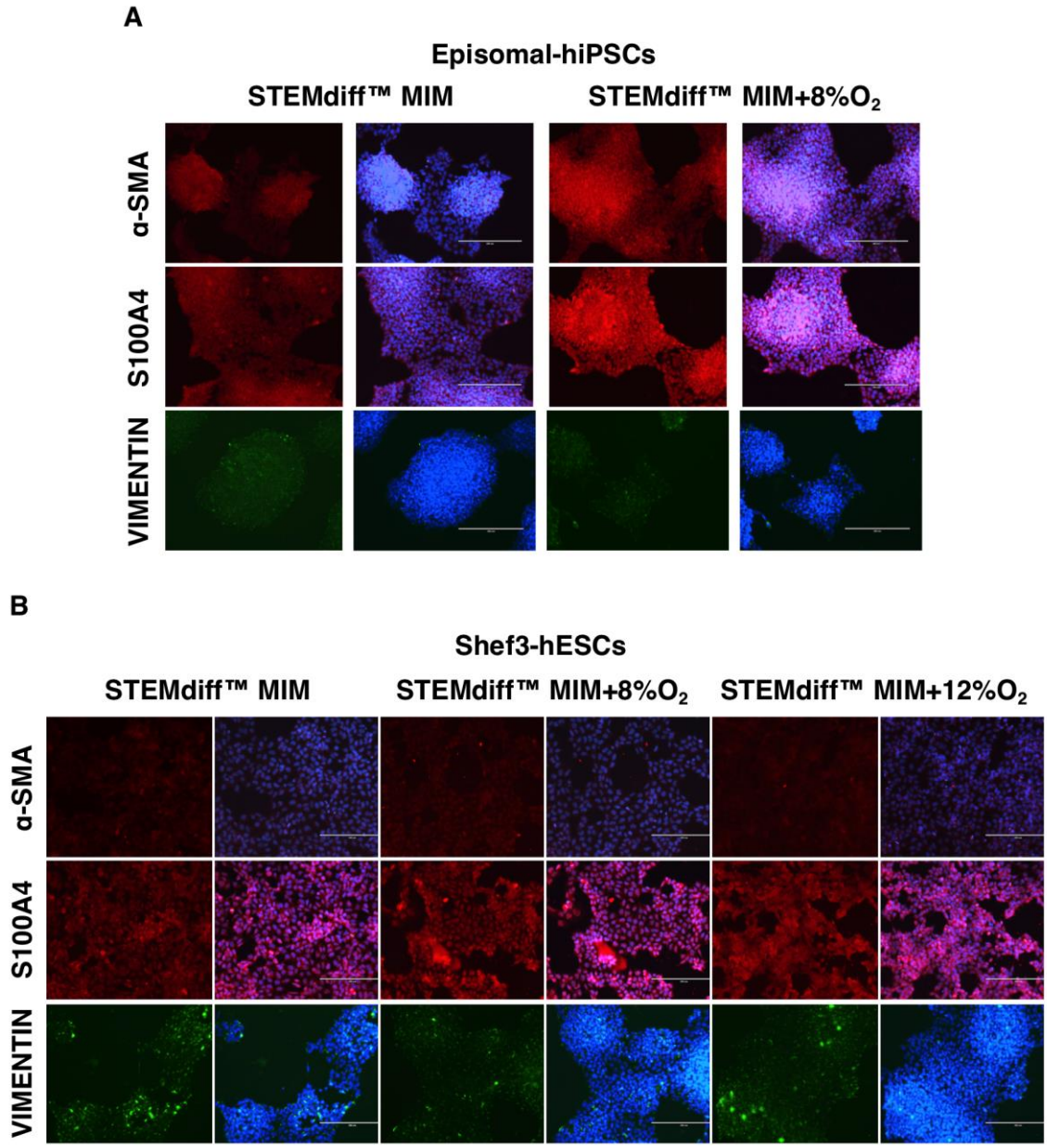

Figure 6.19 Up-regulation of the mesenchymal markers in EMT-induced cells.
Cells were stained for mesenchymal markers, S100A4 and α-SMA (red) and VIMENTIN (green) in **(A).** Episomal-hiPSCs and **(B).** Shef3-hESCs. Nuclei were stained by DAPI (blue), and the corresponding merged image is represented in the right-hand panel for each condition (Magnification 20X, bar= 200μm).

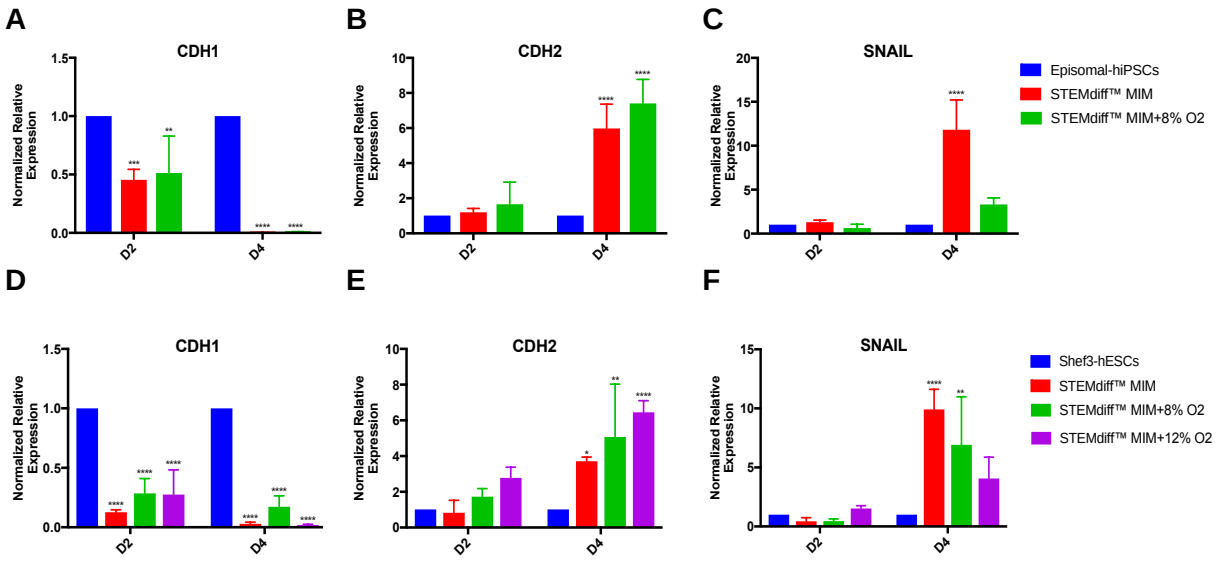

Figure 6.20 Time-course analysis EMT-related genes expression using RT-qPCR. Expression of cytoskeleton markers CDH1 and CDH2 as well as SNAIL in **(A-C)** Episomal-hiPSCs and **(D-F)** in D2 and D4. Episomal-hiPSCs and Shef3-hESCs cultured under STEMdiff™MIM, STEMdiff™MIM + 8% O_2 and STEMdiff™MIM +12% O_2 for 4 days. All data have been normalized to β-actin and 1 for undifferentiated cells cultured at 20% O_2. Data are shown as mean ± SD, Two-way ANOVA with Dunnett's multiple comparisons test was used for statistical analysis *(p≤ 0.05), **(p≤0.01), ***(p≤0.001), ****(p≤0.0001) (n = 3).

6.4 DISCUSSION AND CONCLUSION

Stem cells differentiation is a major hurdle for successful translation of stem cell research to clinical applications. Developing embryo undergoes dynamic changes in oxygen tensions, ranging from ~1.5% O_2 in the first trimester toward ~8% O_2 starting from the second trimester until birth, which why it is thought that oxygen gradients define an embryo's fate (Jauniaux et al. 2000; Poh, et al. 2014). Thus, it is not surprising that low oxygen tension influences the differentiation into many cell types. Regarding the effects of oxygen tension on spontaneous differentiation of hPSCs toward derivatives of all three germ layers, the literature is surprisingly limited. Indeed, while multiple studies have been demonstrating directed differentiation of hPSCs, attention has primarily been focused on the derivation of mature cell types instead of the early events of germ layer formation, which could play a significant role in improving the effectiveness of the differentiation controls. We aimed to highlight the role of oxygen only, by allowing the cells to differentiate spontaneously without the restriction of any growth factors or small molecules, and accordingly study their behaviour in response to different levels of oxygen.

The data presented here demonstrated that the manipulation of oxygen conditions induced striking morphological differences during the culture period (4days). These include enlargement of the cell area and volume, reorganization of focal contacts, and loss cell polarization in both cell lines. Different morphological subpopulations were observed; small triangular cells, large star-shaped with accentuated membrane regions cells, flattened mesenchymal-like cells and elongated spindle-shaped cells. Several studies have classified morphological subgroups within the hMSCs culture; for example, small triangular cells were classified as rapidly self-renewing mesodermal progenitors (Colter et al. 2000; Colter et al. 2001; Prockop et al. 2001; Smith et al. 2004). Another study went further and classified more mature hMSCs into elongated spindle-shaped cells (Muraglia et al. 2000) and large, flattened cells (Docheva et al. 2008; Haasters et al. 2009). A study has shown that hypoxia level (1% O_2) induced profound changes in Fibroblast cells architecture (Vogler et al. 2013). Collectively, our data with others suggest that (i) morphological heterogeneity in a culture does not only indicate the existence of distinct cell types but also might represent different stages of cells and hypoxia might be a significant inducer and (ii)

cytoskeleton changes of cell shape are hypoxia-dependent; however, the details remain unclear.

A hypoxic microenvironment is one of the critical 'niche' components in regulating stem cells fate (Davy & Allsopp 2011). However, it is arguable to which direction between self-renewal and differentiation hypoxia drives stem cells. Our results revealed that there was an overall down-regulation of pluripotency markers including OCT4, NANOG, and GDF3 in both cell lines. It was found that hypoxia promotes hESCs multilineage differentiation by suppressing OCT4 expression via direct binding of HIF-1A to reverse hypoxia-responsive elements (rHREs) in the OCT4 promoter (Lee et al. 2012). Although mRNA expression of HIF-1A- is known to be down-regulated in a variety of cells under hypoxic conditions, due to post-transcriptional regulation (Ziello et al. 2007; Forsyth et al. 2008; Westfall et al. 2008). Our RT-qPCR results showed that levels of HIF-1A were slightly up-regulated, especially in Episomal-hiPSCs under some oxygen conditions but not at normoxia condition (20% O_2). This data may support finding from (Lee et al. 2012) and implies that under hypoxia, the differentiation of Episomal-hiPSCs into specific lineage was HIF-1A-dependent. In our data, we showed that HIF-2A was up-regulated during SP.D under 0%, 2%, 5%, 8% and 12% O_2 conditions in both cell lines. The expression was found to be more pronounced at D4. This confirms a previous finding that HIF-2A mediates the late/chronic hypoxic response (Catherine E. Forristal et al. 2013). This also mimics the *in vivo* situation during embryonic development, which is coordinated by the interplay between HIF-1A and HIF-2A (Koh & Powis 2012a). We also found that HIF-2A was constitutively stabilized under normoxic condition (20% O_2), which is in line with others (Liu et al. 2003; Bracken et al. 2006; Fang et al. 2009).

Cellular adaptation to oxygen gradients greatly depends on HIF-A regulation. The 'classical response' to hypoxia involves up-regulation of hypoxia-related genes including VEGF, LDHA and GLUT1, the latter two genes involved during the switching from aerobic to anaerobic metabolism (Gassmann et al. 1996; Wenger et al. 1997). Our data showed that the expression of VEGF, LDHA, and GLUT1 were all up-regulated during SP.D under 0%, 2%, 5%, 8% O_2 but not under 12% and 20% O_2 conditions in both cell lines. These results suggest an increase in glucose

metabolism, which may play a role in the early differentiation of hPSCs as a part of the coordinated response to hypoxia. *In vivo*, reduced oxygen tension experienced by the embryo stimulates angiogenesis to enhance local oxygen delivery by up-regulating VEGF (Chen et al. 2009). The data suggest that our findings mimic the *in vivo* situation during the formation of three germ layers, which is consistent with previous studies (Behrooz & Ismail-Beigi 1997; Lim et al. 2011; Gilkes et al. 2013).

Regarding spontaneous differentiation under different oxygen conditions, we demonstrated that Episomal-hiPSCs and Shef3-hESCs seemed to be differentiated into mixtures of cells of three germ layers under different oxygen tensions. For example, we found that the induction into endodermal lineage in Episomal-hiPSCs was observed under almost all oxygen conditions including 0%, 2%, 5%, 12% and 20% O_2. However, the induction was faster under 0% and 2% O_2 than those observed with higher oxygen conditions. Delayed induction into endodermal lineages was also observed in Shef3-hESCs under higher oxygen conditions (5%, 12% and 20% O_2). Several studies have demonstrated the acceleration effect of hypoxia during the *in vitro* differentiation of many cell types; however, the underlying mechanism hasn't been addressed yet. For instance, the differentiation of mESCs and hESCs into pancreatic lineages was accelerated under hypoxic culture conditions, and Insulin-producing Cells were generated within 2–3 weeks (Hakim et al. 2014), although *in vivo* these cells are not generated until week 10 after endoderm specification (Spence & Wells 2007). Also, it was found that FIH-1 (a negative regulator of HIF-1A function) (Mahon et al. 2001) inhibited Notch activity, which resulted in accelerated myogenic differentiation under hypoxia conditions (Zheng et al. 2008). Moreover, hypoxia conditions accelerated the formation of contracting EBs during Cardiomyocytes differentiation protocol of ESCs (Bianco et al. 2009). Also, short-term hypoxia accelerated vascular-lineage differentiation through HIF-1A-mediated response (Lee et al. 2012). *In vivo*, it is well-established that the activation of HIF-1A has been repeatedly shown to accelerate the physiologic wound healing processes (Higgins et al. 2007; Kalucka et al. 2013; Ruthenborg et al. 2014) and bone regeneration (Wan et al. 2008) and in tumour angiogenesis (Dewhirst et al. 2008). These processes are associated with multiple events of cellular differentiation through EMT (Sturrock et al. 2018). As discussed previously, EMT is a key process during ESCs differentiation. Therefore, we suggest

that the observed accelerated differentiation is mainly mediated by HIF-1A through EMT, as demonstrated previously (Kuschel et al. 2012), HIF-1A is post-transcriptional regulated, which facilitates immediate response. Also supported by data presented in chapter 5, the stabilization of HIF-1A protein in response to lower oxygen tensions (≤5% O_2) was fast (30min), which could result in an accelerated response. While under normoxia, HIF-1A protein was not detected, which might explain the delayed onset of differentiation seen under this condition in both cell lines.

Our results showed that the induction into ectodermal lineage was transient in Episomal-hiPSCs, based on PAX6 expression at D2 only, under all oxygen conditions. However, oxygen tension differentially regulated specification into ectoderm in Shef3-hESCs, as PAX6 expressed at later time point under 0%, 2% and 5% O_2. Several studies demonstrated perturbed ectoderm specification under hypoxic conditions (Agca et al. 2009; Pimton et al. 2014; Burr et al. 2018). Interestingly, it was found that HIF-1A (-/-) mESCs failed to induce endodermal differentiation but rather shifted toward ectoderm (Pimton et al. 2014). Moreover, a study has found that re-oxygenation during hypoxic protocol resulted in the preferential formation of ectoderm over mesoderm and endoderm lineages (Fynes et al. 2014). These data suggest that hypoxia is not the main regulator in ectoderm differentiation. Collectively, our data suggest the existence of a 'temporal window' during the early stages of hPSCs differentiation where the expression of different germ layers markers may overlap. We also observed remaining unexplained variance in gene expression pattern that might account for some of the inherent differences between different cell types or experiments conditions.

To the best of our knowledge, the present study demonstrates for the first time that mild hypoxia induced the mesoderm differentiation in hPSCs via EMT mechanism. *In vivo*, during the EMT process, epithelial cells transition from a polarized tightly connected cells to non-polarized, and migratory mesenchymal cells (Serrano-Gomez et al. 2016). The data revealed that higher numbers of cell migration events and epithelial foci were observed in Episomal-hiPSCs and Shef3-hESCs under mild hypoxia (8% and 12% O_2), respectively. Similar morphological features have been reported *in vitro* when mesenchymal progenitors were derived from hESCs and

underwent EMT (Lee et al. 2006; Boyd et al. 2009; Kovacic et al. 2012; Li et al. 2012; Chen et al. 2013; Vogler et al. 2013; Daly et al. 2017). The results showed that under mild hypoxia, these populations expressed EMT-related proteins including α-SMA, S100A4, and VIMENTIN, while under other oxygen conditions the expression was reduced or absent. Additionally, our data showed that the SP.D of hPSCs in monolayer culture was associated with an E- to N-cadherin switch that was coincided with a significant up-regulation of SNAIL. Our findings are in line with others (Ciruna & Rossant 2001; Eastham et al. 2007; U Ullmann et al. 2007; Spencer et al. 2007; Evseenko et al. 2010; Gheldof & Berx 2013; Kim et al. 2014; Yeo et al. 2017). Collectively, these observations indicate that mild hypoxia induced the acquisition of EMT-like event during the mesodermal commitment of hPSCs, similar to that observed *in vivo* during early gastrulation. It must be noted that there was unexpected increase in the expression of pluripotency markers including OCT4, NANOG and GDF3 were observed in Shef3-hESCs cultured under 12% O_2 conditions. Overexpression of OCT4 has been shown to shift the differentiation into mesoendoderm derivatives (Niwa et al. 2000; Karwacki-Neisius et al. 2013). These data provide further evidence on the preferential differentiation of mesoderm observed with Shef3-hESCs cultured under 12% O_2 condition.

Given that mild hypoxia is optimum for mesoderm differentiation based on our findings, directed mesoderm differentiation medium (STEMdiffTM MIM) was used to test whether combining mild hypoxia would improve the differentiation efficiency into mesoderm lineage and whether it is through EMT. Our data showed that combining mild hypoxia (STEMdiffTM MIM+8% O_2 and STEMdiffTM MIM+12% O_2) led to more rapid and pronounced mesoderm differentiation as evident by the increased expression of BRACHYURY, especially in Shef3-hESCs line. Also, directed differentiation into mesoderm using STEMdiffTM MIM was through EMT. Indeed, classic features of EMT such as cell migration, epithelial foci formation, expression of α-SMA, S100A4 and VIMENTIN, losing cell polarization that is associated with E- to N- cadherin switch as well as SNAIL up-regulation all of which were observed under STEMdiffTM MIM in a very comparable manner to those observed during SP.D under mild hypoxia in both cell lines. Most importantly, the data revealed that combining mild hypoxia accelerated the acquisition of EMT-like event in both cell lines. These findings imply that (i) hypoxia is a critical factor in regulating stem cells

fate and (ii) that mild hypoxia positively impacts the *in vitro* differentiation of hPSCs into mesodermal lineage in a way that mimics *in vivo* situation. EMT-like event previously described as being involved during *in vitro* directed differentiation of hESCs into endoderm (D'Amour et al., 2005) mesoderm (Evseenko et al. 2010; Gill et al. 2011). A later study has found that activation of EMT by Snail induced mesoderm commitment while suppressing the differentiation into ectoderm, which might explain why hypoxia failed to induce ectoderm commitment in this study.

To conclude, this study demonstrated the generation of mesoderm precursors from SP.D hPSCs cultured under mild hypoxia (8% and 12% O_2) without exogenous factors, which was through EMT. Our study also showed further evidence that hypoxia accelerated the induction into germ layers when compared to normoxic conditions, which is on agreements (Rathjen et al. 1999; Ramírez-Bergeron et al. 2004; Hammoud et al. 2016). Moreover, using simple monolayer differentiation protocol, we demonstrated that timing, duration, and level of exposure to hypoxia differentially regulate hPSCs fate toward precursors of germ layers. Mild hypoxia was found optimum for mesoderm differentiation and showed positive impact when combined with the directed mesoderm culture system. Establishing the optimum oxygen level for the generation of each germ layer progenitors will be critical in realizing the promise of stem cells for not only regenerative therapies but also as accurate *in vitro* systems for disease modelling and toxicity screening tools. To accomplish this goal, understanding the underlying molecular mechanisms regulating early stem cell fate decisions is critical. See **Table 6-1**, **Table 6-2** and Figure 6.21 for concluding remarks.

Table 6-1 Concluding Remarks – Episomal-hiPSCs

O_2 Level (%)	Morphology		Pluripotency			Hypoxia		Differentiation			EMT		
	D2	D4	OCT4	NANOG	GDF3	HIF-1A	HIF-2A*	SOX17 Endoderm	B Mesoderm	PAX6 Ectoderm	Proteins	Cadherin switch	SNAIL
0%	Heterogeneous population		Decreased sig.		Increased sig.	Increased sig. D2&D4	Gradual increase reached sig. levels at D4	Increased sig. D2&D4	Increased sig. D2&D4	Increased sig. at D2, absent at D4	Weak	Slight increase at D2	Slight increase at D2&D4
2%	Heterogeneous population					Decreased D2&D4		Increased sig. D2&D4	Slight increase		Weak	Decreased	Increased sig. at D4
5%	Heterogeneous population				Decreased sig.	Increased D2&D4		Slight increase	Slight increase		Weak to moderate	Decreased	Slight increase at D4
8%	Heterogeneous population + Sig. increase in cell migration events				Decreased sig.	Increased D2&D4		Increase at D2	Increased sig. D2&D4		Strong	Increased sig. at D2	Increased sig. at D4
12%	Heterogeneous population				Decreased sig.	Decreased at D2, increased at D4		Increased sig. at D4	Slight decrease		-ve	Decreased	Decreased
20%	Heterogeneous population				Decreased sig.	Decreased at D2 & D4			Slight increase		-ve	Decreased	Slight increase

Continued in next page >>

Table 6-2 Concluding Remarks – Shef3-hESCs

<table>
<tr><th rowspan="2">O_2 Level (%)</th><th colspan="2">Morphology</th><th colspan="3">Pluripotency</th><th colspan="2">Hypoxia</th><th colspan="3">Differentiation</th><th colspan="3">EMT</th></tr>
<tr><th>D2</th><th>D4</th><th>OCT4</th><th>NANOG</th><th>GDF3</th><th>HIF-1A</th><th>HIF-2A*</th><th>SOX17 Endo</th><th>B Meso</th><th>PAX6 Ecto</th><th>Proteins</th><th>Cadherin switch</th><th>SNAIL</th></tr>
<tr><td>0%</td><td colspan="2">Heterogeneous population</td><td rowspan="3">Decreased</td><td rowspan="3">Decreased</td><td rowspan="3">Decreased</td><td>Slight increase at D2</td><td rowspan="6">Gradual increase reached high levels at D4</td><td rowspan="2">Decreased</td><td>Slight increased at D4</td><td rowspan="3">Increased sig at D4</td><td>Strong</td><td>Increased sig at D2&D4</td><td>Decreased</td></tr>
<tr><td>2%</td><td colspan="2">Heterogeneous population</td><td>Slight increase at D2&D4</td><td>Decreased</td><td>Weak</td><td>Slight increased</td><td>Decreased</td></tr>
<tr><td>5%</td><td colspan="2">Heterogeneous population</td><td rowspan="3">Decreased</td><td>Increase sig. at D4</td><td>Slight increased at D4</td><td>Weak</td><td>Decreased</td><td>Increased sig. at D4</td></tr>
<tr><td>8%</td><td colspan="2">Heterogeneous population + epithelial foci</td><td rowspan="3">Decreased</td><td>Decreased</td><td>Slight increased at D4</td><td rowspan="3">Slight increase</td><td>Strong</td><td>Increased sig. at D2</td><td>Slight increase at D4</td></tr>
<tr><td>12%</td><td colspan="2">Heterogeneous population</td><td colspan="2">Increased sig at D4</td><td>Increased</td><td rowspan="2">Increase sig. at D4</td><td>Slight increased at D4</td><td>Strong to moderate</td><td>Increase at D2&D4</td><td>Increased sig. at D4</td></tr>
<tr><td>20%</td><td colspan="2">Heterogeneous population</td><td colspan="2">Decreased</td><td>Increased sig. at D4</td><td>Increased sig. at D4</td><td>Weak</td><td>Increased sig.at D2</td><td>Increased sig. at D4</td></tr>
</table>

(*) HIF-2A mediated the chronic response during the *in vitro* differentiation in both cell-lines, which mimic *in vivo* situation.
(–) Higher oxygen tensions ≥8% O_2 seemed to be more effective in inducing the differentiation of hPSCs into mesoendoderm lineages.
(Grey cell) 2% O_2 induced only marginal potentiation of mesoendoderm differentiation.
Abbreviation: sig; significant, Meso; mesoderm, Endo; endoderm, Ecto; ectoderm

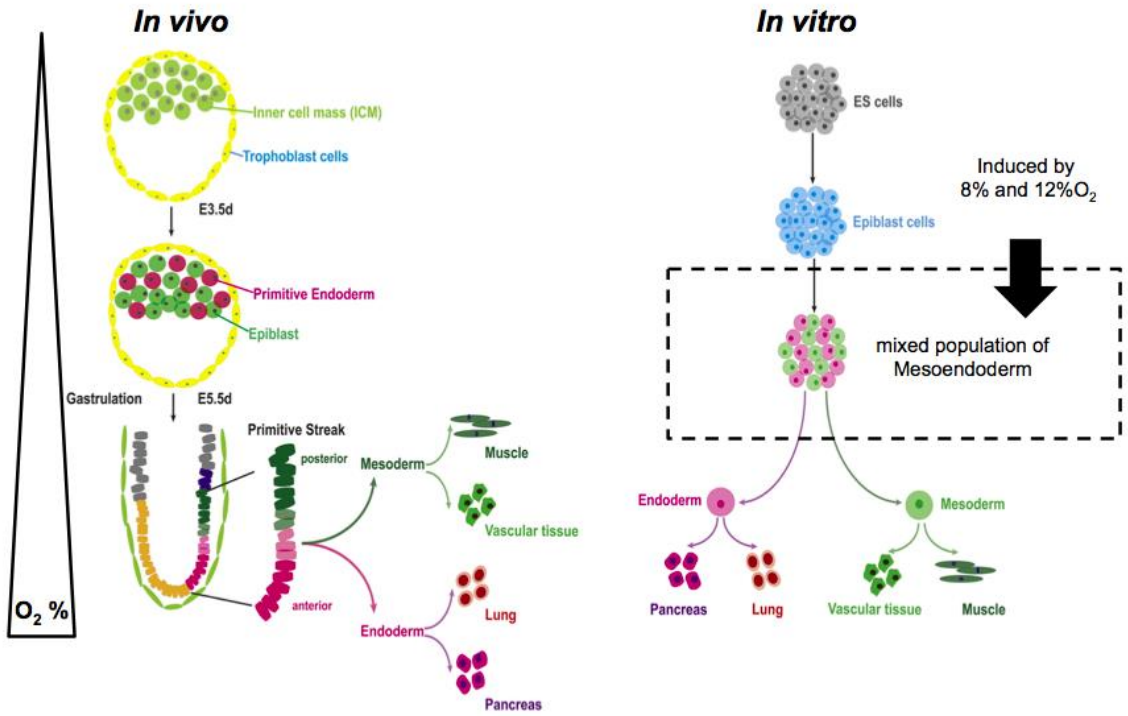

Figure 6.21 Concluding remarks, mild hypoxia enriched the hPSCs with mesendoderm popluation that mimics the *in vivo* formation of the Primitive streak during mouse embryogenesis.

In vivo: mouse embryo develops to a blastocyst (embryonic day 3.5), with the outer cells becoming trophoblast cells and the inner cells forming the ICM. The ICM is further differentiated into pluripotent Epiblast and the cells that contribute to the primitive endoderm. At about embryonic day 5.5, gastrulation begins: epiblast cells form a transient structure-primitive streak, which is the source of three germ layers. The anterior part of the primitive streak forms endoderm tissues (e.g., pancreas, stomach and liver) while the posterior part develops mesoderm tissues (e.g., bone, heart and muscle). ***In vitro*:** ES cells are derived from the ICM can differentiate into any cell types from the three germ layers (ectoderm, mesoderm, and endoderm). When ES cells are differentiating, they become Epiblast cells, which have the potential to differentiate into all layers except the trophoblast. Epiblast cells can further differentiate to Mesoendoderm, which is equivalent to the primitive streak, and subsequent mesoderm and endoderm tissues (Wang 2016).

7 CHAPTER 7: RECOMMENDATION OF FUTURE WORK

The culture of hPSCs under atmospheric conditions does not replicate the low oxygen microenvironment of the uterus where ESCs reside, as well as BM and SVZ where HSCs and NSCs are resided, respectively which may result in cellular impairment during culture including ROS production and genomic instability. To overcome these limitations, we have cultured hPSCs under culture conditions similar to those experienced *in vivo*. We have explored the effect of a wide range of oxygen levels on the proliferation and differentiation potentials of hPSCs.

Based on the results demonstrated in this thesis, and the current state of the field, many areas would benefit from further investigation.

Throughout this project, cells were maintained under the desired optimal conditions using C-Shuttle Glove Box. Cells were exposed to suboptimal conditions (20% O_2) when they were being harvested for analysis. However, all sample-harvested procedures were performed carefully on ice (e.g. fixation, morphological observation under the microscope, cell harvesting for PCR or cell count). It was necessary to harvest cells on ice due to the short half-life of HIF-1A, given its universal role in many downstream cellular processes which was the focus of this project. Given that, also as procedures that require real-time O_2 monitoring was not needed (e.g. lifetime imaging), C-Shuttle Glove Box, discussed in **chapter 3,** was sufficient as it serves the purpose of this project. However, to perform *in vitro* bioprocesses for cells expansion/differentiation protocols that require full O_2 control, including downstream examination, the Biosherix X3 CytoCentric platform (Biospherix, Ltd., Syracuse, NY) could be more useful (Figure 7.1). This system provides full-time optimization, where O_2%, CO_2%, pH and temperature during incubation and cell handling can be monitored. Additionally, all third-party machines such as microscopes, centrifuges, bioreactors and plate reader can be incorporated. This full time and dynamic control would indeed reduce variability between studies and lead to greater reproducibility.

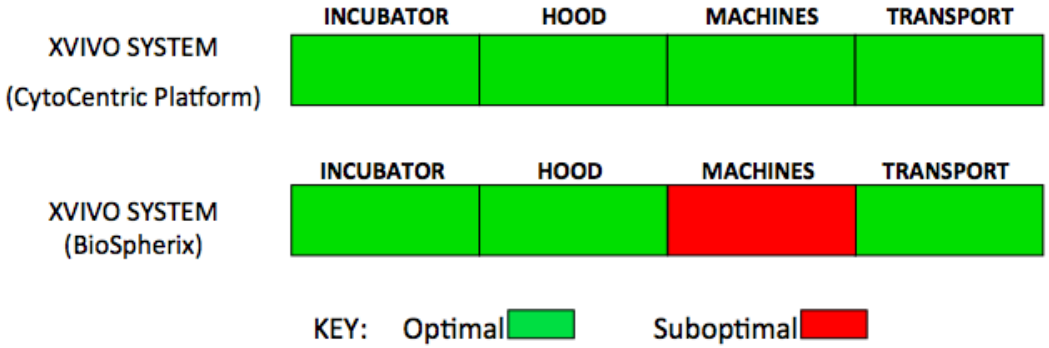

Figure 7.1 Differences in workflow during culturing cells within the CytoCentric Platform and C-Shuttle Glove Box.

Although the results from **chapter 4**, showed that the hPSCs were pluripotent, based on morphology, protein & gene analysis, and represented a suitable starting material to test our hypotheses. However, we don't know whether the populations are stem cell-enriched and what the estimated percentage of purity is and if this had an impact on the outcomes obtained from experiments in **chapter 5 and 6**. Therefore, Flow Cytometry analysis is highly recommended to quantify the proportion of stem cells expressing pluripotency makers. Moreover, as variability in starting population can lead to mixed population and variable and unpredictable results, the thing that complicates scaling up the differentiation protocols, it would be interesting to physically sort heterogeneous subpopulations into the pure and homogeneous population to start with using Fluorescence-Activated Cell Sorting (FACS). This will increase the efficiency of differentiation protocols.

The results in **chapters 5 and 6** indicate that Episomal-hiPSCs have an inherently different tendency to differentiate into a particular lineage, when compared to Shef3-hESCs, which highlights; (i) the possibility of selecting specific cell lines for specific differentiation protocols and (ii) the need to include at least two cell lines for each cell type to assess whether the changes observed are cell line-specific or due to variability in cell culture conditions.

The results from experiments performed in **chapter 5**, showed that the culture condition of 0% O_2 generated massively higher numbers of floating cells. Although the consistent presence of floating cells is a common phenomenon in hPSCs

cultures, it is highly recommended to involve more detailed analysis (e.g. Annexin V - PI staining) to gain a greater understanding of their nature. As according to (Krishna Dasa SS et al. 2014), not all floating cells are dead cells. Additionally, some discrepancies were observed in the metabolic profiles of hPSCs. As so, including other metabolites analysis including glutamine and ammonia will create a better understanding of energy metabolism experienced by the cells under different oxygen tensions.

In chapter 6, during the SP.D protocol, we observed that the Episomal-hiPSCs pellets that were cultured under mild hypoxia (8% O_2) were hardly dissociated into single cells when the downstream analysis was performed, which might be an indication of matrix synthesis. This observation is of particular interest because hypoxia is known in modulating surrounding ECM (e.g. collagen type II and proteoglycan) and focal adhesion compositions (Grimmer et al. 2006; Coyle et al. 2008; Lim et al. 2011a; Gilkes et al. 2013; Maldonado & Nam 2013; Makris et al. 2013; Gilkes et al. 2014; Zieseniss 2014). Therefore, further analysis to identify specific ECM component is highly recommended.

The data presented here have clear implications for stem cell bioprocessing, as they offer a short and cost-effective option for differentiating hPSCs into different lineage by only manipulating O_2 levels. However, we need to gain a deep understanding of the role of oxygen tension on stem cells fate decision. One valuable lesson we learn from *in vivo* embryonic development is that the few early stages of maturation of all tissues occur under low oxygen level, while the maturation proceeds the oxygen level increase but never reaches 20% O_2 in the human body until adult age. Therefore, one of our long-term goals is to optimize hPSCs bioprocessing by applying stage- and time-dependent oxygen culture protocol to efficiently generate the most clinically important lineages (e.g. Cardiomyocytes and βeta cells) from hPSCs (Figure 7.2).

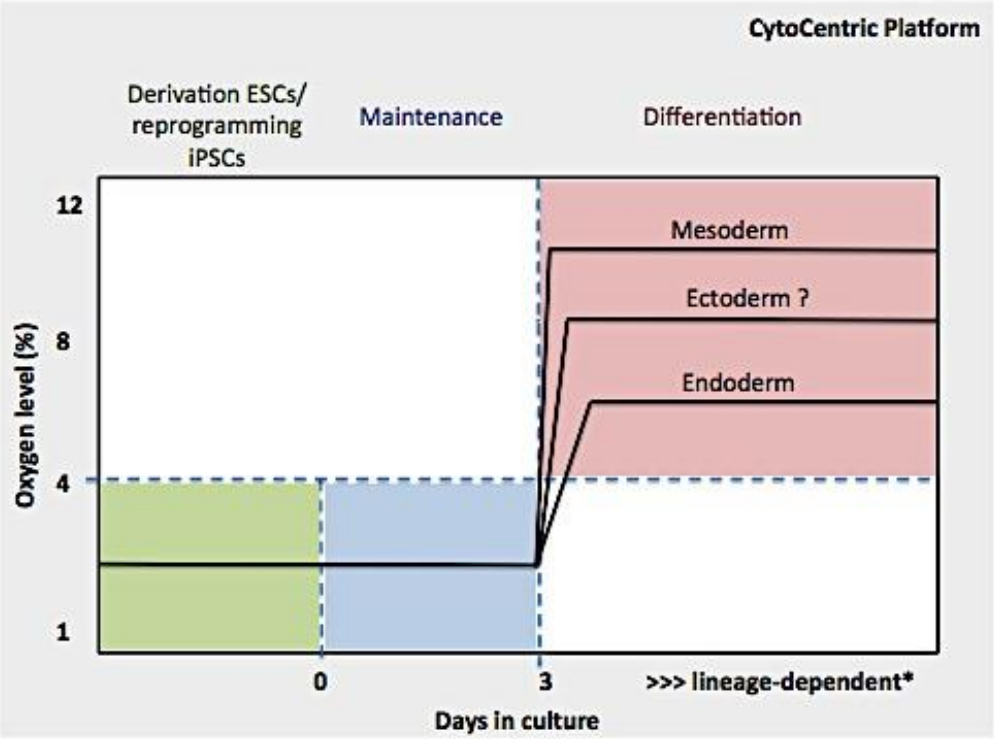

Figure 7.2 The Main Stages Within Stem Cell Bioprocess Development
This illustrative diagram depicts the whole bioprocess from Stem Cells derivation, maintenance and differentiation. Traditionally the primary considerations were attempting to obtain a target cell type, but now, increasingly, research focuses on the downstream bioprocessing of the cells, at each stage trying to maximise the reproducibility, safety, and efficiency of the bioprocess. Derivation of the cells should be performed in similar conditions where the cells are derived from. During the maintenance stage, a short-culture period is adequate, as the hypoxic cascade is immediate and universals. The duration of differentiation protocols is lineage-dependent. The cells during all these stages should not be exposed to suboptimal conditions (20%O_2), and this can be possible using the CytoCentric system.

8 CHAPTER 8: Appendices

8.1 Appendix

8.1.1 Validation plots for CO_2/O_2 controllers.

This data refers to the experiments discussed in **Section 3.3.2**
Known O_2 gas mixtures (0%, 2%, 5%, 8% and 12% O_2) were used after each calibration procedure to validate calibration. After ~10 mins, steady state was reached, and average CO_2 concentrations were recorded (from 5 consecutive readings) over a period of 24 hours by ProCO_2 Model120. Error bars represent the standard deviation (SD) for 8 replicates.

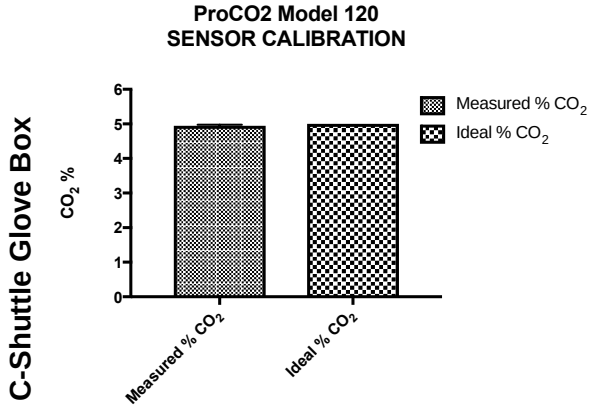

8.2 Appendix

This data refers to the experiments discussed in **Section 5.3.1.2**
To investigate the effects of different oxygen tensions on the self-renewal and proliferation properties of Episomal-hiPSCs and Shef3-hESCs, cells were passaged as a single cell suspension using TrypLE^{TM} to allow for uniform and consistent Initial Seeding Density (ISD)-corresponds to 0hrs- ($0.6X10^5$ cells/cm^2). Then, cells were maintained in parallel under normoxic (20% O_2) and hypoxic (0%, 2%, 5%, 8% and 12% O_2) conditions for 72hrs. Total counts for adherent and floating cells were monitored throughout the culture period of 72hrs. It was noticed that the absolute number of adherent cells increased under all oxygen conditions, but not 12% O_2 culture condition; 0% O_2 $0.01x10^6$ to $0.028x10^6$), 2% O_2 ($0.013x10^6$ to $0.025x10^6$),

5% O_2 (0.014x10^6 to 0.026x10^6), 8% O_2 (0.013x10^6 to 0.061x10^6) and 20% O_2 (0.019x10^6 to 0.066x10^6). Our results showed that Episomal-hiPSCs cultured under normoxic condition displayed a high growth rate as evident by the increased number of adherent cells during the culture periods of 48hrs and 72hrs. The number of adherent cells was higher than all oxygen conditions and the difference was significant under 0% O_2 condition (p=0.0036). Similar growth pattern was observed after 72hrs, the data showed that there was more pronounced cell growth under 8% and 20% O_2 conditions, and the difference was significant under 0%, 2%, 5% and 12% O_2 (p<0.0001). This indicates an increased growth rate of Episomal-hiPSCs under normoxia.

Table 8.2.A: Adherent CellsX10^6/cm2 (Episomal-hiPSCs)

O_2%	Time (hrs)	Mean	SD (±)
0%	0hrs	0.06	0
	24hrs	0.0106666666666667	0.00152752523165195
	48hrs	0.00866666666666666	0.00251661147842358
	72hrs	0.0286666666666667	0.00472581562625261
2%	0hrs	0.06	0.0050251666639028
	24hrs	0.0133333333333333	0.00208166599946613
	48hrs	0.0156666666666667	0.000577350269189626
	72hrs	0.0246666666666667	0.00115470053837925
5%	0hrs	0.06	0.00115470053837925
	24hrs	0.0143333333333333	0.00251661147842358
	48hrs	0.0256666666666667	0.0055075705472861
	72hrs	0.0263333333333333	0.0161658075373095
8%	0hrs	0.06	0.00577350269189626
	24hrs	0.0126666666666667	0.000577350269189625
	48hrs	0.025	0.003
	72hrs	0.061	0.00854400374531753
12%	0hrs	0.06	0.00577350269189626
	24hrs	0.02	0.01
	48hrs	0.02	0
	72hrs	0.0166666666666667	0.00577350269189626
20%	0hrs	0.06	0.00577350269189626
	24hrs	0.0186666666666667	0.00208166599946613
	48hrs	0.025	0.00264575131106459
	72hrs	0.0656666666666667	0.00763762615825973

Similar results were observed with the other cell line -Shef3-hESCs- as there was an increase in the adherent cell count number under all oxygen conditions throughout the culture period of 72hrs; 0% (0.047 x10^6 to 0.077 x10^6), 2% (0.031 x10^6 to 0.133 x10^6), 5% (0.018 x10^6 to 0.082 x10^6), 8% (0.069 x10^6 to 0.164 x10^6), 12% (0.037 x10^6 to 0.105 x10^6) and 20% O_2 (0.038 x10^6 to 0.341 x10^6). The results showed that

at 24hrs of the culture period, the number of adherent cells under 8% O_2 was significantly higher than 20% O_2 condition (p=0.0434). Additionally, significantly higher cell count was observed in the culture maintained under 20% O_2 in compare to all other O_2 conditions (P=0.0001) following 48hrs and 72hrs. This result comes in agreement with Episomal-hiPSCs, as the cells were highly proliferative under normoxic condition (20% O_2).

Table 8.2.B: Adherent cellsX10^6/cm2 (Shef3-hESCs)

O_2%	Time (hrs)	Mean	SD (±)
0%	0hrs	0.06	0.00577350269189626
	24hrs	0.0473333333333333	0.00378593889720019
	48hrs	0.0505982373333333	0.00327044737627459
	72hrs	0.0773666666666667	0.0102080033960287
2%	0hrs	0.06	0.00128315996364444
	24hrs	0.03051	0.00131160207380135
	48hrs	0.0345166666666667	0.00352857383844144
	72hrs	0.133136666666667	0.0112696953522858
5%	0hrs	0.06	0.007
	24hrs	0.0176666666666667	0.00416333199893227
	48hrs	0.0203333333333333	0.00416333199893227
	72hrs	0.0816666666666667	0.0188767935130237
8%	0hrs	0.06	0.01
	24hrs	0.0686666666666667	0.0055075705472861
	48hrs	0.127666666666667	0.00503322295684717
	72hrs	0.164	0.0398873413503583
12%	0hrs	0.06	0.00577350269189626
	24hrs	0.0366666666666667	0.00577350269189626
	48hrs	0.09	0.02
	72hrs	0.103333333333333	0.0115470053837925
20%	0hrs	0.06	0.00577350269189626
	24hrs	0.038	0.00519615242270663
	48hrs	0.204843333333333	0.0278758611227229
	72hrs	0.341192593333333	0.0292802587518644

Cell counts of floating cells under all oxygen conditions were also evaluated every 24 hours over the maintenance culture We found a gradual decrease in the absolute number of floating cells under all oxygen condition over the culture period of 72hrs; 0% O_2 ($0.07x10^6$ to $0.01x10^6$), 2% O_2 ($0.06x10^6$ to $0.019x10^6$), 5% O_2 ($0.08x10^6$ to $0.02x10^6$), 8% O_2 ($0.062x10^6$ to $0.02x10^6$), 12% O_2 ($0.12x10^6$ to $0.03x10^6$) and 20% O_2 ($0.075x10^6$ to $0.018x10^6$). More specifically, after 24hrs of cell culture, the number of floating cells under 8% O_2 was significantly lower compared to normoxic cells (p=0.0230). After 48hrs, the number of floating cells under 20% O_2 was significantly lower than 0% O_2 (p=0.0082), 2% O_2 (p=0.0339) and 5% O_2 (p=0.0022). However,

cells maintained under 12% O_2 condition showed different phenomena. As shown in the results, the absolute adherent cell number decreased throughout the culture period of 72hrs ($0.02x10^6$ to $0.017x10^6$), and the number of floating cells was significantly higher than the cells cultured under 20% O_2 at all time pointed examined ($P<0.0001$).

Table 8.2.C: Floating Cells$X10^6$/cm2 (Episomal-hiPSCs)

O_2%	Time (hrs)	Mean	SD (±)
0%	24hrs	0.0776666666666667	0.000577350269189626
	48hrs	0.0346666666666667	0.00351188458428425
	72hrs	0.0156666666666667	0.0045092497528229
2%	24hrs	0.0686666666666667	0.00585946527708231
	48hrs	0.0323333333333333	0.00665832811847939
	72hrs	0.019	0.003
5%	24hrs	0.0826666666666667	0.00152752523165195
	48hrs	0.0366666666666667	0.00513160143944688
	72hrs	0.0236666666666667	0.00472581562625261
8%	24hrs	0.0626666666666667	0.00929157324317757
	48hrs	0.0236666666666667	0.00251661147842358
	72hrs	0.0293333333333333	0.00251661147842358
12%	24hrs	0.12	0
	48hrs	0.05	0.01
	72hrs	0.0366666666666667	0.00577350269189626
20%	24hrs	0.075	0.007
	48hrs	0.0206666666666667	0.00321455025366432
	72hrs	0.0186666666666667	0.00251661147842358

In Shef3-hESCs; the number of floating cells decreased under 2% ($0.046\ x10^6$ to $0.027\ x10^6$) and 5% ($0.052\ x10^6$ to $0.019\ x10^6$), but interestingly, it was noted that the number of floating cells increased in culture conditions of 0% ($0.060\ x10^6$ to $0.6\ x10^6$), 8% ($0.048\ x10^6$ to 0.126 x106), 12% (0.060 x106 to 0.143 x106) and 20% O_2 (0.041 x106 to 0.047 x106), with more pronounced increase under 0% O_2. As illustrated in Table 8.2.D; the number of floating cells at 48hrs of culture period was significantly higher under 8% than 20% O_2 ($p=0.0023$). Moreover, the results showed that the number of floating cells under 0%, 8% and 12% O_2 conditions after 72hrs was significantly higher than 20% O_2 ($p<0.0001$), ($p=0.0005$) and ($p=0.0001$), respectively. Furthermore, there was a noticeable increase in the floating cell number of cells cultured under 8% and 12% O_2 conditions. The data suggest that there was higher proliferation rate under conditions of 8%, 12% and 20% O_2. Additionally, culture conditions of 2% and 5% O_2 seemed to be favourable condition for the maintenance of Shef3-hESCs, as the cells showed steady growth during the

culture period that was associated with a noticeable decrease in floating cells number. However, on morphological prospective, cells cultured 2% O_2 condition formed more homogenous morphology of stem-like phenotype and no signs of differentiation were observed (Figure 5.3). Interesting, the data suggest that the cells might tend to divide slower under 2% O_2 condition as indicated by the adherent cells count at final time point (72hrs). These findings come in agreements with previous findings observed in Episomal-hiPSCs.

Table 8.2.D: Floating cellsX10^6/cm2 (Shef3-hESCs)

O_2%	Time (hrs)	Mean	SD (±)
0%	24hrs	0.0656666666666667	0.00416333199893227
	48hrs	0.0406666666666667	0.00208166599946613
	72hrs	0.67323	0.0778125369076218
2%	24hrs	0.0455333333333333	0.0146237250156495
	48hrs	0.02951	0.00150009999666689
	72hrs	0.0268433333333333	0.00276832681115025
5%	24hrs	0.052	0.0101488915650922
	48hrs	0.0213333333333333	0.00152752523165195
	72hrs	0.0193333333333333	0.00208166599946613
8%	24hrs	0.048	0.00264575131106459
	48hrs	0.100666666666667	0.0240069434400411
	72hrs	0.126	0.0199248588451713
12%	24hrs	0.06	0.01
	48hrs	0.05	8.49837472194074e-018
	72hrs	0.143333333333333	0.0351188458428425
20%	24hrs	0.0406666666666667	0.00305505046330389
	48hrs	0.0306966666666667	0.00684222429721018
	72hrs	0.0465266666666667	0.0162693617985873

8.3 Appendix

This data refers to the experiments discussed in **Section 5.3.2.1**

Confocal images show the absence of HIF-1A nuclear protein expression (green) in **Episomal-hiPSCs** during the acute response to different oxygen tensions after 24hrs.

A

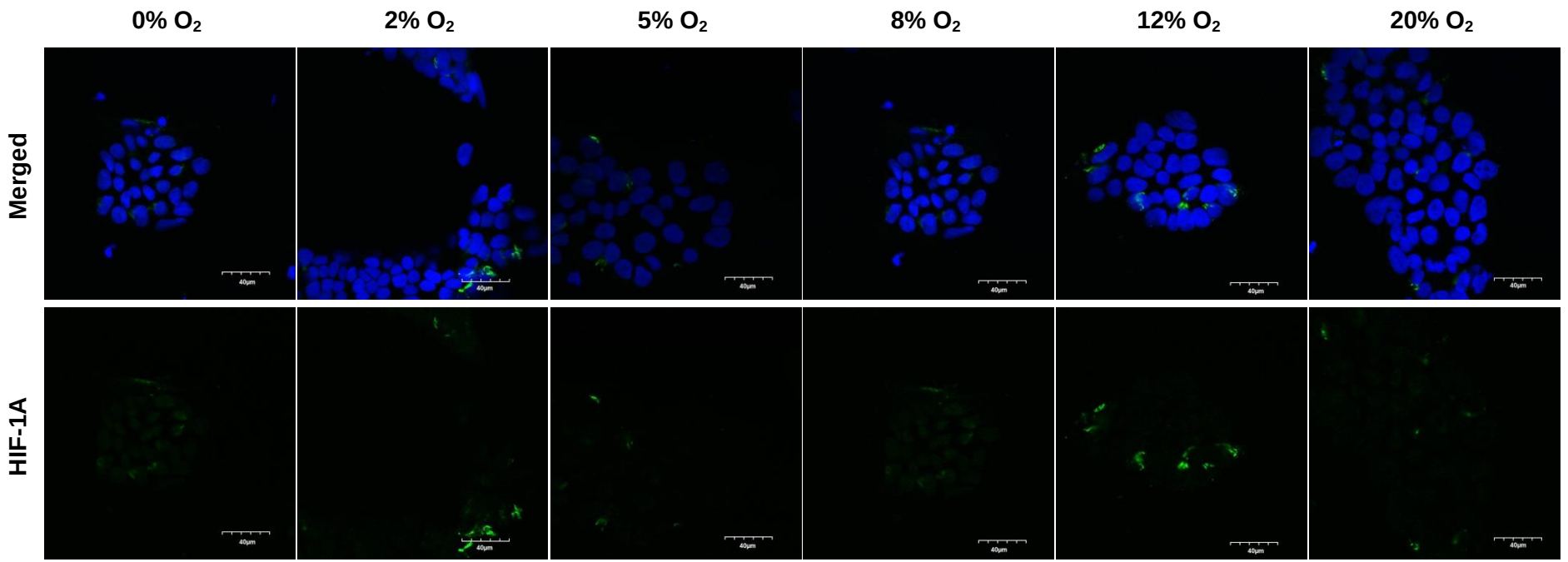

Nuclei were counterstained with DAPI (blue), and the corresponding merged image is represented in the upper panel (Magnification X100, bar = 40µm).

Microscopic analysis show the absence of HIF-1A nuclear protein expression (green) in **Shef3-hESCs** during the acute response to different oxygen tensions after 24hrs.

B

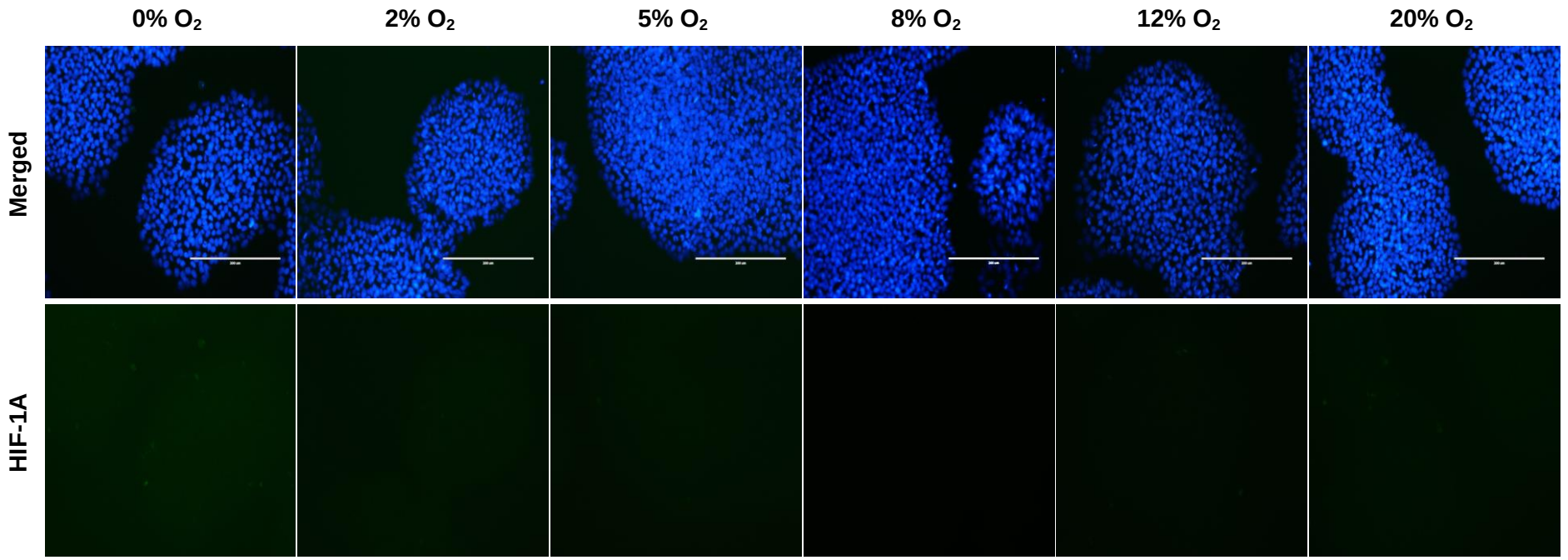

Nuclei were counterstained with DAPI (blue), and the corresponding merged image is represented in the upper panel (Magnification X20, bar = 200µm).

9 CHAPTER 9: REFERENCES

Abbott, M.E., 1936. A History of Embryology : (A Review). *Canadian Medical Association Journal*, 34(1), p.82. Available at: https://www.ncbi.nlm.nih.gov/pmc/articles/PMC1561353/ [Accessed August 16, 2018].

Acloque, H. et al., 2009. Epithelial-mesenchymal transitions: the importance of changing cell state in development and disease. *The Journal of clinical investigation*, 119(6), pp.1438–49. Available at: http://www.ncbi.nlm.nih.gov/pubmed/19487820 [Accessed October 17, 2018].

Akberdin, I.R. et al., 2018. Pluripotency gene network dynamics: System views from parametric analysis Q. Wu, ed. *PLOS ONE*, 13(3), p.e0194464. Available at: http://dx.plos.org/10.1371/journal.pone.0194464 [Accessed October 12, 2018].

Alvarez-Buylla, A. & Garcia-Verdugo, J.M., 2002. Neurogenesis in adult subventricular zone. *The Journal of neuroscience : the official journal of the Society for Neuroscience*, 22(3), pp.629–34. Available at: http://www.ncbi.nlm.nih.gov/pubmed/11826091 [Accessed November 21, 2018].

Amit, M. et al., 2000. Clonally Derived Human Embryonic Stem Cell Lines Maintain Pluripotency and Proliferative Potential for Prolonged Periods of Culture. *Developmental Biology*, 227(2), pp.271–278. Available at: http://www.ncbi.nlm.nih.gov/pubmed/11071754 [Accessed November 22, 2018].

Amit, M. et al., 2003. Human Feeder Layers for Human Embryonic Stem Cells1. *Biology of Reproduction*, 68(6), pp.2150–2156. Available at: http://www.ncbi.nlm.nih.gov/pubmed/12606388 [Accessed November 22, 2018].

Aoi, T. et al., 2008. Generation of pluripotent stem cells from adult mouse liver and stomach cells. *Science (New York, N.Y.)*, 321(5889), pp.699–702. Available at: http://www.ncbi.nlm.nih.gov/pubmed/18276851 [Accessed November 19, 2014].

Aplin, J.D. et al., 1998. Anchorage in the developing placenta: an overlooked determinant of pregnancy outcome? *Human fertility (Cambridge, England)*, 1(1), pp.75–79. Available at: http://www.ncbi.nlm.nih.gov/pubmed/11844314 [Accessed November 17, 2018].

Appelhoff, R.J. et al., 2004. Differential Function of the Prolyl Hydroxylases PHD1, PHD2, and PHD3 in the Regulation of Hypoxia-inducible Factor. *Journal of Biological Chemistry*, 279(37), pp.38458–38465. Available at: http://www.ncbi.nlm.nih.gov/pubmed/15247232 [Accessed October 16, 2018].

Armstrong, L. et al., 2006. The role of PI3K/AKT, MAPK/ERK and NFκβ signalling in the maintenance of human embryonic stem cell pluripotency and viability highlighted by transcriptional profiling and functional

analysis. *Human Molecular Genetics*, 15(11), pp.1894–1913. Available at: http://www.ncbi.nlm.nih.gov/pubmed/16644866 [Accessed November 22, 2018].

Avilion, A.A. et al., 2003. Multipotent cell lineages in early mouse development depend on SOX2 function. *Genes & development*, 17(1), pp.126–40. Available at: http://www.pubmedcentral.nih.gov/articlerender.fcgi?artid=195970&tool=pmcentrez&rendertype=abstract [Accessed July 20, 2014].

Baker, D.E.C. et al., 2007. Adaptation to culture of human embryonic stem cells and oncogenesis in vivo. *Nature Biotechnology*, 25(2), pp.207–215. Available at: http://www.ncbi.nlm.nih.gov/pubmed/17287758 [Accessed November 22, 2018].

Ban, H. et al., 2011. Efficient generation of transgene-free human induced pluripotent stem cells (iPSCs) by temperature-sensitive Sendai virus vectors. *Proceedings of the National Academy of Sciences of the United States of America*, 108(34), pp.14234–9. Available at: http://www.pubmedcentral.nih.gov/articlerender.fcgi?artid=3161531&tool=pmcentrez&rendertype=abstract [Accessed January 12, 2015].

Baraniak, P.R. & McDevitt, T.C., 2012. Scaffold-free culture of mesenchymal stem cell spheroids in suspension preserves multilineage potential. *Cell and Tissue Research*, 347(3), pp.701–711. Available at: http://www.ncbi.nlm.nih.gov/pubmed/21833761 [Accessed November 23, 2018].

Batalov, I. & Feinberg, A.W., 2015. Differentiation of Cardiomyocytes from Human Pluripotent Stem Cells Using Monolayer Culture. *Biomarker insights*, 10(Suppl 1), pp.71–6. Available at: http://www.ncbi.nlm.nih.gov/pubmed/26052225 [Accessed November 23, 2018].

Beattie, G.M. et al., 2005. Activin A Maintains Pluripotency of Human Embryonic Stem Cells in the Absence of Feeder Layers. *Stem Cells*, 23(4), pp.489–495. Available at: http://www.ncbi.nlm.nih.gov/pubmed/15790770 [Accessed November 22, 2018].

BECKER, A.J., McCULLOCH, E.A. & TILL, J.E., 1963. Cytological demonstration of the clonal nature of spleen colonies derived from transplanted mouse marrow cells. *Nature*, 197, pp.452–4. Available at: http://www.ncbi.nlm.nih.gov/pubmed/13970094 [Accessed November 15, 2018].

Behr, R. et al., 2005. Epithelial-Mesenchymal Transition in Colonies of Rhesus Monkey Embryonic Stem Cells: A Model for Processes Involved in Gastrulation. *Stem Cells*, 23(6), pp.805–816. Available at: http://doi.wiley.com/10.1634/stemcells.2004-0234 [Accessed October 19, 2018].

Bongso, A. et al., 1994. Isolation and culture of inner cell mass cells from human blastocysts. *Human reproduction (Oxford, England)*, 9(11), pp.2110–7. Available at: http://www.ncbi.nlm.nih.gov/pubmed/7868682 [Accessed November 22, 2018].

Boyd, N.L. et al., 2009. Human embryonic stem cell-derived mesoderm-like epithelium transitions to mesenchymal progenitor cells. *Tissue engineering. Part A*, 15(8), pp.1897–907. Available at:

http://www.ncbi.nlm.nih.gov/pubmed/19196144 [Accessed October 19, 2018].
Bradley, A. et al., 1984. Formation of germ-line chimaeras from embryo-derived teratocarcinoma cell lines. *Nature*, 309(5965), pp.255–6. Available at: http://www.ncbi.nlm.nih.gov/pubmed/6717601 [Accessed January 25, 2015].
Brandenberger, R. et al., 2004. MPSS profiling of human embryonic stem cells. *BMC developmental biology*, 4, p.10. Available at: http://www.ncbi.nlm.nih.gov/pubmed/15304200 [Accessed November 22, 2018].
Burridge, P.W. et al., 2007. Improved Human Embryonic Stem Cell Embryoid Body Homogeneity and Cardiomyocyte Differentiation from a Novel V-96 Plate Aggregation System Highlights Interline Variability. *Stem Cells*, 25(4), pp.929–938. Available at: http://www.ncbi.nlm.nih.gov/pubmed/17185609 [Accessed November 23, 2018].
Burton, G.J. & Jaunaiux, E., 2001. Maternal vascularisation of the human placenta: Does the embryo develop in a hypoxic environment? In *Gynecologie Obstetrique et Fertilite*. pp. 503–508.
Busuttil, R.A. et al., 2003. Oxygen accelerates the accumulation of mutations during the senescence and immortalization of murine cells in culture. *Aging Cell*, 2(6), pp.287–294. Available at: http://www.ncbi.nlm.nih.gov/pubmed/14677631 [Accessed November 21, 2018].
Buta, C. et al., 2013. Reconsidering pluripotency tests: Do we still need teratoma assays? *Stem Cell Research*, 11(1), pp.552–562. Available at: http://www.ncbi.nlm.nih.gov/pubmed/23611953 [Accessed November 22, 2018].
Carlson, B.M., 2014. *Human embryology and developmental biology*, Elsevier/Saunders. Available at: https://www.sciencedirect.com/book/9781455727940/human-embryology-and-developmental-biology [Accessed November 17, 2018].
Carpenter, M.K. et al., 2004. Properties of four human embryonic stem cell lines maintained in a feeder-free culture system. *Developmental Dynamics*, 229(2), pp.243–258. Available at: http://www.ncbi.nlm.nih.gov/pubmed/14745950 [Accessed November 22, 2018].
Carpenter, M.K., Rosler, E. & Rao, M.S., 2003. Characterization and Differentiation of Human Embryonic Stem Cells. *Cloning and Stem Cells*, 5(1), pp.79–88. Available at: http://www.ncbi.nlm.nih.gov/pubmed/12713704 [Accessed September 21, 2018].
Chambers, I. & Tomlinson, S.R., 2009. The transcriptional foundation of pluripotency. *Development*, 136(14), pp.2311–2322. Available at: http://www.ncbi.nlm.nih.gov/pubmed/19542351 [Accessed November 22, 2018].
Chen, C.-T. et al., 2008. Coordinated Changes of Mitochondrial Biogenesis and Antioxidant Enzymes During Osteogenic Differentiation of Human Mesenchymal Stem Cells. *Stem Cells*, 26(4), pp.960–968. Available at: http://www.ncbi.nlm.nih.gov/pubmed/18218821 [Accessed November 21,

2018].
Chen, G. et al., 2011. Chemically defined conditions for human iPSC derivation and culture. *Nature Methods*, 8(5), pp.424–429. Available at: http://www.ncbi.nlm.nih.gov/pubmed/21478862 [Accessed October 27, 2018].
Cheng, L. et al., 2003. Human Adult Marrow Cells Support Prolonged Expansion of Human Embryonic Stem Cells in Culture. *Stem Cells*, 21(2), pp.131–142. Available at: http://www.ncbi.nlm.nih.gov/pubmed/12634409 [Accessed November 22, 2018].
Chilov, D. et al., 1999a. Induction and nuclear translocation of hypoxia-inducible factor-1 (HIF-1): heterodimerization with ARNT is not necessary for nuclear accumulation of HIF-1alpha. *Journal of cell science*, 112 (Pt 8, pp.1203–1212.
Chilov, D. et al., 1999b. Induction and nuclear translocation of hypoxia-inducible factor-1 (HIF-1): heterodimerization with ARNT is not necessary for nuclear accumulation of HIF-1alpha. *Journal of cell science*, 112 (Pt 8), pp.1203–12. Available at: http://www.ncbi.nlm.nih.gov/pubmed/10085255 [Accessed September 13, 2018].
Cho, Y.M. et al., 2006. Dynamic changes in mitochondrial biogenesis and antioxidant enzymes during the spontaneous differentiation of human embryonic stem cells. *Biochemical and Biophysical Research Communications*, 348(4), pp.1472–1478. Available at: https://www.sciencedirect.com/science/article/pii/S0006291X06018213?via%3Dihub [Accessed November 21, 2018].
Cipolleschi, M.G., Dello Sbarba, P. & Olivotto, M., 1993. The role of hypoxia in the maintenance of hematopoietic stem cells. *Blood*, 82(7), pp.2031–7. Available at: http://www.ncbi.nlm.nih.gov/pubmed/8104535 [Accessed November 21, 2018].
Collins, J.E. & Fleming, T.P., 1995. Epithelial differentiation in the mouse preimplantation embryo: making adhesive cell contacts for the first time. *Trends in Biochemical Sciences*, 20(8), pp.307–312. Available at: https://www.sciencedirect.com/science/article/pii/S096800040089057X?via%3Dihub [Accessed November 16, 2018].
Correia, C. et al., 2014. Combining hypoxia and bioreactor hydrodynamics boosts induced pluripotent stem cell differentiation towards cardiomyocytes. *Stem cell reviews*, 10(6), pp.786–801. Available at: http://www.ncbi.nlm.nih.gov/pubmed/25022569 [Accessed October 22, 2018].
Crisan, M. et al., 2008. A Perivascular Origin for Mesenchymal Stem Cells in Multiple Human Organs. *Cell Stem Cell*, 3(3), pp.301–313. Available at: http://www.ncbi.nlm.nih.gov/pubmed/18786417 [Accessed November 21, 2018].
D'Ippolito, G. et al., 2006. Low oxygen tension inhibits osteogenic differentiation and enhances stemness of human MIAMI cells. *Bone*, 39(3), pp.513–522. Available at: http://www.ncbi.nlm.nih.gov/pubmed/16616713 [Accessed November 21, 2018].
Daly, C. et al., 2017. Hypoxia modulates the stem cell population and induces EMT in the MCF-10A breast epithelial cell line. *Oncology Reports*,

pp.483–490. Available at: http://www.spandidos-publications.com/10.3892/or.2017.6125.
Dings, J. et al., 1998. Clinical experience with 118 brain tissue oxygen partial pressure catheter probes. *Neurosurgery*, 43(5), pp.1082–95. Available at: http://www.ncbi.nlm.nih.gov/pubmed/9802852 [Accessed November 21, 2018].
Doetsch, F. et al., 1999. Subventricular zone astrocytes are neural stem cells in the adult mammalian brain. *Cell*, 97(6), pp.703–16. Available at: http://www.ncbi.nlm.nih.gov/pubmed/10380923 [Accessed November 21, 2018].
Dunwoodie, S.L., 2009. The role of hypoxia in development of the Mammalian embryo. *Developmental cell*, 17(6), pp.755–73. Available at: http://www.sciencedirect.com/science/article/pii/S1534580709004821 [Accessed February 16, 2015].
Duplomb, L. et al., 2006. Concise Review: Embryonic Stem Cells: A New Tool to Study Osteoblast and Osteoclast Differentiation. *STEM CELLS*, 25(3), pp.544–552. Available at: http://www.ncbi.nlm.nih.gov/pubmed/17095705 [Accessed November 23, 2018].
Eastham, A.M. et al., 2007. Epithelial-mesenchymal transition events during human embryonic stem cell differentiation. *Cancer research*, 67(23), pp.11254–62. Available at: http://www.ncbi.nlm.nih.gov/pubmed/18056451 [Accessed October 19, 2018].
Eastham, A.M. et al., 2007. Epithelial-Mesenchymal Transition Events during Human Embryonic Stem Cell Differentiation. *Cancer Research*, 67(23), pp.11254–11262. Available at: http://www.ncbi.nlm.nih.gov/pubmed/18056451 [Accessed November 2, 2018].
Eckert, J.J. & Fleming, T.P., 2008. Tight junction biogenesis during early development. *Biochimica et Biophysica Acta (BBA) - Biomembranes*, 1778(3), pp.717–728. Available at: https://www.sciencedirect.com/science/article/pii/S0005273607003562?via%3Dihub [Accessed November 16, 2018].
Edmondson, R. et al., 2014. Three-dimensional cell culture systems and their applications in drug discovery and cell-based biosensors. *Assay and drug development technologies*, 12(4), pp.207–18. Available at: http://www.ncbi.nlm.nih.gov/pubmed/24831787 [Accessed November 23, 2018].
Eggenschwiler, R. & Cantz, T., 2009. Induced pluripotent stem cells generated without viral integration. *Hepatology (Baltimore, Md.)*, 49(3), pp.1048–9. Available at: http://www.ncbi.nlm.nih.gov/pubmed/19242974 [Accessed January 26, 2015].
Eliasson, P. & Jönsson, J.-I., 2010. The hematopoietic stem cell niche: Low in oxygen but a nice place to be. *Journal of Cellular Physiology*, 222(1), pp.17–22. Available at: http://doi.wiley.com/10.1002/jcp.21908 [Accessed November 21, 2018].
Elks, P.M. et al., 2011. Activation of hypoxia-inducible factor-1 (Hif-1) delays inflammation resolution by reducing neutrophil apoptosis and reverse migration in a zebrafish inflammation model. Available at: www.bloodjournal.org [Accessed October 2, 2018].

Erecińska, M. & Silver, I.A., 2001. Tissue oxygen tension and brain sensitivity to hypoxia. *Respiration physiology*, 128(3), pp.263–76. Available at: http://www.ncbi.nlm.nih.gov/pubmed/11718758 [Accessed June 7, 2015].

Evans, M.J. & Kaufman, M.H., 1981. Establishment in culture of pluripotential cells from mouse embryos. *Nature*, 292(5819), pp.154–156. Available at: http://dx.doi.org/10.1038/292154a0 [Accessed January 13, 2015].

Ezashi, T., Das, P. & Roberts, R.M., 2005. Low O2 tensions and the prevention of differentiation of hES cells. *Proceedings of the National Academy of Sciences of the United States of America*, 102(13), pp.4783–8. Available at: http://www.pubmedcentral.nih.gov/articlerender.fcgi?artid=554750&tool=pmcentrez&rendertype=abstract [Accessed February 2, 2015].

Facucho-Oliveira, J.M. et al., 2007. Mitochondrial DNA replication during differentiation of murine embryonic stem cells. *Journal of Cell Science*, 120(22), pp.4025–4034. Available at: http://www.ncbi.nlm.nih.gov/pubmed/17971411 [Accessed November 21, 2018].

Fehrer, C. et al., 2007. Reduced oxygen tension attenuates differentiation capacity of human mesenchymal stem cells and prolongs their lifespan. *Aging Cell*, 6(6), pp.745–757. Available at: http://www.ncbi.nlm.nih.gov/pubmed/17925003 [Accessed November 21, 2018].

FEKETE, E. & FERRIGNO, M.A., 1952. Studies on a transplantable teratoma of the mouse. *Cancer research*, 12(6), pp.438–40. Available at: http://www.ncbi.nlm.nih.gov/pubmed/14936010 [Accessed November 15, 2018].

Ferrara, N., Gerber, H.-P. & LeCouter, J., 2003. The biology of VEGF and its receptors. *Nature Medicine*, 9(6), pp.669–676. Available at: http://www.ncbi.nlm.nih.gov/pubmed/12778165 [Accessed November 18, 2018].

Fischer, B. & Bavister, B.D., 1993. Oxygen tension in the oviduct and uterus of rhesus monkeys, hamsters and rabbits. *Journal of reproduction and fertility*, 99(2), pp.673–9. Available at: http://www.ncbi.nlm.nih.gov/pubmed/8107053 [Accessed February 1, 2015].

Fontes, A. et al., 2013. Generation of human-induced pluripotent stem cells (hiPSCs) using episomal vectors on defined Essential 8^{TM} Medium conditions. *Methods in molecular biology (Clifton, N.J.)*, 997, pp.57–72. Available at: http://www.ncbi.nlm.nih.gov/pubmed/23546748 [Accessed January 27, 2015].

Forgács, G. & Newman, S. (Stuart A.., 2005. *Biological physics of the developing embryo*, Cambridge University Press. Available at: https://www.nhbs.com/biological-physics-of-the-developing-embryo-book [Accessed November 17, 2018].

Forristal, C.E. et al., 2010. Hypoxia inducible factors regulate pluripotency and proliferation in human embryonic stem cells cultured at reduced oxygen tensions. *Reproduction*, 139, pp.85–97.

Forsyth, N.R. et al., 2006. Physiologic oxygen enhances human embryonic stem cell clonal recovery and reduces chromosomal abnormalities. *Cloning and stem cells*, 8(1), pp.16–23. Available at:

http://www.ncbi.nlm.nih.gov/pubmed/16571074 [Accessed January 27, 2015].

Forsyth, N.R. et al., 2008. Transcriptome alterations due to physiological normoxic (2% O_2) culture of human embryonic stem cells. *Regenerative Medicine*, 3(6), pp.817–833. Available at: https://www.futuremedicine.com/doi/10.2217/17460751.3.6.817 [Accessed September 19, 2018].

Fraisl, P. et al., 2009. Regulation of Angiogenesis by Oxygen and Metabolism. *Developmental Cell*, 16(2), pp.167–179. Available at: https://www.sciencedirect.com/science/article/pii/S1534580709000318?via%3Dihub#fig1 [Accessed October 17, 2018].

Fujiwara, H. et al., 2007. Regulation of mesodermal differentiation of mouse embryonic stem cells by basement membranes. *Journal of Biological Chemistry*, 282(40), pp.29701–29711.

Fusaki, N. et al., 2009. Efficient induction of transgene-free human pluripotent stem cells using a vector based on Sendai virus, an RNA virus that does not integrate into the host genome. *Proceedings of the Japan Academy. Series B, Physical and biological sciences*, 85(8), pp.348–62. Available at: http://www.pubmedcentral.nih.gov/articlerender.fcgi?artid=3621571&tool=pmcentrez&rendertype=abstract [Accessed January 17, 2015].

Gassmann, M. & Wenger, R., 1997. HIF-1, a Mediator of the Molecular Response to Hypoxia. *Physiology*, 12(5), pp.214–218. Available at: http://www.physiology.org/doi/10.1152/physiologyonline.1997.12.5.214 [Accessed October 2, 2018].

Genbacev, O. et al., 1996. Hypoxia alters early gestation human cytotrophoblast differentiation/invasion in vitro and models the placental defects that occur in preeclampsia. *Journal of Clinical Investigation*, 97(2), pp.540–550. Available at: http://www.ncbi.nlm.nih.gov/pubmed/8567979 [Accessed November 18, 2018].

Gheldof, A. & Berx, G., 2013a. *Cadherins and epithelial-to-mesenchymal transition* 1st ed., Elsevier Inc. Available at: http://dx.doi.org/10.1016/B978-0-12-394311-8.00014-5.

Gheldof, A. & Berx, G., 2013b. Cadherins and Epithelial-to-Mesenchymal Transition. *Progress in Molecular Biology and Translational Science*, 116, pp.317–336. Available at: https://www.sciencedirect.com/science/article/pii/B9780123943118000145?via%3Dihub [Accessed October 19, 2018].

Gille, J.J. & Joenje, H., 1992. Cell culture models for oxidative stress: superoxide and hydrogen peroxide versus normobaric hyperoxia. *Mutation research*, 275(3–6), pp.405–14. Available at: http://www.ncbi.nlm.nih.gov/pubmed/1383781 [Accessed August 22, 2018].

Grayson, W.L. et al., 2007. Hypoxia enhances proliferation and tissue formation of human mesenchymal stem cells. *Biochemical and Biophysical Research Communications*, 358(3), pp.948–953. Available at: https://www.sciencedirect.com/science/article/pii/S0006291X07010091 [Accessed November 23, 2018].

Greer, S.N. et al., 2012. The updated biology of hypoxia-inducible factor. *The EMBO journal*, 31(11), pp.2448–60. Available at: http://emboj.embopress.org/content/31/11/2448.abstract [Accessed June 29, 2015].

Guilak, F. et al., 2009. Control of Stem Cell Fate by Physical Interactions with the Extracellular Matrix. *Cell Stem Cell*, 5(1), pp.17–26. Available at: http://www.ncbi.nlm.nih.gov/pubmed/19570510 [Accessed November 23, 2018].

Hall, B.K. (Brian K., 1998. *Evolutionary developmental biology*, Chapman & Hall. Available at: https://books.google.co.uk/books?id=JhSwumfgTQ4C&pg=PA132&redir_esc=y#v=onepage&q&f=false [Accessed November 16, 2018].

Hanna, J. et al., 2008. Direct reprogramming of terminally differentiated mature B lymphocytes to pluripotency. *Cell*, 133(2), pp.250–64. Available at: http://www.pubmedcentral.nih.gov/articlerender.fcgi?artid=2615249&tool=pmcentrez&rendertype=abstract [Accessed January 26, 2015].

Harms, K.M., Li, L. & Cunningham, L.A., 2010. Murine Neural Stem/Progenitor Cells Protect Neurons against Ischemia by HIF-1α–Regulated VEGF Signaling R. Linden, ed. *PLoS ONE*, 5(3), p.e9767. Available at: http://dx.plos.org/10.1371/journal.pone.0009767 [Accessed November 21, 2018].

Harvey, A.J. et al., 2004. Oxygen-Regulated Gene Expression in Bovine Blastocysts1. *Biology of Reproduction*, 71(4), pp.1108–1119. Available at: http://www.ncbi.nlm.nih.gov/pubmed/15163614 [Accessed November 23, 2018].

Heinis, M. et al., 2010. Oxygen Tension Regulates Pancreatic B-cell Differentiation Through Hypoxia-Inducible Factor 1a. *Diabetes*, 59(March), pp.662–669. Available at: https://www.sugarsync.com/pf/D6989864_8893700_646284%5Cnhttp://www.ncbi.nlm.nih.gov/pubmed/20009089.

Hewitt, Z. et al., 2006. Fluorescence-Activated Single Cell Sorting of Human Embryonic Stem Cells. *Cloning and Stem Cells*, 8(3), pp.225–234. Available at: http://www.ncbi.nlm.nih.gov/pubmed/17009898 [Accessed September 19, 2018].

Hong, S.-H. et al., 2010. Multiparameter comparisons of embryoid body differentiation toward human stem cell applications. *Stem Cell Research*, 5(2), pp.120–130. Available at: http://www.ncbi.nlm.nih.gov/pubmed/20605758 [Accessed November 23, 2018].

Hu, K. & Slukvin, I., 2013. Generation of transgene-free iPSC lines from human normal and neoplastic blood cells using episomal vectors. *Methods in molecular biology (Clifton, N.J.)*, 997, pp.163–76. Available at: http://www.ncbi.nlm.nih.gov/pubmed/23546755 [Accessed January 27, 2015].

Ishii, T. et al., 2008. Effects of extracellular matrixes and growth factors on the hepatic differentiation of human embryonic stem cells. *American Journal of Physiology-Gastrointestinal and Liver Physiology*, 295(2), pp.G313–G321. Available at: http://www.ncbi.nlm.nih.gov/pubmed/18535293 [Accessed November 23, 2018].

Ito, K. & Suda, T., 2014. Metabolic requirements for the maintenance of self-renewing stem cells. *Nature reviews. Molecular cell biology*, 15(4), pp.243–56. Available at: http://www.ncbi.nlm.nih.gov/pubmed/24651542 [Accessed October 1, 2018].

Itskovitz-Eldor, J. et al., 2000. Differentiation of human embryonic stem cells into embryoid bodies compromising the three embryonic germ layers. *Molecular medicine (Cambridge, Mass.)*, 6(2), pp.88–95. Available at: http://www.pubmedcentral.nih.gov/articlerender.fcgi?artid=1949933&tool=pmcentrez&rendertype=abstract [Accessed December 29, 2014].

Ivanović, Z. et al., 2000. Primitive human HPCs are better maintained and expanded in vitro at 1 percent oxygen than at 20 percent. *Transfusion*, 40(12), pp.1482–8. Available at: http://www.ncbi.nlm.nih.gov/pubmed/11134568 [Accessed November 23, 2018].

Iyer, N. V et al., 1998a. Cellular and developmental control of O2 homeostasis by hypoxia-inducible factor 1 alpha. *Genes & development*, 12(2), pp.149–62. Available at: http://www.pubmedcentral.nih.gov/articlerender.fcgi?artid=316445&tool=pmcentrez&rendertype=abstract [Accessed February 25, 2015].

Iyer, N. V et al., 1998b. Cellular and developmental control of O2 homeostasis by hypoxia-inducible factor 1 alpha. *Genes & development*, 12(2), pp.149–62. Available at: http://www.ncbi.nlm.nih.gov/pubmed/9436976 [Accessed August 20, 2018].

Jaakkola, P. et al., 2001. Targeting of HIF-alpha to the von Hippel-Lindau Ubiquitylation Complex by O2-Regulated Prolyl Hydroxylation. *Science*, 292(5516), pp.468–472. Available at: http://www.ncbi.nlm.nih.gov/pubmed/11292861 [Accessed October 2, 2018].

Jackson, E.B. & Brues, A.M., 1941. *Studies on a Transplantable Embryoma of the Mouse**, Available at: http://cancerres.aacrjournals.org/content/canres/1/6/494.full.pdf [Accessed November 15, 2018].

James, J.L., Stone, P.R. & Chamley, L.W., 2006. The effects of oxygen concentration and gestational age on extravillous trophoblast outgrowth in a human first trimester villous explant model. *Human Reproduction*, 21(10), pp.2699–2705. Available at: https://academic.oup.com/humrep/article-abstract/21/10/2699/2914109 [Accessed August 18, 2018].

Jauniaux, E. et al., 2000. Onset of Maternal Arterial Blood Flow and Placental Oxidative Stress. *The American Journal of Pathology*, 157(6), pp.2111–2122. Available at: http://www.ncbi.nlm.nih.gov/pubmed/11106583 [Accessed October 26, 2018].

Jauniaux, E., Gulbis, B. & Burton, G.J., 2003. The human first trimester gestational sac limits rather than facilitates oxygen transfer to the foetus--a review. *Placenta*, 24 Suppl A, pp.S86-93. Available at: http://www.ncbi.nlm.nih.gov/pubmed/12852418 [Accessed November 18, 2018].

Jin-qiao, S. et al., 2009. Basic fibroblast growth factor stimulates the proliferation and differentiation of neural stem cells in neonatal rats after ischemic brain injury. *Brain and Development*, 31(5), pp.331–340.

Available at: http://www.ncbi.nlm.nih.gov/pubmed/18657919 [Accessed November 21, 2018].
Jones, D.L. & Wagers, A.J., 2008. No place like home: anatomy and function of the stem cell niche. *Nature Reviews Molecular Cell Biology*, 9(1), pp.11–21. Available at: http://www.ncbi.nlm.nih.gov/pubmed/18097443 [Accessed November 21, 2018].
Kachamakova-Trojanowska, N. et al., 2016. Generation of functional endothelial cells with progenitor-like features from murine induced pluripotent stem cells. *Vascular Pharmacology*, 86, pp.94–108. Available at: http://www.ncbi.nlm.nih.gov/pubmed/27568462 [Accessed November 23, 2018].
Kalluri, R. & Weinberg, R. a, 2009. Review series The basics of epithelial-mesenchymal transition. *Journal of Clinical Investigation*, 119(6), pp.1420–1428.
Kaneko, S. & Takamatsu, K., 2012. Cell Handling and Culture Under Controlled Oxygen Concentration. *Biomedical Tissue Culture*, pp.19–34. Available at: http://cdn.intechopen.com/pdfs/40230/InTech-Cell_handling_and_culture_under_controlled_oxygen_concentration.pdf.
Karsenty, G., 2003. The complexities of skeletal biology. *Nature*, 423(6937), pp.316–318. Available at: http://www.ncbi.nlm.nih.gov/pubmed/12748648 [Accessed November 18, 2018].
Keith, B., Johnson, R.S. & Simon, M.C., 2012. HIF1α and HIF2α: sibling rivalry in hypoxic tumour growth and progression. *Nature reviews. Cancer*, 12(1), pp.9–22. Available at: http://www.pubmedcentral.nih.gov/articlerender.fcgi?artid=3401912&tool=pmcentrez&rendertype=abstract [Accessed February 23, 2015].
Khalife, R. & Mason, P.C., 2015. The effect of the nutritional microenvironment on stem cell differentiation. , (August).
Khan, W.S., Adesida, A.B. & Hardingham, T.E., 2007. Hypoxic conditions increase hypoxia-inducible transcription factor 2α and enhance chondrogenesis in stem cells from the infrapatellar fat pad of osteoarthritis patients. *Arthritis Research & Therapy*, 9(3), p.R55. Available at: http://www.ncbi.nlm.nih.gov/pubmed/17537234 [Accessed September 23, 2018].
Kim, J.B. et al., 2008. Pluripotent stem cells induced from adult neural stem cells by reprogramming with two factors. *Nature*, 454(7204), pp.646–50. Available at: http://www.ncbi.nlm.nih.gov/pubmed/18594515 [Accessed January 8, 2015].
KLEINSMITH, L.J. & PIERCE, G.B., 1964. MULTIPOTENTIALITY OF SINGLE EMBRYONAL CARCINOMA CELLS. *Cancer research*, 24, pp.1544–51. Available at: http://www.ncbi.nlm.nih.gov/pubmed/14234000 [Accessed January 26, 2015].
Koay, E.J. & Athanasiou, K.A., 2008. Hypoxic chondrogenic differentiation of human embryonic stem cells enhances cartilage protein synthesis and biomechanical functionality. *Osteoarthritis and cartilage / OARS, Osteoarthritis Research Society*, 16(12), pp.1450–6. Available at: http://www.sciencedirect.com/science/article/pii/S1063458408001246 [Accessed May 28, 2015].
Koh, M.Y., Darnay, B.G. & Powis, G., 2008. Hypoxia-Associated Factor, a Novel E3-Ubiquitin Ligase, Binds and Ubiquitinates Hypoxia-Inducible

Factor 1 , Leading to Its Oxygen-Independent Degradation. *Molecular and Cellular Biology*, 28(23), pp.7081–7095. Available at: http://www.ncbi.nlm.nih.gov/pubmed/18838541 [Accessed November 18, 2018].

Koh, M.Y. & Powis, G., 2012. Passing the baton: The HIF switch. Available at: https://www.ncbi.nlm.nih.gov/pmc/articles/PMC3433036/pdf/nihms395757.pdf [Accessed November 18, 2018].

Koivunen, P. et al., 2004. Catalytic Properties of the Asparaginyl Hydroxylase (FIH) in the Oxygen Sensing Pathway Are Distinct from Those of Its Prolyl 4-Hydroxylases. *Journal of Biological Chemistry*, 279(11), pp.9899–9904. Available at: http://www.ncbi.nlm.nih.gov/pubmed/14701857 [Accessed November 18, 2018].

Koshiji, M. et al., 2004. HIF-1α induces cell cycle arrest by functionally counteracting Myc. *The EMBO Journal*, 23(9), pp.1949–1956. Available at: http://www.ncbi.nlm.nih.gov/pubmed/15071503 [Accessed November 21, 2018].

Kozak, K.R., Abbott, B. & Hankinson, O., 1997. ARNT-deficient mice and placental differentiation. *Developmental biology*, 191(2), pp.297–305. Available at: http://www.ncbi.nlm.nih.gov/pubmed/9398442 [Accessed February 25, 2015].

Kronenberg, H.M., 2003. Developmental regulation of the growth plate. *Nature*, 423(6937), pp.332–336. Available at: http://www.ncbi.nlm.nih.gov/pubmed/12748651 [Accessed November 18, 2018].

Kubota, Y., Takubo, K. & Suda, T., 2008. Bone marrow long label-retaining cells reside in the sinusoidal hypoxic niche. *Biochemical and Biophysical Research Communications*, 366(2), pp.335–339. Available at: http://www.ncbi.nlm.nih.gov/pubmed/18047833 [Accessed November 21, 2018].

Kumar, H. & Choi, D.-K., 2015. Hypoxia Inducible Factor Pathway and Physiological Adaptation: A Cell Survival Pathway? *Mediators of inflammation*, 2015, p.584758. Available at: http://www.ncbi.nlm.nih.gov/pubmed/26491231 [Accessed October 2, 2018].

Kuschel, A., Simon, P. & Tug, S., 2012. Functional regulation of HIF-1α under normoxia-is there more than post-translational regulation? *Journal of Cellular Physiology*, 227(2), pp.514–524. Available at: http://doi.wiley.com/10.1002/jcp.22798 [Accessed October 10, 2018].

Laflamme, M.A. et al., 2007. Cardiomyocytes derived from human embryonic stem cells in pro-survival factors enhance function of infarcted rat hearts. *Nature Biotechnology*, 25(9), pp.1015–1024. Available at: http://www.ncbi.nlm.nih.gov/pubmed/17721512 [Accessed November 23, 2018].

Larsen, W.J. (William J. et al., 2001. *Human embryology*, Churchill Livingstone. Available at: https://books.google.co.uk/books?id=H5qw-jiMc44C&pg=PA20&redir_esc=y [Accessed November 16, 2018].

Lefebvre, V. & Smits, P., 2005. Transcriptional control of chondrocyte fate and differentiation. *Birth Defects Research Part C: Embryo Today: Reviews*, 75(3), pp.200–212. Available at:

http://www.ncbi.nlm.nih.gov/pubmed/16187326 [Accessed November 18, 2018].
Lim, H.-J. et al., 2011. Biochemical and morphological effects of hypoxic environment on human embryonic stem cells in long-term culture and differentiating embryoid bodies. *Molecules and cells*, 31(2), pp.123–132.
Liu, Y. V. & Semenza, G.L., 2007. RACK1 vs. HSP90: Competition for HIF-1α Degradation vs. Stabilization. *Cell Cycle*, 6(6), pp.656–659. Available at: http://www.ncbi.nlm.nih.gov/pubmed/17361105 [Accessed November 18, 2018].
Ludwig, T.E. et al., 2006. Derivation of human embryonic stem cells in defined conditions. *Nature Biotechnology*, 24(2), pp.185–187. Available at: http://www.nature.com/articles/nbt1177 [Accessed September 19, 2018].
Luo, W. et al., 2010. Hsp70 and CHIP Selectively Mediate Ubiquitination and Degradation of Hypoxia-inducible Factor (HIF)-1α but Not HIF-2α. *Journal of Biological Chemistry*, 285(6), pp.3651–3663. Available at: http://www.ncbi.nlm.nih.gov/pubmed/19940151 [Accessed November 18, 2018].
Ma, T. et al., 2009. Hypoxia and stem cell-based engineering of mesenchymal tissues. *Biotechnology progress*, 25(1), pp.32–42. Available at: http://www.ncbi.nlm.nih.gov/pubmed/19198002 [Accessed November 23, 2018].
Maes, C., Carmeliet, G. & Schipani, E., 2012. Hypoxia-driven pathways in bone development, regeneration and disease. *Nature Reviews Rheumatology*, 8(6), pp.358–366. Available at: http://www.nature.com/articles/nrrheum.2012.36 [Accessed November 17, 2018].
Mahon, P.C., Hirota, K. & Semenza, G.L., 2001. FIH-1: a novel protein that interacts with HIF-1alpha and VHL to mediate repression of HIF-1 transcriptional activity. *Genes & development*, 15(20), pp.2675–86. Available at: http://genesdev.cshlp.org/content/15/20/2675.abstract [Accessed August 27, 2015].
Malladi, P. et al., 2006. Effect of reduced oxygen tension on chondrogenesis and osteogenesis in adipose-derived mesenchymal cells. *American Journal of Physiology-Cell Physiology*, 290(4), pp.C1139–C1146. Available at: http://www.ncbi.nlm.nih.gov/pubmed/16291817 [Accessed November 21, 2018].
Mario R. Cappechi, Martin J. Evans, and O.S., 1989. *Gene modification in mice*, Available at: https://www.nobelprize.org/uploads/2018/06/advanced-medicineprize2007.pdf [Accessed November 15, 2018].
Mater, J. et al., 2016. Edinburgh Research Explorer Pluripotent stem cell derived hepatocytes: Using materials to define cellular differentiation and tissue engineering Pluripotent stem cell derived hepatocytes: using materials to define cellular differentiation and tissue engineering. Available at: www.rsc.org/MaterialsB [Accessed November 23, 2018].
Matsui, Y., Zsebo, K. & Hogan, B.L., 1992. Derivation of pluripotential embryonic stem cells from murine primordial germ cells in culture. *Cell*, 70(5), pp.841–7. Available at: http://www.ncbi.nlm.nih.gov/pubmed/1381289 [Accessed January 26, 2015].

Matsumoto, A. et al., 2005. Absolute oxygen tension (pO2) in murine fatty and muscle tissue as determined by EPR. *Magnetic Resonance in Medicine*, 54(6), pp.1530–1535. Available at: http://www.ncbi.nlm.nih.gov/pubmed/16276490 [Accessed November 21, 2018].

Maxwell, P.H., Pugh, C.W. & Ratcliffe, P.J., 2001. Activation of the HIF pathway in cancer. *Current opinion in genetics & development*, 11(3), pp.293–9. Available at: http://www.ncbi.nlm.nih.gov/pubmed/11377966 [Accessed November 18, 2018].

Medici, D., Hay, E.D. & Olsen, B.R., 2008. Snail and Slug promote epithelial-mesenchymal transition through beta-catenin-T-cell factor-4-dependent expression of transforming growth factor-beta3. *Molecular biology of the cell*, 19(11), pp.4875–87. Available at: http://www.ncbi.nlm.nih.gov/pubmed/18799618 [Accessed November 22, 2018].

Miharada, K. et al., 2011. Cripto Regulates Hematopoietic Stem Cells as a Hypoxic-Niche-Related Factor through Cell Surface Receptor GRP78. *Cell Stem Cell*, 9(4), pp.330–344. Available at: http://www.ncbi.nlm.nih.gov/pubmed/21982233 [Accessed November 21, 2018].

Mirzadeh, Z. et al., 2008. Neural Stem Cells Confer Unique Pinwheel Architecture to the Ventricular Surface in Neurogenic Regions of the Adult Brain. *Cell Stem Cell*, 3(3), pp.265–278. Available at: http://www.ncbi.nlm.nih.gov/pubmed/18786414 [Accessed November 21, 2018].

Misra, A. et al., 2012. Hypoxia activated EGFR signaling induces epithelial to mesenchymal transition (EMT). *PloS one*, 7(11), p.e49766. Available at: http://www.ncbi.nlm.nih.gov/pubmed/23185433 [Accessed October 26, 2018].

MITCHELL, J.A. & YOCHIM, J.M., 1968. Intrauterine Oxygen Tension During the Estrous Cycle in the Rat: Its Relation to Uterine Respiration and Vascular Activity. *Endocrinology*, 83(4), pp.701–705. Available at: http://www.ncbi.nlm.nih.gov/pubmed/5693655 [Accessed August 18, 2018].

Mohyeldin, A., Garzón-Muvdi, T. & Quiñones-Hinojosa, A., 2010. Oxygen in stem cell biology: a critical component of the stem cell niche. *Cell stem cell*, 7(2), pp.150–61. Available at: http://www.ncbi.nlm.nih.gov/pubmed/20682444 [Accessed December 4, 2014].

Mole, D.R. et al., 2009. Genome-wide Association of Hypoxia-inducible Factor (HIF)-1α and HIF-2α DNA Binding with Expression Profiling of Hypoxia-inducible Transcripts. *Journal of Biological Chemistry*, 284(25), pp.16767–16775. Available at: http://www.ncbi.nlm.nih.gov/pubmed/19386601 [Accessed October 10, 2018].

Moore, K. a & Lemischka, I.R., 2006. Stem cells and their niches. *Science (New York, N.Y.)*, 311(2), pp.1880–1885.

Morrison, S.J. et al., 2000. Culture in reduced levels of oxygen promotes clonogenic sympathoadrenal differentiation by isolated neural crest stem cells. *The Journal of neuroscience : the official journal of the Society for*

Neuroscience, 20(19), pp.7370–6. Available at: http://www.ncbi.nlm.nih.gov/pubmed/11007895 [Accessed September 23, 2018].

Murry, C.E. & Keller, G., 2008. Leading Edge Review Differentiation of Embryonic Stem Cells to Clinically Relevant Populations: Lessons from Embryonic Development. Available at: https://www.cell.com/action/showPdf?pii=S0092-8674%2808%2900216-X [Accessed November 22, 2018].

Niebruegge, S. et al., 2009. Generation of human embryonic stem cell-derived mesoderm and cardiac cells using size-specified aggregates in an oxygen-controlled bioreactor. *Biotechnology and bioengineering*, 102(2), pp.493–507. Available at: http://www.ncbi.nlm.nih.gov/pubmed/18767184 [Accessed February 5, 2015].

Ohh, M. et al., 2000. Ubiquitination of hypoxia-inducible factor requires direct binding to the β-domain of the von Hippel–Lindau protein. *Nature Cell Biology*, 2(7), pp.423–427. Available at: http://www.ncbi.nlm.nih.gov/pubmed/10878807 [Accessed October 16, 2018].

Ohnuki, M., Takahashi, K. & Yamanaka, S., 2007. *Current Protocols in Stem Cell Biology* M. Bhatia et al., eds., Hoboken, NJ, USA: John Wiley & Sons, Inc. Available at: http://www.ncbi.nlm.nih.gov/pubmed/19536759 [Accessed October 8, 2015].

Okita, K. et al., 2013. An efficient nonviral method to generate integration-free human-induced pluripotent stem cells from cord blood and peripheral blood cells. *Stem cells (Dayton, Ohio)*, 31(3), pp.458–66. Available at: http://www.ncbi.nlm.nih.gov/pubmed/23193063 [Accessed January 8, 2015].

Ottosen, L.D.M. et al., 2006. Observations on intrauterine oxygen tension measured by fibre-optic microsensors. *Reproductive biomedicine online*, 13(3), pp.380–5. Available at: http://www.ncbi.nlm.nih.gov/pubmed/16984770 [Accessed February 25, 2015].

Pasarica, M. et al., 2009. Reduced Adipose Tissue Oxygenation in Human Obesity: Evidence for Rarefaction, Macrophage Chemotaxis, and Inflammation Without an Angiogenic Response. *Diabetes*, 58(3), pp.718–725. Available at: http://www.ncbi.nlm.nih.gov/pubmed/19074987 [Accessed November 21, 2018].

Patestas, M.A. & Gartner, L.P., 2006. *A textbook of neuroanatomy*, Blackwell Pub. Available at: https://books.google.co.uk/books?id=JEEnkNuuYkoC&pg=PA11&redir_esc=y [Accessed November 16, 2018].

Pattappa, G. et al., 2013. Continuous and uninterrupted oxygen tension influences the colony formation and oxidative metabolism of human mesenchymal stem cells. *Tissue engineering. Part C, Methods*, 19(1), pp.68–79. Available at: http://www.ncbi.nlm.nih.gov/pubmed/22731854 [Accessed November 21, 2018].

Patterson, A.J. & Zhang, L., 2010. Hypoxia and fetal heart development. *Current molecular medicine*, 10(7), pp.653–66. Available at: http://www.pubmedcentral.nih.gov/articlerender.fcgi?artid=3075953&tool=pmcentrez&rendertype=abstract [Accessed February 20, 2015].

Peinado, H., Olmeda, D. & Cano, A., 2007. Snail, Zeb and bHLH factors in tumour progression: an alliance against the epithelial phenotype? *Nature Reviews Cancer*, 7(6), pp.415–428. Available at: http://www.ncbi.nlm.nih.gov/pubmed/17508028 [Accessed November 22, 2018].

Pera, M.F., Reubinoff, B. & Trounson, a, 2000. Human embryonic stem cells. *Journal of cell science*, 113 (Pt 1, pp.5–10.

Pierce, G.B., Dixon, F.J. & Verney, E., 1959. Testicular teratomas.I. Demonstration of teratogenesis by metamorphosis of multipotential Cells. *Cancer*, 12(3), pp.573–583. Available at: http://doi.wiley.com/10.1002/1097-0142%28195905/06%2912%3A3%3C573%3A%3AAID-CNCR2820120316%3E3.0.CO%3B2-M [Accessed November 15, 2018].

Pijnenborg, R. et al., 1980. Trophoblastic invasion of human decidua from 8 to 18 weeks of pregnancy. *Placenta*, 1(1), pp.3–19. Available at: http://www.ncbi.nlm.nih.gov/pubmed/7443635 [Accessed October 17, 2018].

Pineda, E.T., Nerem, R.M. & Ahsan, T., 2013. Differentiation Patterns of Embryonic Stem Cells in Two- versus Three-Dimensional Culture. *Cells Tissues Organs*, 197(5), pp.399–410. Available at: http://www.ncbi.nlm.nih.gov/pubmed/23406658 [Accessed November 23, 2018].

Prasad, S.M. et al., 2009. Continuous hypoxic culturing maintains activation of Notch and allows long-term propagation of human embryonic stem cells without spontaneous differentiation. *Cell Proliferation*, 42(1), pp.63–74.

Prokhorova, T.A. et al., 2009. Teratoma formation by human embryonic stem cells is site dependent and enhanced by the presence of Matrigel. *Stem cells and development*, 18(1), pp.47–54. Available at: http://www.ncbi.nlm.nih.gov/pubmed/18393673 [Accessed January 27, 2015].

Provot, S. et al., 2007. Hif-1alpha regulates differentiation of limb bud mesenchyme and joint development. *The Journal of cell biology*, 177(3), pp.451–64. Available at: http://www.pubmedcentral.nih.gov/articlerender.fcgi?artid=2064828&tool=pmcentrez&rendertype=abstract [Accessed February 20, 2015].

Provot, S. & Schipani, E., 2005. Molecular mechanisms of endochondral bone development. *Biochemical and Biophysical Research Communications*, 328(3), pp.658–665. Available at: http://www.ncbi.nlm.nih.gov/pubmed/15694399 [Accessed November 18, 2018].

Rafalski, V.A., Mancini, E. & Brunet, A., 2012. Energy metabolism and energy-sensing pathways in mammalian embryonic and adult stem cell fate. *Journal of cell science*, 125(Pt 23), pp.5597–608. Available at: http://www.ncbi.nlm.nih.gov/pubmed/23420198 [Accessed January 25, 2017].

Rankin, E.B., Giaccia, A.J. & Schipani, E., 2011. A Central Role for Hypoxic Signaling in Cartilage, Bone, and Hematopoiesis. *Current Osteoporosis Reports*, 9(2), pp.46–52. Available at: http://www.ncbi.nlm.nih.gov/pubmed/21360287 [Accessed November 18, 2018].

Raval, R.R. et al., 2005. Contrasting Properties of Hypoxia-Inducible Factor 1 (HIF-1) and HIF-2 in von Hippel-Lindau-Associated Renal Cell Carcinoma. *Molecular and Cellular Biology*, 25(13), pp.5675–5686. Available at: http://www.ncbi.nlm.nih.gov/pubmed/15964822 [Accessed October 10, 2018].

Ravi, R. et al., 2000. Regulation of tumor angiogenesis by p53-induced degradation of hypoxia-inducible factor 1alpha. *Genes & development*, 14(1), pp.34–44. Available at: http://www.ncbi.nlm.nih.gov/pubmed/10640274 [Accessed November 18, 2018].

Red-Horse, K. et al., 2004. Trophoblast differentiation during embryo implantation and formation of the maternal-fetal interface. *Journal of Clinical Investigation*, 114(6), pp.744–754. Available at: http://www.jci.org/articles/view/22991 [Accessed November 23, 2018].

Reubinoff, B.E. et al., 2000. Embryonic stem cell lines from human blastocysts: somatic differentiation in vitro. *Nature Biotechnology*, 18(4), pp.399–404. Available at: http://www.ncbi.nlm.nih.gov/pubmed/10748519 [Accessed September 30, 2018].

Richards, M. et al., 2002. Human feeders support prolonged undifferentiated growth of human inner cell masses and embryonic stem cells. *Nature Biotechnology*, 20(9), pp.933–936. Available at: http://www.ncbi.nlm.nih.gov/pubmed/12161760 [Accessed November 22, 2018].

Ryan, J.M. et al., 2005. Mesenchymal stem cells avoid allogeneic rejection. *Journal of inflammation (London, England)*, 2, p.8. Available at: http://www.ncbi.nlm.nih.gov/pubmed/16045800 [Accessed August 16, 2018].

San-Millán, I. & Brooks, G.A., 2017. Reexamining cancer metabolism: lactate production for carcinogenesis could be the purpose and explanation of the Warburg Effect. *Carcinogenesis*, 38(2), pp.119–133. Available at: http://www.ncbi.nlm.nih.gov/pubmed/27993896 [Accessed November 1, 2018].

Saxena, S. et al., 2008. FGF2 secreting human fibroblast feeder cells: A novel culture system for human embryonic stem cells. *Molecular Reproduction and Development*, 75(10), pp.1523–1532. Available at: http://www.ncbi.nlm.nih.gov/pubmed/18318041 [Accessed November 22, 2018].

Schipani, E. et al., 2001. Hypoxia in cartilage: HIF-1alpha is essential for chondrocyte growth arrest and survival. *Genes & development*, 15(21), pp.2865–76. Available at: http://www.ncbi.nlm.nih.gov/pubmed/11691837 [Accessed November 18, 2018].

Semenza, G.L. et al., 1991. Hypoxia-inducible nuclear factors bind to an enhancer element located 3' to the human erythropoietin gene. *Proceedings of the National Academy of Sciences of the United States of America*, 88(13), pp.5680–4. Available at: http://www.ncbi.nlm.nih.gov/pubmed/2062846 [Accessed November 20, 2018].

Shen, Q. et al., 2008. Adult SVZ Stem Cells Lie in a Vascular Niche: A Quantitative Analysis of Niche Cell-Cell Interactions. *Cell Stem Cell*, 3(3), pp.289–300. Available at: http://www.ncbi.nlm.nih.gov/pubmed/18786416

[Accessed November 21, 2018].
Shin, J.M. et al., 2011. Enhancement of differentiation efficiency of hESCs into vascular lineage cells in hypoxia via a paracrine mechanism. *Stem cell research*, 7(3), pp.173–85. Available at: http://www.ncbi.nlm.nih.gov/pubmed/21907161 [Accessed March 5, 2015].
Shweiki, D. et al., 1992. Vascular endothelial growth factor induced by hypoxia may mediate hypoxia-initiated angiogenesis. *Nature*, 359(6398), pp.843–845. Available at: http://www.ncbi.nlm.nih.gov/pubmed/1279431 [Accessed November 18, 2018].
Shyh-Chang, N. et al., 2013. Influence of Threonine Metabolism on S-Adenosylmethionine and Histone Methylation. *Science*, 339(6116), pp.222–226. Available at: http://www.ncbi.nlm.nih.gov/pubmed/23118012 [Accessed November 21, 2018].
Simon, M.C. & Keith, B., 2008. The role of oxygen availability in embryonic development and stem cell function. *Nature reviews. Molecular cell biology*, 9(4), pp.285–96. Available at: http://www.pubmedcentral.nih.gov/articlerender.fcgi?artid=2876333&tool=pmcentrez&rendertype=abstract [Accessed September 23, 2014].
Singh, A.M. et al., 2012. Signaling Network Crosstalk in Human Pluripotent Cells: A Smad2/3-Regulated Switch that Controls the Balance between Self-Renewal and Differentiation. *Cell Stem Cell*, 10(3), pp.312–326. Available at: http://www.ncbi.nlm.nih.gov/pubmed/22385658 [Accessed November 22, 2018].
Spencer, H.L. et al., 2007. E-cadherin inhibits cell surface localization of the pro-migratory 5T4 oncofetal antigen in mouse embryonic stem cells. *Molecular biology of the cell*, 18(8), pp.2838–51. Available at: http://www.ncbi.nlm.nih.gov/pubmed/17507657 [Accessed October 19, 2018].
Stacpoole, S.R.L. et al., 2013. High Yields of Oligodendrocyte Lineage Cells from Human Embryonic Stem Cells at Physiological Oxygen Tensions for Evaluation of Translational Biology. *Stem Cell Reports*, 1(5), pp.437–450. Available at: http://www.ncbi.nlm.nih.gov/pubmed/24286031 [Accessed September 23, 2018].
Stadtfeld, M., Brennand, K. & Hochedlinger, K., 2008. Reprogramming of pancreatic beta cells into induced pluripotent stem cells. *Current biology : CB*, 18(12), pp.890–4. Available at: http://www.pubmedcentral.nih.gov/articlerender.fcgi?artid=2819222&tool=pmcentrez&rendertype=abstract [Accessed January 9, 2015].
Staun-Ram, E. & Shalev, E., 2005. Human trophoblast function during the implantation process. *Reproductive biology and endocrinology : RB&E*, 3, p.56. Available at: http://www.ncbi.nlm.nih.gov/pubmed/16236179 [Accessed August 19, 2018].
STEVENS, L.C., 1960. Embryonic potency of embryoid bodies derived from a transplantable testicular teratoma of the mouse. *Developmental biology*, 2, pp.285–97. Available at: http://www.ncbi.nlm.nih.gov/pubmed/13834544 [Accessed November 15, 2018].
Suter, D.M. et al., 2009. A Sox1 to Pax6 Switch Drives Neuroectoderm to Radial Glia Progression During Differentiation of Mouse Embryonic Stem

Cells. *Stem Cells*, 27(1), pp.49–58. Available at: http://doi.wiley.com/10.1634/stemcells.2008-0319 [Accessed March 25, 2019].

Takahashi, K. et al., 2007. Induction of pluripotent stem cells from adult human fibroblasts by defined factors. *Cell*, 131(5), pp.861–72. Available at: http://www.ncbi.nlm.nih.gov/pubmed/18035408 [Accessed July 9, 2014].

Takahashi, K. & Yamanaka, S., 2006. Induction of pluripotent stem cells from mouse embryonic and adult fibroblast cultures by defined factors. *Cell*, 126(4), pp.663–76. Available at: http://www.ncbi.nlm.nih.gov/pubmed/16904174 [Accessed July 9, 2014].

Takubo, K. et al., 2013. Regulation of glycolysis by Pdk functions as a metabolic checkpoint for cell cycle quiescence in hematopoietic stem cells. *Cell stem cell*, 12(1), pp.49–61. Available at: http://www.sciencedirect.com/science/article/pii/S1934590912005929 [Accessed January 16, 2015].

Thiery, J.P. et al., 2009. Epithelial-Mesenchymal Transitions in Development and Disease. *Cell*, 139(5), pp.871–890. Available at: http://www.ncbi.nlm.nih.gov/pubmed/19945376 [Accessed October 19, 2018].

Thomson, J.A. et al., 1998. Embryonic stem cell lines derived from human blastocysts. *Science (New York, N.Y.)*, 282(5391), pp.1145–7. Available at: http://www.ncbi.nlm.nih.gov/pubmed/9804556 [Accessed October 17, 2014].

Tian, H., McKnight, S.L. & Russell, D.W., 1997. Endothelial PAS domain protein 1 (EPAS1), a transcription factor selectively expressed in endothelial cells. *Genes & development*, 11(1), pp.72–82. Available at: http://www.ncbi.nlm.nih.gov/pubmed/9000051 [Accessed September 12, 2015].

Tian, L. et al., 2016. Efficient and Controlled Generation of 2D and 3D Bile Duct Tissue from Human Pluripotent Stem Cell-Derived Spheroids. *Stem Cell Reviews and Reports*, 12(4), pp.500–508. Available at: http://www.ncbi.nlm.nih.gov/pubmed/27138846 [Accessed November 23, 2018].

Trelstad, R.L., Hay, E.D. & Revel, J.-P., 1967. Cell contact during early morphogenesis in the chick embryo. *Developmental Biology*, 16(1), pp.78–106. Available at: https://www.sciencedirect.com/science/article/pii/0012160667900188?via%3Dihub [Accessed November 16, 2018].

Trelstad, R.L., Revel, J.P. & Hay, E.D., 1966. Tight junctions between cells in the early chick embryo as visualized with the electron microscopy. *The Journal of cell biology*, 31(1), pp.C6-10. Available at: http://www.ncbi.nlm.nih.gov/pubmed/5971977 [Accessed November 16, 2018].

Trounson, A., 2002. Human embryonic stem cells: mother of all cell and tissue types. *Reproductive biomedicine online*, 4 Suppl 1, pp.58–63. Available at: http://www.ncbi.nlm.nih.gov/pubmed/12470337 [Accessed November 23, 2018].

van Tuyl, M. et al., 2005. Role of oxygen and vascular development in epithelial branching morphogenesis of the developing mouse lung.

American journal of physiology. Lung cellular and molecular physiology, 288(1), pp.L167-78. Available at: http://www.ncbi.nlm.nih.gov/pubmed/15377493 [Accessed February 20, 2015].

Uchida, T. et al., 2004. Prolonged hypoxia differentially regulates hypoxia-inducible factor (HIF)-1alpha and HIF-2alpha expression in lung epithelial cells: implication of natural antisense HIF-1alpha. *The Journal of biological chemistry*, 279(15), pp.14871–8. Available at: http://www.ncbi.nlm.nih.gov/pubmed/14744852 [Accessed October 16, 2018].

Ufer, C. & Wang, C.C., 2011. The Roles of Glutathione Peroxidases during Embryo Development. *Frontiers in molecular neuroscience*, 4, p.12. Available at: http://www.pubmedcentral.nih.gov/articlerender.fcgi?artid=3148772&tool=pmcentrez&rendertype=abstract [Accessed February 20, 2015].

Vallier, L., Alexander, M. & Pedersen, R.A., 2005. Activin/Nodal and FGF pathways cooperate to maintain pluripotency of human embryonic stem cells. *Journal of Cell Science*, 118(19), pp.4495–4509. Available at: http://www.ncbi.nlm.nih.gov/pubmed/16179608 [Accessed September 23, 2018].

Vićovac, L. & Aplin, J.D., 1996. Epithelial-mesenchymal transition during trophoblast differentiation. *Acta anatomica*, 156(3), pp.202–16. Available at: http://www.ncbi.nlm.nih.gov/pubmed/9124037 [Accessed November 17, 2018].

Viswanathan, S.R., Daley, G.Q. & Gregory, R.I., 2008. Selective Blockade of MicroRNA Processing by Lin28. *Science*, 320(5872), pp.97–100. Available at: http://www.ncbi.nlm.nih.gov/pubmed/18292307 [Accessed November 21, 2018].

Wakui, T. et al., 2017. Method for evaluation of human induced pluripotent stem cell quality using image analysis based on the biological morphology of cells. *Journal of Medical Imaging*, 4(04), p.1. Available at: https://www.spiedigitallibrary.org/journals/journal-of-medical-imaging/volume-4/issue-04/044003/Method-for-evaluation-of-human-induced-pluripotent-stem-cell-quality/10.1117/1.JMI.4.4.044003.full [Accessed October 27, 2018].

Wang, G.L. et al., 1995. Hypoxia-inducible factor 1 is a basic-helix-loop-helix-PAS heterodimer regulated by cellular O2 tension. *Proceedings of the National Academy of Sciences of the United States of America*, 92(12), pp.5510–4. Available at: http://www.ncbi.nlm.nih.gov/pubmed/7539918 [Accessed November 20, 2018].

WARNECKE, C. et al., 2004. Differentiating the functional role of hypoxia-inducible factor (HIF)-1α and HIF-2α (EPAS-1) by the use of RNA interference: erythropoietin is a HIF-2α target gene in Hep3B and Kelly cells. *The FASEB Journal*, 18(12), pp.1462–1464. Available at: http://www.ncbi.nlm.nih.gov/pubmed/15240563 [Accessed November 20, 2018].

Warr, M.R. & Passegué, E., 2013. Metabolic Makeover for HSCs. *Cell Stem Cell*, 12(1), pp.1–3. Available at: http://www.ncbi.nlm.nih.gov/pubmed/23290130 [Accessed November 21, 2018].

Wenger, R.H. et al., 1997. Hypoxia-inducible factor-1α is regulated at the post-mRNA level. *Kidney International*, 51(2), pp.560–563.

Westfall, S.D. et al., 2008. Identification of oxygen-sensitive transcriptional programs in human embryonic stem cells. *Stem cells and development*, 17, pp.869–881.

WIESENER, M.S. et al., 2003. Widespread hypoxia-inducible expression of HIF-2α in distinct cell populations of different organs. *The FASEB Journal*, 17(2), pp.271–273. Available at: http://www.ncbi.nlm.nih.gov/pubmed/12490539 [Accessed November 20, 2018].

Wu, D. & Yotnda, P., 2011. Induction and testing of hypoxia in cell culture. *Journal of visualized experiments : JoVE*, (August), pp.2–5.

Yang, G. et al., 2008. PTEN deficiency causes dyschondroplasia in mice by enhanced hypoxia-inducible factor 1 signaling and endoplasmic reticulum stress. *Development*, 135(21), pp.3587–3597. Available at: http://www.ncbi.nlm.nih.gov/pubmed/18832389 [Accessed November 18, 2018].

Yang, M.-H. et al., 2008. Direct regulation of TWIST by HIF-1α promotes metastasis. *Nature Cell Biology*, 10(3), pp.295–305. Available at: http://www.ncbi.nlm.nih.gov/pubmed/18297062 [Accessed November 22, 2018].

Yeo, C.D. et al., 2017. The role of hypoxia on the acquisition of epithelial-mesenchymal transition and cancer stemness: a possible link to epigenetic regulation. *The Korean journal of internal medicine*, 32(4), pp.589–599. Available at: http://www.ncbi.nlm.nih.gov/pubmed/28704917 [Accessed October 19, 2018].

Yin, T. & Li, L., 2006. The stem cell niches in bone. *Journal of Clinical Investigation*, 116(5), pp.1195–1201. Available at: http://www.ncbi.nlm.nih.gov/pubmed/16670760 [Accessed November 21, 2018].

Ying, Q.L. et al., 2003. BMP induction of Id proteins suppresses differentiation and sustains embryonic stem cell self-renewal in collaboration with STAT3. *Cell*, 115(3), pp.281–92. Available at: http://www.ncbi.nlm.nih.gov/pubmed/14636556 [Accessed January 25, 2015].

Zannettino, A.C.W. et al., 2008. Multipotential human adipose-derived stromal stem cells exhibit a perivascular phenotype in vitro and in vivo. *Journal of Cellular Physiology*, 214(2), pp.413–421. Available at: http://www.ncbi.nlm.nih.gov/pubmed/17654479 [Accessed November 21, 2018].

Zeisberg, M. & Neilson, E.G., 2009. Biomarkers for epithelial-mesenchymal transitions. *The Journal of clinical investigation*, 119(6), pp.1429–37. Available at: http://www.ncbi.nlm.nih.gov/pubmed/19487819 [Accessed October 19, 2018].

Zelzer, E. et al., 2004. VEGFA is necessary for chondrocyte survival during bone development. *Development*, 131(9), pp.2161–2171. Available at: http://www.ncbi.nlm.nih.gov/pubmed/15073147 [Accessed November 18, 2018].

Zhang, J. et al., 2011. UCP2 regulates energy metabolism and differentiation potential of human pluripotent stem cells. *The EMBO Journal*, 30(24),

pp.4860–4873. Available at: http://www.ncbi.nlm.nih.gov/pubmed/22085932 [Accessed October 12, 2018].

Zheng, G. et al., 2009. Disruption of E-cadherin by matrix metalloproteinase directly mediates epithelial-mesenchymal transition downstream of transforming growth factor-beta1 in renal tubular epithelial cells. *The American journal of pathology*, 175(2), pp.580–91. Available at: http://www.ncbi.nlm.nih.gov/pubmed/19590041 [Accessed November 22, 2018].

Zhou, W. et al., 2012. HIF1α induced switch from bivalent to exclusively glycolytic metabolism during ESC-to-EpiSC/hESC transition. *The EMBO Journal*, 31(9), pp.2103–2116. Available at: http://www.ncbi.nlm.nih.gov/pubmed/22446391 [Accessed November 21, 2018].

Zhu, H. et al., 2011. The Lin28/let-7 Axis Regulates Glucose Metabolism. *Cell*, 147(1), pp.81–94. Available at: http://www.ncbi.nlm.nih.gov/pubmed/21962509 [Accessed November 21, 2018].